

Forschungszentrum Karlsruhe
Technik und Umwelt

Wissenschaftliche Berichte
FZKA 6127

European Helium Cooled Pebble Bed (HCPB) Test Blanket

**ITER Design Description Document
Status 1.12.1998**

Edited by:

L. V. Boccaccini

Contributors:

**H. Albrecht, L. V. Boccaccini,
L. Berardinucci, M. Dalle Donne,
H. J. Fiek, U. Fischer, S. Gordeev,
S. Hermsmeyer, E. Hutter, K. Kleefeldt,
T. Lechler, M. Lenartz, P. Norajitra,
G. Piazza, G. Reimann, P. Ruatto,
F. Scaffidi-Argentina, K. Schleisiek,
I. Schmuck, H. Schnauder, H. Tsige-Tamirat**

**Association FZK-Euratom
Projekt Kernfusion**

März 1999



Forschungszentrum Karlsruhe
Technik und Umwelt
Wissenschaftliche Berichte

FZKA 6127

European Helium Cooled Pebble Bed (HCPB) Test Blanket

**ITER Design Description Document
Status 1.12.1998**

**Edited by:
L.V. Boccaccini**

**Contributors:
H. Albrecht, L.V. Boccaccini, L. Berardinucci, M. Dalle Donne, H.J. Fiek,
U. Fischer, S. Gordeev, S. Hermsmeyer, E. Hutter, K. Kleefeldt, T. Lechler,
M. Lenartz, P. Norajitra, G. Piazza, G. Reimann, P. Ruatto, F. Scaffidi-Argentina,
K. Schleisiek, I. Schmuck, H. Schnauder, H. Tsige-Tamirat**

**Association FZK-Euratom
Projekt Kernfusion**

**Forschungszentrum Karlsruhe GmbH, Karlsruhe
1999**

Als Manuskript gedruckt
Für diesen Bericht behalten wir uns alle Rechte vor

Forschungszentrum Karlsruhe GmbH
Postfach 3640, 76021 Karlsruhe

Mitglied der Hermann von Helmholtz-Gemeinschaft
Deutscher Forschungszentren (HGF)

ISSN 0947-8620

European Helium Cooled Pebble Bed (HCPB) Test Blanket ITER Design Description Document. Status 1.12.1998

Abstract

The Helium Cooled Pebble Bed (HCPB) blanket is based on the use of separate small lithium orthosilicate and beryllium pebble beds placed between radial toroidal cooling plates. Cooling is provided by circulating helium at 8 MPa. The tritium produced in the pebble beds is purged by a separate flow of helium at 0.1 MPa. The structural material is martensitic steel.

A milestone for the development of the HCPB Demo Blanket Design is the test in ITER. For this purpose a Test Blanket System - a test module placed in plasma contact and its ancillary systems - has been designed. The analyses performed show that the Test Blanket System allows to conduct a suitable test programme in ITER and meets all the integration requirements in the fusion reactor. Finally, the test system will operate with sufficient reliability and will not impede the safe operation of ITER.

Europäisches Heliumgekühltes Feststoff-Testblanket ITER Design Description Document. Status 1.12.1998

Kurzfassung

Das HCPB Feststoffblanket ist aus Schichtungen kleiner Lithium-Orthosilikat- und Berylliumkugel aufgebaut (HCPB steht für die englische Bezeichnung helium cooled pebble bed). Die einzelnen Schüttungen sind durch radial-toroidal verlaufende Kühlplatten voneinander getrennt. Die Kühlung erfolgt durch gasförmiges Helium bei einem Druck von 8 MPa. Das in den Kugelbetten erzeugte Tritium wird durch einen separaten Heliumstrom von 0.1 MPa herausgespült. Als Strukturmaterial wird martensitischer Stahl verwendet.

Ein Meilenstein für die Entwicklung des HCPB Blanket Designs stellt der Test in ITER dar. Zu diesem Zweck wurde ein Testblanket-System entwickelt, das sich als Testmodul mit seinen Hilfssystemen direkt in der Umgebung des Plasmas befindet. Die Analysen zeigen, daß das Testblanket-System die Durchführung geeigneter Testprogramme in ITER erlaubt und die gesamten Anforderungen an die Integration in den Fusionsreaktor erfüllt. Außerdem arbeitet das Testsystem mit ausreichender Zuverlässigkeit und wird den sicheren Betrieb von ITER nicht behindern.

Introductory Remarks

The present report is the final version of the Design Description Document (DDD) for the Helium Cooled Pebble Bed (HCPB) Test Blanket Module (TBM) to be irradiated in ITER. In fact, one of the goals of the ITER Engineering and Design Activities (EDA) is the definition of an in-reactor test program of blanket concepts developed for a demonstration reactor. For this purpose it is foreseen that 3 of the 20 horizontal ports of ITER house TBMs based on blanket concepts selected in the frame of the Test Blanket Working Group (TBWG). The European Union is represented by two concepts, namely the Water Cooled Lithium Lead (WCLL) and the HCPB blanket. Japanese, Russian and US concepts complete the list of the selected blankets. In addition a 4th port is reserved for testing the Breeding Blanket of ITER, which will replace the shielding blanket during the enhanced performance phase to produce part of the tritium necessary for the operation of the machine.

As the Test Blanket Modules are in-vessel components of ITER, a detailed DDD for each test device like the other components of ITER is required. These documents are written in accordance with a scheme given by the ITER Joint Central Team (JCT) and account for the comments made by the JCT in different stages of the work. At the end of the EDA phase, the DDDs of the Test Blanket Modules have been included in the Final Design Report of ITER (ITER FDR, Section 5.6).

The DDD for the HCPB Test Blanket Module has been conceived as an electronic document (WORD 6.0) that has grown steadily during the three year (1996-1998) of the TBM design activities. Two previous hardcopy versions of this document have been already distributed among the members of the TBWG and ITER JCT. The version submitted to ITER for the Final Design Report is dated December 5, 1997 (except the Section 2.7 that was subsequently updated on April 30, 1998). The version presented in this FZKA Report is dated December 1, 1998 and represents the final version of this document. It doesn't differ substantially from the FDR version; only few more recent results of the 1997-1998 European Blanket Programme have been included.

This work has been performed in the framework of the Nuclear Fusion Project of the Forschungszentrum Karlsruhe and it is supported by the European Union within the European Fusion Technology Program.

List of Abbreviations and Acronyms

ALARA	As low as reasonably achievable
ASME	American Society of Mechanical Engineers
BOL	Beginning of life
BPP	Basic Performance Phase
BZ	Breeding Zone
CD	Centered Disruption
CEA	Commissariat a l'Énergie Atomique
CEN	Centre d'Etude de l'Énergie Nucléaire
CFC	Carbon fibre composite
CFD	Computational fluid dynamics
CP	Cooling plate
CPS	Coolant Purification Subsystem
DBTT	Ductile to brittle transition temperature
DDD	Design Description Document
DEMO	Demonstration (reactor)
EB	Electro beam
ECN	Energieonderzoek Centrum Nederland
EDA	Engineering Design Activities
EM	Electromagnetic
ENEA	Ente per le Nuove Tecnologie, l'Energia e l'Ambiente
EPP	Enhanced Performance Phase
FE, FEM	Finite Element, FE Method
FMEA	Failing Modes and Effects Analysis
FW	First Wall
FZK	Forschungszentrum Karlsruhe
GDRD	General Design Requirements Document
GS	Gas chromatograph
GSEDC	General Safety and Environmental Design Criteria
HVAC	Heating, ventilation, air conditioning
HCPB	Helium Cooled Pebble Bed
HX	Heat Exchanger
IAEA	International Atomic Energy Agency
IBB	Inboard Blanket
ICRP	International Council on Radiation Protection
IG	ITER Grade
ISDC	ITER Structural Design Criteria
ISS	Isotope Separation System
ITER	International Thermonuclear Experimental Reactor
I&C	Instrumentation and control
JCT	Joint Central Team
LA	Low Activation
LF	Lorentz Force
LIM	Limiter
LOCA	Loss of Coolant Accident
LOFA	Loss of Flow Accident

MANET	Martensitic-steel for NET
MF	Magnetisation Force
MRM	Magnesium Reduction Method
MS	Melting and Spray
MTTR	Mean time to repair
NDT	Non destructive testing
NET	Next European Torus
NSSR	Non-site Specific Safety Report
OBB	Outboard Blanket
PIE	Postulated Initiating Event
PFC	Plasma Facing Components
REM	Rotating Electrode Method
RH	Remote Handling
R&D	Research and Development
SCK	Studiecentrum voor Kernenergie
SEHD	Safety Environmental Health Division
SIC	Safety Importance Class
SS	Stainless steel
TBA	Test Blanket Assembly
TBD	To be determined
TBM	Test Blanket Module
TBS	Test Blanket Subsystem
TBWG	Test Blanket Working Group
TES	Tritium Extraction Subsystem
TF	Toroidal Field
TIG	Tungsten inert gas
VDE	Vertical Displacement Event
VV	Vacuum Vessel
WCLL	Water Cooled Lithium Lead
WDS	Water Detriation System

Table of Contents

SUMMARY	1
1 FUNCTIONS AND DESIGN REQUIREMENTS	3
1.1 Functions.....	3
1.2 Design Requirements.....	3
1.2.1 General Requirements.....	3
1.2.2 Vacuum Requirements.....	4
1.2.3 Structural Requirements.....	5
1.2.4 Electromagnetic Requirements.....	5
1.2.5 Thermal-hydraulic Requirements.....	5
1.2.6 Mechanical Requirements.....	6
1.2.7 Electrical Requirements.....	6
1.2.8 Nuclear Requirements.....	7
1.2.9 Remote Handling Requirements.....	7
1.2.10 Chemical Requirements.....	9
1.2.11 Seismic Requirements.....	9
1.2.12 Manufacturing Requirements.....	9
1.2.13 Construction Requirements.....	10
1.2.14 Assembly Requirements.....	10
1.2.15 Testing Requirements.....	10
1.2.16 Instrumentation & Control Requirements.....	11
1.2.17 Decommissioning Requirements.....	11
1.2.18 Electrical Connections / Earthing / Insulation Requirements.....	11
1.2.19 Material Requirements.....	11
1.2.20 HVAC Requirements.....	12
1.2.21 Lay-out Requirements.....	12
1.3 Safety Requirements.....	12
1.3.1 Safety Functions.....	13
1.3.2 Safety Classification of Items.....	13
1.3.3 Safety Design Limits and Analysis Requirements.....	14
1.3.4 Safety Assessment.....	14
1.3.5 Specific Safety Design Requirements.....	15
1.4 R&D Requirements.....	16
1.5 Operation and Maintenance.....	16
1.6 Surveillance and In-Service Inspection.....	16
1.7 Quality Assurance.....	17
1.8 System Configuration & Essential Features.....	17
1.9 Interfacing Systems.....	17
1.10 Codes and Standards.....	20

1.11 Reliability Requirements	20
1.12 Other Special Requirements	20
2 DESIGN DESCRIPTION	21
2.0 Summary Description	21
2.0.1 General	21
2.0.2 Test Blanket Subsystem	23
2.0.3 Tritium Extraction Subsystem	30
2.0.4 Helium Cooling Subsystem	32
2.0.5 Coolant Purification Subsystem	34
2.0.6 Test Blanket Remote Handling Subsystem	36
2.0.7 Safety	37
2.1 Detailed System Description	39
2.1.1 General Design Description	39
2.1.1.1 Test Blanket Subsystem Design Description	39
2.1.1.1.1 Nuclear Design	47
2.1.1.1.2 Thermohydraulic and thermal design	63
2.1.1.1.2.1 Calculational assumptions	63
2.1.1.1.2.2 Models	64
2.1.1.1.2.3 Results	66
2.1.1.1.3 Structural Design	76
2.1.1.1.4 Mechanical Design	87
2.1.1.1.5 Maintenance/Remote Handling	91
2.1.1.1.6 Fabrication and Assembly	92
2.1.1.1.6.1 Reference Manufacturing Procedure	92
2.1.1.1.6.2 Alternative Manufacturing Procedure	95
2.1.1.1.7 Materials	96
2.1.1.1.8 Electromagnetic Design	98
2.1.1.1.9 Tritium Control	104
2.1.1.1.9.1 Tritium permeation	104
2.1.1.1.9.2 Tritium inventory	106
2.1.1.2 Tritium Extraction Subsystem	107
2.1.1.3 Helium Cooling Subsystem	115
2.1.1.3.1 Thermal-hydraulic design	115
2.1.1.3.2 Primary Heat Removal Loops	116
2.1.1.3.3 Secondary Heat Removal Loops	120
2.1.1.3.4 Maintenance/Remote Handling	120
2.1.1.3.5 Assembly	121
2.1.1.3.6 System Start-up, Control, and Shutdown	121
2.1.1.3.7 Materials	122
2.1.1.3.8 Safety	122
2.1.1.4 Coolant Purification Subsystem	127
2.1.1.5 Test Blanket Remote Handling Subsystem	134
2.1.1.5.1 Mechanical Design	137
2.1.1.5.2 Decay Heat Removal During Remote Handling	138
2.1.1.6 Reliability Analysis	142
2.1.1.7 Test Program	146
2.1.1.7.1 Test objectives	146

2.1.1.7.2 ITER requirements	146
2.1.1.7.3 Test Plan	147
2.1.2 Supporting Design Documents	149
2.2 System Performance Characteristics	150
2.2.1 Operating State Description	150
2.2.2 Operating State Data	150
2.3 System Arrangement.....	153
2.4 Component Design Description	154
2.4.1 List of Components.....	154
2.4.2 Test Blanket Subsystem	156
2.4.3 Tritium Extraction Subsystem	158
2.4.4 Helium Cooling Subsystem.....	165
2.4.5 Coolant Purification Subsystem.....	166
2.4.6 Test Blanket Remote Handling Subsystem	171
2.5 Instrumentation and Control	172
2.6 System Interfaces	175
2.6.1 Plasma Interface.....	175
2.6.2 Blanket System Interface.....	175
2.6.3 Vacuum Vessel Interface.....	175
2.6.4 Remote Handling Interface	176
2.6.5 Cryostat Interface	176
2.6.6 Primary and Secondary Heat Transfer Interface	177
2.6.7 Vacuum Pumping and Leak Detection Interface	178
2.6.8 Tritium Plant Interface	178
2.6.9 Tokamak Operations and Control Interface.....	179
2.6.10 Building and Transporter Interface	179
2.6.11 Hot Cell Interface.....	180
2.6.12 Other Interfaces.....	180
2.7 Safety analysis of reference events.....	181
2.7.1 Large in-vessel TBM coolant leaks.....	186
2.7.1.1 Case 1a: Failure of first wall (Cat. IV)	186
2.7.1.2 Case 1b: Failure of FW plus Be/steam reaction (Cat. V)	195
2.7.1.3 Case 1c: Large leak inside module (Cat. IV).....	199
2.7.1.4 Case 1d: Small leak inside module (Cat. III)	204
2.7.2 Large ex-vessel TBM coolant leaks.....	207
2.7.2.1 Case 2a: Main pipe break in the vault (Cat. IV)	207
2.7.2.2 Case 2b: Main pipe break in vault plus failure of FW (Cat. IV)	213
2.7.2.3 Case 2c: Main pipe break in the vault plus large leak inside module (Cat IV).....	219
2.7.2.4 Case 2d: Loss of flow plus FW failure at beryllium melting (Cat. V)	225
2.7.3 Safety analysis data base.....	231
2.7.3.1 Materials and toxic materials inventory	231
2.7.3.2 Energy sources	232
2.7.3.3 Material data used in safety analysis	235
2.7.3.4 The 1D heat transport model	240

Appendixes:

Appendix A 9Cr RCC-MR properties data	247
Appendix B Li_4SiO_4 pebble bed	264
Appendix C Beryllium pebble bed.....	268

Summary

One of the main engineering performance goals of ITER is to test and validate design concepts of tritium breeding blankets relevant to a DEMO or a power producing reactor. The tests foreseen on modules include the demonstration of a breeding capability that would lead to tritium self-sufficiency in a reactor and the extraction of high-grade heat suitable for electricity generation. To accomplish these goals, a number of the ITER horizontal ports are available to test the Test Blanket Systems, both in the Basic Performance Phase (BPP) and the Extended Performance Phase (EPP). One of the ports will be dedicated to the testing of the tritium breeding blanket which will be used in the EPP of ITER.

The blanket test program will investigate various design concepts of tritium breeding blankets proposed by the Parties. The Design Description Document(s) of the Test Blanket System addresses the requirements and the design description of the Test Blanket System(s) with the ITER device, auxiliaries, facilities, machine operations, safety, reliability, and maintenance.

The European Fusion Program proposes two DEMO relevant blanket concepts for testing in ITER. One is the Water Cooled Lithium Lead (WCLL) blanket, the other the Helium Cooled Pebble Bed (HCPB) blanket. Both use martensitic steel as structural material. The present part of the EU DDD covers the design specifications for the HCPB.

During the ITER Basic Performance Phase the blanket test module shall occupy half of the test port allocated to the helium cooled blankets, the other half being occupied by the Japanese helium cooled ceramic breeder blanket module. During the Extended Performance Phase the HCPB test modules may occupy the whole or half of one port according to the numbers of blanket concepts to be tested and to the number of ports available for the blanket module testing. Parts of the tests, in particular those related to tritium control and fluid dynamics (helium flow distribution, pressure drop), may be conducted before the first plasma ignition.

The purpose of the tests is to validate the design principles and the operational feasibility for the demonstration blanket system. The tests in ITER include the simultaneous function of all subsystems including first wall, blanket module and shield as well as cooling and tritium systems and - to a smaller extent - blanket specific equipment for remote handling. Safety, reliability, maintenance and dismantling will be equally addressed. To assess those qualities and characteristics, the test blanket systems are to be exposed directly to the ITER plasma for relatively long, continuous operating periods. These test blanket modules will be replacing shielding blanket modules, thus they must meet all applicable ITER shielding blanket requirements, including heat removal, shielding protection for the Vacuum Vessel welds and Toroidal Field magnets, and reduction of neutron streaming.

Breeding and recovery of tritium are important goals of the test program. Lithium ceramic compounds will be used as the breeder materials to be investigated. Subsystems to recover the bred tritium will be demonstrated along with test facilities to separate and remove the tritium from the coolant or purge streams. Special design provisions and tritium handling facilities will be required to meet the ITER safety goals and requirements. Generation and extraction of high temperature coolant

helium will demonstrate the suitability of fusion for commercial power generation. The high temperature coolant will transfer the rejected heat to the ITER facility water coolant system.

The Test Blanket Modules will be designed to: (1) conform to the same safety requirements as other in-vessel components, (2) be robust against the thermal and mechanical loads produced on them by disruption, and (3) have a minimum impact on reactor operation and availability due to any unscheduled test module removal.

The Test Blanket Systems are to be installed and maintained through the horizontal test ports. Standard ITER remote handling equipment and procedures will be used to the maximum extent. All Test Blanket System's plumbing and instrumentation and control shall be contained within the vacuum chamber horizontal port extensions and pass through the horizontal port or shielding doors. Maintenance rails and other remote handling equipment are to be provided for use within the horizontal ports. Space shall be provided in the region immediately outside the biological shield, near the ports, for the helium coolant loops while the Test Blanket Systems are in place and for storage of test equipment during maintenance actions. Furthermore space shall be provided for the tritium handling equipment but not necessarily near the horizontal port. Transport from the horizontal ports to the Hot Cells is to be provided as well as facilities in the Hot Cells for storage, maintenance, testing, refurbishing, and dismantling the test articles.

1 Functions and Design Requirements

1.1 Functions

The test blanket system has to fulfil the following tasks:

1.1.1 Tritium breeding to demonstrate the feasibility of the process and to ultimately enable the extrapolation to a full size blanket and the validation of analytical tools.

1.1.2 High grade heat production and removal to demonstrate the feasibility of electricity production.

1.1.3 Remove the surface heat flux and the nuclear heating within the allowable temperature, stress and deformation limits.

1.1.4 Reduce the nuclear responses in the vacuum vessel structural material for the ITER fluence goal.

1.1.5 Contribute to the protection of superconducting magnets against excessive nuclear heating and radiation damage.

1.1.6 Contribute to the passive stabilisation of the plasma.

1.1.7 Contribute to the reduction of neutral particle density between the divertor and the main plasma chamber by $\sim 10^4$.

1.1.8 Provide a maximum degree of mechanical and structural self-support to: (1) minimise the loads transmitted to the vacuum vessel, and (2) decouple the operating temperature ranges between the test blanket system, the backplate and the vacuum vessel.

1.2 Design Requirements

1.2.1 General Requirements

1.2.1.1 The system must be designed for the power requirements set for ITER (Ref. GDRD Sect 2.2.1.2.1 and 2.2.6.1)

a. Maximum Nominal Fusion Power	1.5 GW
b. Maximum Fusion Power Excursions	20%
c. Duration of Excursion Time	~ 10 sec
d. Pulse Duration	1000 sec
e. Pulse Repetition time	2200 sec

1.2.1.2 The primary wall of the Test Blanket shall provide a vacuum tight, cooled barrier between the plasma and the underlying blanket/shield structure capable of removing the surface heat flux (≈ 0.5 MW/m² Peak, 0.25 MW/m² Average) and the highest level of nuclear heating (≈ 25 MW/m³) [per Ref. GDRD Sect 1.4-3.4].

1.2.1.3 The Test Blanket shall be designed for an average FW boundary fluence of $> 0.3 \text{ MWa/m}^2$ if testing is during the BPP and $> 1.0 \text{ MWa/m}^2$ if testing is during the EPP.

1.2.1.4 The Test Blanket System shall demonstrate a tritium breeding ratio sufficiently high to perform measurements and to allow reliable extrapolation of the breeding ratio to a full size blanket.

1.2.1.5 The Test Blanket System shall provide adequate neutron shielding protection to the vacuum vessel and magnets (per GDRD 5.5.2.1.2).

1.2.1.6 The Test Blanket System shall demonstrate its capacity to generate high grade heat and to remove the power from the blanket system at reactor relevant coolant conditions (outlet temperatures 450°C).

1.2.1.7 The Test Blanket System shall be designed for installation, routine maintenance, and removal by remote handling equipment through horizontal test ports in the cryostat and vacuum vessel. The time required by these operations shall be minimised.

1.2.1.8 Due to its high level of importance in the successful operation of ITER and its potentially large effect on the overall machine availability, the Test Blanket System design, R&D, procurement, manufacture, test, installation, and operation has to be to high quality standards.

1.2.1.9 The Test Blanket System will be designed according to the Test Blanket Program standards and to the applicable codes, manuals, and guidelines specified. The system shall be designed in compliance with the applicable structural design criteria.

1.2.1.10 System and component reliability requirements are TBD pending outcome of FMEA, Reliability, and other System Engineering Studies.

1.2.2 Vacuum Requirements

1.2.2.1 A double barrier with intermediate leak detection will be used as the primary tritium containment boundary at vulnerable locations (i.e. flanges, bellows, etc.). For the Test Blanket System, this boundary will be established at the nominal Vacuum Vessel.

1.2.2.2 The leak rate inside the primary vacuum must be $< 10^{-7} \text{ Pa m}^3 \text{ s}^{-1}$. The Test Blanket System should have a leak rate $< 10^{-8} \text{ Pa m}^3 \text{ s}^{-1}$.

1.2.2.3 The Test Blanket System and its components will have to undergo both hot and cold vacuum leak tests before and after installation. The possibility of repair work shall be foreseen.

1.2.2.4 Materials, design, tolerances and surface finish must be consistent with the generation and maintenance of high quality vacuum and with the ITER outgassing requirements.

1.2.2.5 The design of the Test Blanket System shall enable bake-out of the structures at 240°C before (to avoid plasma pollution) and after an operation period (to avoid risk of hydrogen embrittlement in the test blanket structure).

1.2.3 Structural Requirements

1.2.3.1.(deleted)

1.2.3.2 The Test Blanket System shall be supported by the vacuum vessel extension and be cantilevered into its nominal position using an appropriate support structure. It shall be designed to withstand the following conditions:

1.2.3.2.1 The external pressure inside the vessel will be 10^{-6} Pa during normal operation, 0.5 MPa for off-normal conditions, and 0.1 MPa for maintenance.

1.2.3.2.2 The pressure of the cooling helium will be 8 MPa in normal operation. The pressures during off-normal conditions and system tests are 120% of nominal.

1.2.3.2.3 Electromagnetic loads as defined in 1.2.4.

1.2.3.2.4 (deleted)

1.2.3.3 The shield structure must accommodate the loads resulting from the coolant pressure, the external pressure within the vacuum vessel, and the full range of electromagnetic loads.

1.2.3.4 The Test Blanket System structure must react the range of axisymmetric radial and poloidal loads on the components that it supports. The weight, net vertical, and net toroidal loads will be transmitted to the vacuum vessel extension.

1.2.4 Electromagnetic Requirements

1.2.4.1 The system must be designed to withstand the electromagnetic loads resulting from the interaction of the magnetic fields and eddy currents induced in the system during plasma transient conditions. The combination of these currents and fields existing in the device may result in radial, toroidal, and/or poloidal pressures on different faces of the modules. The direction and magnitude of these loads must be determined based on design dependent factors such as: location, electrical characteristics, size, segmentation, and connection to other components. The loads at all positions must be calculated for:

- a. normal operation, including start-up and shut-down
- b. the system must be designed to withstand a reduced set of electromagnetic induced loads resulting from centered plasma disruptions and vertical displacement events (VDE's) with the parameters described in GDRD Section 2.2.7 and for the number of disruptions specified in section 2.2.7.4. Specific values are TBD.

1.2.5 Thermal-hydraulic Requirements

1.2.5.1 System Requirements at nominal power of 1.5 GW. The power deposition has to be calculated for a full size test module (to account for the presence of the Japanese half module) and a first wall of martensitic steel with a 5 mm thick beryllium protective layer. The two test modules may be assumed to be 50-60 mm recessed in respect of the contour of the ITER first wall. A surface heat flux of 0.25 MW/m² shall be used for the design of the helium coolant system, while a peak value of 0.5 MW/m² shall be used for the first wall design.

1.2.5.2 System Requirements in off-normal conditions are TBD

1.2.5.3 The power of the test blanket shall be iteratively recalculated as the design and material data evolve.

1.2.5.4 First Wall and Breeder Zone shall be cooled in series by the high pressure (8 MPa) helium coolant. An overpressure of 20 % and steady state conditions shall be assumed for the coolant loop design. The test blanket power shall be dissipated to a low pressure, low temperature cooling loop provided by ITER. Peak requirements in the heat exchangers are TBD. The loops shall be equipped with a control system enabling to decrease the helium mass flow during the plasma dwell time. The coolant system should be able to raise the temperature of the test blanket modules to the prescribed value in approximately 2 to 4 h.

1.2.5.5 The test blanket systems will be designed to operate at elevated temperatures relative to the shield blanket systems. This will allow the test blanket to demonstrate the tritium breeding capability and generation of high grade heat. The maximum temperatures for the coolant helium will be in the range of 450 °C, structural material in the range 500 - 550 °C and solid breeder material up to 900 °C.

1.2.6 Mechanical Requirements

1.2.6.1 The Test Blanket System including its support structure and shield shall be supported by the vacuum vessel extension and be cantilevered into its nominal position using an appropriate support structure. The corresponding dimensional tolerances and loads (mechanic, thermomechanic and electromagnetic) are TBD.

1.2.6.2 The coolant and breeder pipework as well as eventual gas ducts, electrical wires or diagnostic cables will be routed through the horizontal test port and will be designed to allow movements during thermal transients.

1.2.6.3 The penetrations of all pipework through the Vacuum Vessel and the Cryostat shall fulfil all requirements of a vacuum and safety boundary.

1.2.6.4 Welds in contact with water and in high fluence and/or stress level regions, such as near the first wall, are subject to irradiation assisted stress corrosion cracking and should be avoided.

1.2.6.5 The TBM structure shall be bakeable to 240°C.

1.2.6.6 The TBM shall be designed to be removable (RH Class 1) by remote handling through the horizontal test ports. The required time for this operation shall be minimised.

1.2.6.7 The TBM structural connections shall use remote handling compatible connectors, accessible from the back side.

1.2.7 Electrical Requirements

1.2.7.1 The in-vessel portion of the Test Blanket System shall contribute to meeting the requirements that the combined toroidal resistance of the blanket in-vessel structures and the Vacuum Vessel must be larger than 4 $\mu\Omega$ as specified in GDRD Section 5.3.3.3.1.

1.2.7.2 A continuous electrical connection (poloidal and toroidal) between all FW of adjacent modules is desirable to decrease the above electromagnetic loads at the expense of large localised effects on these connections.

1.2.7.3 The connection from the tokamak assembly to the outside, through the supply pipes of the blanket system, shall have a resistance of TBD.

1.2.8 Nuclear Requirements

1.2.8.1 The Test Blanket System shall provide enough shielding so that the Vacuum Vessel remains reweldable at specific locations until at least an average fluence of 1 MWa/m² is reached on the FW (Ref. GDRD 5.5.2.3.3.1).

1.2.8.2 The Test Blanket System shall be designed so that the nuclear responses for at least 1 MWa/m² at the First Wall are limited to a helium production of < 1 appm at all components that may need to be rewelded, such as Vacuum Vessel, blanket components, or piping.

1.2.8.3 The blanket system (including the Test Blanket System), in combination with the vacuum vessel and divertor, shall be designed so that the power dissipated by the attenuated radiation in the cryogenic toroidal magnet remains within the limits specified in GDRD Section 5.3.3.6. The peak insulator dose shall be limited to 3 x 10⁸ rad with neutron fluence of 1 MW a/m² at the First Wall.

1.2.8.4 Provisions shall be provided to breed tritium in the test blankets during the Basic and Enhanced Performance Phases with a tritium breeding ratio from which the self-sufficiency in power reactors can be foreseen. Bred tritium will be extracted in-situ from the test blankets.

1.2.9 Remote Handling Requirements

1.2.9.1 All systems inside the biological shield boundary shall be remotely maintainable. The Test Blanket System and its supporting subsystems shall be designed in complete compliance with the remote handling requirements applicable to their respective remote handling classification. All Test Blanket System components are to be considered as Class 1, except the frames interposing between the modules and the back plate, which are RH Class 2.

1.2.9.2 (deleted)

1.2.9.3 The in-vessel Test Blanket System components may be removed and installed without disturbing any ITER Blanket Modules.

1.2.9.4 The Test Blanket System and its supporting in-vessel subsystems must be capable of insertion/removal through the horizontal test ports by use of horizontal test remote handling equipment.

1.2.9.5 Welded joints within the plasma chamber and the Vacuum Vessel extensions shall be avoided; unavoidable welds shall be done, repaired and leak tested remotely.

1.2.9.6 For any maintenance actions, the more important corrective action should meet the following design goals, see GDRD Section 5.5.1.3.3.3 and 5.19.3.9.3.1.

Test Blanket:

- a. be able to replace a module in 8 weeks,
- b. be able to repair a leak at a fluid joint within 6 weeks (not including the time required to locate and isolate the leak) after a failure of a Test Blanket Module with impact on normal ITER operation,
- c. be able to correct or remove faulty module or test article within 2 weeks,
- d. be able to install repaired module within 4 weeks during scheduled maintenance period.

1.2.9.7 At prescribed intervals (TBD) and after significant off-normal, including electromagnetic, events it shall be possible, using existing in-vessel inspection equipment, to:

- a. inspect/verify modules position,
- b. inspect/verify First Wall integrity,
- c. conduct all specified pre-operational tests.

1.2.9.8 Special assembly and maintenance tools shall be provided for structural attachment of the test blanket article to the port extension:

I for welded connections

wall thickness	TBD cm
speed:	
welding	TBD cm/s
cutting	TBD cm/s
inspection	TBD cm/s

II. for mechanical connections:

end effectors	type and capacity are TBD
tools	type and capacity are TBD

III. for pipe welding, cutting, and inspection of manifolds to blanket module/FW connections:

pipe size	TBD cm OD
wall thickness	TBD cm
position	from inside pipe
speed:	
welding	TBD cm/s
cutting	TBD cm/s
inspection	TBD cm/s

be capable of joining, cutting, and leak testing the breeder and cooling manifolds of the test blanket article.

IV. Others TBD

1.2.9.9 Other in-vessel requirements include:

- a. Gripping points must be provided on all replaceable components or assemblies capable of supporting their full weight over the full range of motion required for installation and removal.
- b. The structural supports, coolant line joints, instrumentation, and all other interfaces necessary for (dis)assembly must be compatible with the capability of the remotely operated tools.
- c. Sufficient space for the insertion and removal of tools must be assured.
- d. All liquid and gas pressure bearing joints must be capable of being leak detected by remote means.

- e. Mechanical guides should be provided to aid the transporter for final positioning and alignment and to protect adjacent components from damage due to collisions.
- f. The maximum Test Article weight to be attached to the Vacuum Vessel is TBD kg.

1.2.9.10 Transporter Requirements

- a. The size of the Test Blanket Article, the transportable support equipment shall remain within the internal transporter dimensions accounting for covers as well as α and γ protection walls on the transporter and space occupation of transporter service equipment (requirements are TBD). The maximum transported mass is < TBD kg. Afterheat removal of the test article must be assumed during the transport time from the test port to the storage room and the hot cell. Remote surveillance may be required (TBD).

1.2.10 Chemical Requirements

The Test Blanket System and its supporting subsystems, in particular breeder and cooling systems, have to be compatible with the materials with which they are in contact. The coolant chemistry shall be defined to limit corrosion, electrochemical, and neutronic effects to acceptable levels over the system lifetime. Neutron absorbers, tritium generating chemicals (e.g. LiOH) and matter with bad activation characteristics as well as toxic and reactive chemicals shall be avoided in the coolant. The presence of hydrogen isotopes, in particular tritium, in breeder and cooling circuits shall be continuously monitored. The need of double confinement of tritium carrying plumbing is TBD.

1.2.11 Seismic Requirements

The earthquake resistance of the Test Blanket System and subsystems shall be consistent with the specifications adopted for the ITER building. The Test Blanket System shall in particular contribute to the efficient confinement of radioactive material and chemicals during an earthquake so that the allowable release will not be exceeded.

1.2.12 Manufacturing Requirements

The Test Blanket article and its surroundings shall be manufactured according to the ASME code class 1 (TBD) with particular emphasis on tolerances between the Test Blanket article and the shielding blanket in the following situations:

- a. shut-down including installation, shut-down after operation, and shut-down before removal;
- b. nominal operation taking into account the pulsed conditions and irradiation effects (e.g. swelling);
- c. accidental situations which could lead to deformations.

The manufacture of the test blanket system shall be accompanied by an approved quality assurance plan and pass an acceptance test prior to shipment. (Other testing requirements see 1.2.15). These acceptance tests are TBD but shall include among others:

- pressure and flow testing of all fluid channels
- vacuum/He leak testing
- NDT certification of structural and seal welds
- certification of bonding of dissimilar melts
- certification of critical dimensions

1.2.13 Construction Requirements

Construction requirements are TBD; however, it is anticipated that specific requirements will be applied during transport, handling, storing and dismantling of the various components of the Test Blanket System.

1.2.14 Assembly Requirements

1.2.14.1 The primary wall of the Shielding Blanket shall be installed within ± 10 mm of the corresponding magnetic surface, as defined in GDRD Section 2.2.4.5 (including ripples) at operating temperature. To help protect the first wall of the Test Blanket, the Test Blanket First Wall will be recessed below the adjacent Shielding Blanket First Wall and, thus, will not have an explicit requirement for alignment to the magnetic surface.

1.2.14.2 The Test Blanket System will also have the requirement to minimise any gap to adjacent modules in order to minimise neutron streaming.

1.2.14.3 The Test Blanket System shall be installed from the horizontal test port using remote handling equipment. The structural support element for the blanket portion of the Test Blanket System shall be attached to the Vacuum Vessel Extension by bolting or welding. Provisions are to be provided to react design basis shear loads.

1.2.14.4 (delete)

1.2.14.5 All assembly techniques must be compatible with maintaining the vacuum requirements on the system. Handling, cleaning, limits on the use of potential contaminants, etc. must be in compliance with the vacuum specifications.

1.2.15 Testing Requirements

1.2.15.1 The Test Blanket System must pass both a hot and cold leak test after completion of its assembly within the vacuum vessel and prior to start of operation. This will supplement the Test Blanket System full operational test in the Hot Cell prior to installing on the ITER device.

Leak tests

a	Internal pressure	TBD MPa with helium
b	External pressure	1 Pa
c	Component temperature cold/hot	20°C / 240°C (TBD)
d	Leak rate acceptance level into plasma chamber	1×10^{-8} Pa m ³ s ⁻¹

1.2.15.2 The system must be pressure tested with operational coolant at 1.38 (TBD) times nominal operating value after welding of the shield and first wall coolant connections to their respective manifolds. Each flow circuit must be flow tested to demonstrate the required flow rate at the design pressure differential.

1.2.16 Instrumentation & Control Requirements

1.2.16.1 Instrumentation required for operation:

- (1) Monitor the system temperatures, flow rates, pressure, and stressed /deflections (to insure that they are within prescribed values).
- (2) Maintain temperature differentials between different points in the system to prescribed values (TBD) as determined by thermal stress limits
 - a. Cooling temperature sensors; number and position TBD
 - b. Flow sensors; number and position TBD
 - c. Others TBD

1.2.16.2 Instrumentation to signal acceptability to operate or need to shut down:

- a. Stresses/ deflection detectors; number and location TBD
- b. Temperature sensors; number, location TBD
- c. Flow sensors; number and position TBD
- d. Leak sensors; number and position TBD
- e. Others TBD

1.2.16.3 Other: TBD

1.2.17 Decommissioning Requirements

The Test Blanket System shall be designed to minimise the disposal rating. Since the rating criteria are site specific, the specific criteria are TBD.

1.2.18 Electrical Connections / Earthing / Insulation Requirements

The grounding requirements are TBD.

1.2.19 Material Requirements

1.2.19.1 The materials of the in-vessel components will be chosen according to the test blanket requirements, the compatibility between materials, their outgassing requirements and to the physics requirements with the objective of limiting the impurity level inside the machine.

1.2.19.2 The materials of the in-vessel components have to be consistent with the generation and maintenance of a high quality vacuum.

1.2.19.3 Materials shall be used with well characterised mechanical, structural and irradiation properties for their respective service conditions (temperature, stress, irradiation, hydrogen etc.) in order to obtain a high degree of confidence in their performance capability. The materials used in the test blanket are anticipated to be:

Structural material	martensitic steel (grade is TBD)
First wall structural material	martensitic steel (grade is TBD)
First wall protection	Beryllium
Breeder material	overstoichiometric lithiumorthosilicate, i.e. Li_4SiO_4 + 2.2 wt% SiO_2 (alternatives: Li_2ZrO_3 or Li_2TiO_3)
Multiplier material	Beryllium
Shielding	stainless steel (water cooled)
Coolant	Helium
Piping	martensitic steel (grade is TBD)

1.2.20 HVAC Requirements

Not directly applicable.

1.2.21 Lay-out Requirements

1.2.21.1 Structural and leak tightness welds shall be removed as far away as possible from high neutron flux locations.

1.2.21.2 Welds shall be isolated from gaps whenever possible. Field welds shall be protected by sufficient shielding to allow rewelding.

1.2.21.3 (deleted)

1.2.21.4 (deleted)

1.2.21.5 Special attention shall be given to gaps between modules. Radiation streaming shall be minimised by the design.

1.2.21.6 The Test Blanket system shall be sized for insertion and removal through the horizontal mid-plane test port and the transporter shall be sized to accommodate the Test Blanket System and/or ancillary equipment (TBD).

1.2.21.7 Wherever structural welding is required, the module arrangement shall include a (TBD) mm space adjacent to welds for remote welding/cutting equipment. This layout must include an unobstructed route, of this cross-sectional size, between the weld and the point of entry for the welding equipment.

1.2.21.8 Other Services. The ancillary systems for the Test Blanket article depend on a reliable supply of the following infrastructure services that ITER shall provide (details and redundancy are TBD): electrical power, data connections, secondary cooling water, He detritiation.

1.3 Safety Requirements

The safety requirements for the Test Blanket System are derived from the General Safety and Environmental Design Criteria (GSEDC), the General Design Requirements Document (GDRD) and functional safety requirements (confinement, fusion power shutdown, decay heat removal, monitoring, and control of physical and

chemical energies) which are generally necessary for ITER. All criteria and requirements build upon the fundamental safety principles stated below:

- Design, construction, operation, and decommissioning shall meet technology-independent radiological dose and radioactivity release limits for the public and site personnel based on recommendations by international bodies such as IAEA and ICRP.
- During normal operation, including maintenance and decommissioning, radiation exposure of site personnel and the public shall remain below the prescribed limits and be kept as low as reasonably achievable (ALARA).
- ITER shall make maximum use of favourable safety characteristics which are inherent to fusion. Uncertainties of plasma physics shall not have an effect on public safety.
- The defence in depth concept shall be applied to all safety activities so that multiple levels of protection are provided to prevent or minimise the consequences of accidents.
- Special attention should be given to passive safety.
- The design shall minimise the amounts of radioactive and toxic materials and the hazards associated with their handling.
- All conventional (non-nuclear) safety and environmental impacts from construction, operation, and decommissioning shall meet common industrial standards for industrial practice. This includes chemical toxins and electromagnetic hazards.

1.3.1 Safety Functions

The Test Blanket System may contain "experimental" components to which no safety function will be assigned. The Test Blanket System may, however, support the safety function "fusion power shutdown" in off-normal situations by passive or active action; however, the definition of and requirements on this type of system are not yet defined.

1.3.2 Safety Classification of Items

The Test Blanket System equipment shall be classified according to its importance to safety into four classes according to Table 4.1.2.-3 "Safety Importance Classification" in [GDRD - Safety v.5(4/21/95)] and the associated rules. The following provisional Safety Importance Classes (SIC) are suggested by the Safety Environmental and Health Division (SEHD):

Table: 1.3.2-1: Safety Importance Classification

Component	SIC	Comment
In-vessel part of the Test Blanket system	3 or 4 TBD	No design and related safety analyses are presently available

Ex-vessel part of Test Blanket System and blanket coolant loops	2	SIC-2 for confinement SIC-4 for decay heat removal
---	---	---

1.3.3 Safety Design Limits and Analysis Requirements

The safety limits shall be determined by iterating deterministic and probabilistic safety analyses with the design of the Test Blanket System. The safety analyses shall use the process adopted by the project which aims at systematic identification, modelling, and analysis of the representative event sequences. Depending on the required degree of detail, this process will be graded from qualitative analysis up to detailed simulations and calculations. Accident initiating events will be identified through Failure Modes and Effects Analysis (FMEA) and then grouped into Postulated Initiating Event (PIE) categories. The PIEs will be supplemented by the related accident source terms (tritium, activation products), determined in a conservative manner. Particularly, detailed fault analysis shall be performed where there is a potential for challenging confinement barriers.

Provisional safety design limits are as follows:

- If beryllium (Be) is used as FW armour material, short term temperatures shall stay below 800°C (TBD) to avoid Be-steam ignition scenarios.
- If carbon (CFC) is used as FW armour material, short term temperatures shall stay below 1800°C (TBD); the use of radiatively cooled (i.e. very hot) carbon tiles shall be limited as far as possible.
- If Be is used as first wall armour material, long term (decay heat driven) Be temperatures shall be limited to 500°C (TBD) to avoid excessive H₂ production.
- If CFC is used as first wall armour material, long term (decay heat driven) temperatures shall be limited to 800°C (TBD) to avoid excessive H₂ production.
- Maximum steel temperatures are TBD and depend on the final material choice. Environmental effects (e.g. DBTT or hydrogen embrittlement) shall be accounted for.
- The inventory of Be dust inside the vacuum vessel shall be limited to 100 kg (TBD). This value is provided provisionally fore ease of EDA design.
- The total mobilizable tritium inventory inside the PFCs (first wall, divertor, limiters, launchers) shall be limited to 1 kg.
- The corrosion products in the blanket cooling loops shall be limited to a total of 10 kg (TBD).

1.3.4 Safety Assessment

The safety analyses will include but are not limited to the following events:

- Plasma disturbances (such as disruptions, VDEs, power excursions) resulting in an overload of the Blanket.
- Over-pressure in the VV from water LOCAs causing steam formation and H₂ generation on hot FW armour surfaces.
- Temperature transients of the Blanket due to LOFAs in the primary heat transfer system and from in- and ex-vessel LOCAs.
- Pressure and temperature transients with related chemical reactions inside the Breeding Blanket due to water ingress by LOCAs.
- Pressure and temperature transients and related chemical reactions at the FW surface due to air ingress into the VV.
- Mechanical loads to the Blanket from magnetic accidents.

1.3.5 Specific Safety Design Requirements

1.3.5.1 The design basis for the Test Blanket System shall take into account the initiating events and potential loads due to accidents as identified by the safety analysis.

1.3.5.2 The design of the blanket module support structure shall react a large portion of the load acting on the modules thus minimising the load on the Vacuum Vessel, the first radioactivity confinement barrier.

1.3.5.3 The Test Blanket System shall not significantly contribute to the ITER radioactivity source term and the blanket parameters shall be chosen accordingly.

1.3.5.4 The design should minimise the volume of liquid spills from the Test Blanket article into the Vacuum Vessel.

1.3.5.5 The design should assure fast thermal relaxation of an overheated FW to avoid self-sustained chemical reactions between plasma facing materials and coolants/air. This requires the provision of reliable means (such as good thermal contact between FW and bulk blanket) to cool down the hot FW surface in the course of an accident (such as ex-vessel LOCA, LOFA or plasma disturbance). Otherwise the accident may cause an in-vessel LOCA with the related concerns, i.e. mobilisation/release of tritium and activation products, and chemical reactions (H₂ production). This requirement is quantified in terms of temperature limits set out in Section 1.3.3.

1.3.5.6 The design should limit the long term (several hours after shutdown) decay heat driven FW temperatures to avoid H₂ concentrations in the Vacuum Vessel which are prone to deflagration/detonation if air ingress in the Vacuum Vessel cannot be excluded. This requirement is quantified in terms of temperature limits set out in Section 1.3.3.

1.3.5.7 It is suggested to segment the Test Blanket System cooling loops so that sufficient independence is provided. This measure would serve the implementation of the single failure criterion.

1.3.5.8 Attention should be paid to potentially asymmetric temperature distributions due to these measures which should not cause thermal stress in the first wall/blanket equipment above permissible limits.

1.3.5.9 Off-normal heat removal should be as passive as possible. It is suggested to design the heat transport system to allow for removal of decay heat by natural coolant circulation. It is suggested further to increase by adequate treatment, if the vacuum requirements allow, the relative emissivity of thermal radiation between the adjacent surfaces of Test Blanket System and Vacuum Vessel to values significantly above the natural ones (such as 0.8 vs. 0.3).

1.3.5.10 (deleted)

1.3.5.11 In general, the design should strive for:

- Limitation of the inventory of radioactive dust inside the Vacuum Vessel.
- Limitation of the mobilizable tritium inventory inside the Test Blanket System.
- Limitation of the corrosion products in the Test Blanket System cooling loops.
- Limitation of the tritium concentration in the Test Blanket System coolant systems.

1.3.5.12 Monitoring shall be provided to indicate whether the above requirements are being met.

1.3.5.13 The design of decontamination, shielding, remote operation, flask transfer functions should minimise the dose to personnel in the course of maintenance and decommissioning.

1.3.5.14 Amounts and radio-toxicity of radioactive waste from operation and decommissioning of the Test Blanket System equipment should be minimised within the limits set by the applicable material. Potentially high radio-toxicity of breeder, multiplier, and braze materials should be considered in this context.

1.3.5.15 The experimental nature of the FW leads to the design requirement for the Vacuum Vessel that failures of the FW should not cause rupture of the vessel which is the first radioactivity confinement barrier.

1.4 R&D Requirements

The R&D requirements for the Test Blanket development are concept dependent except for the development and the complete characterisation of a suitable structural steel with martensitic steel being the currently preferred material. The associated R&D is regularly revised to adjust priorities and effort, and to account for the latest technical progress in the different fields of R&D. This program is closely linked to the development of a blanket for a demonstration (DEMO) reactor for which the Test Blanket article should be a representative module.

1.5 Operation and Maintenance

The operational and maintenance requirements for the Test Blanket System are included in Section 1.2.1 and 1.2.9.

1.6 Surveillance and In-Service Inspection

The surveillance and in-service inspection requirements are included in Section 1.2.9.

1.7 Quality Assurance

The quality assurance requirements are included in Section 1.2.1., 1.2.12 and 1.2.15.

1.8 System Configuration & Essential Features

The configuration and essential features are included in Section 1.2.21.

1.9 Interfacing Systems

In order to successfully complete all test objectives, the Test Blanket System must work in co-operation with many of the other ITER systems and facilities. These interrelationships are many and complex, involving both geometric and functional requirements. Below is a list of the systems that have a significant impact on the operational capability of the Test Blanket System. A brief description of the geometric and functional requirements is given for each interfacing system.

Vacuum Vessel

The Vacuum Vessel System is to provide twenty horizontal ports for systems to access the plasma chamber. Specifically, this involves ports or access chambers of a particular size and structural capability to properly accommodate the port systems, including ancillary equipment, and the associated remote handling equipment.

The unique requirements imposed by the Test Blanket System will involve the mounting configuration onto the Vacuum Vessel Wall, the structural requirements during operation and maintenance periods, the thermal conditions of the shield and ancillary equipment, and accommodations for routing of plumbing lines. The main interface requirements are as follows:

- number of test ports required
- Horizontal port size/geometry
- Load support requirements
- Thermal requirements
- Coolant plumbing requirements
 - size/location
 - mechanical loads and displacements
 - special seal requirements
 - penetration requirements

Shielding Blanket

The Test Blanket System will work in close co-operation with this system.

There must be a high level of geometric synergism between these two systems to meet the ITER requirements for the neutronic streaming and not have contact load transfer between system modules.

In order to provide limited protection from direct plasma ion impingement on the Test Blanket First Wall, the Test Blanket will be recessed behind the general contour of

the surrounding Shielding Blanket First Wall. This will impose additional surface heating requirements on the adjacent Shielding Blanket First Wall components. The temperatures and surface conditions (emissivity, absorptivity, and surface area) of the interfacing surfaces will have to be determined to estimate the anticipated heat transfer. The main interface requirements are:

- geometry
- mechanical loads
- physical loads
- thermal loads

Remote Handling Equipment

Remote handling equipment will be required to install, inspect, and maintain diagnostic, plasma heating, maintenance, test blanket modules, and shield port systems through the horizontal access port. The specific interface requirements for the Test Blanket System will involve unique geometry, weight, positioning, and thermal constraints. The geometry will involve not only the Test Blanket, which may be separated into two elements, but will also include the ancillary equipment that will be positioned behind the blanket in the Vacuum Vessel Extension area. Special-use end effectors will be the responsibility of the Test Blanket System. Some of the interface requirements are listed below:

- maximum supported weight
- positioning accuracy
- kinematics requirements
- inspection requirements
- accommodation of special end effectors
- accommodation of special materials and coolants

Cryostat

The Cryostat System is to provide twenty horizontal ports for access to the Vacuum Chamber. Additionally, the Cryostat is to provide the Second Tokamak Confinement Boundary.

The unique requirements imposed by the Test Blanket System will involve the unique geometry constraints and special maintenance requirements. Plumbing lines shall be accommodated in the port areas. Main requirements are:

- number of test ports required
- horizontal port size/geometry
- thermal requirements
- coolant plumbing requirements with respect to:
 - size/location
 - mechanical loads and displacements
 - special seal requirements
 - penetration requirements

Primary Heat Transport System

This system is to provide water coolant to remove the heat generated in the test blanket and shield. Detailed information needed;

- Number of loops
- Inlet and outlet temperature for each loop

- Flow rate for each loop

Vacuum Pumping System

The blanket system is partially contained within the primary boundary and effects the volume pumped by the Vacuum Pumping System. As a result, emissions from surfaces and leaks from the blanket system must be within the capability of the pumping system. In addition, the vacuum pumping may include specific components, such as tracer gas sources, for remote leak checking. These components must be permanently mounted on the blanket components near high potential leak sources. Important interface requirements are:

- outgassing requirement
- leakage rate

Tritium Plant

The use of unique materials will effect the Tritium Plant System involving the possible airborne elements.

Tokamak Operations and Control

The Test Blanket System instrumentation needs shall be integrated into the Tokamak Operations and Control System.

Building

The building space external to the cryostat and biological shield shall accommodate the Test Blanket System maintenance scheme. Space and support services (power, cooling water, He, ventilation etc.) shall be provided for operational support equipment near the horizontal test ports. Radial space must be provided to remove the modules from the mid-plane maintenance ports and transport them to the hot cells. Main interface requirements are related to:

- location and size of needed space
- support services (electrical, I&C, fluids)

Waste Treatment and Storage

The Test Blanket System will impose some additional requirements on the Waste Treatment and Storage system. This will evolve from the use of unique materials (see section 1.2.19) and coolants.

General Testing Equipment

The Test Blanket System will impose some additional requirements on the General Testing Equipment system. This will evolve from the use of unique materials (see section 1.2.19) and coolants.

Hot Cells

The Test Blanket System should be designed in such a way that the following operations can be performed in the hot cells:

1. to separate the components of the Test Blanket Subsystem:
 - remove the Test Blanket Subsystem from its location in the Transporter;
 - cut the tubes at designed planes;
 - unfasten the bolts between the Shield and the Support Frame (if necessary);

- unfasten the bolts of the mechanical connection between the TBM and the Frame.
2. to perform the following operations on the component at the end of the irradiation time foreseen for the HCPB TBM:
- cut the TBM and remove the beryllium and orthosilicate pebble from the beds for investigation:
 - tritium release test
 - mechanical investigation
 - crush test
 - thermal cycling test
 - cut probes of the structure for investigations.
 - tritium release test
 - swelling test
 - embrittlement test
 - tritium inventory determination
1. to perform the following repairs:
- weld small leakages in the components;
 - replace tubes;
 - replace damaged instrumentation.

1.10 Codes and Standards

The Test Blanket System shall be designed according to the project ITER Structural Design Criteria, (ISDC). Using the rules specified in the ISDC, stresses and other applicable quantities shall be calculated for different load calculations in nominal and accidental situations. Details are TBD

1.11 Reliability Requirements

Reliability requirements are included in Section 1.2.1.

1.12 Other Special Requirements

TBD

2 Design Description

2.0 Summary Description

2.0.1 General

The European fusion program proposes two DEMO relevant blanket concepts for testing in ITER. One is the Water Cooled Lithium Lead (WCLL) blanket, the other the Helium Cooled Pebble Bed (HCPB) blanket. Both use martensitic steel as structural material. The present version of the EU DDD gives a description of the HCPB Test Blanket Module (TBM) and of the related supporting subsystems.

The testing foreseen for Demo blanket includes the demonstration of a breeding capability that would lead to tritium self-sufficiency in a reactor and the extraction of high-grade heat suitable for electricity generation. To accomplish these goals, the ITER horizontal ports will be used to provide a relevant fusion plasma and the appropriate nuclear environment.

The purpose of the tests is to validate the design principles and the operational feasibility for the demonstration blanket system. This test blanket system includes all the basic support functions for the tritium breeding blanket. The supporting subsystems are:

1. Test Blanket Subsystem (first wall, breeding blanket, shield, and structure);
2. Tritium Extraction Subsystem (tritium removal, handling and processing);
3. Helium Cooling Subsystem (heat transfer, heat transport);
4. Coolant Purification Subsystem (helium purification and conditioning);
5. Test Blanket Remote Handling Subsystem (remote handling as related to the test blanket systems).

In addition, the basic properties and operating characteristics of the systems' materials will be validated. To assess those qualities and characteristics, the test blanket systems are to be exposed directly to the ITER plasma for relatively long, continuous operation periods. These test blanket modules will replace shielding blanket modules; thus they must meet all applicable ITER shielding blanket requirements, including heat removal, shielding protection for the vacuum vessel welds and toroidal field magnets, and reduction of neutron streaming.

Breeding and recovery of tritium are important goals of the test program. Lithium ceramic compounds will be used as the breeder materials to be investigated. Subsystems to recover the bred tritium will be demonstrated along with test facilities to separate and remove the tritium from the coolant or purge streams. Special designs and tritium handling facilities will be required to meet the ITER safety goals and requirements.

Generation and extraction of high temperature helium will demonstrate the suitability of fusion for commercial power generation. The high temperature helium will transfer the rejected heat to the ITER facility water coolant system.

The Test Blanket modules will be designed to: (1) conform to the same safety requirements as other in-vessel components, (2) be robust against the thermal and mechanical loads produced on them by disruption, and (3) have a minimum impact on reactor operation and availability due to any unscheduled test module removal.

The Test Blanket systems are to be installed and maintained through the horizontal test ports. Standard ITER remote handling equipment and procedures will be used to the maximum extent. All Test Blanket systems' plumbing and instrumentation and control shall be contained within the vacuum chamber horizontal port extensions and shall pass through the horizontal port or shielding doors. Maintenance rails and other remote handling equipment are to be provided for use within the horizontal ports. Space shall be provided in the region immediately outside the biological shield, near the ports, for tritium handling equipment while the Test Blankets systems are in place and for storage of test equipment during maintenance actions. Transport from the horizontal ports to the hot cells is to be provided as well as facilities in the hot cells for storage, maintenance, testing, refurbishing, and dismantling the test modules. The installed Test Blanket Subsystem is to be a complete assembly which can be fully tested prior to the installation. This will facilitate the installation and removal process and increase the reliability of the installation and check out procedure.

The European and the Japanese have collaborated in their approach for testing their helium cooled solid breeder test modules. During the ITER Basic Performance Phase (BPP) the European Test Blanket Module (TBM) shall occupy half of the test port allocated to the helium cooled blankets, the other half being occupied by the Japanese helium cooled ceramic breeder blanket module. The tritium systems (extraction and purification) for the two TBMs will be separate and placed in the Tritium Building. The helium coolant loops (heat transfer and heat transport) will also be separated and will be placed in the pit immediately adjacent to the test port.

Parts of the BPP tests, in particular those related to tritium control and fluid dynamics (helium flow distribution, pressure drop), may be conducted before the first plasma ignition.

To facilitate handling operations the two TBMs are mounted from the vacuum vessel extension. They are contained in a water cooled frame to assure neutron shielding. The frame will be supplied with water at approximately 4 MPa and 140 °C with a maximum temperature rise of 50 °C under the maximum quasi steady state heat flux. It will be made of the same materials as the main blanket/shield structure.

During the Extended Performance Phase the HCPB test module may occupy the whole or half of one port according to the numbers of blanket concepts to be tested and to the number of ports available for the blanket module testing.

2.0.2 Test Blanket Subsystem

The Test Blanket subsystem contains the DEMO Blanket test module (TBM) to be validated. In addition, it also must perform all the functions of the basic ITER shielding blanket. Thus both of these main functions must be achieved.

The Test Blanket subsystem must perform the following functions:

- Breed tritium to demonstrate the technical objectives of the DEMO test program.
- Produce high-grade heat that is removed with a suitable coolant medium to demonstrate the technical objectives of the DEMO test program.
- Remove the surface heat flux and the nuclear heating within the allowable temperature and stress limits.
- Reduce the nuclear responses in the vacuum vessel structural material for the ITER fluence goal.
- Protect the superconducting coils, in combination with the vacuum vessel, from excessive nuclear heating and radiation damage.
- Contribute to the passive stabilisation of the plasma.
- Contribute to the reduction of neutral density between the divertor and the main plasma chamber by $\sim 10^4$.
- Provide a maximum degree of mechanical and structural self-support to: (1) minimise the loads transmitted to the back plate, and (2) allow different operating temperature ranges in the test blanket system and the surrounding ITER components (shield blanket, back plate, vacuum vessel).

Most of the functional requirements listed above assure that the test blanket modules perform the functions equally as well as the basic shielding blanket - remove the surface heat, thermalize the neutrons, protect the magnets and vacuum vessel, assure minimal leakage of coolant, and react the electromagnetic loads. The first two requirements of tritium production and power production address the new requirements to verify the DEMO Blanket materials and design approaches.

The Helium Cooled Pebble Bed (HCPB) blanket has been developed within the European Program as a DEMO relevant blanket. Forschungszentrum Karlsruhe (FZK), Commissariat à l'Énergie Atomique (CEA), ENEA (Ente per le Nuove Tecnologie, l'Energia e l'Ambiente), together with ECN Petten and SCK-CEN Mol are collaborating for the further development of the HCPB DEMO blanket and design and construction of the HCPB Test Blanket Modules (TBM).

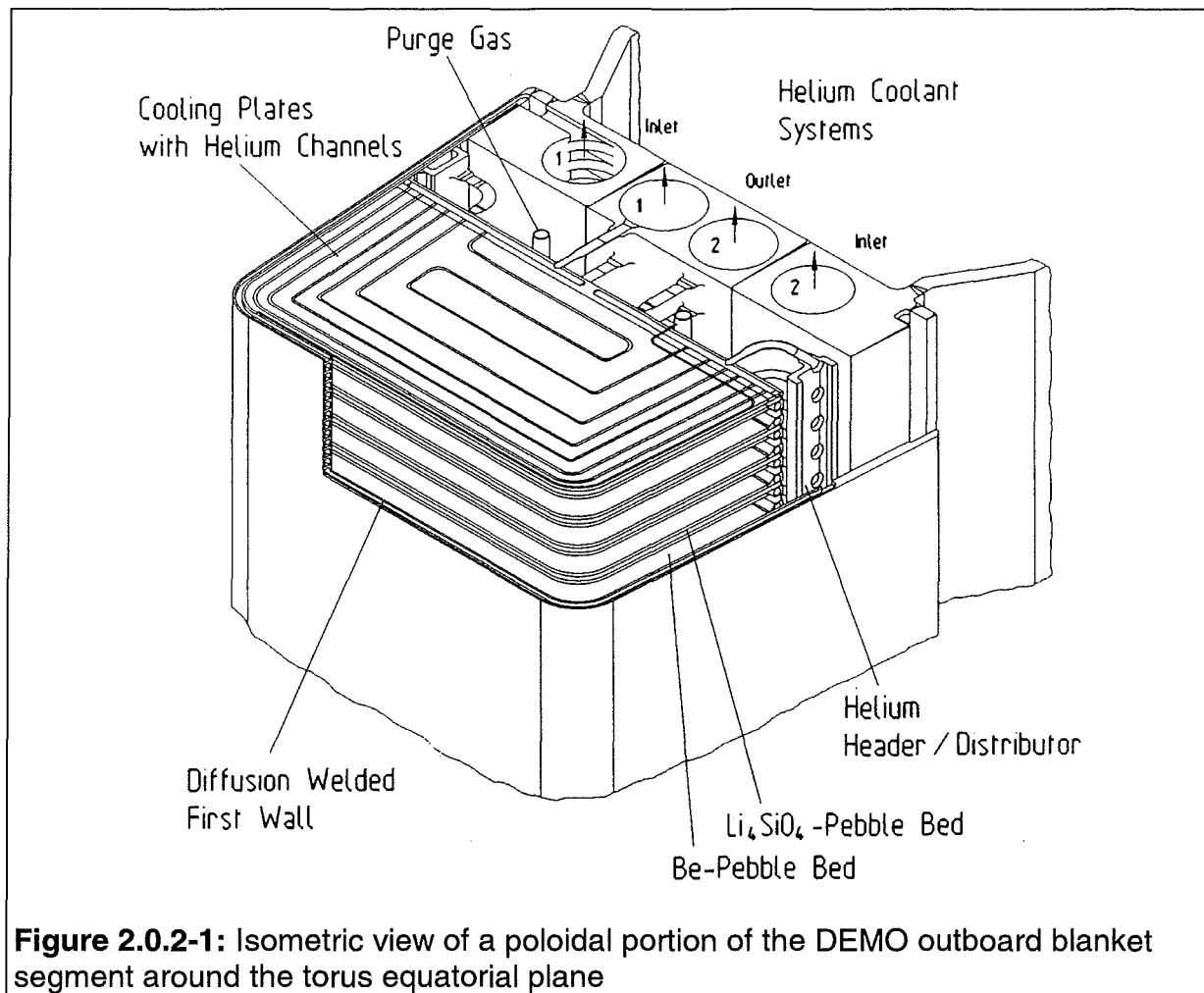


Figure 2.0.2-1: Isometric view of a poloidal portion of the DEMO outboard blanket segment around the torus equatorial plane

Fig. 2.0.2-1 shows an isometric view of the poloidal portion of the DEMO HCPB outboard blanket segment around the torus equatorial plane, where the highest power deposition, highest stresses and temperatures are expected. This portion of the HCPB blanket shall be tested in ITER. The HCPB DEMO blanket exhibits the following basic design features:

1. The ceramic breeder and the neutron multiplier are contained in form of pebbles in a tightly closed box called blanket box.
2. The plasma facing wall of the blanket box is the first wall (FW). The back side of the blanket box is formed by a plate which contains the poloidal helium feeding and collecting manifolds.
3. The blanket box and the blanket structure are cooled by helium at 8 MPa. The coolant flows in series through the blanket box and the blanket structure.
4. The blanket structure consists of 8 mm thick cooling plates placed in toroidal-radial planes. The plates are welded to the front and side wall of the blanket box.
5. Alternatively between the plates there are alternating slits of 9 mm thickness filled by a bed of the breeder pebbles (reference: $\text{Li}_4\text{SiO}_4 + 2.2 \text{ wt\% SiO}_2$ of 0.25 to 0.63 mm diameter), and of 45 mm thickness filled by a binary bed of 1.5 to 2.3

mm and 0.1 to 0.2 mm beryllium pebbles. Alternative breeder materials are Li_2ZrO_3 or Li_2TiO_3 .

6. A separate purge gas system at 0.1 MPa carries away the tritium generated in breeding material and in beryllium.
7. For safety reasons, the coolant flow is divided into two completely independent coolant systems, which feed in series the FW cooling channels and then the coolant plates in alternating flow directions.

More information on the HCPB DEMO design can be found in [2.0.2-1].

The requirement to be able to conduct blanket module testing in ITER while not adversely impacting the availability puts constraints on the design approach to the system configuration and the attendant remote handling equipment and procedures. The general approach employed in the Test Blanket system is to fully test the largest system that can be handled and installed in the horizontal ports. Figure 2.0.2-2 presents the overall scheme for the Test Blanket System installation. The ITER Vacuum Vessel Port Extension is responsible for supporting the static and the dynamic loads generated by any module located within the horizontal port. These loads will be transmitted through a mounting system, which uses guide keys.

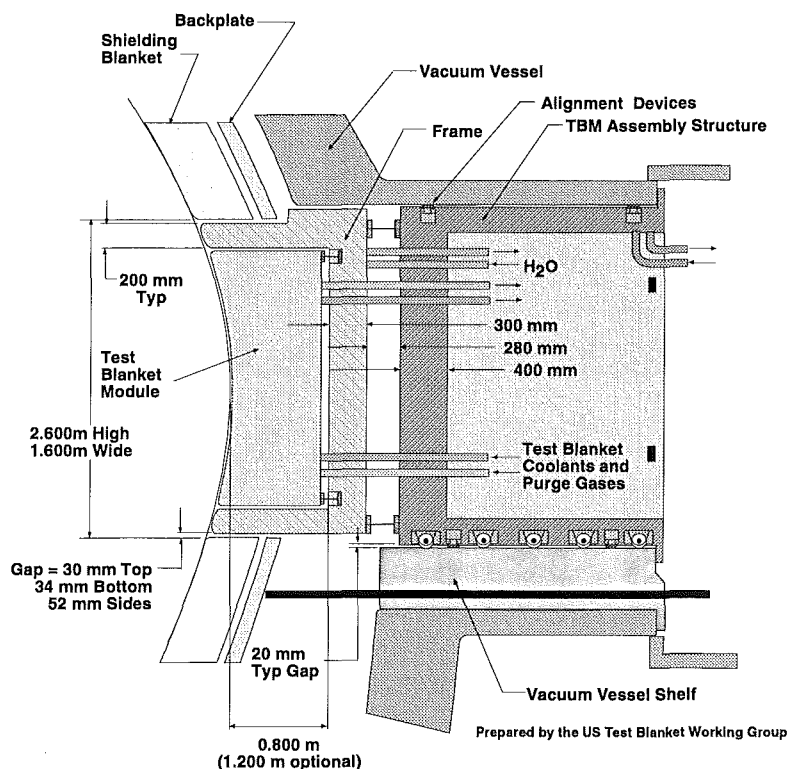


Figure 2.0.2-2: Schematic of Test Blanket Subsystem Elements in Horizontal Port
[Ref. 2.0.2-2]

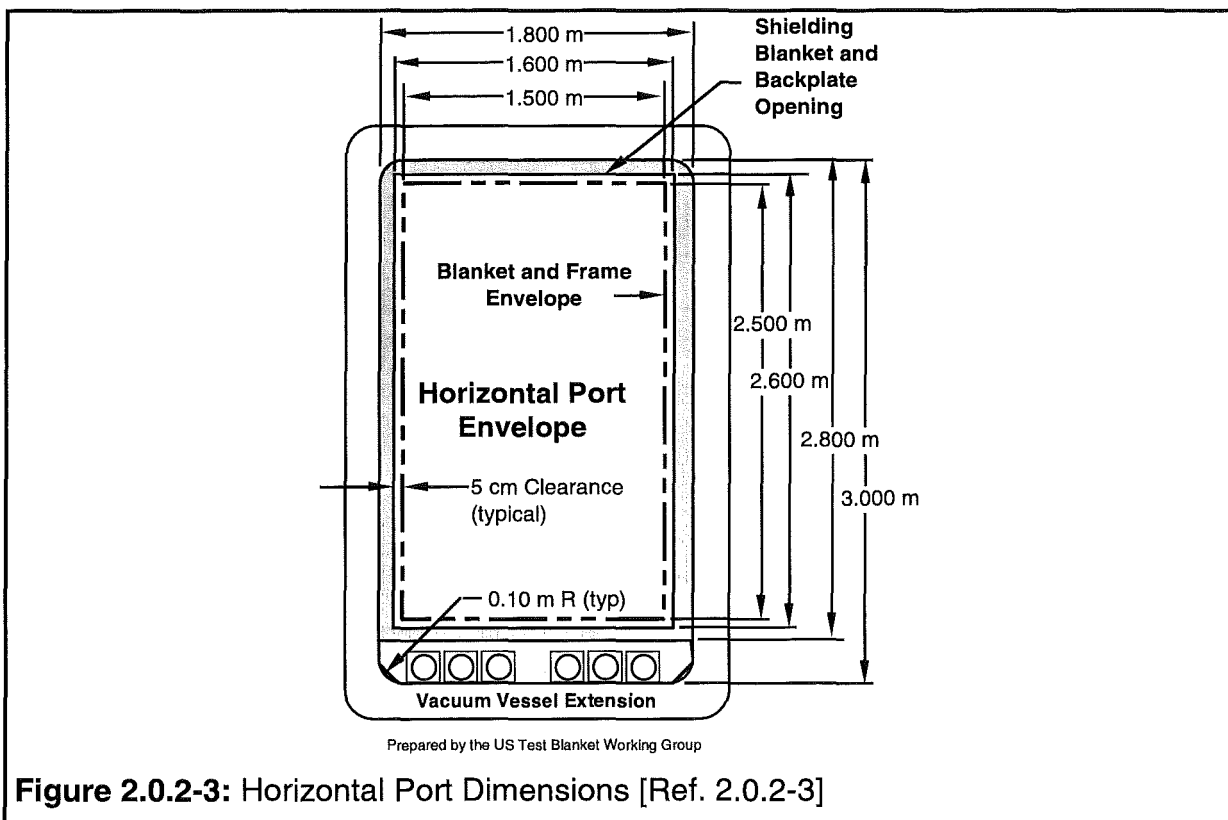
Advantages of this system are:

1. Remote handling operations inside the Vacuum Vessel (V.V.) Port Extension are eliminated.
2. Pipe penetration through V.V. Plug can be seal welded; no bellows are needed.
3. The single assembly which includes test modules, shielding and V.V. plug, can be pre-assembled and fully tested prior to installation into the port.

The current design uses straight pipes running through the cryostat closure plate and the bio-shield plug.

The Test Blanket Modules are contained in a water cooled frame to assure thermal insulation and neutron shielding. Shielding will be provided behind the test blankets to assure the shielding requirements for the vacuum vessel and the magnets are satisfied.

The physical size of the test blanket is determined by the constraints of the ITER horizontal port. The governing dimensions for the vacuum vessel port and the back plate opening are given in the GDRD, Section 5.3.3.5.2 and are shown in Figure 2.0.2-3.



Provisions for cooling pipes on the floor reduce the available height by 20 cm within the vacuum vessel extension region (1.800 m x 2.800 m). Allowing some space for a transport mechanism, alignment features, and load transfer components yields an opening size for the back plate and shielding blanket of 1.600 m x 2.600 m. Within the vacuum vessel extension, the shielding should fill the envelope as much as possible. The radial depth of the blanket is determined by the blanket design

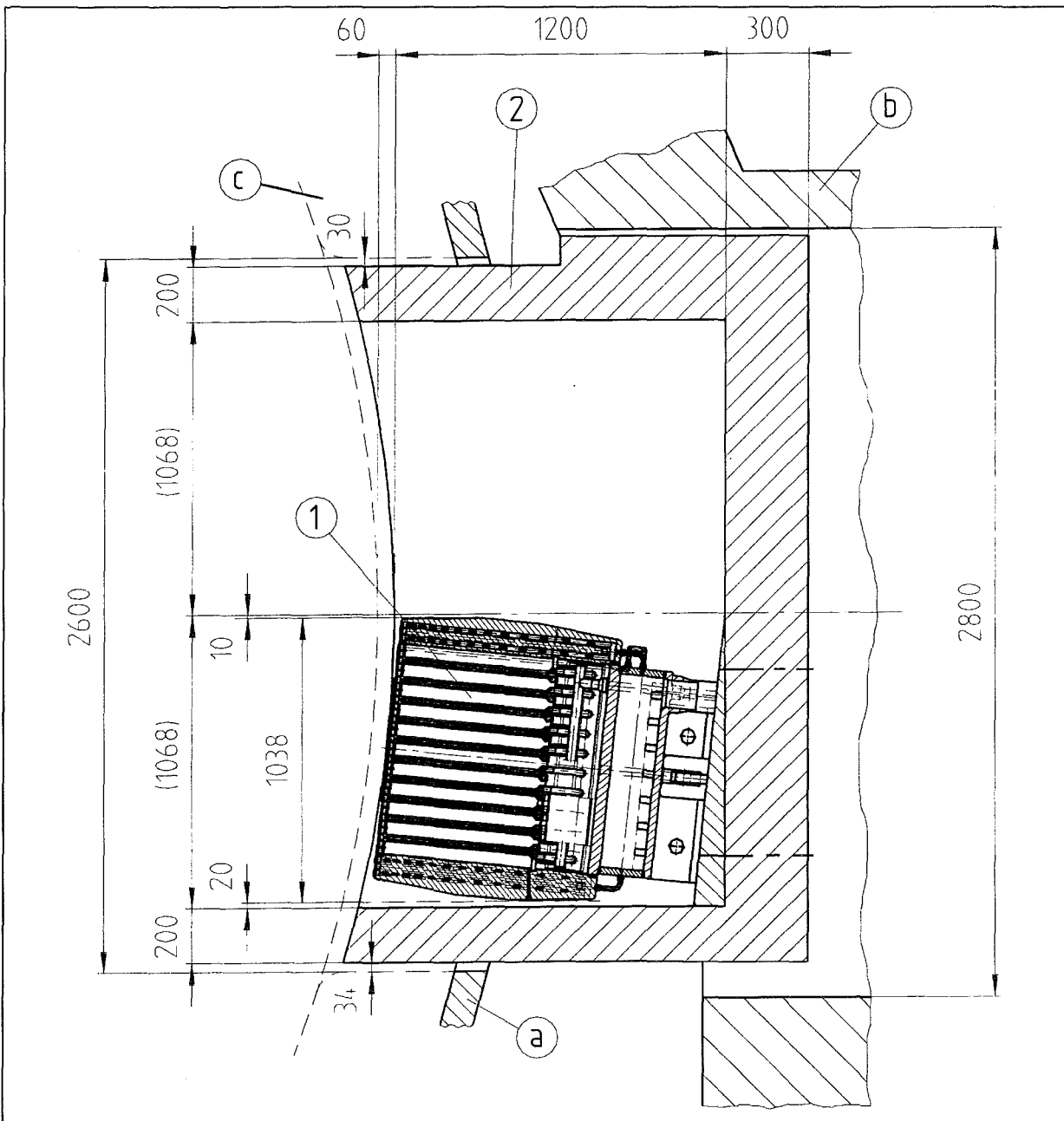
parameters. The first wall surface of the blanket (and frame) may be recessed from the adjacent ITER shielding blanket or limiter modules.

In the Basic Performance Phase the European and Japanese helium cooled Test Blanket Modules shall occupy the same test port. Fig. 2.0.2-4 shows a vertical cross section of the ITER horizontal port with the European HCPB-TBM which occupies its lower half, the upper part being reserved for the Japanese helium cooled TBM.

The HCPB-TBM represents a poloidal portion of the HCPB DEMO blanket. As in DEMO the radial toroidal cooling plates and the first wall are cooled by helium at 8 MPa flowing first in the first wall and then in the cooling plates. For safety reasons the coolant helium flows in two completely separated loops. In the first wall as well as in the adjacent cooling plates the helium is flowing alternating in opposite directions. In this way the TBM temperatures are more uniform. In the reference Test Blanket Module (TBM-I) there are between the cooling plates alternating 9 mm thick ceramic breeder pebble layers and 47 mm thick beryllium pebble layers. The tritium purging gas is helium at about 0.1 MPa flowing in radial direction from the first wall to the back of the module. The plasma side of the first wall is protected by a 5 mm beryllium layer and it recessed from the shield blanket counter by a minimum amount of 60 mm. To improve the alignment with the ITER FW the module is inclined by about 7 degree. At the upper and lower ends the HCPB-TBM is closed by caps capable to sustain a pressure of 2.5 MPa. During normal operation the space in the TBM is at the purge gas pressure of 0.1 MPa. However, in case of a leak from a cooling plate, it could be pressurized up to 2.5 MPa. In such a case a pressure relief system assures that the design pressure of the box of 2.5 MPa will not be exceeded.

The maximum temperature of the structural material and of the ceramic pebble bed for the reference TBM amount to 500 °C and 581 °C, respectively. Power excursions to 120 % of nominal with a duration of 10 s lead to a temperature increase of 20 K in the FW structure. All calculated stresses are below the admissible limits according to RCC-MR. The thermal time constant of the TBM (with the exception of the poloidal headers at the back side of the module) is much less than the scheduled ITER burn time; i.e. steady-state conditions are prevailing in the TBM during most of the burn time.

The second version of the test module with a modified flow scheme in the FW and an increased thickness of the ceramic pebble bed (TBM-II) allows a significant increase of the helium outlet temperature and of the maximum ceramic bed temperature at about the same FW temperature. TBM-II will be tested in ITER after the TBM-I during BPP. Calculations have also been performed for a third HCPB test module (TBM-III) to be tested during the EPP. These calculations have been performed to size the ancillary loops for the HCPB-TBM, so that the same ancillary loops could be used during the EPP period as well.



- 1. Blanket Test Module
- 2. Frame
- a. Back Plate
- b. Vacuum Vessel
- c. Shield Blanket

Figure 2.0.2-4: Vertical cross section of the support frame with the European HCPB-TBM

Water cooled Frame and Shield

The Frame is made of the same structural material as the shielding blanket and maintained by the cooling water at about the same temperature as the vacuum vessel extension at their contact surfaces. Also the Shield will be cooled by water and maintained at the same temperature as the frame at its contact surfaces.

Supply Pipes

A set of two supply and two return pipes will provide the HCPB blanket test module with high pressure helium coolant. A set of one supply and one return pipe will provide the 0.1 MPa helium for the purging of the tritium produced in the TBM.

A simple set of water pipes will be used to cool the Frame and the Shield. The diagnostic conduit with Instrumentation and Control System leads will penetrate the TBM Back Plate and VV Plug.

Reliability

The reliability of the TBM including the supply pipes inside the vacuum vessel (VV) has been analysed using usual basic failure rates of the components like welds, pipes, and bends. An overall failure rate of less than 0.01 1/a has been obtained which yields with a TBM replacement time of 8 weeks an availability of more than 99.9 %. The reliability is dominantly determined by leaks of the pipes inside the VV. The TBM itself is very fault-tolerant; this is a consequence of the design concept which allows single failures of most internal welds without affecting the operability of the TBM and of ITER. Radiation effects have not yet been taken into account.

References

- [2.0.2-1] M. Dalle Donne et al., "European DEMO BOT Solid Breeder Blanket", KfK 5429, Nov. 1994
- [2.0.2-2] L. Waganer, e-mail of 19.11.1997 to R. Parker
- [2.0.2-3] L. Waganer, Test Port Design Revision by TBWG-5 Agreements, 28 Oct. 1997

2.0.3 Tritium Extraction Subsystem

Tritium is produced in the Test Blanket Module (TBM) by nuclear reactions of the neutrons emitted from the plasma vessel with the lithium atoms (Li^6) contained in the breeder material. The tritium extraction is achieved with the help of a helium purge gas containing up to 0.1 % H_2 ; the addition of hydrogen is needed to facilitate the tritium release by isotopic exchange.

The tasks of the Tritium Extraction Subsystem are:

- Removal of tritium produced in the Test Blanket Module,
- Separation and intermediate storage of the two main chemical forms of tritium, i.e. HTO and HT,
- Purification and conditioning of the purge gas.

It is a main aspect of the design that the system can be operated for one campaign of the reactor (max. 6 days) without intermediate unloading or regeneration of single components. In addition, no valve switching actions, temperature cycling or tritium transfer operations will be needed within this time span.

Principle of Operation (Fig. 2.0.3-1):

The helium purge gas stream containing 0.1% H_2 is sent through the breeder and beryllium pebble beds to extract the accumulated tritium (mainly by isotopic exchange).

Removal of tritium and excess hydrogen from the helium carrier gas is accomplished in two steps:

- tritiated water (HTO and HO) is frozen out in a cold trap operated at -100°C ,
- molecular hydrogen isotopes (HT, H_2) and gaseous impurities are adsorbed on a molecular sieve bed operated at -196°C .

The clean helium is then sent through a make-up unit where hydrogen is again added to provide a He : H_2 swamping ratio of 1000.

At the end of an experimental cycle, the tritiated water collected in the cold trap is transferred to the Water Detritiation System (WDS) which is part of the installations for the primary fuel cycle ^{a)}. Desorption of the molecular hydrogen isotopes from the molecular sieve bed is carried out in a secondary helium loop containing a circulation pump and a Pd/Ag diffuser. The pure hydrogen isotopes obtained at the secondary side of the diffuser are stored in uranium getter beds and, later on, transferred to the Isotope Separation System (ISS).

The Tritium Extraction Subsystem is located in the Tritium Building.

^{a)} see J.E. Koonce, O. K. Kveton: Design Description Document (DDD) - Tritium Plant 3.2, Chapter 3.2E and Appendix to this report, Chapter 3.2WE

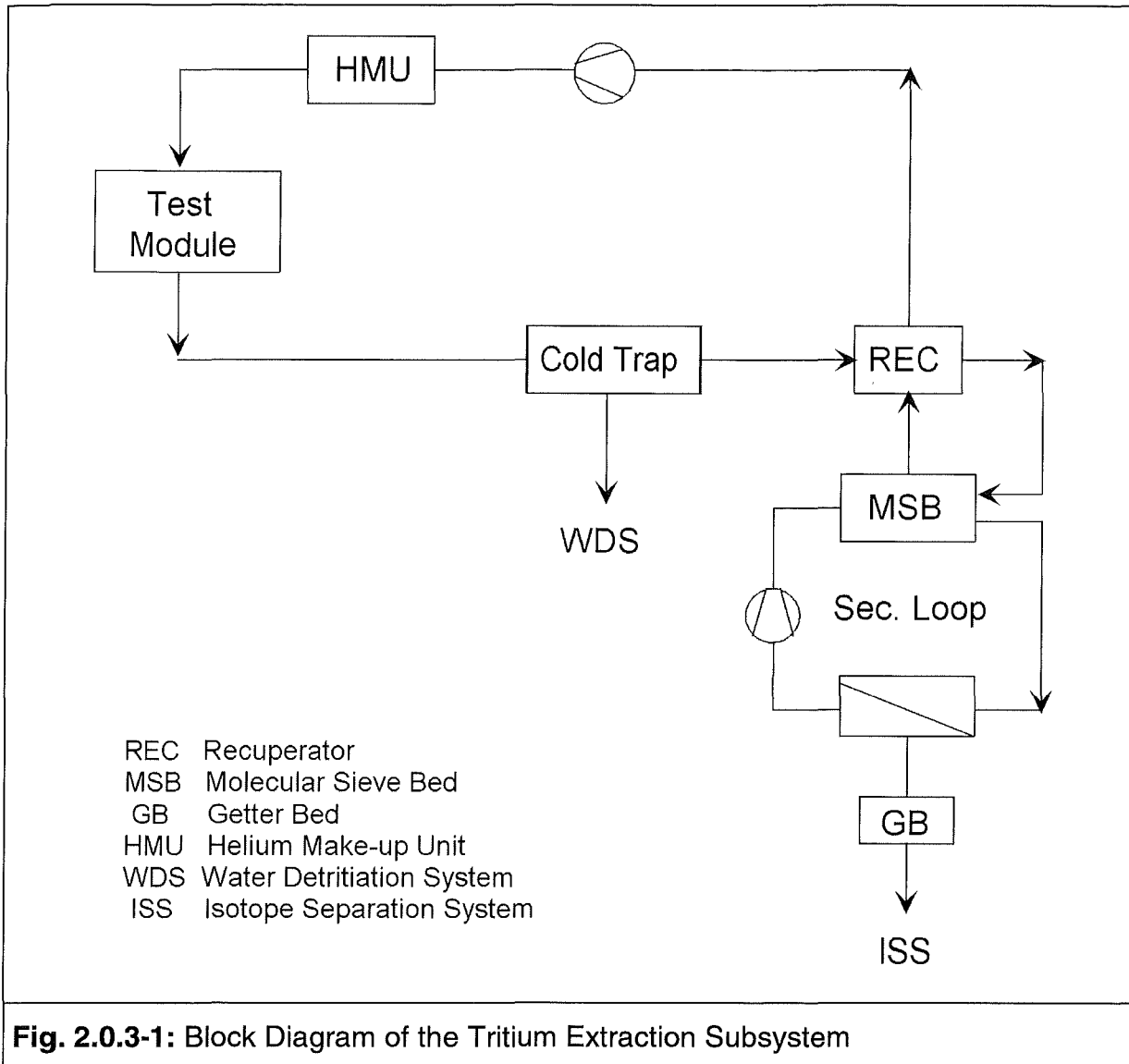


Fig. 2.0.3-1: Block Diagram of the Tritium Extraction Subsystem

2.0.4 Helium Cooling Subsystem

The cooling subsystem is designed for the European helium-cooled pebble bed (HCPB) test module to be installed in the bottom half of an equatorial test port in ITER, presumably port No. 01. It includes the primary helium heat transport loops with all components, and the pressure control unit. The secondary water loop subsystem with the ultimate heat sink is part of the ITER cooling system providing water flow at low temperature. A further interface to the cooling subsystem are the connections to the helium purification subsystem, taking a bypass flow of 0.1% of the main mass flow rate. Two separate primary heat transport loops of 2 x 50% heat capacity are foreseen for redundancy purposes during decay heat removal in accordance with the DEMO blanket design. The cooling subsystem will be housed in the wedge-shaped pit outside of the cryostat at the same level as the test module. A schematic flow diagram is shown in Figure 2.0.4-1.

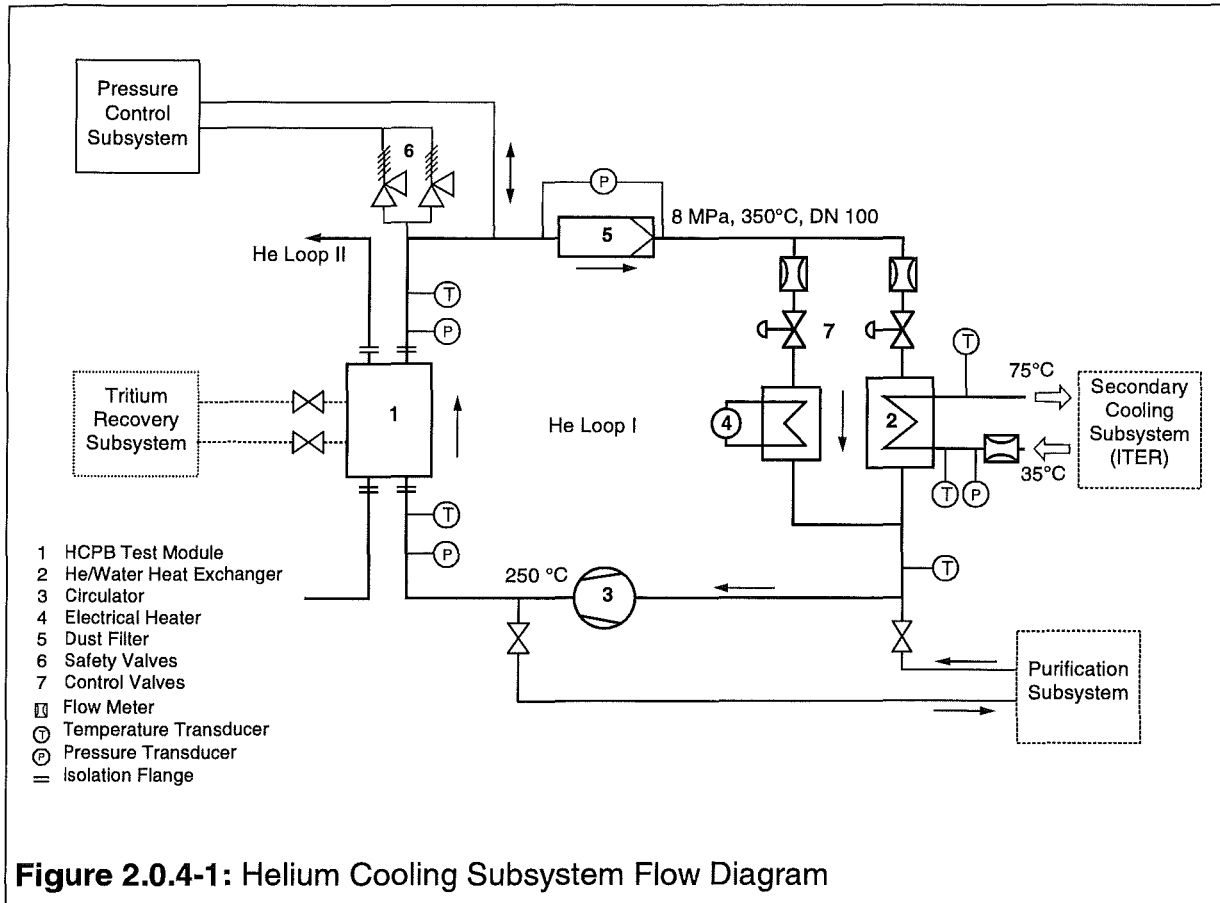
The thermal-hydraulic design parameters are as follows: The maximum heat to be removed from the test module amounts to 2.3 MW. Nominal primary helium coolant conditions are 250°C and 350°C (later on 250 and 450°C) at module inlet and outlet, respectively, and 8 MPa of pressure. The total flow rate in both primary helium loops is 3.7 kg/s. The secondary cooling water provided by ITER has a temperature of 35/75°C at the heat exchanger inlet/outlet, a pressure of 0.5 to 1.0 MPa, and a maximum mass flow rate of 13.8 kg/s.

Main components in each loop are the heat exchanger, circulator, electrical heater, dust filter, and pipework. The total helium mass inventory in one loop amounts to 6.9 kg, and the overall pressure loss is about 0.36 MPa, half of which occurring in the test module proper. The heat exchanger is assumed to be a straight tube bundle heat exchanger, or alternatively consisting of U-tubes, with high pressure helium flowing inside the tubes. The design specification for the circulator is as follows: temperature 300°C, pressure 9.6 MPa, mass flow rate 1.9 kg/s at a pumping head of 0.36 MPa at 80% of maximum speed and at 250°C inlet temperature, speed variation max/min of at least 4. The electrical heater with a power of 100 kW which is installed in a bypass to the heat exchanger is needed for baking the test module first wall at 240°C and for heating the whole cooling subsystem. A filter unit is installed in the hot leg of the main loop, accumulating residual dust and particles from fabrication, and erosion particles down to a size of typically 10^{-6} m. For the main pipework an outer diameter of 101.6 mm and a wall thickness of 6.3 mm have been chosen. This results in a flow velocities of between 40 and 50 m/s. The number of valves in the main loops has been kept at a minimum to avoid inadvertent closure which would mean loss of heat sink. All of the piping and components in the primary cooling subsystem will be constructed of austenitic stainless steel.

The pressure control unit is needed for evacuation, helium supply, pressure control, and overpressure protection. The components are conventional and of relatively small size, except for the storage and dump tanks.

Activation of cooling subsystem components is expected to be generally low allowing controlled personnel access. Remote handling is envisaged for connection and disconnection of the TBM by the aid of the transporter, and for replacement of the dust filter insert. All components of the cooling subsystem such as heat exchangers,

circulators, electrical heaters, dust filters, tanks, and valves will be pre-assembled at the factory and delivered to the site as functional units. High quality assurance standards are applied to all assembly procedures. The large components of the cooling subsystem installed in the pit require lifting equipment with a load capacity of about 2 tons.



The following preliminary subsystem control scheme is proposed for pulsed operation: The principal objective is to keep the test module inlet temperature at 250°C. The secondary cooling water inlet temperature is kept at 35°C, the circulator is operated at rated speed, the electrical heaters are turned off, and flow partition through the HX and heater bypass is controlled as to maintain the inlet temperature close to 250°C. During longer shutdown periods decay heat removal is achieved at reduced circulator speed, or by natural convection.

2.0.5 Coolant Purification Subsystem

Two coolant purification systems are provided, one for each of the two main cooling systems (Fig. 2.03-1). They are designed to purify 0.1% of the helium coolant stream. The specific tasks of a purification system are:

- to extract hydrogen isotopes as well as solid, liquid or gaseous impurities from the main coolant system; of particular importance is the extraction of tritium, permeating into the coolant from the breeder zone and from the first wall.
- to remove condensed water that may be entrained in the cooling gas due to leakages or failures of the heat exchanger tubes.

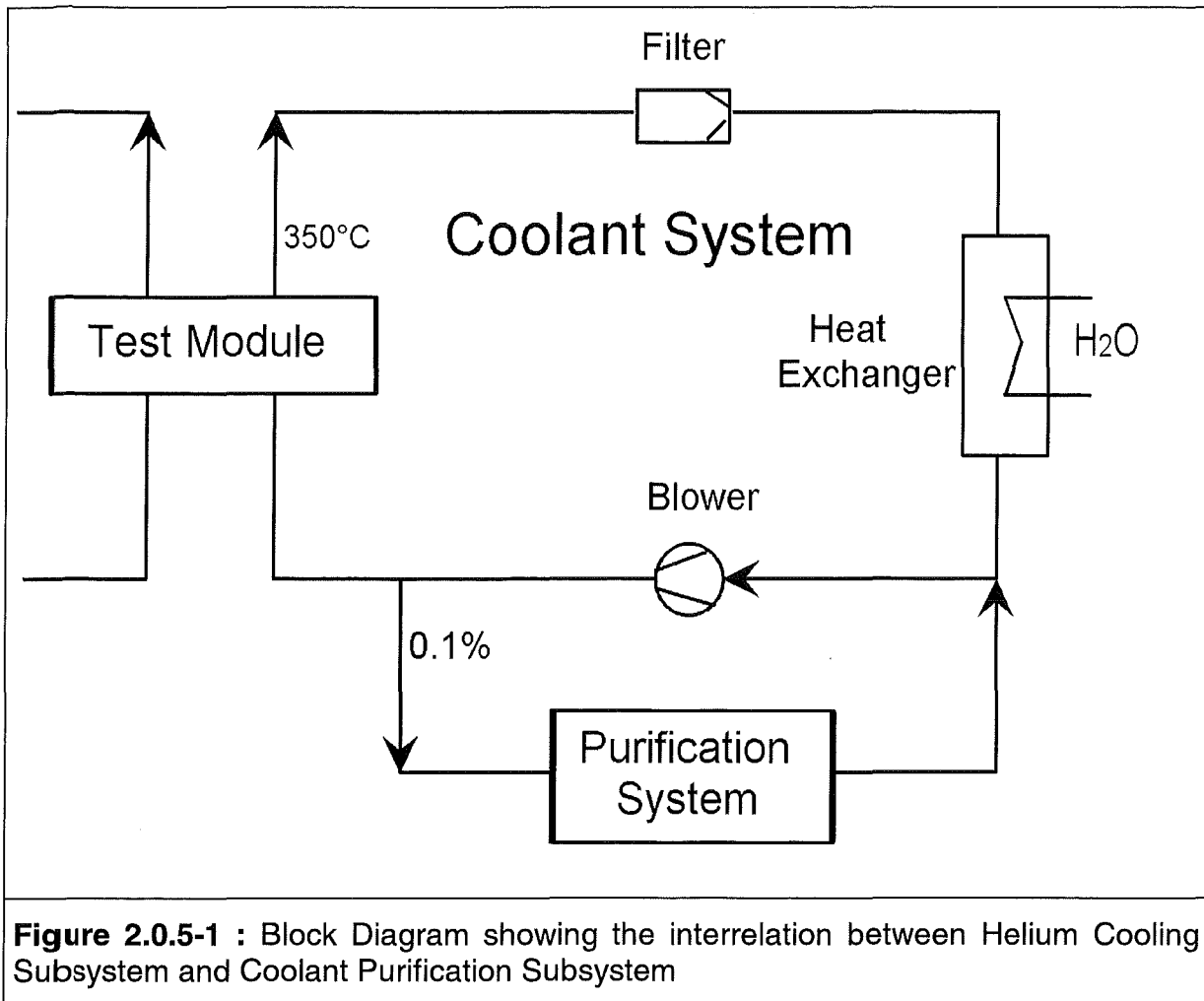
The interrelation between Cooling Subsystem and Coolant Purification Subsystem is shown in Figure 2.0.5-1. The latter is located in the Tritium Building in the vicinity of the Tritium Extraction Subsystem.

Principle of Operation

The 0.1 % fraction of the coolant gas leaving the cooling subsystem downstream of the coolant blower can be sent through a water separator to remove condensed water that may be present as a consequence of water leakages in the heat exchanger. Then, an oxidizer unit is employed to convert all molecular hydrogen isotopes into water ($Q_2 \rightarrow Q_2O$, $Q = H, D, T$). This water is frozen out in a cold trap operated at $\leq -100^\circ\text{C}$ while the remaining impurities are adsorbed on a molecular sieve bed operated at LN_2 temperature (-196°C). The pure helium is warmed up again and returned into the main coolant loop upstream of the blower.

The coolant purification system can be operated for one reactor campaign (max. 6 days) without intermediate unloading or regeneration of single components. In addition, no valve switching actions, temperature cycling or tritium transfer operations will be needed during this time span.

At the end of a campaign, the cold trap is warmed up, the liquified water is drained into a mobile water container and then transferred to the Water Detritiation System. The gaseous impurities desorbing from the molecular sieve bed during regeneration are sent to the Radioactive Waste Gas System.



2.0.6 Test Blanket Remote Handling Subsystem

All equipment to be used in the horizontal ports should be designed for radial installation and removal of components through the port extensions. Since the equipment will be inside the Bioshield and will be highly activated after reactor operation, it will be necessary to use remote handling systems for all operations within the Bioshield boundaries. This requirement will apply to the Test Blanket Subsystem.

The design of the remote handling system of the test blanket modules is dependent upon the piping system layout within the port extension. One of the project recommendations is to minimise the amount of remote operations inside the port extension. A concept was developed which combines the blanket modules, the shielding assembly, the coolant pipes and the vacuum vessel closure plate as one super assembly. This allows full functional testing of the assembly prior to installation within the port. This will also reduce the amount of time required to remove and install a test blanket assembly and eliminate remote operations inside the port extension.

The remote handling system for the blanket assemblies will take full advantage of the equipment designed by the JCT to minimise duplication of efforts and to standardise system operations. The transporter is the standard JCT design with overall dimension of 8 m long, 3.8 wide and 5 m high. All operations that are identical to other ITER operations will use the same ITER system to perform, such as removing the bioshield plug and the cryostat closure plate. Operations that are specific to the test blanket system will be integrated into the overall system design.

2.0.7 Safety

The safety considerations of the Test Blanket Module (TBM) focus on the accidental safety aspects to the extent that conceivable failures of the TBM system can impede the safe operation of ITER. On the other side, occupational safety and waste generation issues have not been elaborated so far, since they are small compared to those associated with the basic ITER machine.

An attempt was made by the ITER Joint Central Team to harmonise the spectrum of events to be analysed for each type of test blanket modules. Two event families were found to be the most demanding occurrences with respect to potential damage in ITER, associated with the release of radioactive material (in particular tritium) into the containment, i.e., in-vessel TBM coolant leaks and ex-vessel TBM coolant leaks. These two groups were investigated in different variants or in combination with a set of postulated aggravating occurrences that could be triggered by the postulated initiating event (PIE). The following event sequences were studied for the HCPB TBM.

Large in-vessel TBM coolant leaks	Large ex-vessel TBM coolant leaks
1a) FW cooling channel failure	2a) Main pipe break in the vault
1b) FW failure plus pebble bed beryllium/steam chemical reaction	2b) Main pipe break plus subsequent failure of FW
1c) Large leak inside module	2c) Main pipe break plus large leak inside TBM
1d) Small leak inside module	2d) Main pipe break (or loss of flow) plus FW failure at beryllium melting

The assessment addresses a number of concerns or issues that are directly caused by the TBM system failure. Any consequences which may result from subsequent damage to the ITER machine (e.g., via a heavy disruption) are beyond the scope of this work. The concerns addressed for the different event sequences, where applicable, are the following: (a) vacuum vessel pressurisation, (b) vault pressure build-up, c) purge gas system pressurisation, (d) temperature evolution in the TBM, (e) decay heat removal capability, (f) tritium and activation products release from the TBM system, (g) hydrogen and heat production from Be/steam reaction, and (h) Be/air reaction exothermic heat production.

Three methods of analyses have been applied: RELAP analysis for short-term thermal-hydraulic system transients, FIDAP analysis for short-term local TBM temperature evolution, and a 1D heat transport model for long-term passive decay heat removal assessment. The chemical aspects of Be/air and Be/steam reactions have been treated as bounding estimates based on correlations specified for ITER application. The analysis refers to the TBM-I type test module design as described in this document with EUROFER as structural material and for a lifetime planned to be achieved in the basic performance phase of ITER. This corresponds to a fluence level at the first wall of 0.36 MWa/m², including 20 % margin for poloidal peaking. The thermal-hydraulics analysis is based on the cooling subsystem layout according to section 2.1.1.3.

The transient analysis results are summarised as follows. The concerns identified for the individual event sequences revealed to be uncritical. The VV pressurisation upon release of the total helium inventory from the TBM system is very small (3500 Pa). In cases of large ex-vessel leakage from one loop the pressure rises in the vault by 4500 Pa within 5 seconds, i.e., 4.5 % above nominal. This seems to be too small to use the vault pressure for shutdown signal generation. Pressurisation of the TBM box and the connected tritium extraction subsystem upon a leak inside the module occurs within a fraction of a second and requires fast acting isolation valves in the purge gas lines. Relief of the box pressure will be needed for stress control reasons, where the direct discharge into the VV would be the most straightforward solution. The temperature evolution in the TBM first wall during transients is dictated by the disruption loads and by the delay time needed to shutdown the plasma. At continued plasma operation the first wall temperature rises at a rate of 7.5 K/s if one cooling system fails and 8.3 K/s if both systems are lost. On the other hand, temperatures in the breeding zone are hardly affected by the delay time. Therefore, the long-term temperature development in the TBM is just a matter of decay heat and boundary conditions assumed. The 1D heat transport model showed that passive decay heat removal from the TBM is assured in all cases at temperature levels below 500°C, even if adiabatic boundary conditions are assumed at the back. As a result chemical heat in cases of air or steam ingress into the pebble beds is insignificant. In the hypothetical scenario 2d the chemical heat at the TBM surface can reach the order of the regular surface heat flux. For the hydrogen production in scenario 1b with steam ingress into the pebble beds an upper bound of 100 grams is predicted.

The tritium release from the TBM system is inherently small. The most mobile fraction of the order 1 mg only is carried with the helium coolant and will be released in almost all cases investigated. The amount of tritium which could be liberated from the beryllium pebbles in the scenario 2c is estimated to be less than 60 mg. The tritium which might be released from the tritium extraction subsystem in cases where the purge gas system is involved (1b, 1c, 1d, 2c) has not been evaluated, but is judged to be negligible if the isolation valves are closed. Activation products in the helium cooling subsystem are expected to be small anyway. They are negligible for any in-vessel leak event.

Uncertainties in the data base and in the analysis do not seem to have considerable impact on the outcome of the study. Most of the effects are inherently small (like pressurisation, heat production, radioactive inventory) compared to the consequences resulting for ITER as a whole from the postulated disruption damage.

2.1 Detailed System Description

2.1.1 General Design Description

The HCPB Test Blanket System is based on the requirements listed in Section 1.

The detailed design of the system components will be analysed to demonstrate that these requirements can be met within allowable engineering parameters. The analyses refer to the reference ceramic breeder material Lithium Orthosilicate. The principal components in the test blanket system are:

1. the Test Blanket Subsystem (first wall, breeding blanket, shield, and structure);
2. the Tritium Extraction Subsystem (tritium removal, handling, and processing);
3. the Helium Cooling Subsystem (heat transfer and transport);
4. the Coolant Purification Subsystem;
5. the Test Blanket Remote Handling Subsystem (remote handling as related to the test blanket systems).

2.1.1.1 Test Blanket Subsystem Design Description

The Test Blanket Subsystem (TBS) encompasses the functions of the first wall, breeding blanket, shield, and structure. Like the basic ITER shielding blanket, one of its principal functions is to remove surface heat flux and energy from the plasma during normal and off-normal operational conditions. It also incorporates a shield section designed to reduce the nuclear responses in the vacuum vessel and, together with the vacuum vessel, shield the superconducting coils. In addition to these requirements, the test blankets breed sufficient tritium to demonstrate self sufficiency in a DEMO reactor and to produce and extract high grade heat suitable for electric power production. The TBS also has structural elements that provide the structural and thermal attachment from the vacuum vessel. The heat generated within the test blanket is removed with a compatible heat removal system that provides both thermal and safety protection. The TBS is designed so that it is sufficiently reliable and can be readily removed and replaced so that the availability of ITER is not adversely impacted. It also is designed to be compatible with the primary vacuum and safety boundaries so that the basic ITER safety requirements can be met.

These functions correspond to the requirements documented in Section 2.0.2 of this document. The ITER GDRD also lists the test blanket system functional, configurational, and specific requirements in 5.19.

During the Basic Performance Phase of ITER two test blanket modules (TBM) will be tested. The first (TBM-I) will have the same configuration of the DEMO blanket, however with a higher Li-6-enrichment (90 % instead of 40 % of the DEMO). Fig. 2.1.1.1-1 shows a vertical and a horizontal cross section of TBM-I which can be

considered as an about 1 m long poloidal section of the HCPB DEMO outboard blanket segment. The main components of the module are:

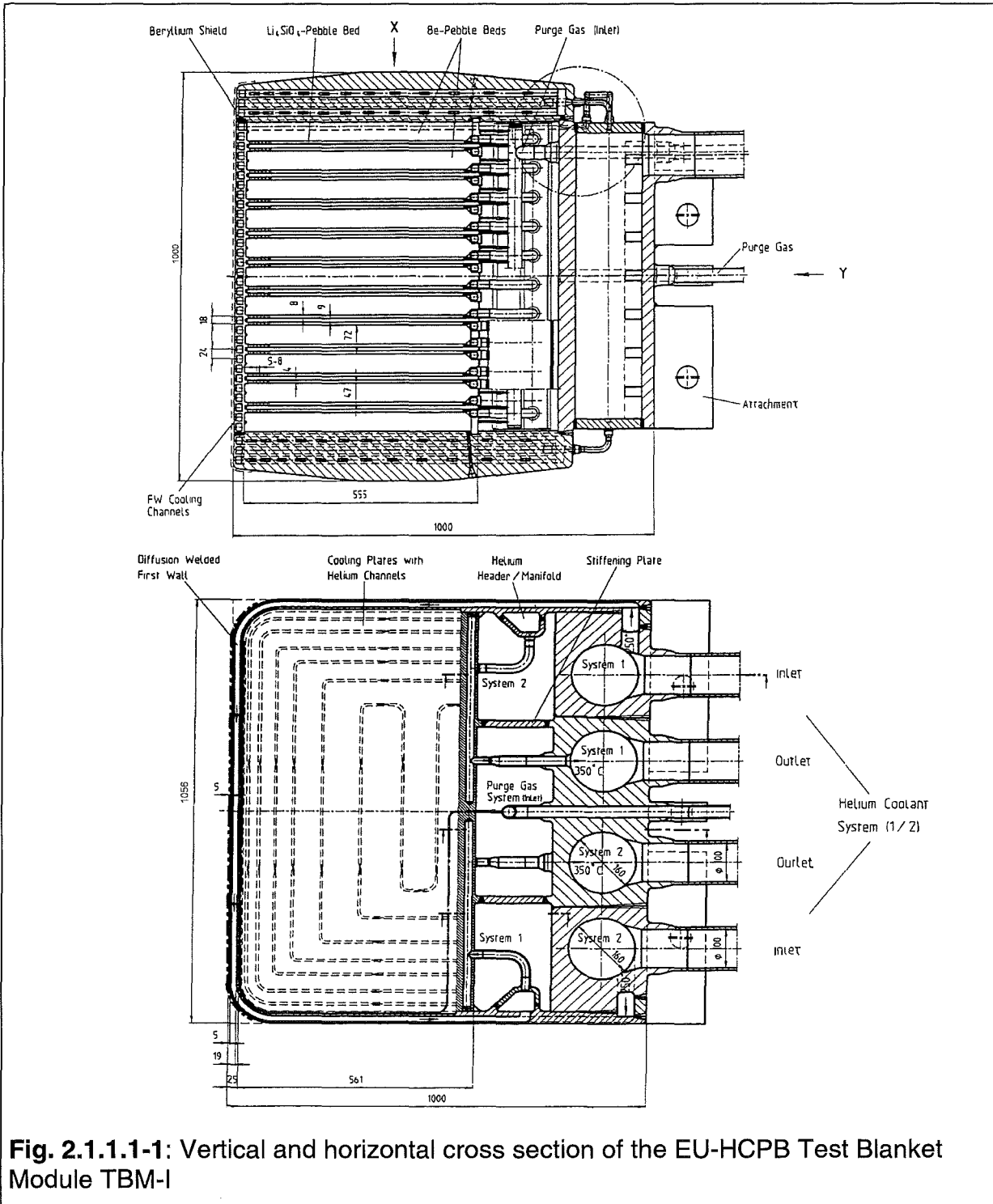


Fig. 2.1.1.1-1: Vertical and horizontal cross section of the EU-HCPB Test Blanket Module TBM-I

- The U-shape box of 25 mm thickness with integrated radial/toroidal cooling channels of 14 x 18 mm cross section. The FW is covered with protective Be layer of 5 mm thickness.
- The breeding zone consisting of 9 mm thick ceramic breeder pebble beds and 47 mm thick Be multiplier pebble beds, separated by 8 mm thick cooling plates. In total the breeding zone consists of 10 breeder and 11 Be pebble beds. The latter number includes the Be beds between the outermost cooling plates and the caps.
- The main coolant headers at the back side of the module for the He supply to the FW cooling channels and the He collection from the cooling plates; two intermediate headers attached to the inner surface of the box serve to redistribute the coolant from the FW channels to the cooling plates.
- The purge gas supply and collection system.
- The caps at the poloidal ends of the module with a maximum thickness of about 120 mm.

Reference ceramic breeder material is Li_4SiO_4 with 2.2 wt% SiO_2 in form of pebbles of 0.25 to 0.63 mm diameter. The packing factor of the bed amounts to 0.62. The Be bed is a binary bed with pebbles of 1.5 to 2.3 and 0.1 to 0.2 mm diameter. The packing factor is 0.8. The 9 % Cr martensitic steel EUROFER is used as structural material. However, because thermophysical and mechanical data of EUROFER are not yet available, it has been replaced by the 9% Cr martensitic steel Z10CDVNb9-1 (T91) in the thermal and mechanical calculations.

For the cooling of the modules two completely separated Helium systems are available operating at a pressure of 8 MPa. Helium is flowing at first through the module box including the FW and then through the cooling plates. To obtain a more homogeneous temperature distribution the flow directions in the FW and the cooling plates are alternating. The He flow in the caps is parallel to the main part of the module. Each cap is connected to both cooling systems.

The purge gas is fed to the plasma-near side of the pebble beds, flows radially to the rear side and further on via perforated closure plates into the collection chamber between the breeder zone and the He headers. The nominal operating pressure of the purge gas system is 0.1 MPa.

The second module (TBM-II) will also have a Li-6-enrichment of 90 %, however the geometry of the blanket and the coolant flow scheme will be slightly modified to achieve higher, and thus more relevant, temperatures at the coolant outlet and in the ceramic breeder pebbles. A vertical cross section of TBM-II is shown in Fig. 2.1.1.1-2. The ceramic breeder and Be pebble beds have thickness of 15 and 53 mm, respectively. With the same poloidal height of the module as TBM-I this yields 9 ceramic breeder and 10 Be pebble beds.

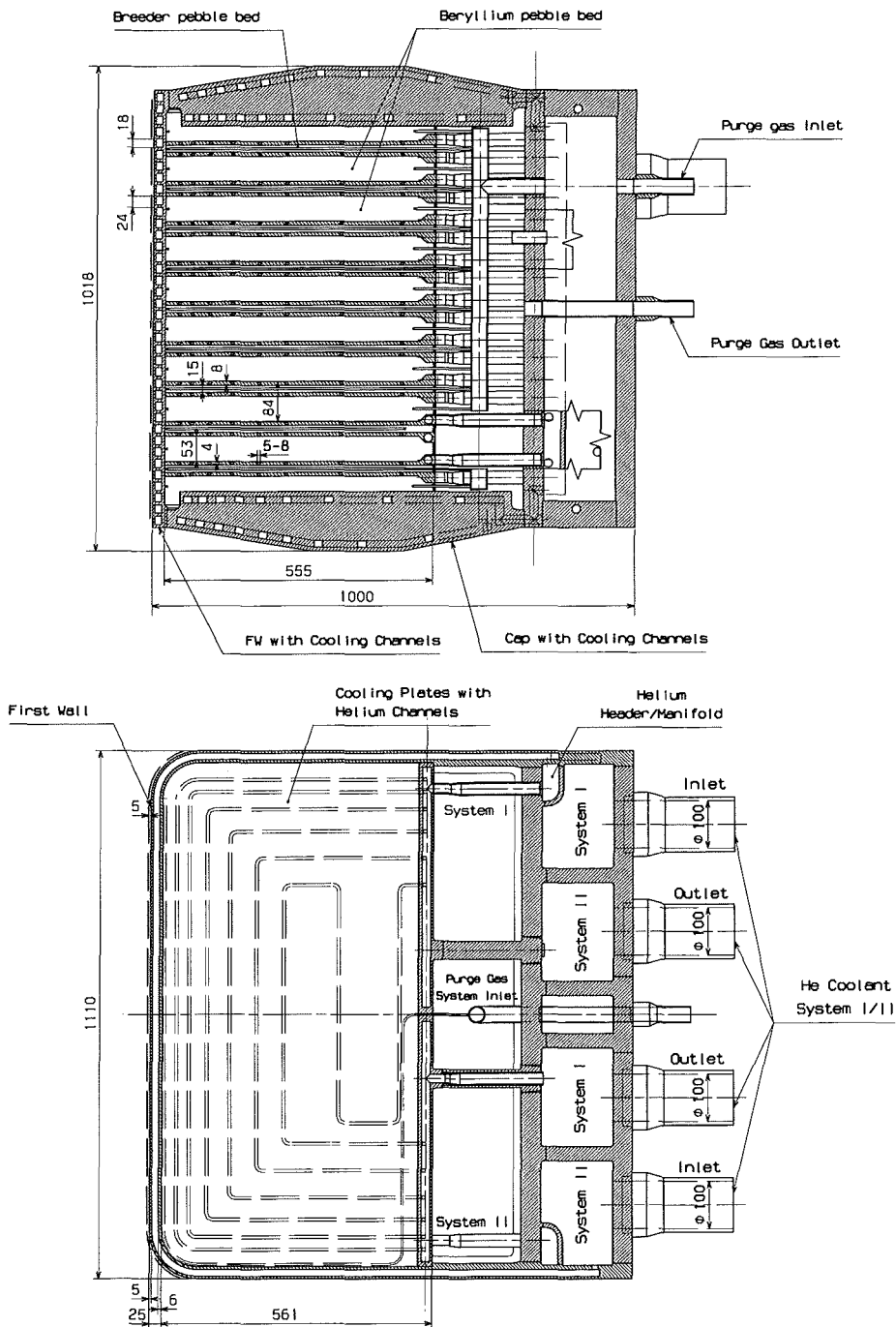


Fig. 2.1.1.1-2: Vertical and horizontal cross section of the EU-HCPB Test Blanket Module TBM-II

The basic flow scheme of the He in TBM-II is the same as in TBM-I with the exception that the coolant is flowing twice through the box with a U-turn at the rear end of the side wall. 32 of the 38 cooling channels in the FW are connected via the intermediate headers to the cooling plates. The remaining 6 channels (3 at each poloidal end) and the caps are connected in parallel to the main helium headers. In the outermost channels He is flowing through the FW in a single pass. This flow scheme leads to higher coolant velocities, and hence, higher heat transfer coefficients which allows higher He temperatures at about the same structural temperatures.

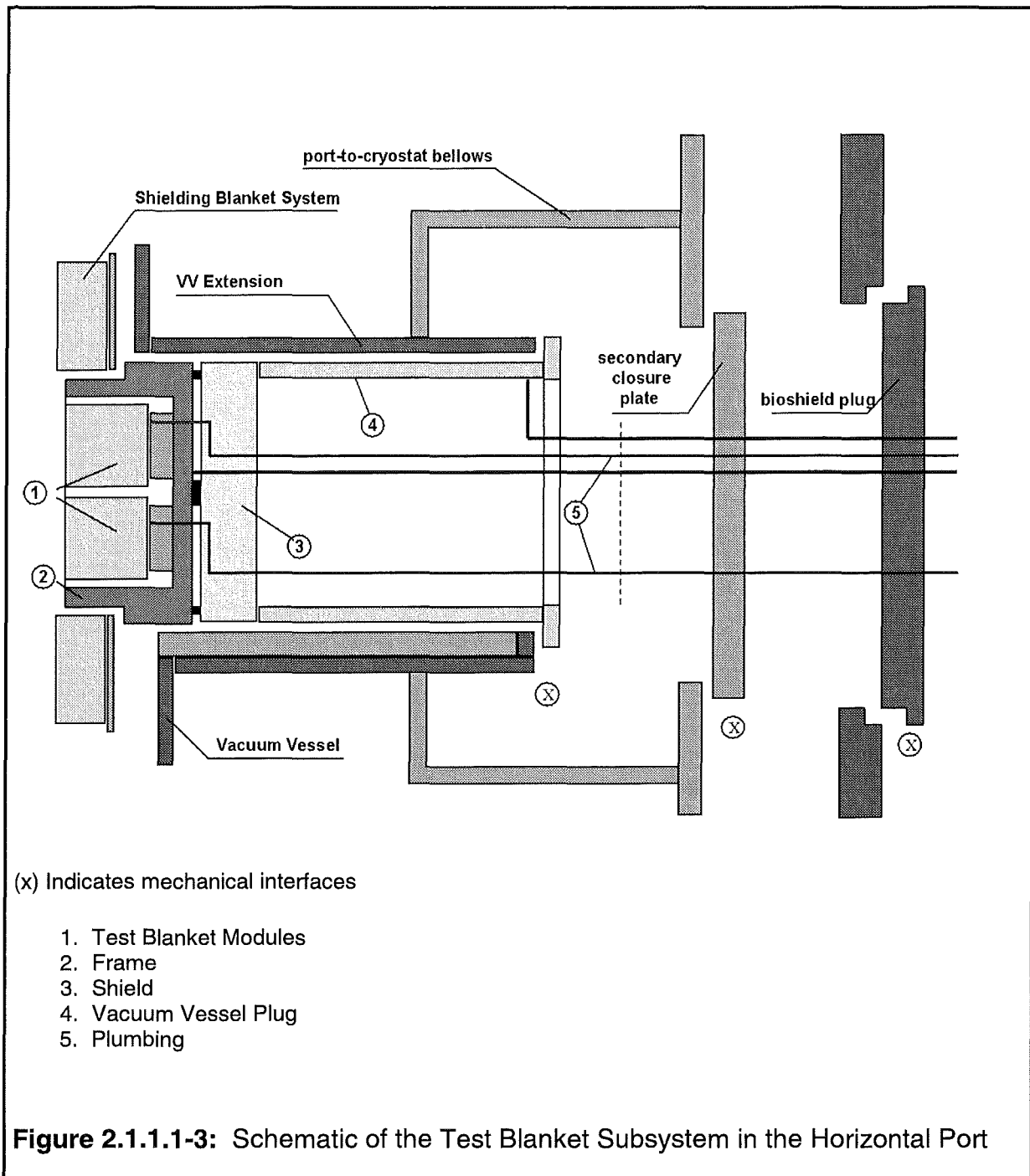
Another difference as compared to TBM-I is the design of the caps. The welds between the caps and the box are placed at the poloidal surfaces of the module with the advantage that the welding of the FW region can be avoided. The groove in the caps near the FW increases the elasticity of the connection between the caps and the box which reduces the loads transmitted from the caps into the FW in the case of an accidental pressure increase in the box. Of course, the cap design and the He flow scheme of TBM-II can likewise be applied to TBM-I, and inverse.

Neutronic and thermomechanical design calculations have been performed also for a TBM to be tested during the EPP (TBM-III). The geometrical configuration is the same as that of TBM-I. These calculations have been performed to assess the requirements posed by the TBM to the ancillary loops (helium coolant loop, helium purification plant, tritium extraction subsystem) during the EPP.

The design of the subsystem and in particular the plumbing layout is strongly dependent on the adopted remote handling procedures. For the solution with attachment from the Vacuum Vessel Port Extension, the arrangement of the Test Blanket Subsystem inside the port is schematically represented by Fig. 2.1.1.1-3. The TBMs (1) are contained in an insulation frame (2). This frame will provide a standardised interface with the ITER basic structure and a better shielding capability as well as neutronic and thermal isolation from the basic shielding blanket.

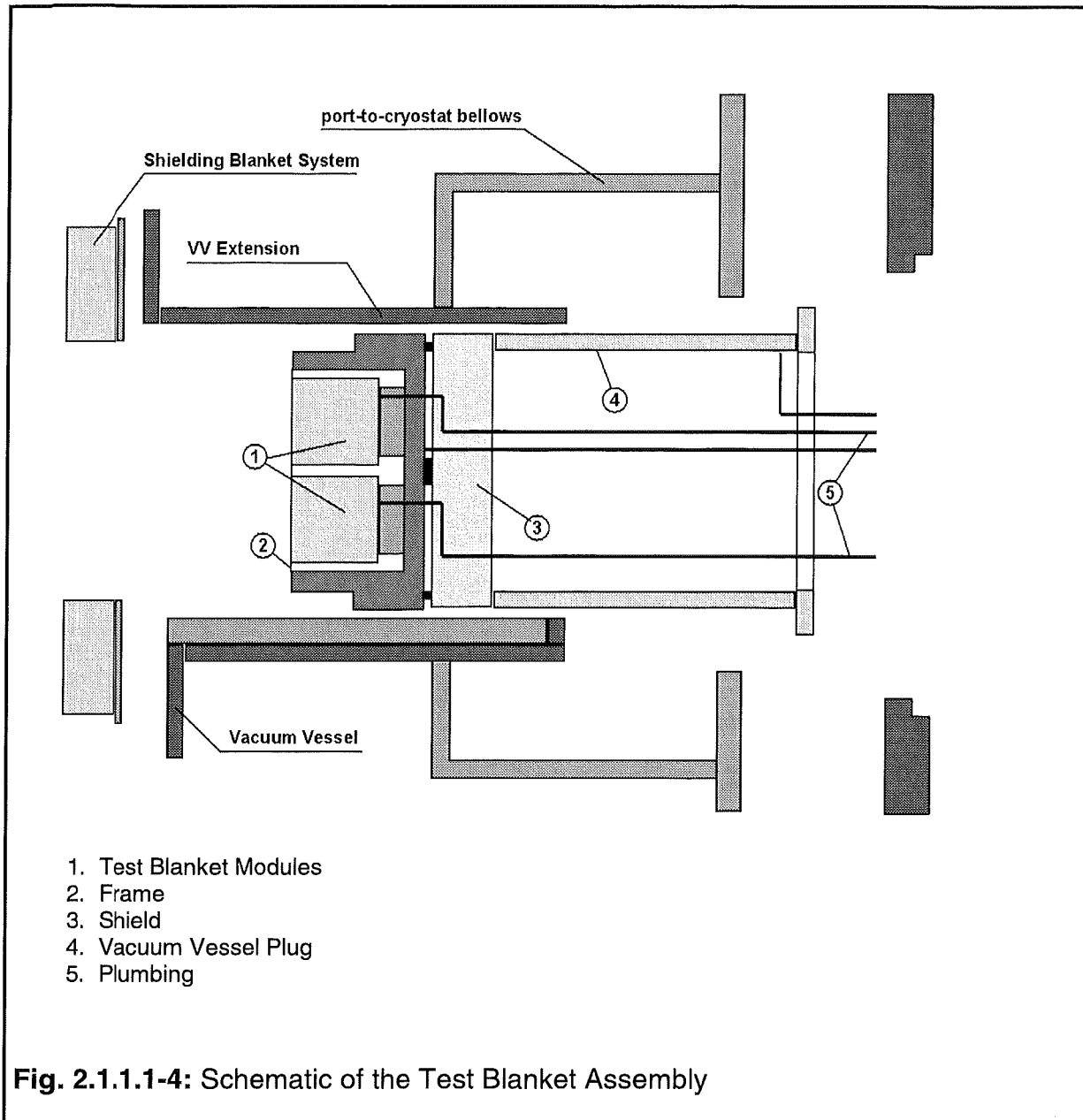
A water cooled Shield (3) is located behind the TBMs and Frame. It will assure neutron protection for the vacuum vessel, magnets and contribute to reduce the neutron load at the VV boundary.

The mechanical interface with the ITER Reactor is provided by the Vacuum Vessel Plug (4). This structure is supported by the Vacuum Vessel Port Extension using guide keys and/or rollers.



The plumbing (5) which extends through the VV closure plate up to the cryostat boundary, is also part of the TBS. Note that all the VV plug penetrations have rigid connection and do not require vacuum tight flexible connections such as bellows.

This arrangement enables the whole Test Blanket Subsystem (TBMs, Frame, Shield, VV Plug and Plumbing) to be a self contained unit (see Fig.2.1.1.1-4), that will be installed and removed as a single piece without remote handling operations inside the VV Port Extension. Indeed this assembly can be completely assembled and tested prior to installation.



Figures 2.1.1.1-5 is an isometric view of the horizontal port illustrating the routing of the test blanket piping. The current design uses straight pipes running through the cryostat closure plate and bio-shield plug. Bellows are used at cryostat and bio-shield boundaries to accommodate relative motion during operations.

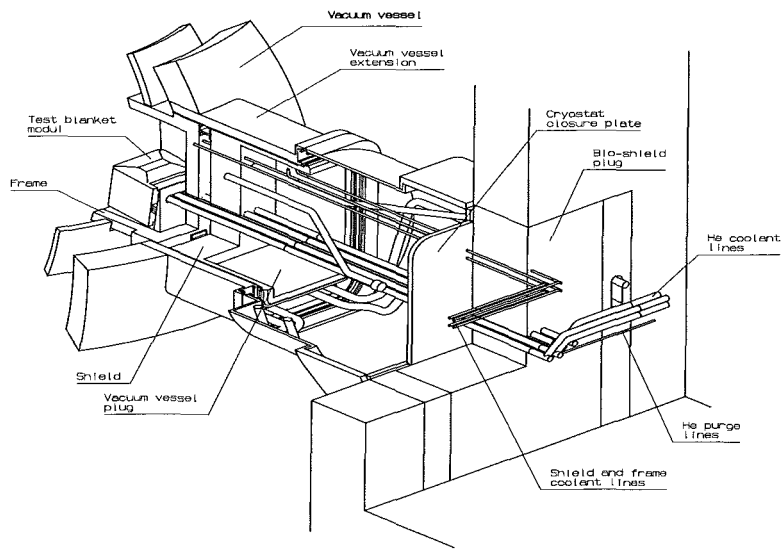


Fig.2.1.1.1-5: Isometric view of the Test Blanket Assembly installed with piping

2.1.1.1.1 Nuclear Design

Calculational procedure and modelling

The nuclear design analyses for the HCPB blanket test modules in ITER are based on three-dimensional Monte Carlo calculations with the MCNP-code [2.1.1.1.1- 1] and nuclear cross-section data from the FENDL-1 data library [2.1.1.1.1-2]. A 9 degree torus sector model, developed on the basis of the current ITER design with 20 toroidal field coils by the ITER Joint Central Team nuclear analysis group, formed the basis of the calculations. A horizontal outboard test blanket port was inserted into the model with the proper dimensions of 260 cm times 160 cm at the level of the blanket back plate.

Inside the horizontal port, a water-cooled steel frame and two test modules of the HCPB type were integrated, see 2.1.1.1.1- 1 for a vertical cross-section of the torus sector model including the test modules. The HCPB test blanket module model was adopted from the Demo blanket model [Ref. 1 of Section 2.0.2] with the following exceptions: in toroidal direction, the blanket test module is rectangular instead of trapezoidal to reduce neutron streaming between the module and the steel frame, see fig. 2.1.1.1.1- 2 for a horizontal cross-section of the port with integrated test blanket modules; in poloidal direction, the modules follow the contour of the ITER shielding blanket first wall with an outward recess of 5 cm. As for ITER, there is a 5 mm beryllium protection layer for the blanket test module first wall. Fig. 2.1.1.1.1-3 shows a vertical cross-section of the port with integrated test blanket modules.

Three different cases were considered in the nuclear analysis: TBM-I and -II for tests in the basic performance phase (BPP) and TBM-III for test in the enhanced performance phase (EPP), see table 2.1.1.1.1-1 for the main features of the three TBM-configurations.

Table 2.1.1.1.1-1: Main features of the different TBM-configurations

	TBM-I	TBM-II	TBM-III
Operation phase	BPP	BPP	EPP
Poloidal height of breeder ceramics pebble bed	9 mm	15 mm	9 mm
Poloidal height of beryllium pebble bed	47 mm	53 mm	47 mm
Breeder material	Li ₄ SiO ₄	Li ₄ SiO ₄	Li ₄ SiO ₄
⁶ Li-enrichment	90 at%	90 at%	90 at%
Structural material	EUROFER	EUROFER	EUROFER

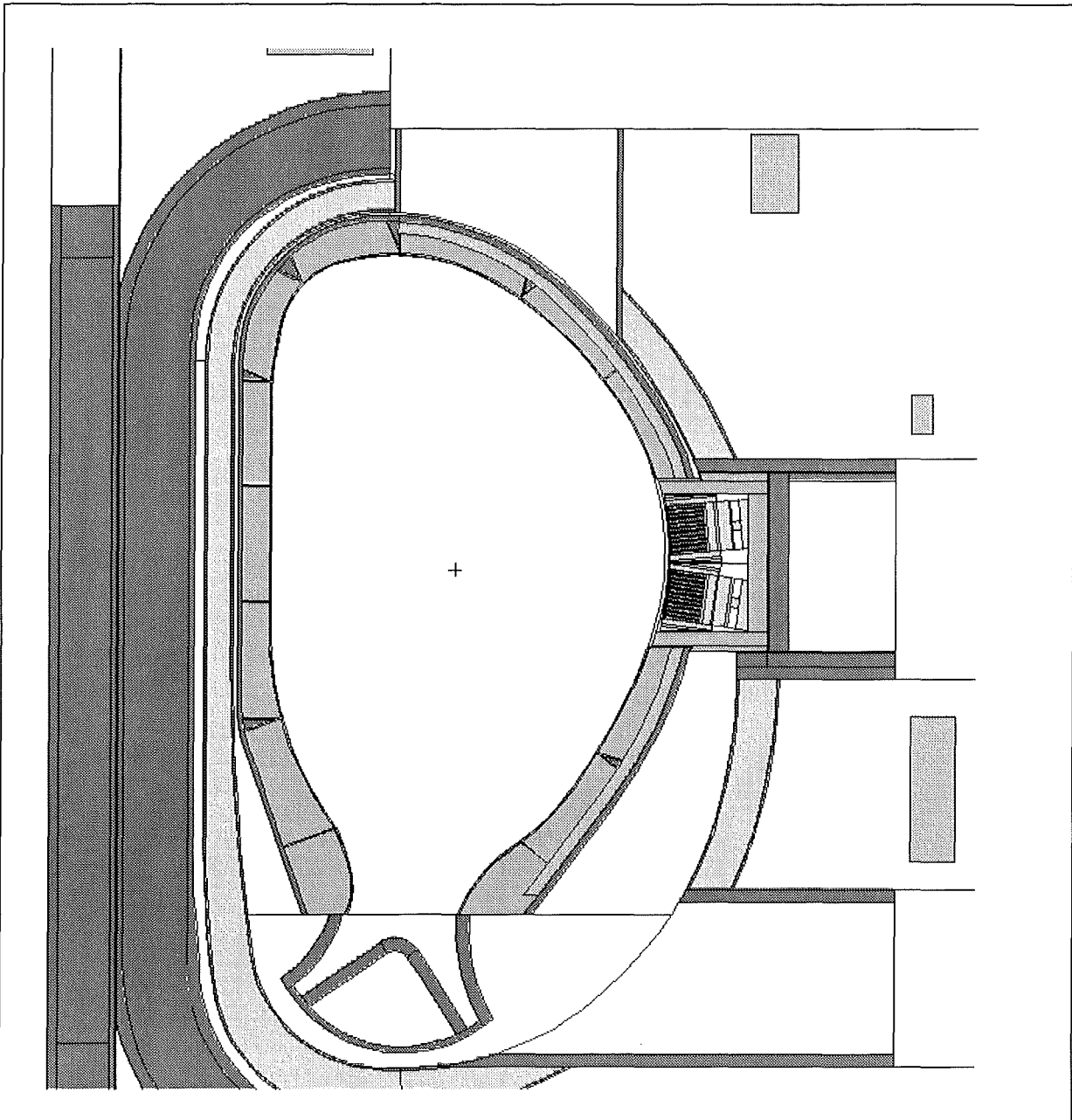


Fig. 2.1.1.1- 1: Vertical cross-section of the 9° torus-sector model with test blanket port and integrated HCPB test blanket modules

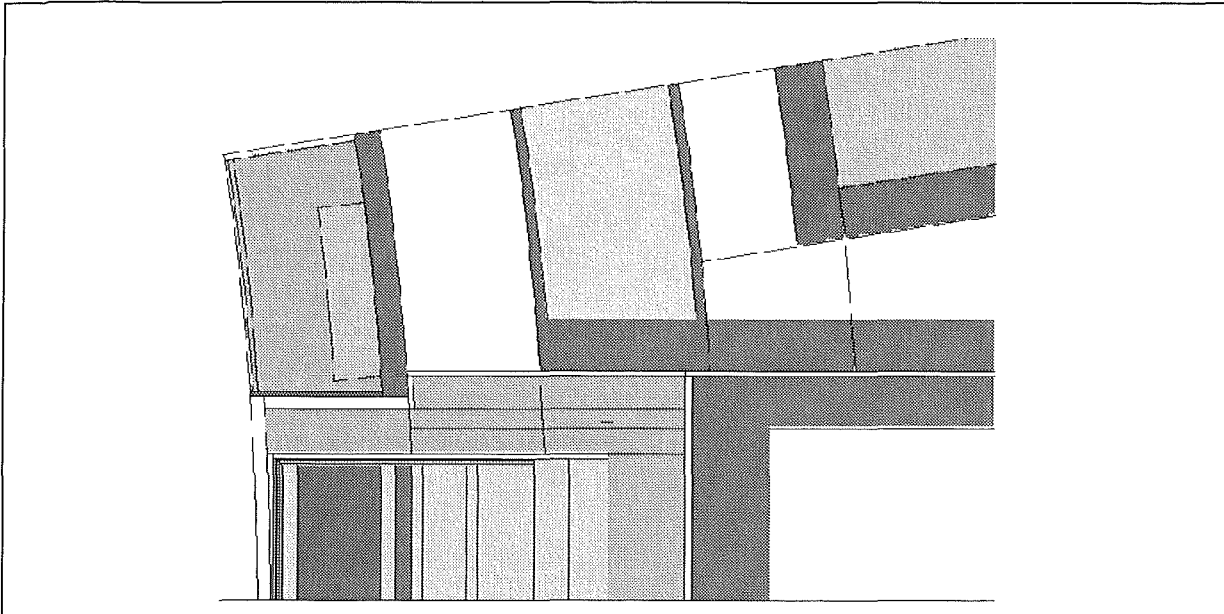


Fig.2.1.1.1.1-2: Horizontal cross-section of the test blanket port with integrated HCPB test blanket module.

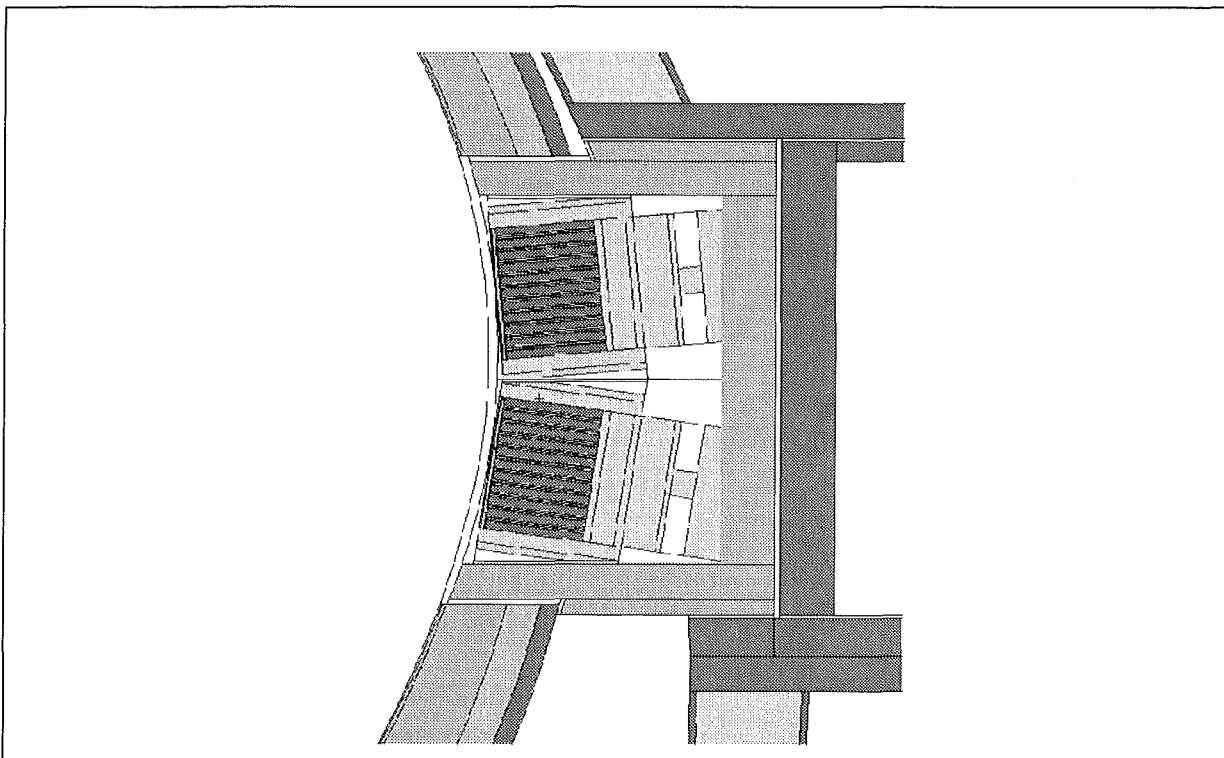


Fig. 2.1.1.1.1-3: Horizontal cross-section of the test blanket port with integrated HCPB test blanket module

With regard to the DEMO blanket configuration, the ^6Li -enrichment has been increased to achieve higher temperatures in the breeder and the helium coolant. In addition, a configuration with a larger breeder pebble bed height (TBM-II) has been taken into account to have available a solution with a further increased nuclear power generation in the breeder. Note that the low activation steel EUROFER is assumed as structural material for the test blanket modules while ITER uses the ferritic SS-316LN steel. For the transport calculation, the following EUROFER composition [w%] is assumed: 89.225 Fe, 9.0 Cr, 0.4 Mn, 1.0 W, 0.07 Ta, 0.2 V, 0.105 C. For calculating the activation and afterheat of the TBM (see below), also the minor constituents of the LA steel EUROFER were taken into account.

For the BPP-calculations, the proper ITER water-cooled shielding blanket is used in the model (assuming SS-316 as structural material) while for the EPP-calculations a simulated ITER driver blanket is applied. In that case, the shielding blanket mixture is replaced by a homogenised mixture of 10 vol% SS-316, 76 vol% Be, 4.5 vol% water and 8.5 vol% Li_2ZrO_3 pebbles (at a Li-6-enrichment of 75 at%) to account for the proper ITER breeder blanket albedo.

Calculational results

MCNP-calculations were performed for the nuclear heating and the tritium production in the lower TBM and to assess the shielding performance with regard to the radiation loads on the TF-coil and the vacuum vessel adjacent to the test blanket port. In addition, the neutron spectra were calculated throughout the TBM in a 175 group structure for subsequent use with the activation calculation (see below). Typically 2 to 5 million source neutron histories were tracked in the MCNP-calculations to ensure a sufficient statistical accuracy for the calculated nuclear responses in the test blanket modules. For the shielding calculation, geometry splitting with Russian Roulette was applied for variance reduction in the scoring regions around the test blanket port. The spatial neutron source distribution was sampled in a special routine linked to MCNP. Use was made of the neutron source density distribution given numerically by ITER on a fine poloidal-radial grid. The calculated nuclear responses (neutron flux, heating, tritium production, etc.) were normalised to a fusion power of 1500 MW.

Neutron wall loading and first wall fluxes

The neutron wall loading was calculated with MCNP for the voided torus sector model showing that 1.94 % of the 14 MeV source neutrons generated in the plasma chamber are entering the TBM first wall with a surface area of $4.87 \cdot 10^3 \text{ cm}^2$ (9° sector). This results in an average neutron wall loading of 1.197 MW/m^2 at the TBM first wall. The corresponding 14 MeV neutron current density amounts to $5.31 \cdot 10^{13} \text{ cm}^{-2}\text{s}^{-1}$. The total neutron flux density at the TBM first wall is $3.90 \cdot 10^{14}$ and $4.64 \cdot 10^{14} \text{ cm}^{-2}\text{s}^{-1}$ for the BPP and the EPP, respectively. The increase by about 20% is mainly due to the higher neutron multiplication of the ITER driver blanket.

Nuclear power generation

The albedo of the surrounding ITER blanket modules affects the nuclear performance of the HCPB blanket test module in the test blanket port. While the ITER breeding blanket neutronicly is similar to the HCPB blanket due to its high beryllium content, the ITER shielding blanket, consisting of a water/steel mixture, is very different. It shows both a lower neutron multiplication and reflection power. Consequently, less neutrons are scattered into the small size blanket test module when surrounded by shielding instead of breeding blanket modules. This has a detrimental effect on the neutronic performance of the HCPB TBM. As compared to the BPP, up to 20% higher power densities are obtained in the EPP in the TBM front region (fig. 2.1.1.1.1-4 and table 2.1.1.1.1-2).

Table 2.1.1.1.1-2: Maximum power densities [W/cm^3] in the HCPB- TBM's

	BPP		EPP
	TBM-I <i>9 mm breeder layer thickness</i>	TBM-II <i>15 mm breeder layer thickness</i>	TBM-III <i>9 mm breeder layer thickness</i>
First wall/beryllium	7.95	8.02	8.04
First wall/steel	10.6	10.1	10.0
Be pebble bed	4.67	4.69	4.68
Ceramics pebble bed	20.2	16.4	24.3
Cooling plate/steel	8.08	8.29	8.01

The power generation in the test module is displayed in table 2.1.1.1.1-3 for the different cases. The energy multiplication (the energy released in the test blanket divided by the neutron energy loaded onto the TBM first wall by the source neutrons) amounts to 1.31 for the BPP and 1.35 for the EPP. Note that the power generated in the water-cooled steel frame, being composed of 80% structural material and 20% H_2O , is higher than in the TBM.

Table 2.1.1.1.1-3: Power generation [MW] in the HCPB-TBM and the steel frame.

	BPP		EPP
	TBM-I <i>9 mm breeder layer thickness</i>	TBM-II <i>15 mm breeder layer thickness</i>	TBM-III <i>9 mm breeder layer thickness</i>
First wall	0.19	0.19	0.18
Beryllium	0.41	0.38	0.41
Breeder	0.44	0.50	0.48
Structure	0.49	0.47	0.50
Total TBM	1.53	1.54	1.57
Steel frame	3.29	3.29	3.56

Tritium generation

The tritium production rate in the HCPB TBM is affected in a similar way by the surrounding blanket modules than is the breeder ceramics power density (fig. 2.1.1.1.1-5). When applying the TBM-I configuration, the local tritium breeding ratio, calculated by dividing the number of tritons produced in the TBM by the number of 14 MeV source neutrons entering the TBM first wall, is below unity for the BPP and above for the EPP operation (table 2.1.1.1.1-4). In terms of the tritium generation potential, TBM-II shows a better performance than TBM-I due to its the larger breeder volume.

Table 2.1.1.1.1-4: Tritium generation in the HCPB-TBM

	BPP		EPP
	TBM-I <i>9 mm breeder layer thickness</i>	TBM-II <i>15 mm breeder layer thickness</i>	TBM-III <i>9 mm breeder layer thickness</i>
Tritium production rate [cm ⁻³ s ⁻¹]	9.40 · 10 ¹²	6.81 · 10 ¹²	1.04 · 10 ¹³
Tritium production rate [g/d]	0.21	0.23	0.23
Local tritium breeding ratio	0.94	1.02	1.04

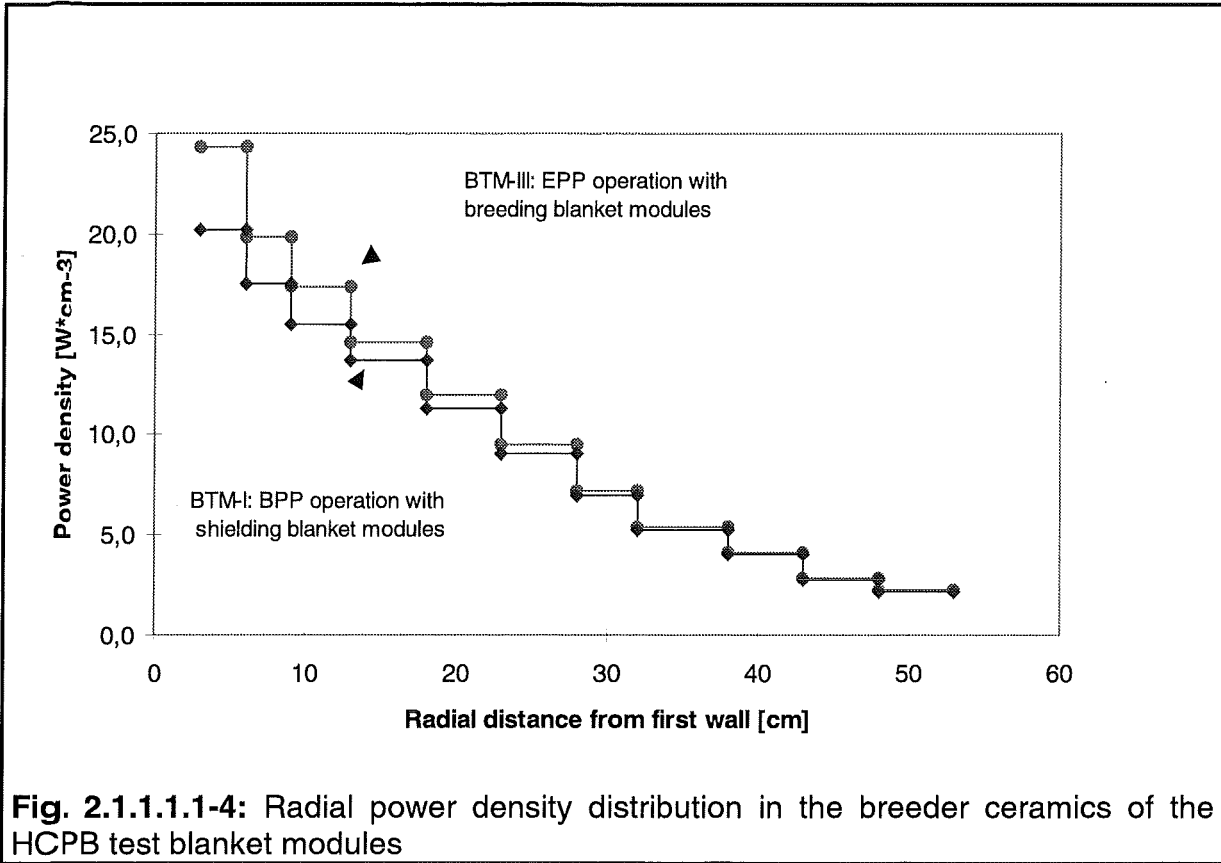


Fig. 2.1.1.1-4: Radial power density distribution in the breeder ceramics of the HCPB test blanket modules

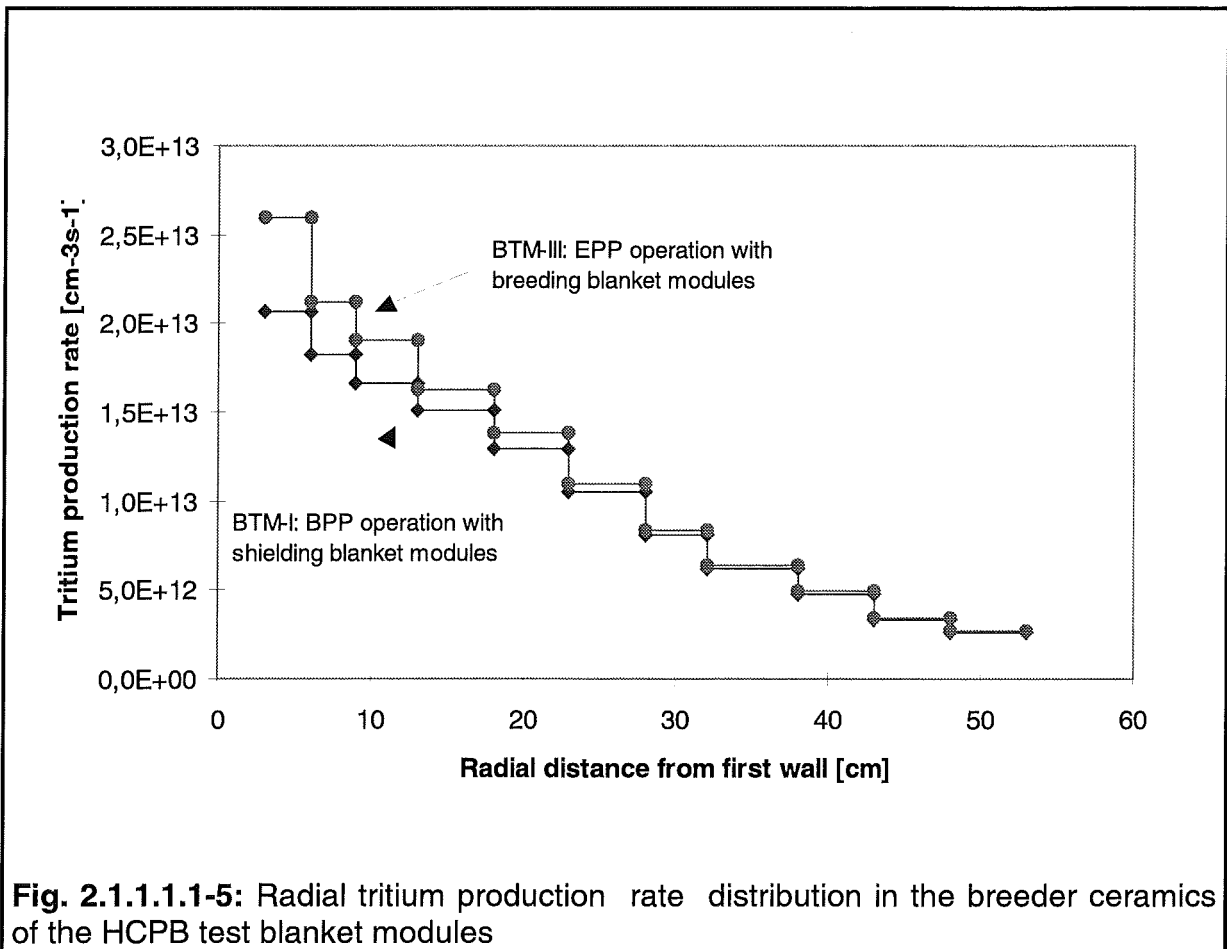


Fig. 2.1.1.1-5: Radial tritium production rate distribution in the breeder ceramics of the HCPB test blanket modules

Shielding efficiency

Neutron streaming through the test blanket port deteriorates the shielding efficiency of the blanket/shield system. The design of the test blanket system therefore has been further developed to reduce void gaps to a minimum and by designing the steel support frame as efficient radiation shield. This includes recent test port design modifications as proposed by TBWG-5 (see figs. 2.1.1.1.1-2/ 3).

According to the requirements specified by ITER, the test blanket system has to be designed for a total first wall fluence of 1 MWa/m². With regard to shielding, the most crucial requirements refer to the reweldability of the vacuum vessel and the peak radiation dose to the electrical insulator of the toroidal field (TF) coil being limited to 3·10⁸ rad. The reweldability criterion results in an upper limit for the helium production of about 1 appm at maximum.

The shielding efficiency was assessed by calculating the radiation loads to the vacuum vessel and the TF-coil adjacent to the test blanket port at the highest loaded locations. For that purpose, the calculated nuclear responses were averaged over the poloidal extension of the TBM which amounts to a height of 84 cm. Over this height, the neutron wall loading is at its maximum. In toroidal direction, the responses apply for parts located closest to the test blanket port.

Table 2.1.1.1.1-5 shows the calculated radiation loads to the TF-coil and the vacuum vessel when assuming two test blanket modules of type TBM-I present in the test blanket port. For the TF-coil, the most crucial radiation load is the radiation dose absorbed by the epoxy resin insulator. With the current test blanket port configuration, the required design limit can be met within a safety factor 3. The other responses are below the design radiation limits by more than one order of magnitude. As referred to the previous port design, these reduced loads are mainly due to fact that the broad gap between the test blanket frame and the vacuum vessel has been reduced by suitably extending the steel frame (figs. 2.1.1.1.1-2/ 3).

The accumulated helium production in the SS-316 front plate of the vacuum vessel amounts to \cong 0.09 appm at the assumed TBM first wall fluence of 1 MWa/m². Hence the joint reweldability criterion is satisfied within a safety margin of one order of magnitude.

Table 2.1.1.1.1-5: Radiation loads to the TF-coil and the vacuum vessel at a TBM first wall fluence of 1 MWA/m².

	HCPB TBM 3d -calculation	Radiation load limits
Vacuum vessel		
Helium production [appm]	0.09	1.0
TF-coil		
Peak dose to electrical insulator (Epoxy) [rad]	$9.4 \cdot 10^7$	$3 \cdot 10^8$
Peak displacement damage to copper stabiliser [dpa]	$2.2 \cdot 10^{-5}$	$6 \cdot 10^{-3}$
Peak fast neutron fluence ($E > 0.1$ MeV) to the NB ₃ Sn superconductor [cm ⁻²]	$6.2 \cdot 10^{16}$	$1 \cdot 10^{19}$
Peak nuclear heating in winding pack [mWcm ⁻³]	0.03	1.0

Activation and Afterheat Calculations

Calculational procedure and irradiation conditions

For TBM-I the afterheat and the activity inventory was calculated by making use of an appropriate code system that allows to perform three-dimensional activation calculations [2.1.1.1.1-4]. The Monte Carlo code transport MCNP [2.1.1.1.1-1] and the fusion inventory code FISPACT [2.1.1.1.1-5] form the central modules of this system and are linked through an appropriate interface. While the MCNP-calculations are based on the FENDL-1 data library [2.1.1.1.1-2], the FISPACT inventory calculations make use of the activation and transmutation cross-section data of the European Activation File EAF-4.1 [2.1.1.1.1-6].

Neutron fluxes and spectra in 175 energy groups are provided by three-dimensional MCNP-calculations for TBM-I (first wall, breeder ceramics, steel plates, side and back walls using an appropriate radial segmentation scheme), the back shield and the support frame using the torus sector model described above. The spectra are routed to the FISPACT-code for performing the inventory calculations in each specified material zone. The individual results of the single zone inventory calculations are merged to get the total activation inventory and the afterheat of the TBM, the back shield and the support frame.

In the activation calculation a continuous irradiation at full power (1500 MW) is assumed over a time period of 0.3 years. As the neutron wall loading at the TBM first wall is 1.197 MW/ m², this results in a total first wall fluence of 0.36 MWA/m² that actually would be achieved over a ten years period according to the operational availability assumed by ITER for the blanket test programme.

Material specification

As specified by the European Blanket Management Committee, the design of the European Demo blanket should be based on the use of the low activation (LA) steel EUROFER as structural material. Accordingly, the nuclear design of the TBM has also been performed using the EUROFER LA-steel for the test module. Other components like the support frame are based on SS-316 as structural material. For the activation and afterheat calculations, the chemical composition according to table 2.1.1.1.1-6 has been used for the involved materials EUROFER [2.1.1.1.1-7], beryllium [2.1.1.1.1-8], Li_4SiO_4 [2.1.1.1.1-9] and SS-316 [2.1.1.1.1-10].

The total masses and volumes associated to the different materials of the TBM-I, the back shield and the support frame are given in table 2.1.1.1.1-7.

Table 2.1.1.1-6: Chemical composition of the materials used in the activation and afterheat calculations for TBM-I (wt%).

Element	EUROFER	Beryllium	Li ₄ SiO ₄	SS-316
Fe	ad 100	0.0435	0.0083	ad 100
Pb	-	0.002	-	-
Li	-	-	20.950	-
O	0.010	0.0512	ad 100	-
Be	-	ad 100	-	-
C	0.105	0.081	0.100	0.800
Ca	-	0.002	0.0083	-
K	-	-	0.0083	-
Mg	-	0.0250	0.0031	-
Na	-	-	0.0071	-
Si	0.050	0.01	24.220	1.000
TE	-	-	1.790	-
Mn	0.400	0.0085	0.00033	2.000
P	0.005	-	-	-
S	0.005	-	-	-
Cr	9.000	0.006	-	17.000
Ni	0.005	0.006	0.0009	12.000
Mo	0.005	0.002	-	2.500
V	0.200	-	-	-
Nb	0.001	-	-	0.010
B	0.001	-	-	-
N	0.030	0.038	-	0.060
Al	0.010	0.025	0.091	0.005
Co	0.005	0.0004	-	0.090
Cu	0.005	0.004	-	0.200
Zr	-	0.001	0.0048	-
Zn	-	0.001	-	-
Bi	-	-	-	-
Cd	-	-	-	-
Ag	-	0.0003	-	0.040
Pt	-	-	-	-
Sn	-	-	-	0.001
Sc	-	0.0005	-	0.001
Ta	0.070	-	-	0.050
Ti	0.010	0.004	0.0101	0.005
W	1.100	0.01	-	-
U	-	0.011	-	-

Table 2.1.1.1.1-7: Volumes and masses of the materials of TBM-I.

	Volume [cm ³]	Mass[kg]
First wall protection layer (beryllium)	4.48E+03	8.31E+00
Neutron multiplier (beryllium)	2.95E+05	4.31E+02
Breeder (Li ₄ SiO ₄)	5.18E+04	7.93E+01
EUROFER blanket structure (FW, cooling plates, side walls)	2.00E+05	1.56E+03
Top/bottom walls (EUROFER)	2.85E+05	2.22E+03
Support frame (SS- 316)	2.25E+06	1.79E+04
Back shield (EUROFER)	9.71E+05	7.57E+03

Results for activity inventory and afterheat generation

Results are given for the integrated activity and afterheat of the different materials of the TBM, the back shield and the support frame in tables 2.1.1.1.1-8 through 2.1.1.1.1-11 and figures 2.1.1.1.1-6 and 2.1.1.1.1-7.

Table 2.1.1.1.1-8: Total activity [Bq] of the different materials in the TBM-I

Time	EUROFER	Ceramics	Beryllium	Total
Shut-down	7.74E+16	4.14E+15	3.97E+16	1.21E+17
1.0 min	7.38E+16	2.18E+15	5.13E+14	7.65E+16
1.0 h	6.33E+16	3.94E+14	3.66E+14	6.40E+16
1.0 d	3.03E+16	1.94E+14	2.52E+14	3.07E+16
30.0 d	1.43E+16	1.15E+14	1.37E+14	1.45E+16
1.0 yr	5.30E+15	7.19E+12	1.25E+14	5.43E+15
10.0 yr	4.21E+14	4.60E+09	7.44E+13	4.95E+14
50.0 yr	7.34E+10	1.38E+09	7.85E+12	7.92E+12
100. yr	1.16E+10	1.25E+09	4.78E+11	4.91E+11

As compared to the direct nuclear heating at full power operation (table 2.1.1.1.1-3) one can see that the afterheat production is no more than 2% of direct power at shut-down, decreasing below 1% after one hour and below 0.1% after a few days. Major source of the afterheat is the EUROFER steel. Only at shut-down time there is a

significant contribution by beryllium (about 30% share) and the Li_4SiO_4 breeder ceramics (about 9% share). The maximum afterheat power density at shut-down amounts to 0.35, 0.11 and 0.21 W/cm^3 for EUROFER (first wall), beryllium (first wall protection) and the Li_4SiO_4 breeder ceramics (first 3 cm of breeder zone). Note that the afterheat generation in the support frame (table 2.1.1.1.1-10) exceeds that in the TBM by about a factor 3.

Table 2.1.1.1.1-9: Total afterheat P_{decay} of the different materials in the TBM-I .

Time	EUROFER	Ceramics	Beryllium	Total afterheat	
	P_{decay} [kW]	P_{decay} [kW]	P_{decay} [kW]	P_{decay} [kW]	$P_{\text{decay}}/P_{\text{direct}}$
shut-down	1.72E+01	2.60E+00	9.91E+00	2.97E+01	1.94E-02
1.0 min	1.67E+01	8.74E-01	6.17E-02	1.77E+01	1.15E-02
1.0 h	1.28E+01	2.67E-02	4.00E-02	1.29E+01	8.44E-03
1.0 d	2.35E+00	1.00E-02	1.27E-02	2.37E+00	1.55E-03
30.0 d	8.64E-01	4.76E-03	1.11E-03	8.70E-01	5.69E-04
1.0 yr	1.85E-01	2.25E-04	3.77E-04	1.85E-01	1.21E-04
5.0 yr	7.90E-03	6.33E-07	1.69E-04	8.07E-03	5.27E-06

Table 2.1.1.1.1-10: Total afterheat P_{decay} [kW] of the back shield and the TBM support frame.

Time	Back shield (EUROFER)	Support frame (SS-316LN)
shut-down	1.28E+00	1.05E+02
1.0 min	1.25E+00	9.83E+01
1.0 h	1.09E+00	7.17E+01
1.0 d	4.39E-01	9.73E+00
30.0 d	1.48E-01	6.35E+00
1.0 y	2.01E-02	1.22E+00

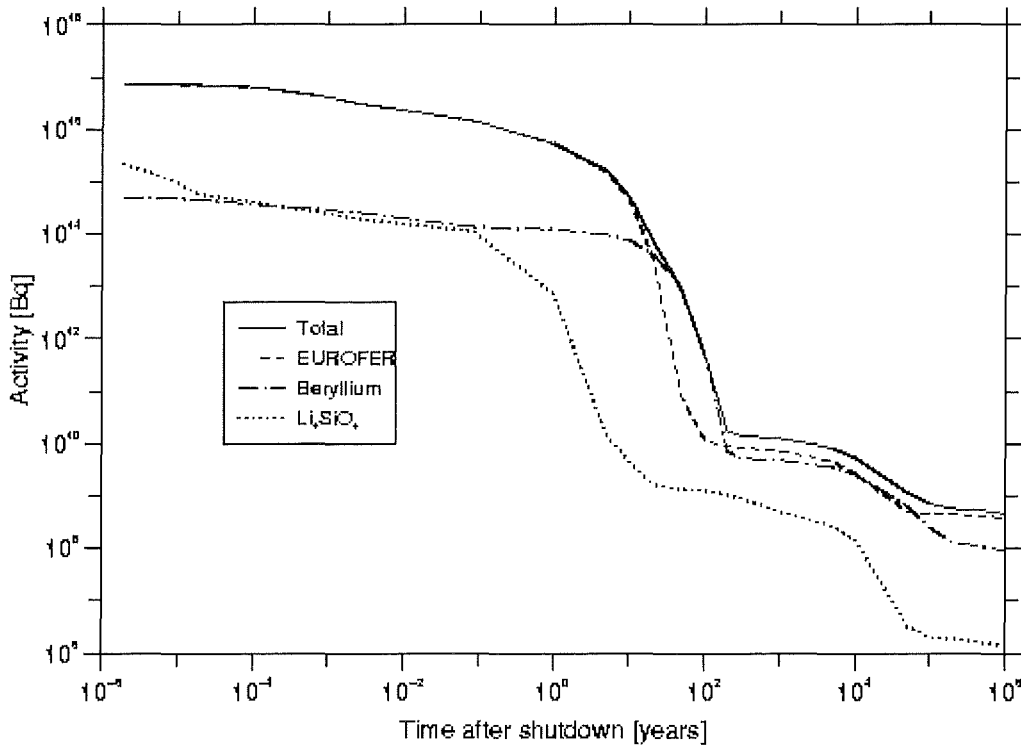


Fig. 2.1.1.1.1-6: Total activity inventory [Bq] in TBM-I as function of cooling time.

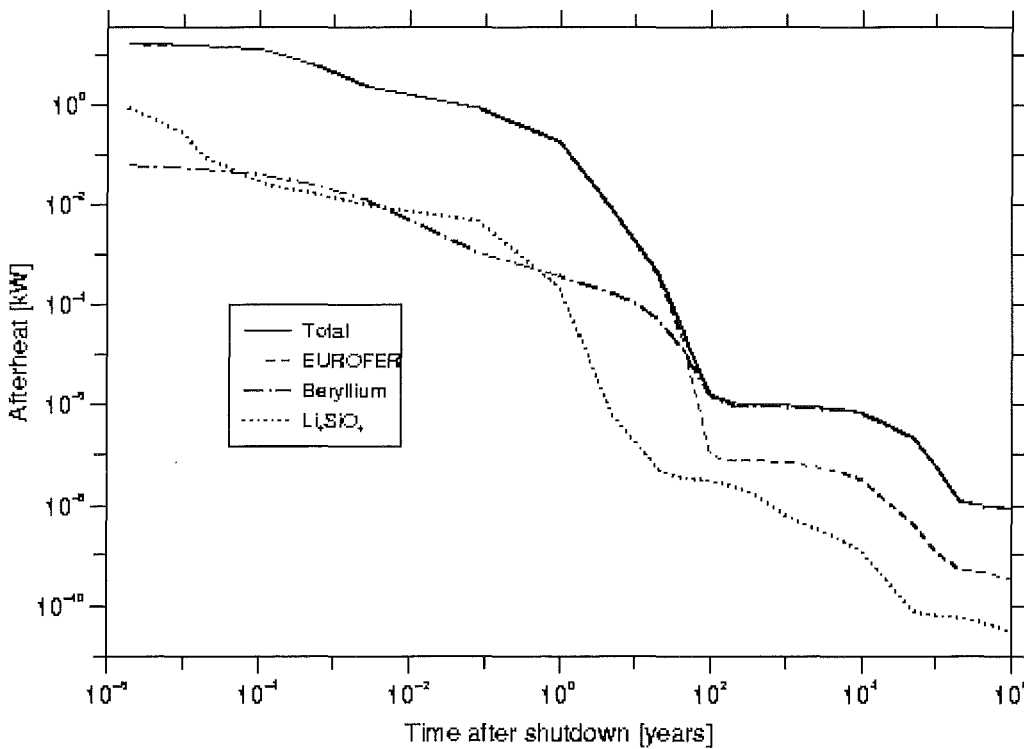


Fig. 2.1.1.1.1-7: Total afterheat power [kW] in TBM-I as function of cooling time.

Afterheat generation in MANET steel

Previously the Demo blanket design has been based on the martensitic steel MANET [2.1.1.1.1-11] as structural material. As the safety analysis described in section 2.1.1.18 also is based on the use of that steel, activation and afterheat calculations have been performed for the ITER test module additionally with MANET as structural material. Actually, there is no significant difference in the afterheat generation of the two steel variants in the relevant time period up to one day after shutdown (table 2.1.1.1.1-11). This is due to the fact that ^{56}Mn (being mainly produced by the $^{56}\text{Fe}(n,p)^{56}\text{Mn}$ -reaction) is the main contributor to the afterheat generation at those cooling times. The iron content of EUROFER and MANET, however, is very similar (87 vs. 89 w%). During the time period one day to about one year after shut-down, the LA steel EUROFER, however, produces more afterheat than MANET. This is caused by activation products (^{187}W , ^{182}Ta and ^{183}Ta) of the EUROFER constituents tungsten and tantalum.

Table 2.1.1.1.1-11: Total afterheat P_{decay} [kW] of the blanket structure of the TBM when using MANET as structural material.

Time	MANET	MANET/EUROFER
shut-down	1.72E+01	1.002
1.0 min	1.68E+01	1.002
1.0 h	1.19E+01	0.930
1.0 d	6.25E-01	0.266
30 d	3.95E-01	0.456
1.0 y	1.38E-01	0.747
5.0 y	1.57E-02	1.993

References

- [2.1.1.1.1-1] J. F. Briesmeister (ed.): MCNP - A General Monte Carlo N-Particle Transport Code, Version 4A, LA-12625-M, November 1993
- [2.1.1.1.1-2] FENDL/MC-1.0 - Library of Continuous Energy Cross-Sections in ACE Format for Neutron-Photon Transport Calculations with the Monte Carlo N-Particle Transport Code System MCNP4A, generated by R. E. MacFarlane by processing FENDL/E-1.0, Summary Documentation by A. B. Pashchenko, H. Wienke and S. Ganesan, IAEA-NDS-169, Rev. 3, November 1995
- [2.1.1.1.1-3] U. Fischer, M. Dalle Donne: Three-dimensional Neutronics Analysis of the European HCPB Blanket Test Module in ITER, 4th Int. Symp. on Fusion Nuclear Technology, Tokyo, Japan, April 6 - 11, 1997.
- [2.1.1.1.1-4] H. Tsige-Tamirat: Aktivierung von Brutmaterialien im Blanket des (d,t)-Fusionsreaktors, Forschungszentrum Karlsruhe, Wissenschaftliche Berichte FZKA 5855, April 1997; see also: H. Tsige-Tamirat: Three-dimensional Activation Analyses for Demo Type Fusion Reactor Blankets, Proc. of the 19th Symp. on Fusion Technology, Lisbon, Portugal, 16-20 Sept. 1996, Vol. 2, p.1559-1562, Elsevier 1997
- [2.1.1.1.1-5] R. A. Forrest , J.-Ch. Sublet: FISPACT 4 User Manual, UKAEA FUS 287, July 1995.
- [2.1.1.1.1-6] J. Kopecky, D. Nierop: The European Activation File EAF-4, Report ECN-C-95-072, December 1995.
- [2.1.1.1.1-7] B. van der Schaaf, ECN Petten, personal communication, September 1997.
- [2.1.1.1.1-8] Brush-Wellmann Material Specification for Beryllium Pebbles.
- [2.1.1.1.1-9] Ch..Adelhelm, FZK-IMF, personal communication, November 1996.
- [2.1.1.1.1-10] J.-Ch. Sublet: Elemental Composition of Structural Materials Including Impurities and Tramp Elements, SEAFP/R-A6/2(93), June 1993.
- [2.1.1.1.1-11] M. Schirra et al.: Untersuchungen zum Vergütungsverhalten, Umwandlungsverhalten und der mechanischen Eigenschaften am martensitischen Stahl 1.4914 (NET-Charge MANET-1), KfK-4561, Juni 1989

2.1.1.1.2 Thermohydraulic and thermal design

Ref. [2.1.1.1.2-1] illustrates in detail the methods of the thermohydraulic and mechanical stress calculations for the DEMO blanket. The present approach extends these methods to achieve a more accurate representation of blanket conditions.

1. The computational fluid dynamics (CFD) code FIDAP has been applied in modelling the 3D interaction of blanket structure and helium coolant to produce an accurate prediction of fluid temperatures along the path of flow. In particular, results of a FW model containing part of the breeding region have shown fluid temperature increases for that breeding zone differing from values according to ref. [2.1.1.1.2-1] and have led to a moderate redistribution of the helium mass flows in the six zones of the breeding region.
2. A finite-element (FE) analysis of a radial-toroidal blanket slice, including the manifold and covering six FW channels in poloidal height for reasons of symmetry has been added mainly for the sake of more accurate stress calculations, but gives the most complete view of the overall blanket temperature distribution.
3. The stationary-operation performance of the blanket-box cap has been analysed in some detail using a 2D FE model. This analysis is limited to the cap design selected for TBM-II (see Fig. 2.1.1.1-2).

2.1.1.1.2.1 Calculational assumptions

The ground rules can be summarized as follows:

1. The effective thermal conductivity of the bed of Li_4SiO_4 pebbles has been updated with recent measurements at FZK [2.1.1.1.2-2]. For the bed of 0.25 - 0.63 mm Li_4SiO_4 pebbles in helium the measured effective thermal conductivity data may be correlated by the equation $k_e [\text{W/mK}] = 0.768 + 4.957 \cdot 10^{-4} T [^\circ\text{C}]$. The heat transfer coefficient between pebble bed and containment wall obeys the correlation $\alpha [\text{W/m}^2\text{K}] = 0.4108 + 3.0321 \cdot 10^{-3} T^{0.6623} [^\circ\text{C}]$.
2. The effective thermal conductivity of the binary beryllium bed (1.5 - 2.3 mm and 0.1 - 0.2 mm pebbles) has been obtained by interpolating the experimental results of similar beryllium and Li_4SiO_4 pebble beds [2.1.1.1.2-3]. The correlations used are:

$$k_e = 6.235 \left\{ 1 + 353 \left[\alpha_{Be}(T_m - T_0) - \alpha_{St}(T_{St} - T_0) + \left(\left(1 + \frac{\Delta V}{V} \right)^{1/3} - 1 \right) \right] \right\}$$

$$\alpha = 3308 \left\{ 1 + 383.1 \left[\alpha_{Be}(T_m - T_0) - \alpha_{St}(T_{St} - T_0) + \left(\left(1 + \frac{\Delta V}{V} \right)^{1/3} - 1 \right) \right] \right\} \cdot [1 + 9.239 \cdot 10^{-4} T_w]$$

where

$K_e [\text{W/mK}]$	= effective thermal conductivity of the bed
$\alpha [\text{W/m}^2\text{K}]$	= heat transfer coefficient between pebble bed and containment wall
$T_m [^\circ\text{C}]$	= average temperature of the pebble bed
$T_0 [^\circ\text{C}]$	= temperature at which the bed filling operation has been performed \approx room temperature

T_{St} [°C]	= average temperature of the bed containing wall of steel
T_w [°C]	= local wall temperature
α_{Be} [K ⁻¹]	= thermal expansion coefficient of beryllium at average between T_0 and T_m [2.1.1.1.2-4]
α_{St} [K ⁻¹]	= thermal expansion of T91 at average between T_0 and T_{St} [2.1.1.1.2-5]
$\Delta V/V$	= volume swelling of beryllium under neutron irradiation

For the present calculations the Beginning Of Life (BOL) situation has been considered where the highest pebble bed temperatures are expected, thus $\Delta V/V=0$. This is a pessimistic assumption as the beryllium swelling increases the bed thermal conductivity. Furthermore in the present calculation the term in T_w for the calculation of the wall heat transfer coefficient α has been neglected to simplify the calculations. This term does not have a large effect on α and in any case it is pessimistic to neglect it.

The power density distribution has been obtained by the three-dimensional neutronic calculations of Section 2.1.1.1.1. For the calculation of the blanket power, and coolant temperatures, an average heat flux on the first wall of 0.25 MW/m² has been assumed. For first-wall maximum-temperature calculations, these coolant temperatures have been employed even though a surface heat flux of 0.5 MW/m², conceivable as a local hot spot, has been applied.

2.1.1.1.2.2 Models

Two types of FE code have been employed for the present calculations. The fluid dynamics code FIDAP [2.1.1.1.2-6] has been applied to model the interaction of blanket structures and helium coolant and produce for both stationary and transient operation structural temperature distributions and fluid temperatures along the path of flow. Of these results, mainly fluid temperatures were input into ABAQUS [2.1.1.1.2-7] FE models to calculate more detailed structural temperature distributions and eventually, in Section 2.1.1.1.3, stresses in the blanket.

Thermohydraulic models

The need of a thermohydraulic model to mesh the fluid area and neighbouring structures with a fine mesh means that a full radial-toroidal slice of the blanket is too large to be treated in a single model. For this reason, the radial-toroidal blanket cross section is cut into a FW region and six U-shaped breeding zones (BZ) that neighbour groups of cooling channels and coincide with those in ref. [2.1.1.1.2-1].

FW/BZ₁ This 3D model of the first wall covers both the FW and the first two channels of the BZ to ensure a good representation of FW/BZ thermal interaction. In poloidal direction, the model covers six FW channels, four cooling plates and two pebble beds of both Li₄SiO₄ and Beryllium. A constant-velocity fluid model is employed; the alternating flow directions of the two helium systems and thermal fluid links according to the flow path have been taken into account.

BZ_i All six parts of the breeding zone are modelled separately by models that are geometrically affine, achieved through replacing fluid channels with an equivalent fluid layer model. The models are quasi-2D, i.e. while they extend radially they do not have any variation in this direction. Their poloidal extension is from the middle of one

beryllium bed to the middle of the next, with a periodic boundary condition for the poloidal heat flux reflecting the kind of symmetry found in the blanket. According to previous results of radial temperature profiles, the thermal interaction between the six models is not accounted for. The fact that in the blanket the BZ channels are passed in series with the FW channels is reflected by applying FW helium outlet temperatures as inlet temperatures to the BZ channels.

Thermohydraulic calculations produce important thermal boundary conditions for successive thermal and structural analyses. They produce structural temperatures, too. However, since the structural analysis models used below have a greater radial extension, they have been chosen to display structural temperature distributions whenever they were available.

Thermal/stress models

The two FE models implemented in ABAQUS differ in the part of blanket they cover. They will be called M2D and M3D here, reflecting the fact that one of them is 2D, the other 3D. The blanket-box cap model is called CAP2D.

M2D This model is described in ref. [2.1.1.1.2-1]. It is a radial-poloidal cross section of six FW channels poloidal height and the full radial depth of the breeding zone. The model takes stationary fluid temperatures at a given toroidal position as input, from both FW/BZ₁ and BZ₁ to BZ₆. Because of its fine mesh, the M2D gives a good impression of the radial-poloidal temperature distribution particularly in the pebble beds.

M3D The mesh of this model of a radial-toroidal blanket slice including the manifold is depicted in Figure 2.1.1.1.2-1. The poloidal height is six FW channels. To limit the model size the breeding zone has got a very coarse radial-toroidal mesh. BZ coolant channels could not be modelled. Instead, cooling plate steel temperatures from the BZ_i have been averaged and applied as thermal constraint. Fluid temperatures along the fully modelled FW channels have been taken from the FW/BZ₁ model.

CAP2D This is a 2D radial-poloidal model of the current design of the blanket box cap. In poloidal direction it covers the cap and the top beryllium bed of the blanket, while having full radial depth. It is worth noting that the FE model was derived inside the CAD system CATIA [2.1.1.1.2-8] from a CAD model of the cap; moreover, the thermal and stress analyses were carried out using the FE module [2.1.1.1.2-9] of the software.

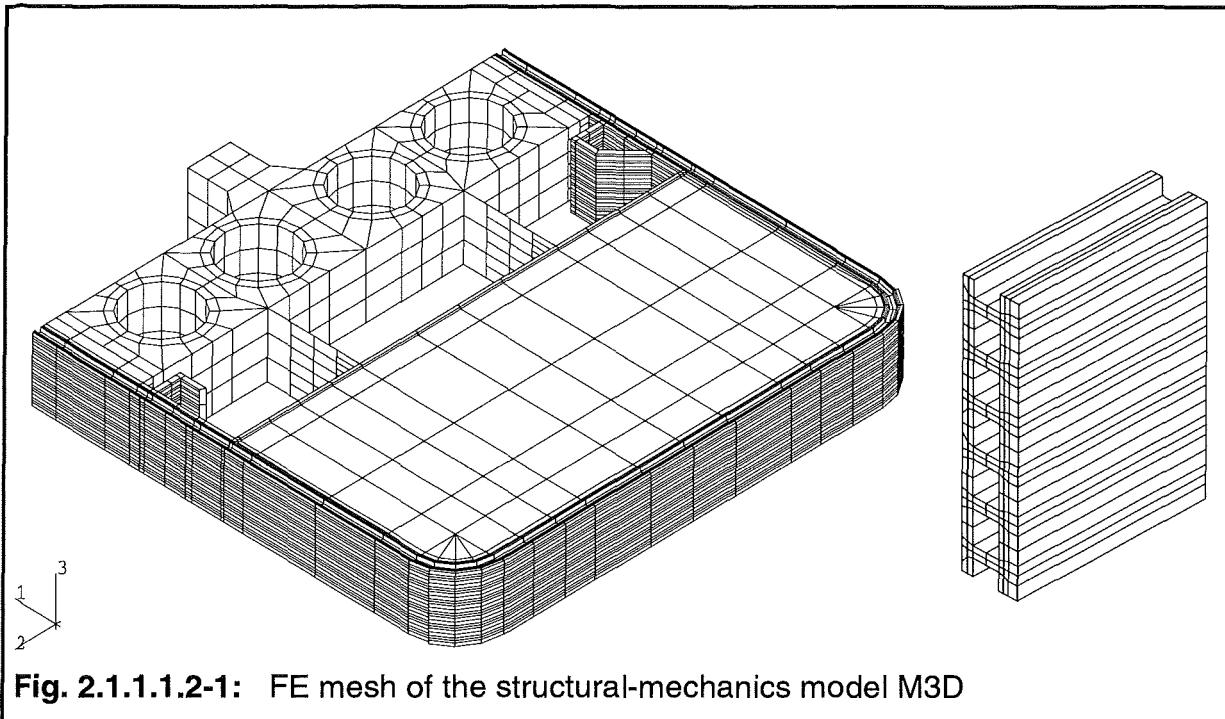


Fig. 2.1.1.1.2-1: FE mesh of the structural-mechanics model M3D

2.1.1.1.2.3 Results

Stationary temperatures

Thermohydraulic calculations for TBM-I, TBM-II and TBM-III have been carried out with the 3D model FW/BZ₁ and the 2D BZ₂ to BZ₆ to produce complete sets of steady-state coolant temperatures along the path of flow. Figure 2.1.1.1.2-2 displays coolant temperatures from FW/BZ₁ for TBM-I, with $T_{in}=250^{\circ}\text{C}$ and $T_{out}=350^{\circ}\text{C}$ design values and $T_{out,FW}=284^{\circ}\text{C}$ reflecting the heat distribution between FW and BZ.

Using stationary fluid temperatures, the ABAQUS models M2D and M3D were employed to predict module temperature distributions. Figure 2.1.1.1.2-3 shows the full-slice temperature distribution from M3D for TBM-I. For the toroidal position 300mm off the centre, radial-poloidal distributions for all concepts TBM-I to TBM-III are displayed in Figures 2.1.1.1.2-4 to 2.1.1.1.2-6. Table 2.1.1.1.2-1 compares key temperatures, i.e. maximum temperatures of pebble beds and structural material, to DEMO values. In all the cases Li-6-enrichment of 90% has been chosen for the TBMs, while an enrichment of 40% is sufficient for DEMO. In case of the module TBM-I, with exactly the DEMO blanket geometry, the maximum FW temperature approaches that of DEMO. However, the temperatures in the blanket are considerably lower than in DEMO. This is due to the fact that the neutron load, and thus the power densities, are considerably smaller than in DEMO, while the maximum surface heat flux on the first wall is the same (0.5 Mw/m^2).

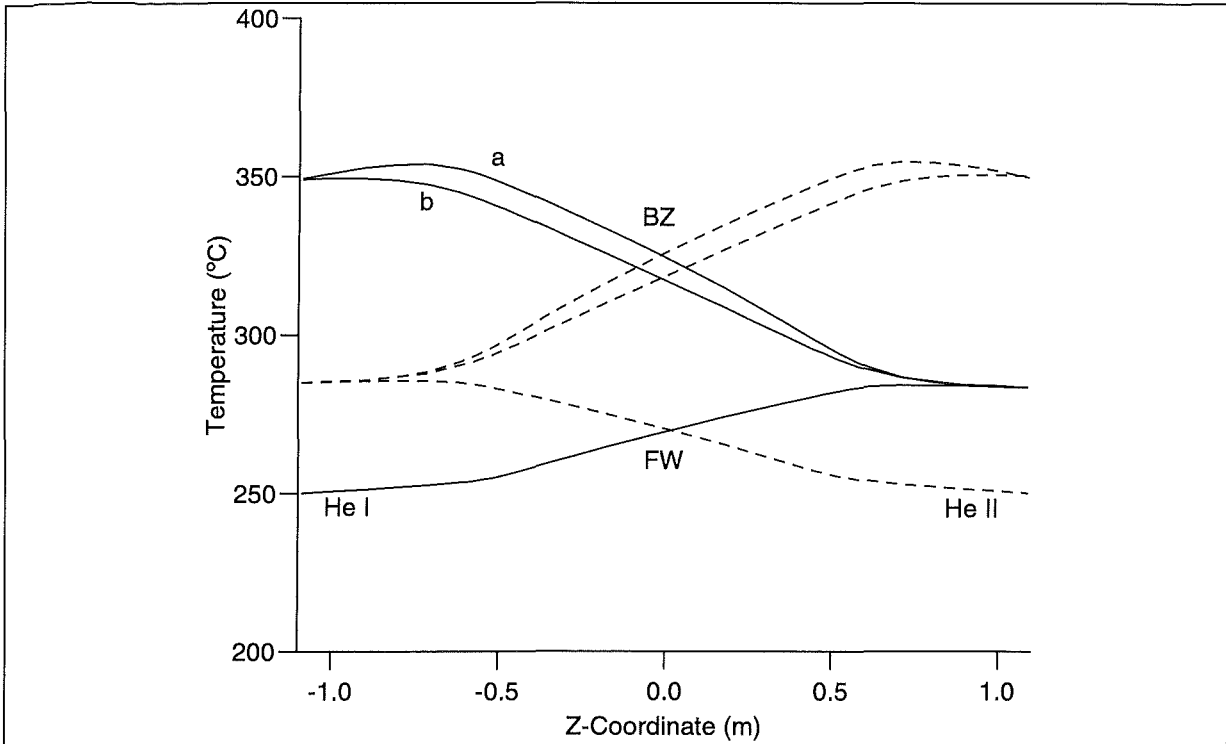


Fig. 2.1.1.1.2-2: Coolant temperatures along the path of flow (TBM-I; a: BZ channel 1, b: BZ channel 2)

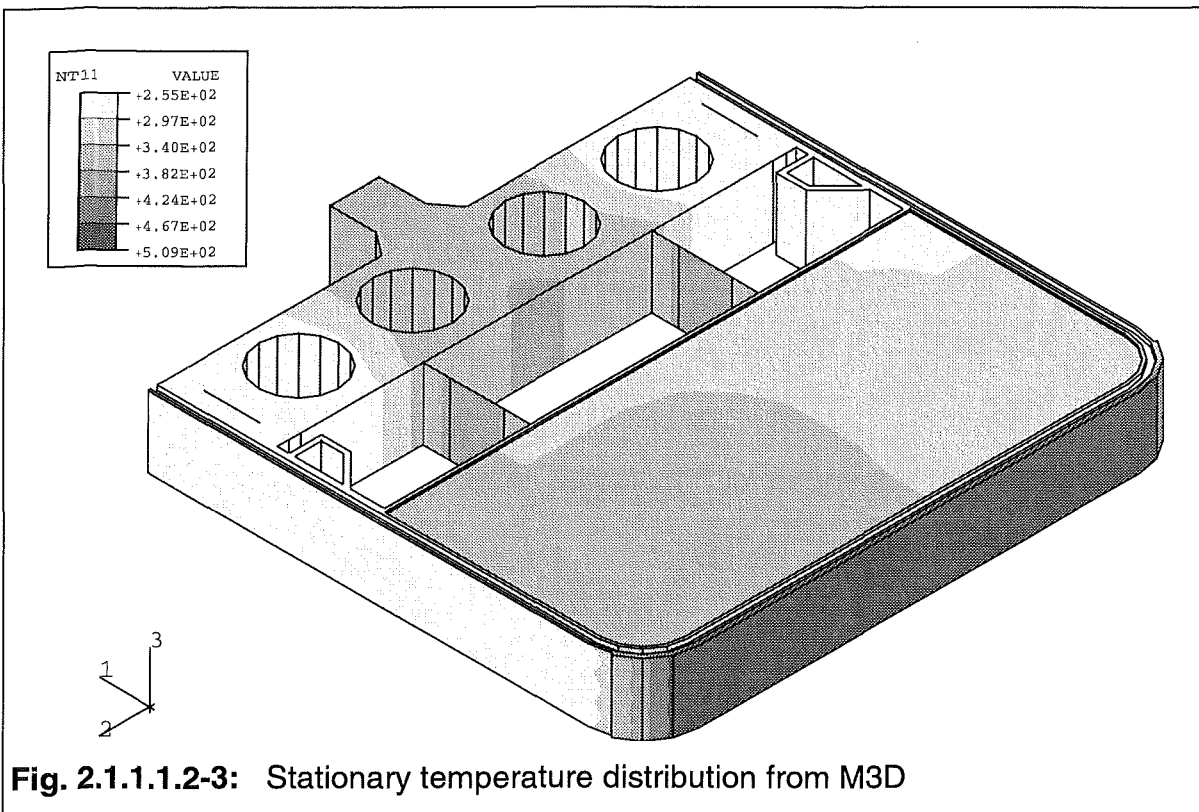


Fig. 2.1.1.1.2-3: Stationary temperature distribution from M3D

As a consequence of the increased bed thickness the maximum ceramic-bed temperature in TBM-II amounts to 837°C, which is close to the DEMO value of 879°C.

Recent neutronic calculations put thermal loads during the EPP close to those expected for TBM-I and lead to almost identical temperatures for TBM-I and TBM-III.

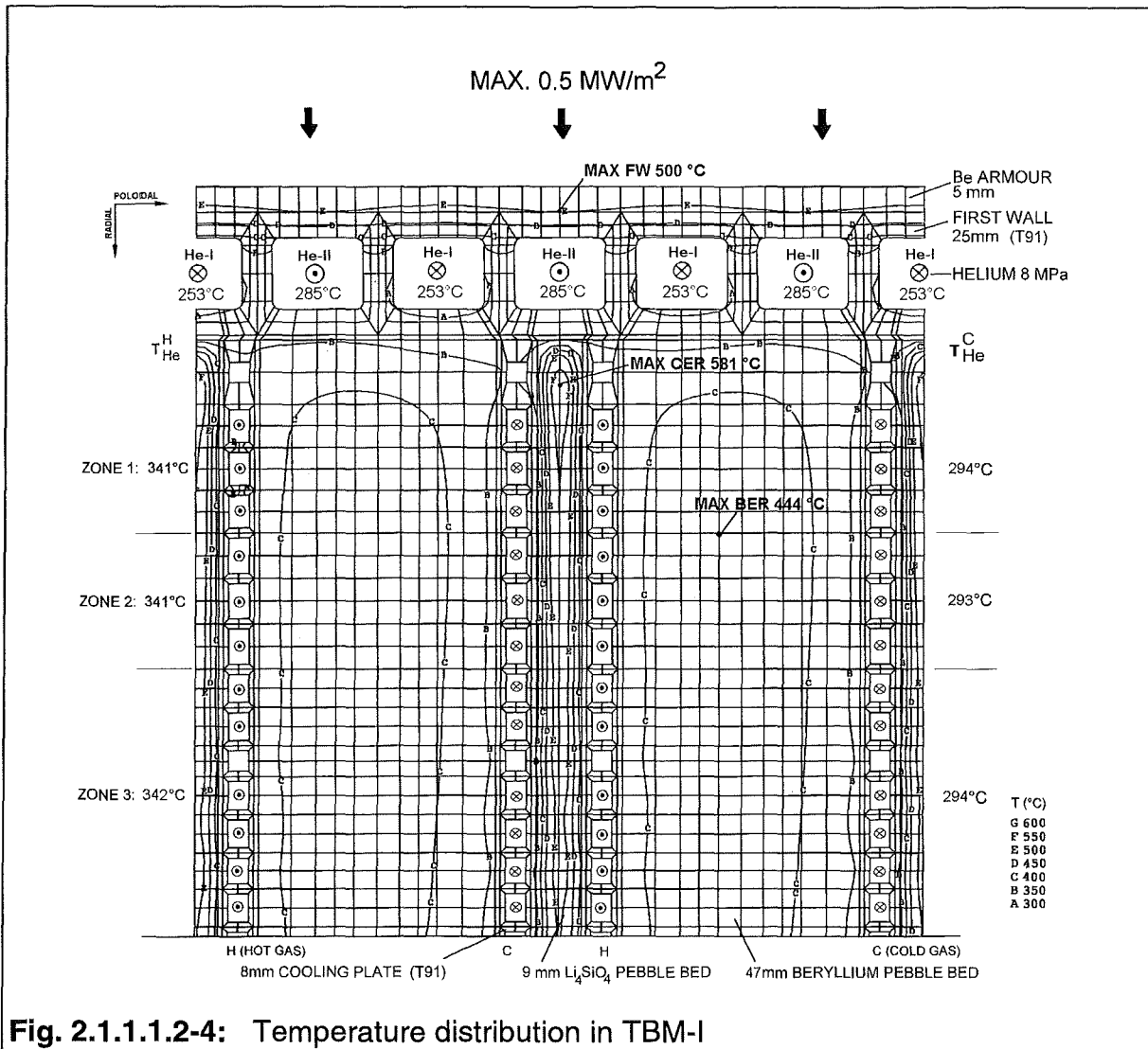


Fig. 2.1.1.2-4: Temperature distribution in TBM-I

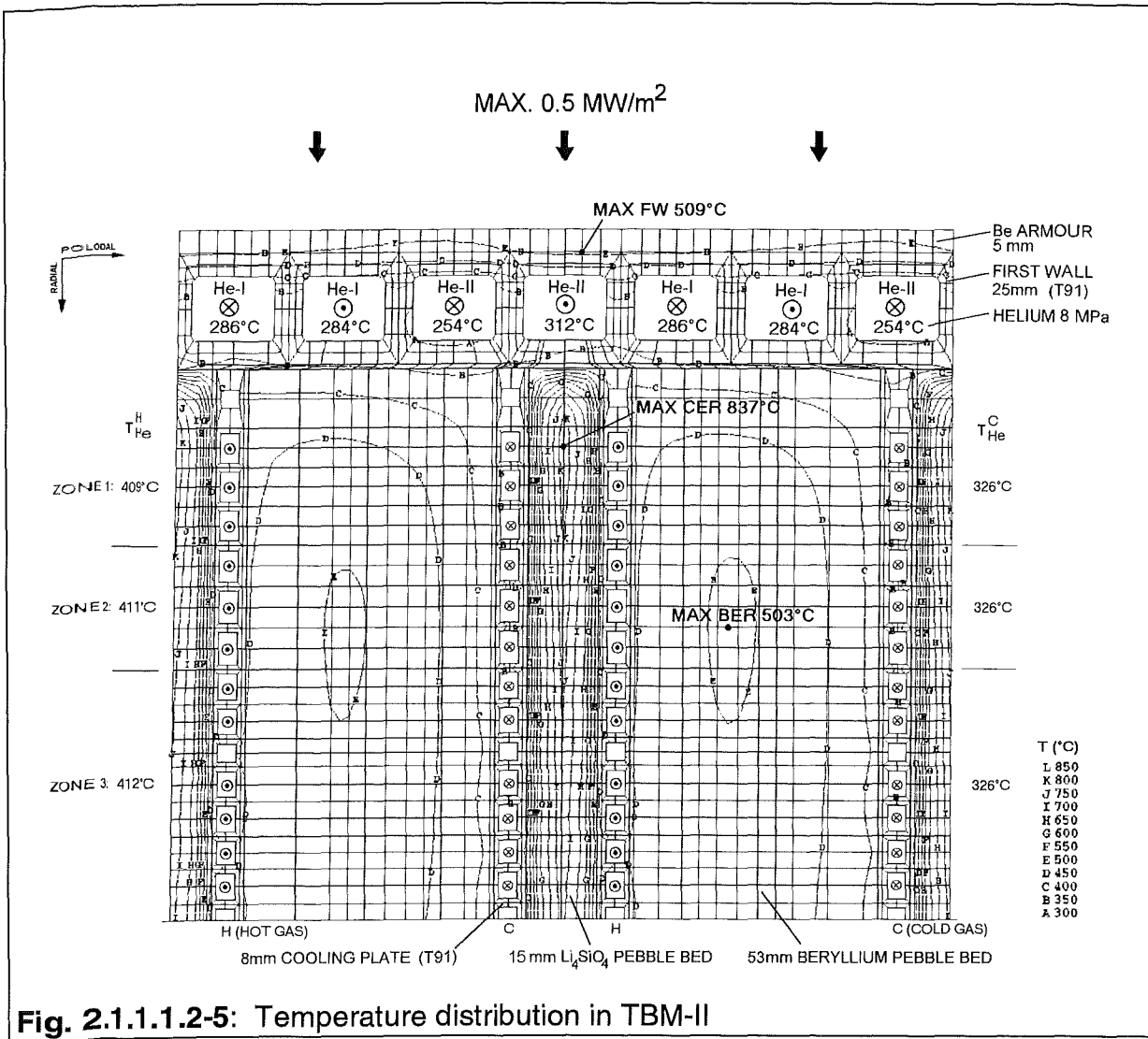


Fig. 2.1.1.1.2-5: Temperature distribution in TBM-II

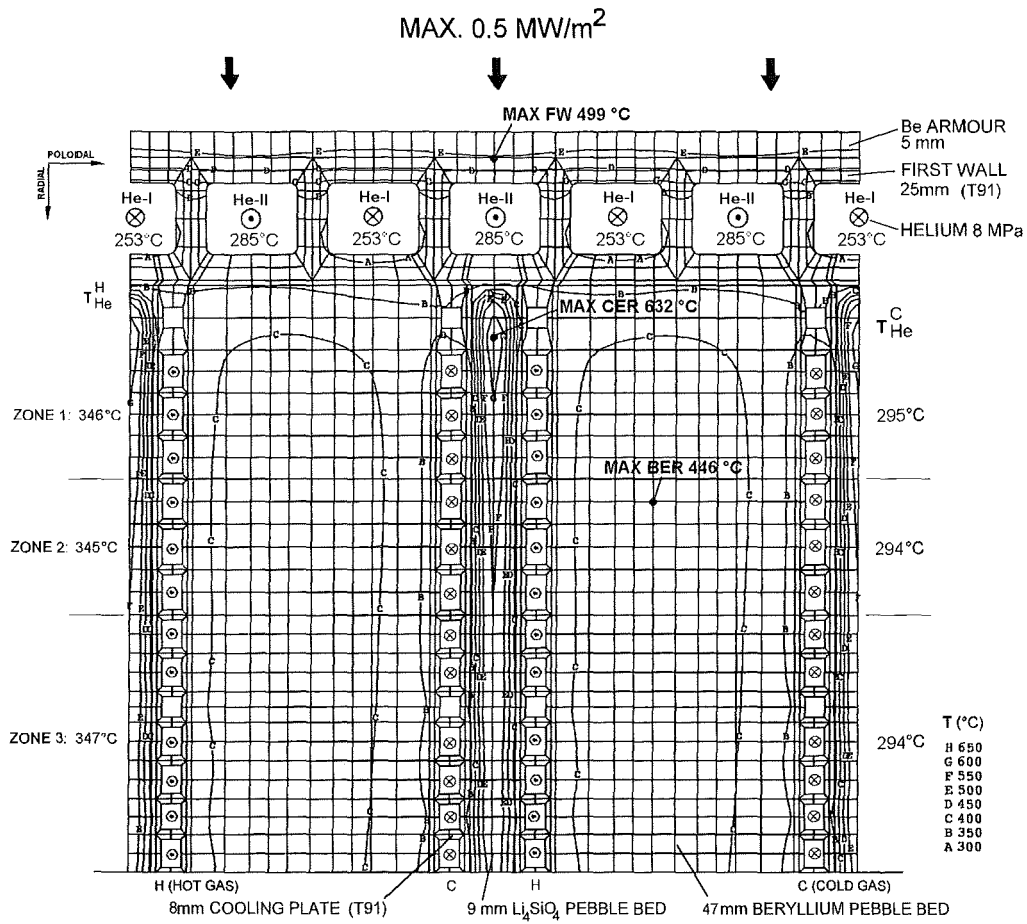


Fig. 2.1.1.2-6: Temperature distribution in TBM-III

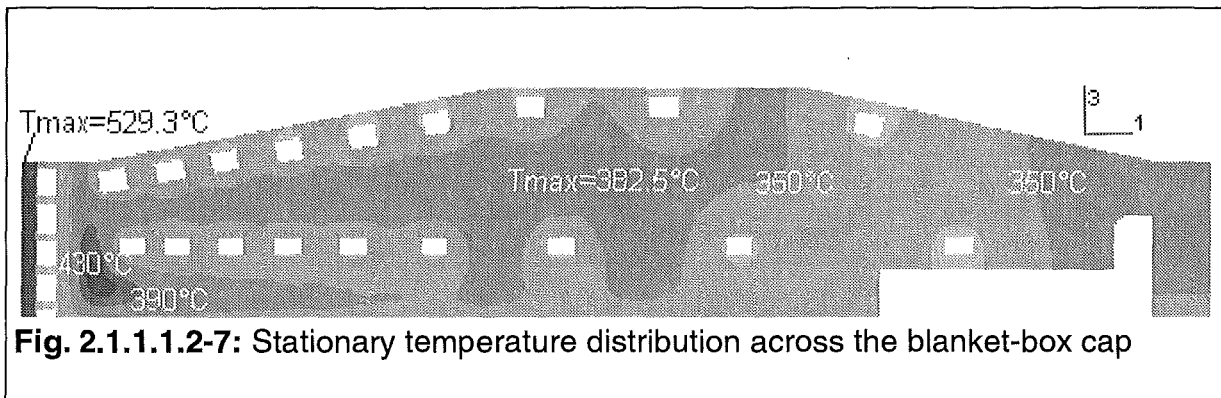
Table 2.1.1.1.2-1: Results of the thermohydraulic calculations for the three TBMs

	ITER Test Module			DEMO
	BPP		EPP	
	TBM-I	TBM-II	TBM-III	Blanket
Li ⁶ -enrichment	90 %	90 %	90 %	40 %
Total Power [MW] (surface flux included)	1.81	1.82	1.85	2500
Total helium mass flow [kg/sec]	3.5	2.1	3.5	2400
Helium pressure [MPa]	8	8	8	8
Helium pressure drop in TBM [MPa]	0.18	0.20	0.18	0.24
Helium inlet/outlet temp. [°C]	250/350	250/420	250/352	250/450
Max. power density [MW/m ³] in				
structural material	11	11	10	25
beryllium pebble bed	5	5	5	14
ceramic pebble bed	20	16	24	43
Maximum temperatures [°C]				
structural material	500	509	499	502
beryllium pebble bed	444	503	446	624
ceramic pebble bed	581	837	632	879

Blanket-box cap

Fluid temperatures were taken to be 270.2°C in the FW channels (from analysis of TBM-I above) and 280°C in the cap channels, assuming that the cap is being cooled in parallel with the FW channels. The thermal loading stems from heat sources in the structure and FW surface heat flux of 0.5MW/m². The temperature of the bottom side of the Be bed has been assumed to be equal to that of the neighbouring cooling plate; this temperature of 345°C was taken from the analysis of TBM-I (above).

Fig. 2.1.1.1.2-7 displays the temperature distribution in the cap, with T=529.3°C the absolute temperature maximum in the FW Beryllium and T=382.5°C the maximum in the cap itself. While the Be bed has been part of the model for its role as a volume heat source, bed temperatures are biased, and a temperature step between Be and steel is missing, due to the omission of the Be-bed/steel heat transfer coefficient.



Temperatures during power cycling

Thermohydraulic calculations with the models FW/BZ₁ and BZ₂ to BZ₆, for TBM-I, have produced a set of transient coolant temperatures during an ITER power cycle. The power history for surface heat flux and internal heat sources is: linear power ramp-up within 50 s; full power burn time 1000 s; linear power ramp-down within 100s; pulse repetition time 2200 s. The coolant inlet temperature was kept constant at 250°C. Transient coolant temperatures at the outlets of FW and BZ channels are depicted in Figure 2.1.1.1.2-8.

Transient fluid temperatures as well as averaged cooling-plate steel temperatures were fed into M3D to determine the temperature distribution in the TBM-I during operational transients.

The result of this calculation is presented in Fig. 2.1.1.1.2-9. It shows the course of maximum temperatures in the Be coating, in the FW steel, in the manifold, the Li₄SiO₄ pebble bed, and the Be pebble bed. The main information derived from this figure and from the thermohydraulic calculation with FW/BZ₁ can be summarized as follows:

- The time constant of the plasma-facing front of the box is short in terms of a power cycle, e.g. 25 s after establishing full power the FW has reached 90% of the temperature rise under steady-state conditions.
- The maximum temperature gradient in the breeder material is 4.5 K/s during ramp-up, and 3.0 K/s during ramp-down.
- The manifold does not reach thermal equilibrium.

To investigate in more detail the blanket's time response to the cyclic power operation, a complementary FIDAP analysis has been carried out for different locations of the breeder zone, using the BZ_i. The results in Tab. 2.1.1.1.2-2 show, for the zones of the breeding region and for the power-up part of the cycle, pebble bed time constants based on the assumption that the beds have a first-order delay characteristic. The behaviour of the ceramic pebble bed is of particular interest: The time constant of between 40s and 50s obtained for the first five zones is comparable to the value obtained for the ramp-up (see above). The time constants increase with the distance from the FW. In the rear part a value of 314.9s for Be is the largest value attained. In general, it can be stated that the time constants of the BZ are sufficiently low for reaching thermal equilibrium in the TBM within the power cycling times specified for ITER.

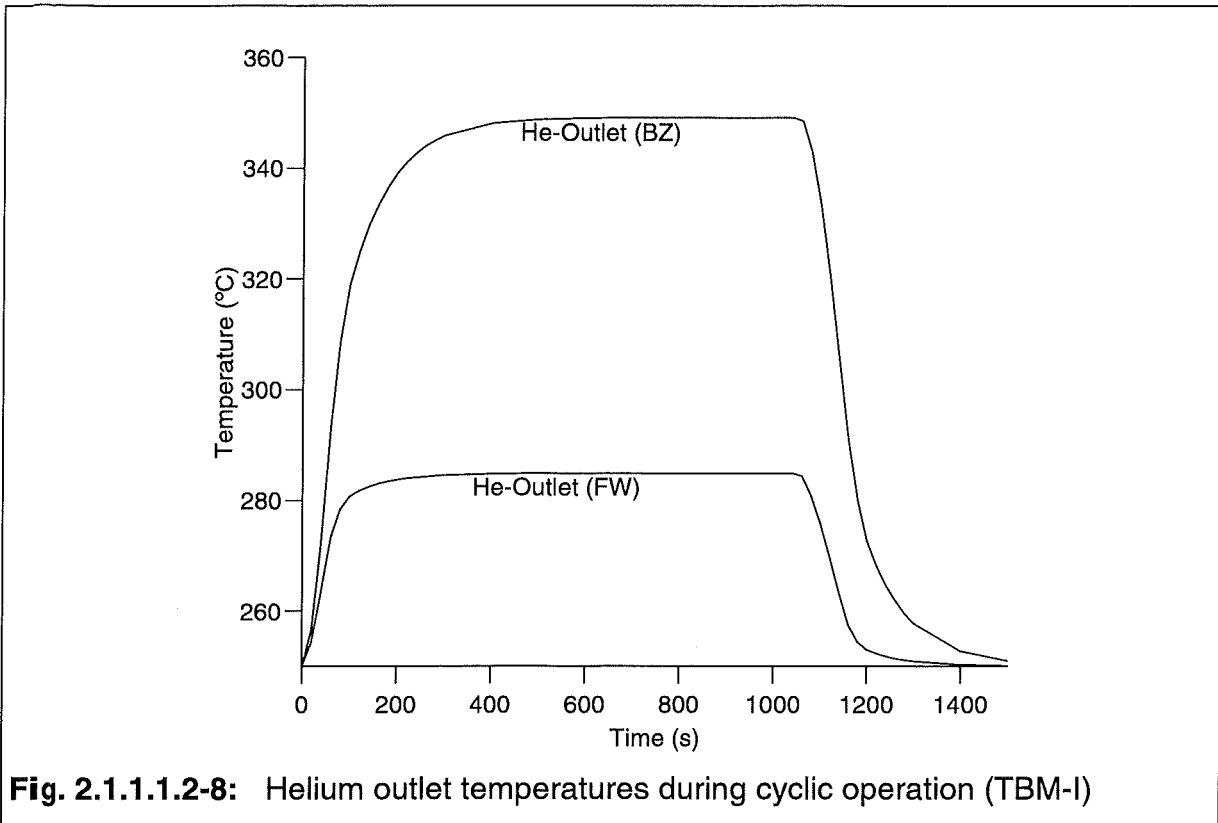


Fig. 2.1.1.1.2-8: Helium outlet temperatures during cyclic operation (TBM-I)

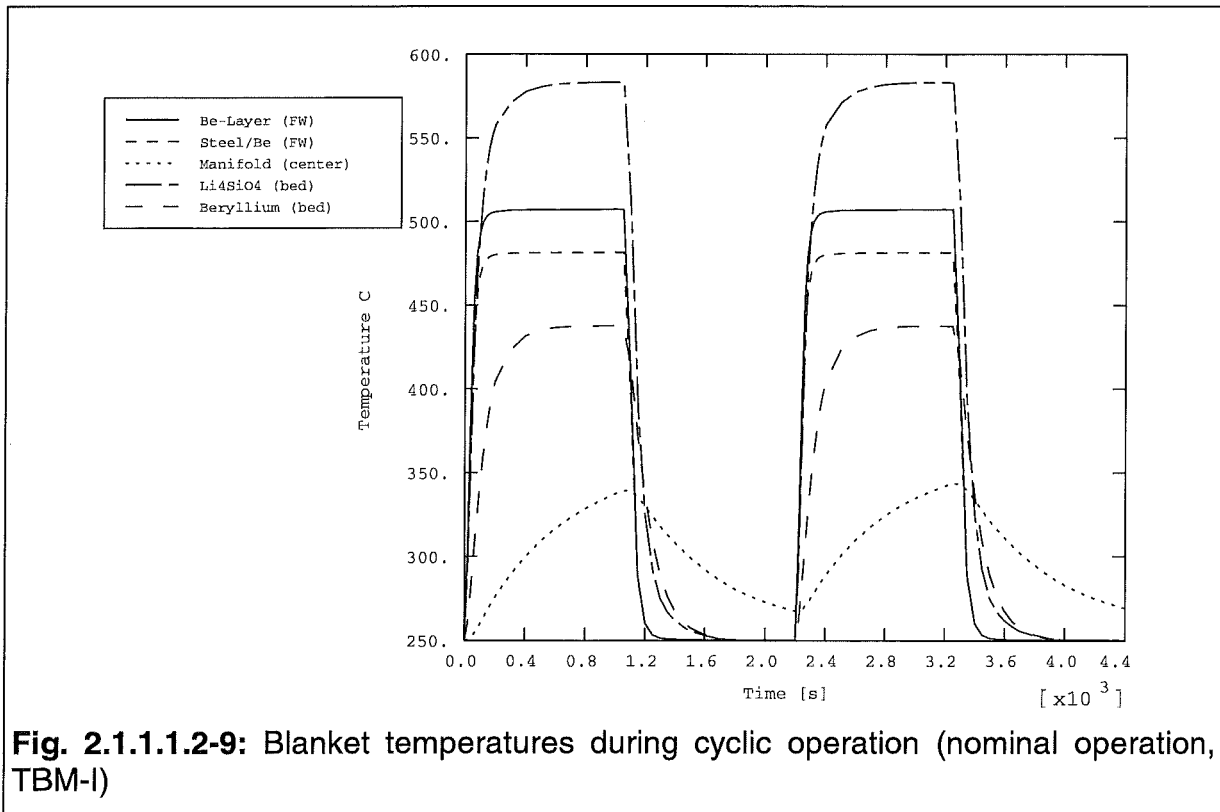


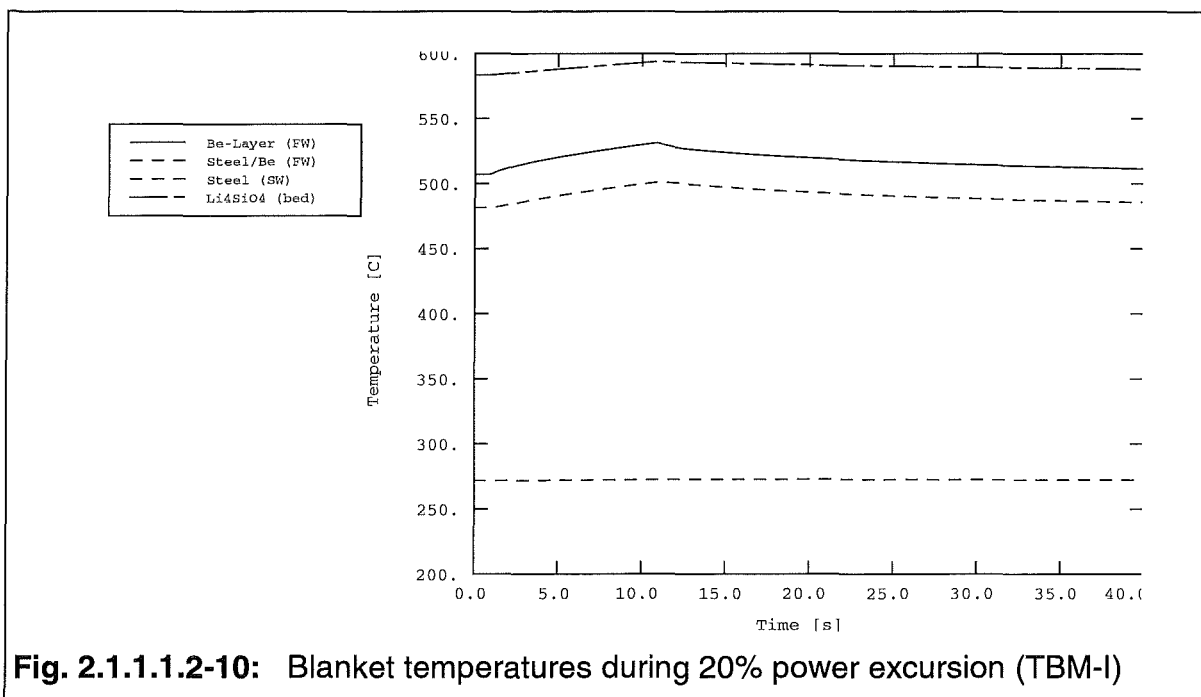
Fig. 2.1.1.1.2-9: Blanket temperatures during cyclic operation (nominal operation, TBM-I)

Table 2.1.1.1.2-2 Pebble-bed time constants

Zone	Distance from FW [mm]	Li ₄ SiO ₄ time constant [s]	Be time constant [s]
1	39.5	41.1	125
2	69.5	43.8	137.4
3	104.5	46.5	151
4	149	52.4	178.8
5	224	66	232.1
6	324	109.7	314.9

Temperatures during power excursion

Transient coolant and structural temperatures during an instantaneous power excursion (surface flux and internal heat sources) to 120% of nominal, and with a duration of 10s, were calculated using FW/BZ₁. The courses of maximum temperatures in the Be coating, in the FW steel, in the manifold, the Li₄SiO₄ pebble bed, and the Be pebble bed are shown in Fig. 2.1.1.1.2-10. The power excursion leads to a temperature increase of 22K and 25K in the FW (steel and beryllium, respectively), and 10K in the breeder zone. The steel temperature of the side wall is only slightly affected.

**Fig. 2.1.1.1.2-10:** Blanket temperatures during 20% power excursion (TBM-I)

References:

[2.1.1.1.2-1] P. Norajitra, Thermohydraulics Design and Thermomechanics Analysis of Two European Breeder Blanket Concepts for DEMO, FZKA 5580 (1995)

[2.1.1.1.2-2] M: Dalle Donne, Personal notes, Karlsruhe (July 1997)

[2.1.1.1.2-3] M: Dalle Donne et al., Heat Transfer and Technological Investigation on Mixed Beds of Beryllium and Li_4SiO_4 Pebbles, Proc. ICFRM 6, Stresa, Italy, Sept. 27 - Oct. 1 (1993).

[2.1.1.1.2-4] M. Kühle, Material Data Base for the NET Test Blanket Design Studies, Test Blanket Advisory Group, KfK, Feb. (1990)

[2.1.1.1.2-5] RCC-MR-Addendum May 1993, A3-18S, pp 451-476

[2.1.1.1.2-6] FIDAP 7.0 - FIDAP Users Manual, Fluid Dynamics International (1993)

[2.1.1.1.2-7] ABAQUS 5.6 - ABAQUS/Standard User's Manual, Vol. I to III, Hibbitt, Karlsson & Sorensen, Inc. (1996)

[2.1.1.1.2-8] CATIA - CAD-System, Ver.4, Dassault Systemes (1997)

[2.1.1.1.2-9] CATIA.ELFINI Solver, User's Reference Manual, Ver.4, Dassault Systemes (1997)

2.1.1.1.3 Structural Design

Various low-activation materials are being investigated within the European Fusion Technology Program. The final choice is likely to have mechanical properties similar to the martensitic steel T91, which has been defined by the Blanket Management Committee for the present calculations. The relevant properties of T91 are from ref. [2.1.1.1.3-1], [2.1.1.1.3-2] and [2.1.1.1.3-3].

While thermal loads have been analysed thoroughly in the previous section, little has been said about the mechanical loads. Nominal loads are a pressure of 8 MPa in the cooling system and 0.1 MPa in the blanket box. In case of accidental leakage from the cooling system inside the TBM the blanket box pressure is bound to rise substantially. Preliminary calculations suggest that the blanket box cap could withstand pressures of 2.5 MPa, requiring pressure load control by e.g. rupture disc or safety valve. This value of 2.5 MPa has been taken as the box accident pressure in the following analyses.

Two and three-dimensional calculations have been carried out with the FE computer code ABAQUS [2.1.1.1.3-4] and CATIA.ELFINI [2.1.1.1.3-5] and have been compared with the RCC-MR (see Appendix A) code.

The FE models M2D, M3D and CAP2D have been introduced in Section 2.1.1.1.2.2.

M2D

The results of the stationary 2D calculations are shown in Table 2.1.1.1.3-1 (TBM-I), Table 2.1.1.1.3-2 (TBM-II) and Table 2.1.1.1.3-3 (TBM-III). The admissible stresses according to RCC-MR are also included. The comparison of the results in all three tables shows that all calculated stresses are below the admissible limits. The distribution of the von Mises stresses (primary and primary plus secondary) in the FW of the three test modules are shown in the Figures 2.1.1.1.3-1 to 2.1.1.1.3-4.

M3D

A generalised plane strain condition was assumed for the nodes on the poloidal model boundaries, i.e. radial-toroidal cross-sections remain plane but may incline. The mechanics of the pebble beds were neglected for the structural calculations. Also, the Young's modulus for the plasma-facing Be layer was diminished onethousandfold to account for the sectioning of this layer, making its structural effect negligible.

Figure 2.1.1.1.3-5 shows, for the geometry of TBM-I and TBM-III, primary stresses and deformations for the assumed accident pressure in the box in addition to the 8MPa operating pressure in the cooling system. Maximum von Mises stresses of up to 65MPa occur at the coolant collector and the stiffening ribs between the breeding region and the manifold. Figure 2.1.1.1.3-6 illustrates, for TBM-I and 200s after the start of the power cycle, the deforming effect of combined primary stresses and thermal expansion. Overall stresses are now dominated, by a factor of 10, by secondary thermal stresses and are thus closely linked to the thermal history of the

module. A plot of von Mises stress histories, see Figure 2.1.1.1.3-7, puts the maximum stress value at the interface between steel and Be layer, close to the toroidal FW corner, at 420MPa 200s into the power cycle, thereafter reducing to a stationary value of 410MPa. Stresses in the side wall are closely linked to the temperature history of the manifold, rising continuously during burn time. However, the stress levels reached are considerably smaller than those in the FW.

A ten-second power excursion to 120% of nominal, starting off from stationary operation, has been analysed and found to increase maximum von Mises stresses by 10%, to 440MPa (see Fig. 2.1.1.1.3-8).

These 3D analyses have yet to be carried out for the cases of TBM-II and TBM-III.

While calculations for M2D are carried out at a location that agrees with the position of maxima in M3D, the values of stationary stress maxima vary by more than 10% (364/410 MPa). The three-dimensionality of M3D, further the fact that it is modelling structures that are bound to have an effect on FW stress, are reasons for the differences of M2D and M3D. They seem to suggest that results of M3D, that still lie within admissible stresses according to RCC-MC, are more credible. Having said that, it should be left to a detailed local analysis to determine accurately pattern and value of stress maxima.

CAP2D

As before, the mechanics of both Be pebble bed and FW Beryllium have been neglected. The mechanical constraint of the cap is imposed by fixing the FW bottom right-hand side node completely and all nodes of the bottom plane of FW and back wall in poloidal direction.

For the assumed accident in the box, 2.5MPa were applied to the inside of the cap in addition to 8MPa in the cooling channels. The primary stress distribution in Fig. 2.1.1.1.3-8 shows von Mises stresses of up to 232MPa at the joint of cap and FW, which is below the limit of $1.5 \cdot S_m$. Stresses at other locations are uncritical.

Secondary stresses in the operational hot cap depend critically on the type of boundary condition for the third dimension, i.e. perpendicular to the modelled cross section. The CATIA.ELFINI FE code allows applying a plane-strain condition together with specifying a reference temperature for the expansion in the unmodelled direction. This temperature was set at 335°C, the cap average known from the thermal analysis. Maximum von Mises stresses of 322MPa occur at the FW Be/steel interface, see Fig. 2.1.1.1.3-10, similar to previous blanket-box calculations.

Table 2.1.1.1.3-1 Results of the stress calculations for TBM-I (Basic Performance Phase)

- a) Maximum von Mises primary stresses [MPa]: occurs at the corners of the plasma side of the FW cooling channels ($T = 380\text{ }^{\circ}\text{C}$):

	$p_{\text{He}} = 8\text{ MPa}$	Admissible limit by RCC-MR (Class A)
Normal operation (pressure p_{He} only in cooling channels, no leakage)	56	267
Leakage from cooling plates (pressure in the whole blanket box controlled at 2.5 MPa)	82	267

- b) Maximum von Mises primary plus secondary stresses [MPa]: occurs at the FW interface between FW and plasma facing beryllium layer ($T = 494\text{ }^{\circ}\text{C}$):

	$p_{\text{He}} = 8\text{ MPa}$	Admissible limit by RCC-MR (Class A)
Normal operation (pressure p_{He} only in cooling channels, no leakage)	332	444
Leakage from cooling plates (pressure in the whole blanket box controlled at 2.5 MPa)	349	444

Table 2.1.1.1.3-2 Results of the stress calculations for TBM-II (Basic Performance Phase)

- a) Maximum von Mises primary stresses [MPa]: occurs at the corners of the plasma side of the FW cooling channels ($T = 396 \text{ }^\circ\text{C}$):

	$p_{\text{He}} = 8 \text{ MPa}$	Admissible limit by RCC-MR (Class A)
Normal operation (pressure p_{He} only in cooling channels, no leakage)	62	262
Leakage from cooling plates (pressure in the whole blanket box controlled at 2.5 MPa)	93	262

- b) Maximum von Mises primary plus secondary stresses [MPa]: occurs at the FW interface between FW and plasma facing beryllium layer ($T = 492 \text{ }^\circ\text{C}$):

	$p_{\text{He}} = 8 \text{ MPa}$	Admissible limit by RCC-MR (Class A)
Normal operation (pressure p_{He} only in cooling channels, no leakage)	329	446
Leakage from cooling plates (pressure in the whole blanket box controlled at 2.5 MPa)	339	446

Table 2.1.1.1.3-3 Results of the stress calculations for TBM-III (Extended Performance Phase)

- a) Maximum von Mises primary stresses [MPa]: occurs at the corners of the plasma side of the FW cooling channels ($T = 380\text{ }^{\circ}\text{C}$)

	$p_{\text{He}} = 8\text{ MPa}$	Admissible limit by RCC-MR (Class A)
Normal operation (pressure p_{He} only in cooling channels, no leakage)	56	267
Leakage from cooling plates (pressure in the whole blanket box controlled at 2.5 MPa)	82	267

- b) Maximum von Mises primary plus secondary stresses [MPa]: occurs at the FW interface between FW and plasma facing beryllium layer ($T = 493\text{ }^{\circ}\text{C}$)

	$p_{\text{He}} = 8\text{ MPa}$	Admissible limit by RCC-MR (Class A)
Normal operation (pressure p_{He} only in cooling channels, no leakage)	331	445
Leakage from cooling plates (pressure in the whole blanket box controlled at 2.5 MPa)	347	445

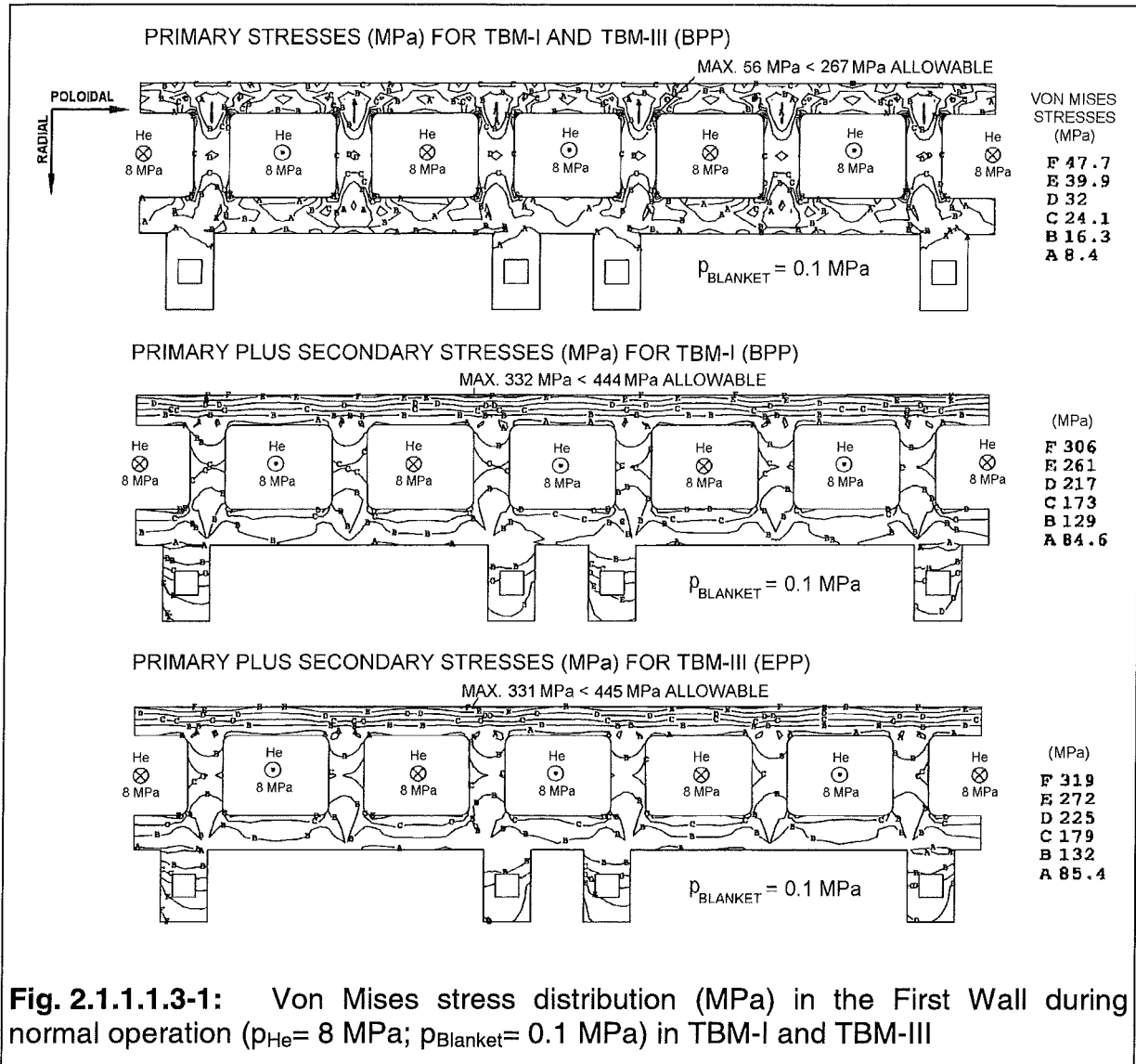
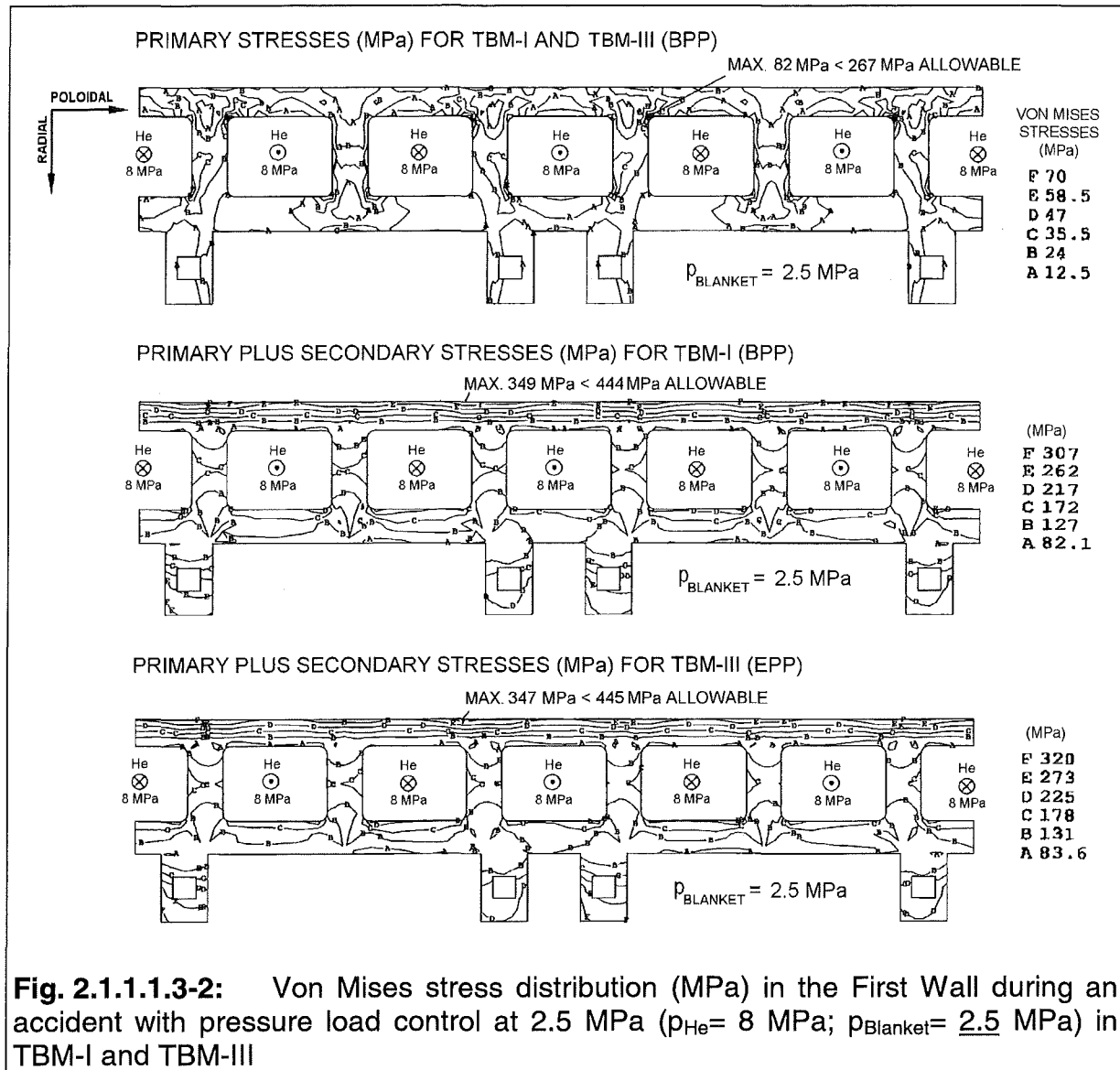
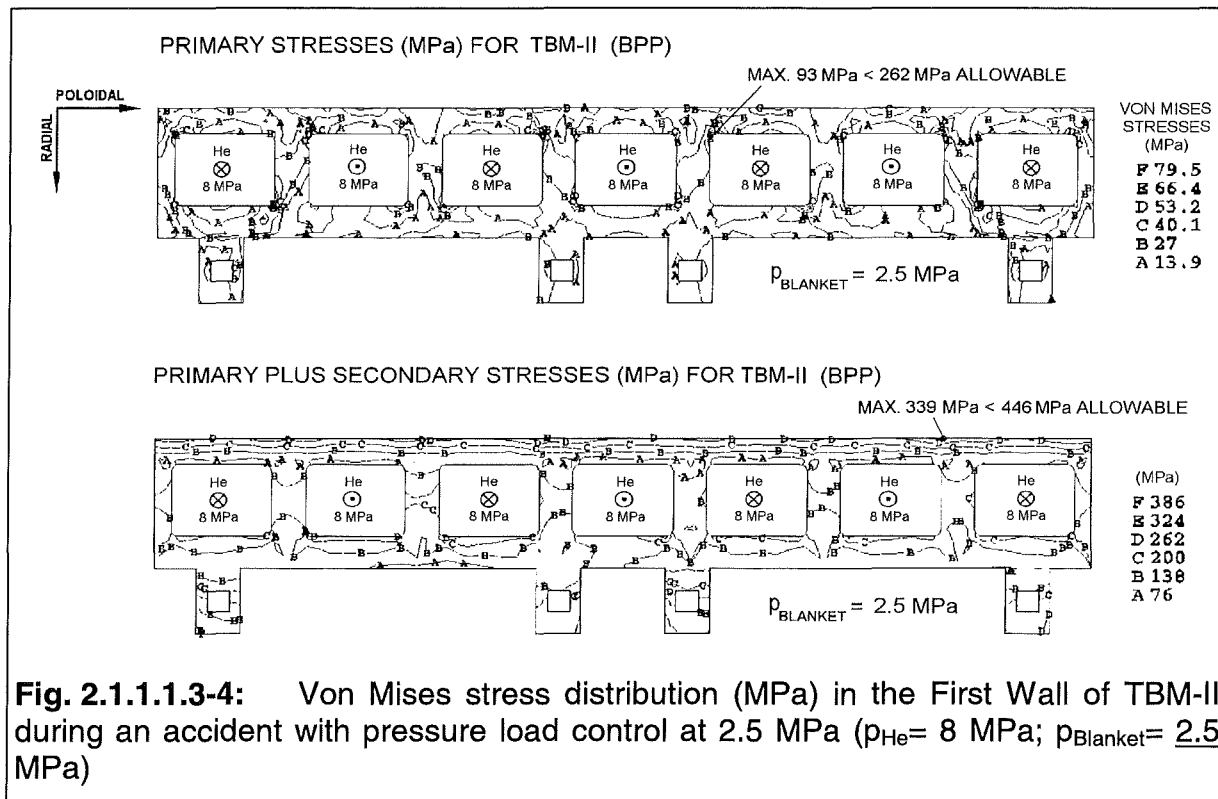
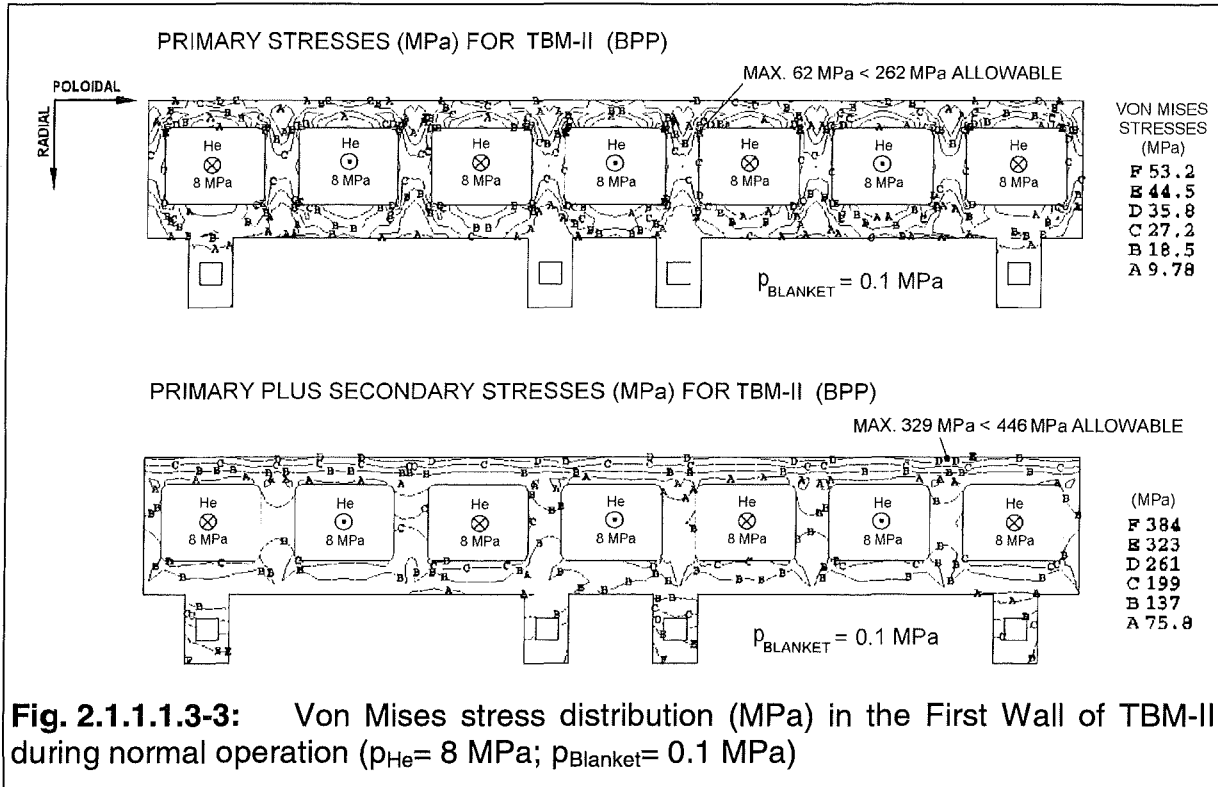
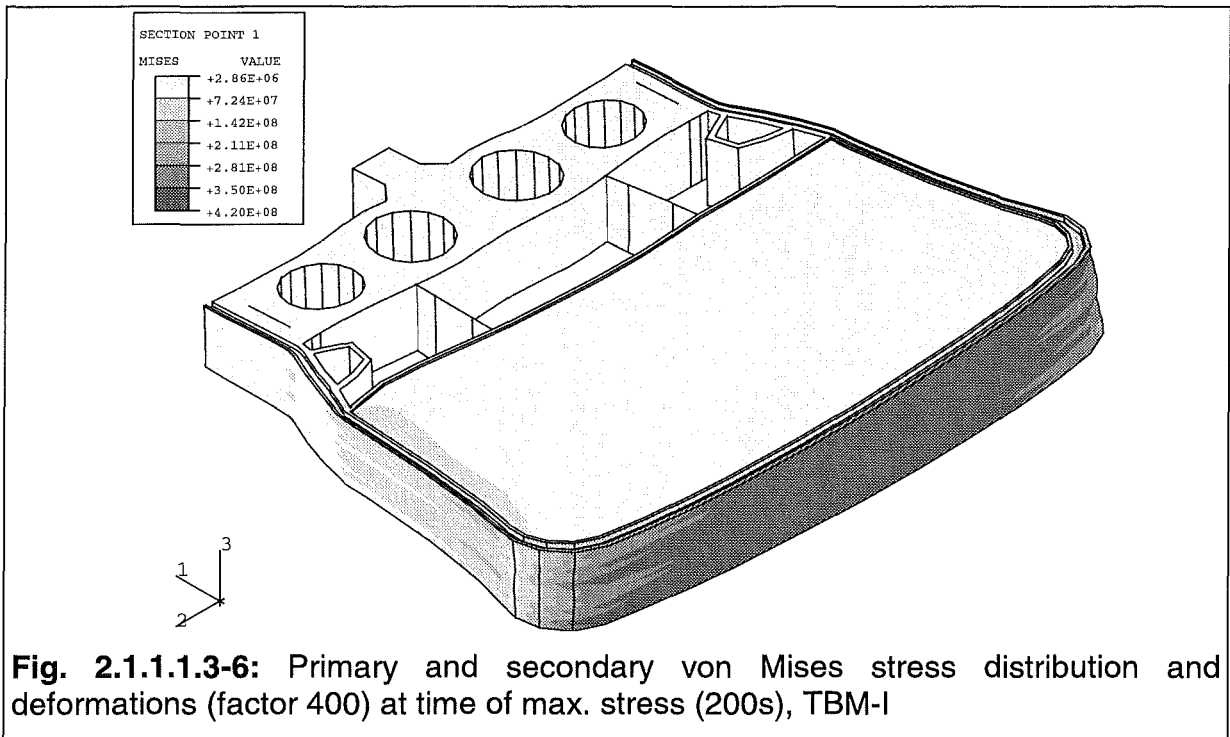
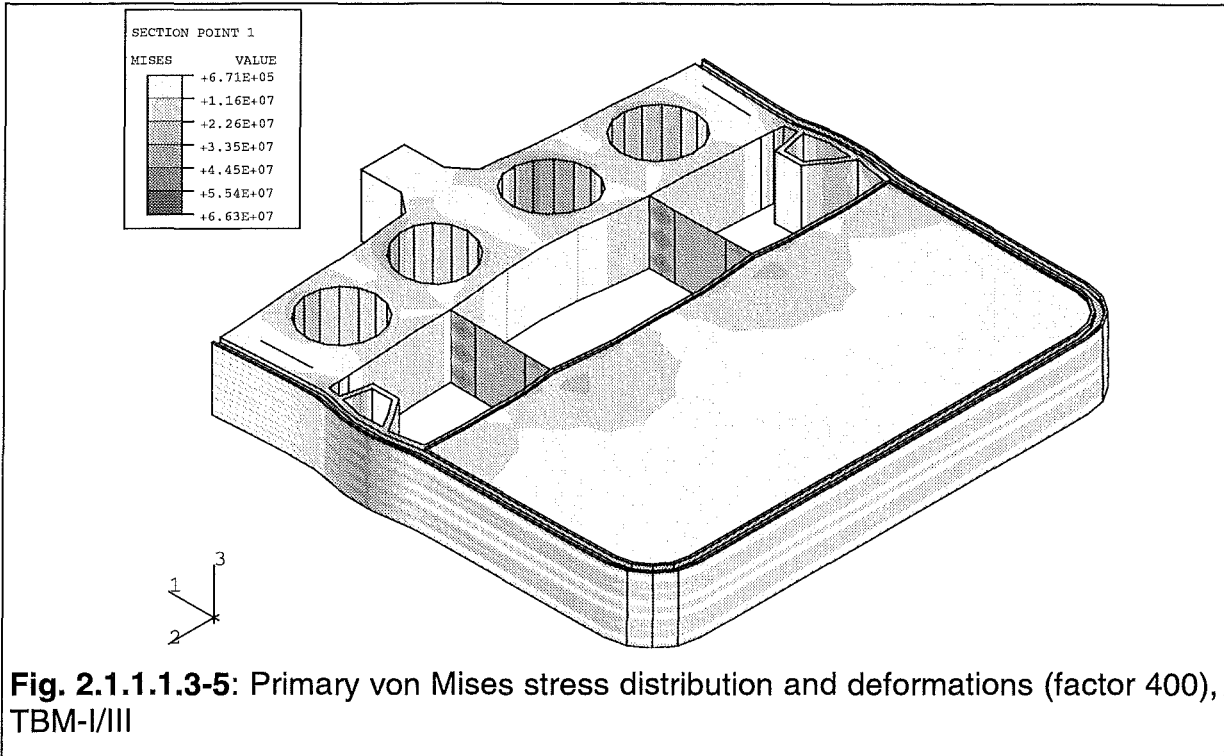
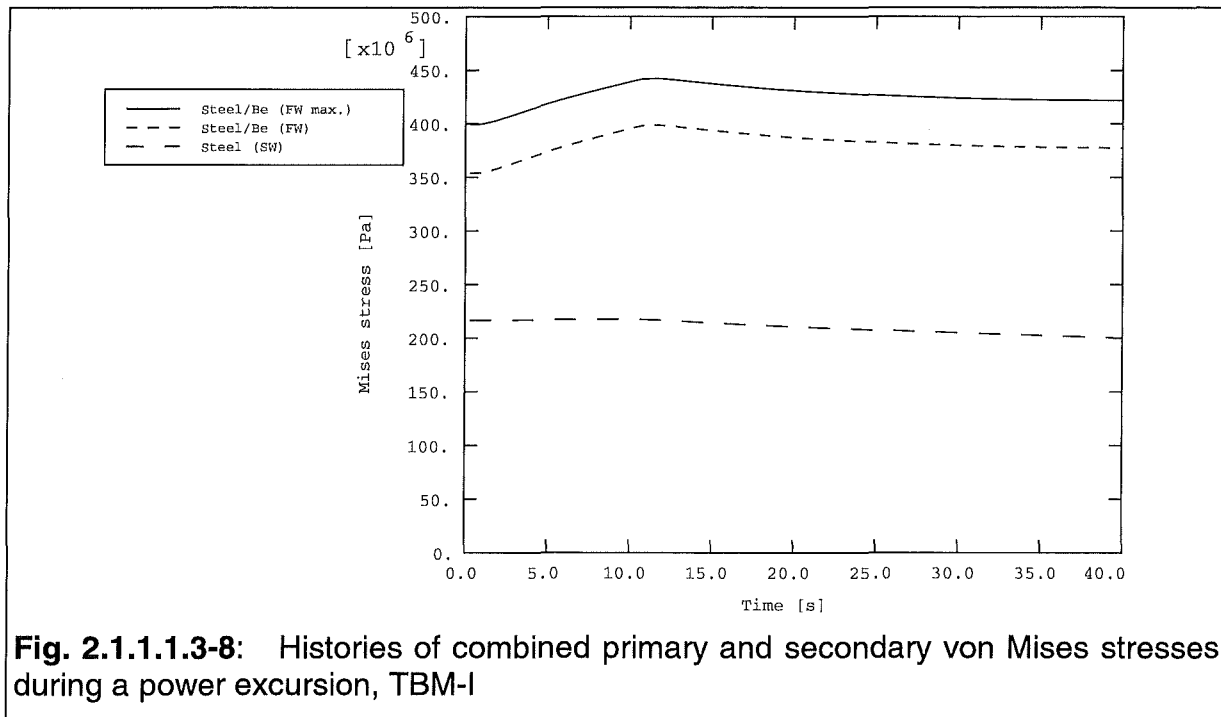
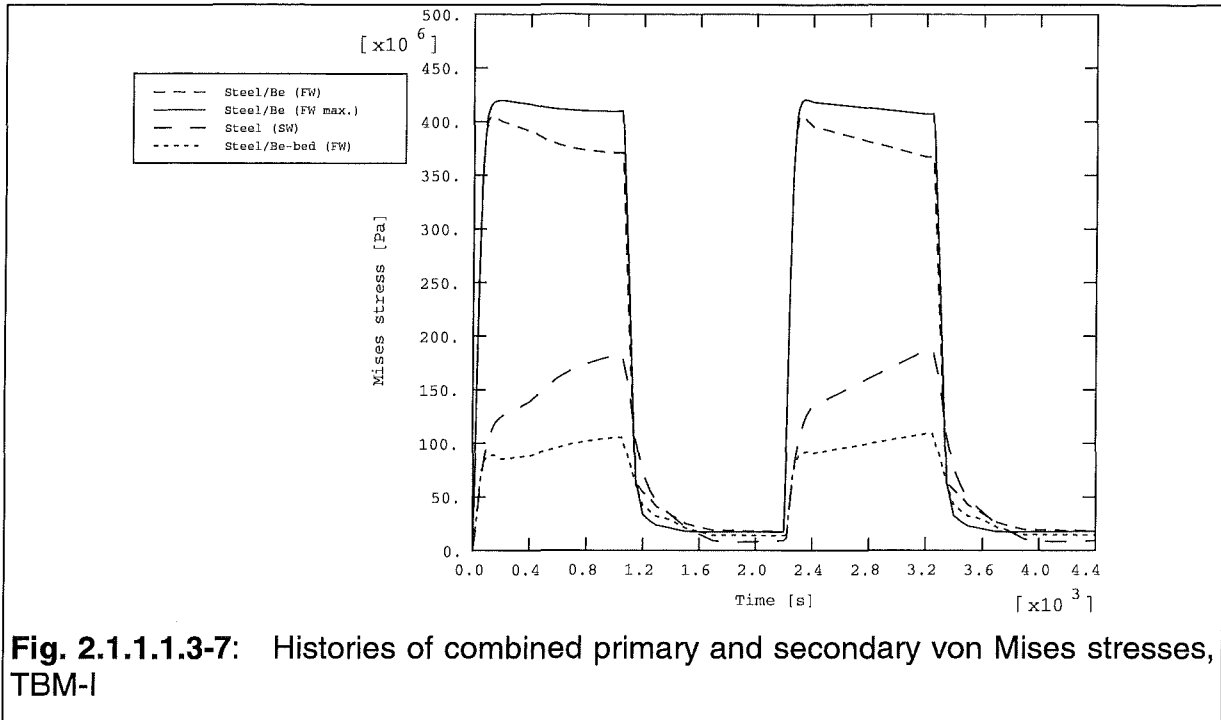


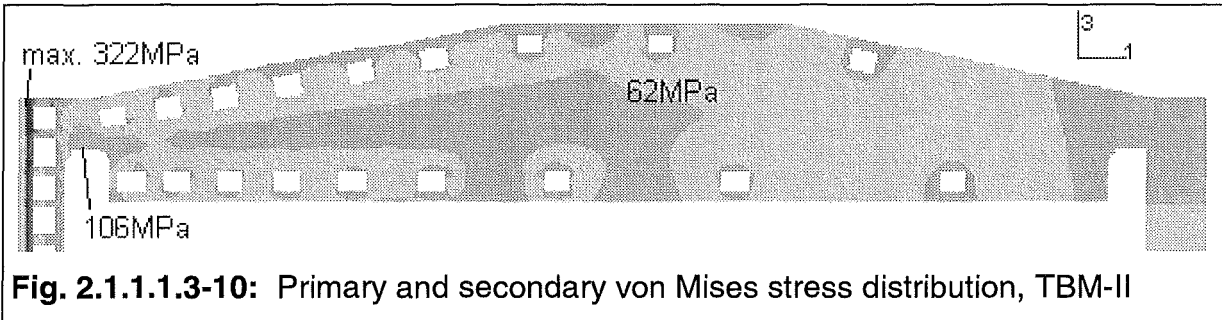
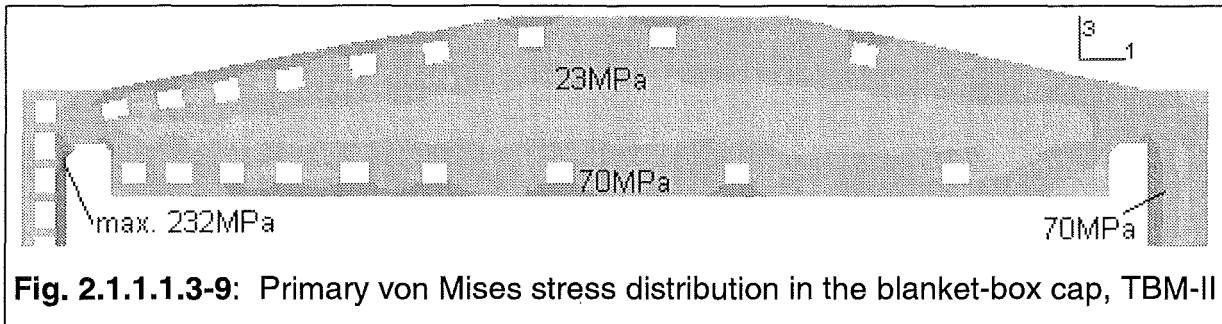
Fig. 2.1.1.1.3-1: Von Mises stress distribution (MPa) in the First Wall during normal operation ($p_{\text{He}} = 8 \text{ MPa}$; $p_{\text{Blanket}} = 0.1 \text{ MPa}$) in TBM-I and TBM-III











References:

[2.1.1.1.3-1] J. Wareing, A-A Tavassoli, Assessment of martensitic steels for advanced fusion reactors.

[2.1.1.1.3-2] RCC-MR-Addendum May 1993, A3-18S, pp 451-476

[2.1.1.1.3-3] RCC-MR-Addendum November 1987, A3-18S, pp 67-94

[2.1.1.1.3-4] ABAQUS 5.6 - ABAQUS/Standard User's Manual, Vol. I to III, Hibbitt, Karlsson & Sorensen, Inc. (1996)

[2.1.1.1.3-5] CATIA.ELFINI Solver, User's Reference Manual, Ver.4, Dassault Systemes (1997)

2.1.1.1.4 Mechanical Design

The test blanket module is installed radially into the horizontal test port and replaces a portion of the shielding blanket. Fig. 2.0.2-4 and 2.1.1.1.4-1 show the arrangement of the Test Blanket Subsystem (TBS) inside the ITER horizontal port.

The TBS is located and supported by the Vacuum Vessel Port Extension (see Section 2.1.1.1). The mechanical interface is provide by the Vacuum Vessel Plug. This component of the TBS fills the port envelope as much as possible with a standard gap allowance of 20 mm.

The Test Blanket Module is contained in an insulating frame, so that the thermal conditions on the side wall of the test blanket module need not be identical to the wall conditions of the facing wall of the shielding blanket. Although the nominal temperature of some of the test blankets may be in the neighbourhood of 300°C to 500°C, the frame is cooled to approximately 150°C. Basic parameters of the frame cooling are similar to ones of the ITER Shielding Blanket Modules. The frame will also contribute to the neutron shielding of the vacuum vessel and the magnets.

The clear opening through the shielding blanket back plate and the blanket modules is 1.600 m wide and 2.600 m high. There is a gap allowance (see Table 2.1.1.1.4-1) completely around the perimeter of the frame to account for the differential motion between the Back Plate and the Vacuum Vessel during operational and off-normal conditions. The wall thickness of the Frame has been chosen of 200 mm; it allows a suitable TBM size and at the same time a good neutron shielding capability (see Section 2.1.1.1.1). The external frame dimensions adjacent to the regular shielding blanket modules are 1.496 m wide by 2.536 m high. In the region outside the back plate there is a step increase in the wall thickness to fill the VV Extension with a gap of 25 mm; this allows a better shielding capability at the side walls and shielding from the neutron streaming through the gap between Frame and ITER Shielding Blanket System.

Table 2.1.1.1.4-1: Clearances around the Test Blanket Subsystem [2.1.1.1.4-1]

dim (mm)		Frame - Back Plate	Frame – VV	VV Plug – VV
Poloidal	Top	30	25	20
	Bottom	34	25	20
Toroidal		52	25	20

The first wall of the Frame follows the FW contour of the adjacent shield blankets modules, but it is receded from it of 60 mm. The frame back wall has a thickness of 300 mm; it also provides the attachment points for the TBM's.

The European and the Japanese teams have collaborated in their approach for testing their helium cooled solid breeder test modules. During the ITER Basic Performance Phase (BPP) the European Blanket Test Module (EU-TBM) shall occupy the lower half of the test port allocated to the helium cooled blankets, the other half being occupied by the Japanese helium cooled ceramic breeder blanket module (JA-TBM).

Taking into account 20 mm gap between TBM's and Frame and between EU- and JA-TBM, the maximum dimensions of each TBM is 1038 high and 1056 wide. The maximum radial dimension (from the Frame FW to inner side of the frame back wall, measured at the middle port plane) necessary for the EU-TBM is about 1.2 m. It is dictated by the radial dimension of the EU-TBM that reproduces at full scale a portion of the European HCPB DEMO blanket.

The first wall of the TBM is planar, without curvature, but it conforms as closely as possible to the first wall of the adjacent shield blankets modules. The deviation from the primary first wall is in the range of 60-75 mm.

The TBM's are being designed to withstand a combination of coolant pressure loads, thermal loads from the plasma, electromagnetic loads, thermal stresses due to temperature gradients inside the TBM and, especially, at interfaces of parts cooled by the water. A more detailed description of the EU-TBM is in Section 2.1.1.1.

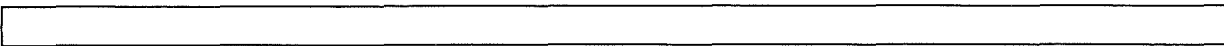
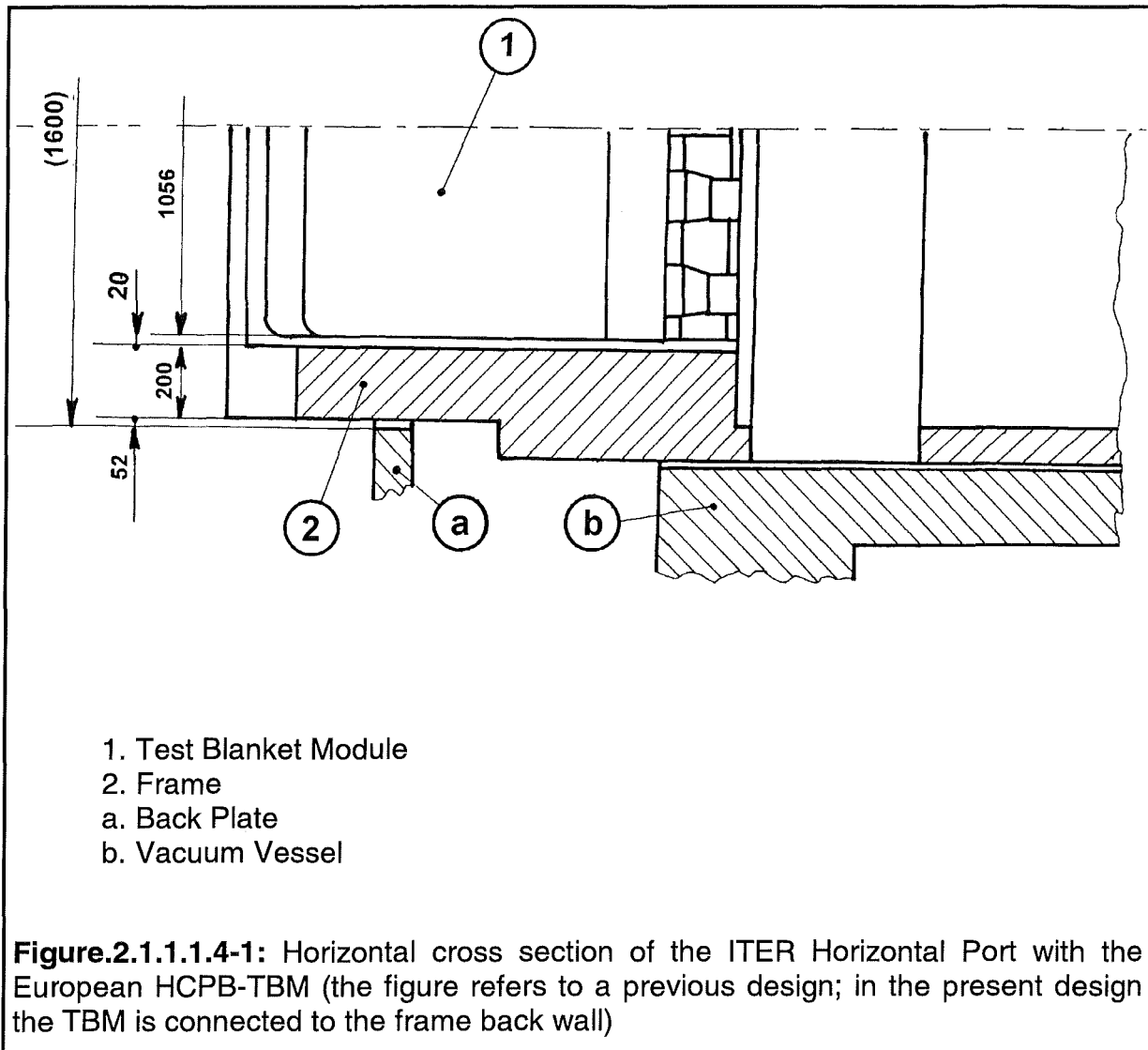
Additional shielding is needed behind the frame to protect the vacuum vessel, the TF-magnet and to reduce the neutron load outside the vacuum vessel boundary. This will be provided by the water cooled Shield. This structure is integrated in the vacuum vessel plug.

For the mechanical connection between the TBM and the frame back wall a groove-and-tongue design is proposed which holds the TBM in the poloidal and toroidal direction (Fig. 2.1.1.1.4-2). Fixation in the radial direction is assured by four bolts with slightly slotted holes. This design allows the transmission of loads and torques in all directions and planes - in particular the large torque vector in the radial direction during disruptions - , and the accommodation of the differential expansions resulting from the different materials and temperatures in the TBM and the frame.

The heat generated inside the supporting structure is transmitted by heat conduction to the cooled regions of the TBM and the frame, respectively, without excessive temperature rises. Heat transfer across the contact areas of the support is not needed for heat removal.

References:

[2.1.1.1.4-1] e-mail of K. Ioki, 13.11.1997



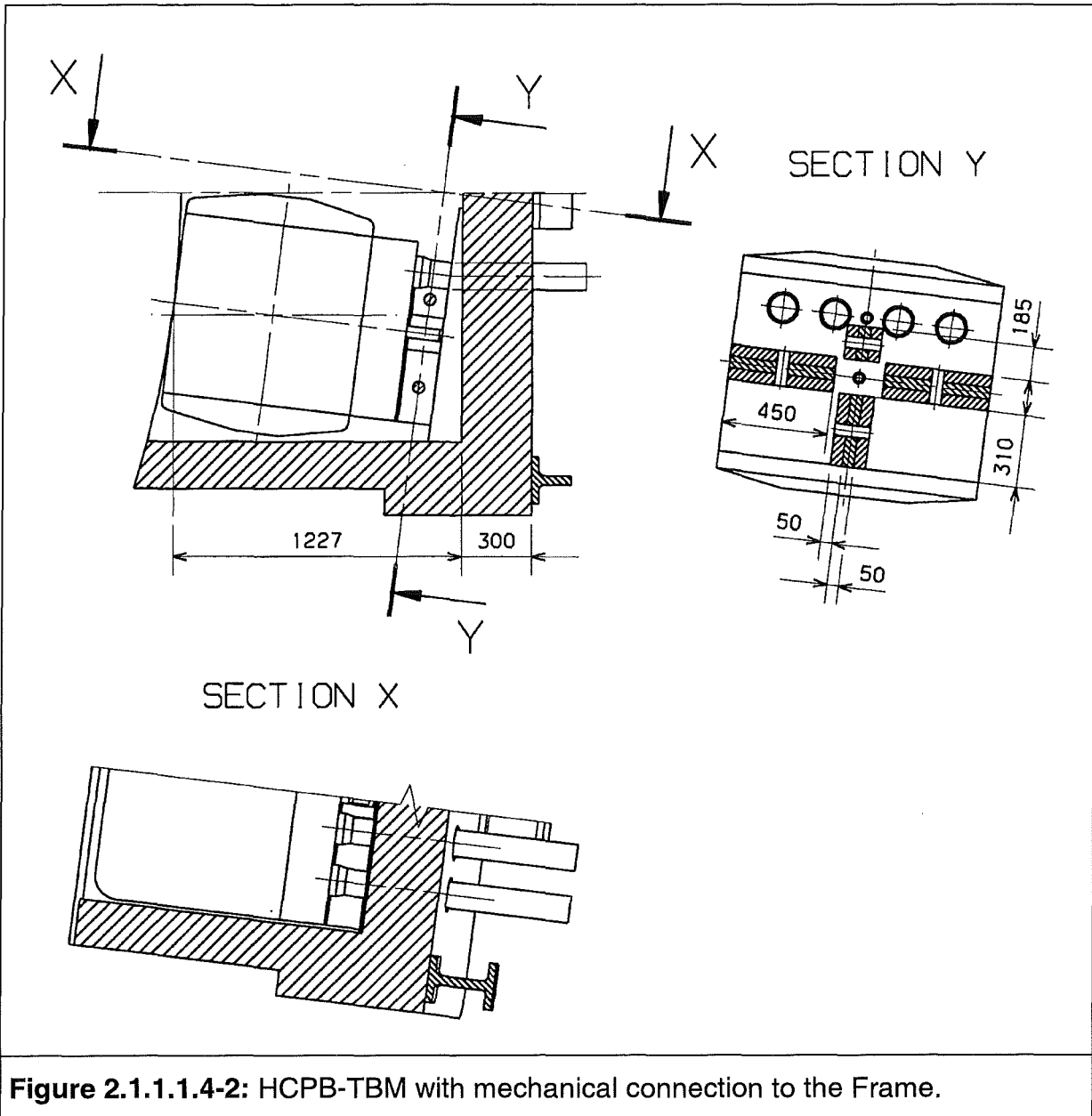


Figure 2.1.1.1.4-2: HCPB-TBM with mechanical connection to the Frame.

2.1.1.1.5 Maintenance/Remote Handling

The TBM's are designed to be removable through the horizontal test port by use of remote handling equipment. The TBM's size is limited to the port dimensions. Since the weight of full TBM is higher than that of the regular Shielding Blanket Module, special attention should be paid to remote handling equipment for TBM's. The mass distribution of the current HCPB-TBM design is as follows:

HCPB-TBM	3.5 t
Frame (without coolant)	TBD t
Shield (without coolant)	TBD t
Vacuum Vessel Plug	TBD t
Plumbing	1 t
<hr/>	
Total (without Japanese TBM)	TBD t

Replacement frequency is estimated as several times (TBD) during BPP. Maintenance procedure description is:

- duration is no more than 8 weeks;
- drainage of water and helium depressurisation;
- removal of cryostat plug to the maintenance cell;
- further steps will depend on the decision of JCT and TBWG on general approach for design of TBM's, all the interfaces and piping, handling equipment for blanket test modules.

2.1.1.1.6 Fabrication and Assembly

2.1.1.1.6.1 Reference Manufacturing Procedure

The high quality required for the fabrication of the Test Blanket Module demands for the application of well-known, reproducible and reliable fabrication-techniques. Non destructive testing and – in case of faults or defects - repair should be possible after each major manufacturing step. Two different manufacturing procedures are being investigated. The reference manufacturing procedure applies as far as possible processes which are 'state of the art'. However some steps of fabrication require adaptation due to the dimensions of the workpiece and the special requirements mentioned above. For fabrication steps which were considered poor or doubtful with respect to feasibility, reliability or reproducibility it was attempted to provide alternatives in order to prevent fabrication aspects from being prohibitive for the construction of the module.

Using the reference procedure the main fabrication and assembly steps are as follows (procedure as applied to TBM-II):

- Step 1: Machine the first wall and cooling plate halves
- Step 2: Diffusion weld the first wall and cooling plates
- Step 3: Bend the first wall to obtain the U-shaped box
- Step 4: Weld the cooling plates into the first wall box
- Step 5: Manufacture and weld the caps to the box
- Step 6: Insert purge gas tubes, fill the Be and Li_4SiO_4 chambers
- Step 7: Close pebble beds with porous plates, connect purge gas lines to header
- Step 8: Install coolant pipes and stiffening plates in the rear chamber of the TBM
- Step 9: Close the rear of the module by EB-welding the plates forming He inlet outlet and purge gas manifolds to the module box
- Step 10: Weld He nozzles, purge gas nozzles and attachment plates to the rear of the module

After each major assembly step non destructive testing – and if needed repair – are possible. So can heat treatment by local or bulk heating. Alternatively heat treatment can be done at the end of manufacturing in a single step by bulk heating.

A development program on the most important manufacturing steps has been carried out using MANET as typical martensitic steel. The results can be summarized as follows:

Step 2: Diffusion Welding of FW and Cooling Plates

Plates with internal channels such as FW- and Cooling Plates have been fabricated by diffusion welding (solid HIP) of two grooved plates. Welding parameters are 980 °C to 1050 °C at 25MPa for 2 hours.

Results:

- The plates produced by diffusion welding withstand an internal pressure of 15 MPa without leaks.
- Metallographic tests showed flawless bonding.
- Destructive tests confirmed the tensile and bending strength of the bonded zone to be nearly the same as that of base material.
- The quality of diffusion welds can be significantly improved by application of a two step HIP-technique: welding parameters of the first HIP cycle (canned) as mentioned above, second HIP cycle (without canning) with significant higher pressure (150 MPa).
- The influence of preparation methods and welding parameters on the ductility of the bonded zone are still being investigated.

An alternative fabrication method for the FW plates is the so-called HIP forming process: A thin-wall tube is inserted into the grooves and tight welded. In the subsequent HIP process with high pressure the tube is expanded until contact with the webs. A small FW plate has been manufactured successfully according to this method.

Step 3: Bending the First Wall

Bending the first wall plate-structure was successfully carried out at room temperature in different radii with and without filling material.

Results:

- The channel height in the bent section was reduced by 8.3% and 10.5% respectively, which is tolerable.
- No surface cracks were detected.
- Accompanying FEM calculations showed that the maximum total strain of approximately 50 % is within the acceptable limits.

Tests with additional material on one side of the plate (for machining the ledges that are needed as weld preparation for the CP to FW seam) are carried out now. The optimum thickness of the additional layer of material on the outside of the bend was found to be 6 mm. For these plates the height reduction in the bent zone was larger but still within acceptable limits. Additional tests to determine the precision that can be achieved by using suitable devices are carried out now.

Step 4: Welding of Cooling Plates into the FW Box

For the fabrication of the module TIG welding is the technique that is expected to be applied for welding the cooling plates to the U-shaped first wall box. The weld preparation for the seams that join the CPs to the FW was optimised. The welding parameters were investigated. The parameters found suitable were successfully applied in a fully mechanised welding test.

Results:

- Mechanised TIG welding can be carried out in one single step for each side without preheating
- No surface cracks occurred, the distortion was below 0.01% which is within acceptable limits.
- High quality can be obtained if the optimum TIG welding parameters are kept constant by means of automatised devices.

Steps 5 and 9: EB-Welding

EB-Welding is intended for welding the module's caps to the FW-box as well as for joining the He-supply headers. One advantage of this welding technique is the small heat affected zone that leads to very small distortions. EB-welding was tested on specimens of different shapes.

Results:

- For MANET workpieces EB-welding is suitable.
- NDT of EB-welded seams can be done by ultrasonic technique.
- Double welds with a leak-detection channel can be carried out from one side (transparent welding). The inspection channel between double seams remains open and is leaktight.

Further investigations are needed to demonstrate the feasibility of welding seam thickness of up to 55 mm and for thick to thin or grooved pieces.

Other Steps:

All other fabrication steps can be carried out with available technologies. In particular, no problems are expected for the orbital welds (round plate to sheet, tube to sheet and tube to tube) that have to be carried out on the Helium supply system. The technique is considered state of the art, all tools and devices are available 'off the shelf'.

2.1.1.1.6.2 Alternative Manufacturing Procedure

Alternative to the conventional manufacturing process by EB- and TIG-welding the HCPB blanket module can be assembled by Solid-HIPing. With this technique the various parts of the blanket module (i.e. FW, cooling plates, manifolds etc) that have been manufactured as usual by conventional techniques, are preassembled and seal welded in a vacuum chamber. Then the module is inserted into the HIP-facility in order to weld the actual bonding zones.

In the HIP-chamber the parts are diffusion welded at temperatures of about 1000 °C and pressures in the 100 MPa range for about three hours. Subsequent to this process the HIPed parts get a thermal treatment in order to restore their mechanical properties.

First tests were done at FZK to determine and optimize the joining parameters for the HIP-process (i.e. pressure, temperature, time and surface preparation) that are needed to produce reliable welds with reproducible quality. In order to proof the quality of the bonding specimens have been investigated by ultra-sonic scanning and metallographic examinations. In addition strength examinations i.e. bending tests, tensile tests and impact tests have been carried out. The first results of the tensile and bending tests evidenced the strength of the base material. The impact tests resulted in values of about 40% of the basic material. Further optimization of the HIP-parameters is necessary.

2.1.1.1.7 Materials

According to the available information the Blanket Test Module Design is based on the use of the following materials:

- The structural material used in the breeding blanket will be a low activation martensitic steel (EUROFER). The exact specifications of this material will be made within the European Fusion Technology Program by the end of 1998. So far only its chemical composition is known. Thus the properties of the ferritic-martensitic steel Z10CDVNB 9-1 (T91) has been used in the design calculations (structural, thermomechanical and electromechanical calculations). This steel is referenced in the code RCC-MR including the thermo-physical and mechanical data [2.1.1.1.7-1] (see also Appendix A). By the neutronic calculations the chemical composition of EUROFER was adopted.
- The reference ceramic breeder is lithium orthosilicate (Li_4SiO_4) + 2.2 wt% SiO_2 (see Appendix B "Li₄SiO₄ pebble bed"). Alternative material are Li_2ZrO_3 or Li_2TiO_3 .
- Beryllium is used in form of pebbles as multiplier and in form of a plasma facing layer protecting the first wall (see Appendix C "Beryllium pebble bed").

In the following the different materials for each component are listed with the estimated weight:

HCPB-TBM

Structural material	EUROFER	3000 Kg
breeder material	Bed of 0.25-0.63 mm of reference ceramic breeder	75 Kg
Multiplier	Binary bed of 1.5 to 2.3 and 0.1 to 0.2 mm beryllium pebbles	415 Kg
plasma facing material	5 mm beryllium layer	1 Kg
Coolant	Helium (8 MPa, 250°-450°C)	Negligible
purge flow	Helium (0.1 MPa, 20°-450°C)	Negligible

Frame

Structural material	316LN-IG	TBD
heat sink	Copper alloy	TBD
plasma facing material	10 mm beryllium layer	TBD
Coolant	Water	TBD

Shield

Structural material	316LN-IG	TBD
Coolant	Water	TBD

VV Plug

TBD	TBD
-----	-----

Plumbing

Helium coolant / water coolant/
Diagnostics

Structural material	EUROFER / 316LN-IG / 316LN-IG	TBD
Coolant	Helium / water / none	TBD

References

[2.1.1.1.7-1] Règles de Conception et de Construction des Matériels Mécaniques des Îlots Nucléaires Rapides (RCC-MR), French Design and Construction Rules for Fast Breeder Reactor Power Stations, AFCEN, Ed.1985 and 2 Modification Files at 1987 and 1993.

2.1.1.1.8 Electromagnetic Design

The TBM is electrically connected to the VV Port Extension, that mostly defines the boundary conditions for induced electric currents determination during transient electromagnetic events.

Electromagnetic (EM) calculations have been performed to evaluate the magnetic forces acting on the various components of the Test Blanket Subsystem. The results of these calculations constitute a basis for the structural analysis of the connection between TBM and Frame and to calculate electromagnetic loads for the stress analysis of the TBM.

The Finite Element Method program AENEAS [2.1.1.1.8-1], developed at FZK to study transient eddy current problems as well as magnetic fields and forces in non-linear magnetic materials [2.1.1.1.8-2], has been used for the electromagnetic analysis of the European Helium Cooled Pebble Bed (HCPB) TBM. All significant ITER components, with a particularly accurate discretization of the HCPB TBM structure, have been included in the Finite Element model (Fig. 2.1.1.1.8-3). Magnetic properties of the steel T91 [2.1.1.1.8-3] have been considered as well as reference poloidal and toroidal field configurations. The plasma behaviour during Centered Disruptions (CD), upward and downward Vertical Displacement Events (VDEs) has been derived [2.1.1.1.8-4] from data obtained by means of the TSC code [2.1.1.1.8-5].

Magnetic behaviour of martensitic steels

Martensitic steels, which exhibit ferromagnetic behaviour, have been proposed as structural material for almost all the Test Blanket Modules (TBMs) which will be tested in ITER. Because of the strong applied magnetic field, the structure is magnetized to the saturation value of the magnetization, so that the magnetic flux density distribution inside the TBMs and in the plasma region close to them changes significantly. The following critical issues have to be investigated by means of an electromagnetic analysis: 1) magnetized matter interacts directly with the external magnetic field causing a magnetic loading (Magnetization Force, MF) on the structure which has to be considered for the mechanical design of the TBMs; 2) when a plasma disruption occurs, an electromagnetic load (Lorentz Force, LF) due to interaction between eddy currents and the magnetic field is added to the structure; the value of this load and the effect of the magnetization on it have to be investigated to assess the capability of the TBM structure to withstand the mechanical effects of plasma disruptions; 3) the magnetized structure of the TBMs produces a non-axisymmetrical magnetic field in the plasma region which can affect plasma stability and lead to disruption. electromagnetic analysis.

Force Calculation

Electromagnetic force distributions have been calculated for CDs (10ms, 25ms and 50ms) and for upward and downward VDEs (50ms). Resultant forces and torques have been derived at the TBM support (Fig. 3). Normal components of forces (F_N) and torques (T_N) for the ITER reference CD (50ms) are shown as a function of time in Fig. 2.1.1.1.8-1 and Fig. 2.1.1.1.8-2, respectively. In addition to the total force and

torque, MF and LF contributions are also pointed out. A pulling F_N of 0.2 MN in the direction of the plasma center acts on the TBM even during normal operation. The resultant F_N of the LF distribution originating during the disruption achieves a max. value of 0.12 MN in positive normal direction, contributing to a reduction of the total F_N acting on the support. However, if we consider the spatial distribution of the forces on the TBM structure, we can observe that whereas the MFs act prevalently in the radial direction, the LFs are differently directed depending on the eddy current patterns in the structure. Therefore, during a disruption the loading of the structure can be locally higher than during normal operation. Considering the T_N (Fig. 2.1.1.8-2) we note that the only significant contribution is given from the LF (max. 0.8 MNm). For faster CDs (10ms and 25ms), analogous behaviours with increasing peak values are obtained for F_N and T_N given by LF contribution (respectively 0.26 MN and 1.75 MNm for a 10ms CD). The effect of the magnetization on the LF (stronger magnetic flux density) has been evaluated carrying out the same electromagnetic analyses for a nonmagnetic structural material. For the reference CD (50ms) peak values of the LF contribution have been calculated as $F_N=0.07$ MN and $T_N=0.65$ MNm. Upward and downward VDE have been also analysed (Fig. 2.1.1.1.8-4), but from Tab. 1 – showing the maximum values of the total resultant forces and torques acting on the support for the reference CD (50ms) and upward and downward VDEs - it is evident that the most critical event for the TBM is represented by a centered plasma disruption.

Tab. 2.1.1.1.8-1 – Maximum Values for reference plasma disruption events.

Max Values	F_N (MN)	$ F_T $ (MN)	T_N (MNm)	$ T_T $ (MNm)
CD (50ms)	-0.20	1.14	0.72	0.32
Up. VDE (50ms)	-0.20	0.08	0.47	0.25
Down. VDE (50ms)	-0.20	0.12	0.49	0.22

Note: For the normal components also the direction is indicated whereas for the tangential components only the magnitudes are presented.

Error Field Calculation

The magnetic field produced by the magnetized matter of the TBM (error field) has been calculated to evaluate the effect of the TBMs on the toroidal magnetic field in the plasma region.

Fig. 2.1.1.8-5 shows the magnitude of the error field as a function of the toroidal angle in the plane $Z=1.7$ m and for different radius values. The solid curve corresponds to a circle taken around the outer edge of the plasma ($R=10.947$ m). Toroidal magnetic field ripple values δ_{Fe} for the same plane are reported in Fig. 6 and have been calculated following [2.1.1.1.8-6]. At $R=10.947$ m results $\delta_{Fe} \cong 0.85\%$, but it can be observed that near the module, δ_{Fe} changes very rapidly with R . Changes in δ_{Fe} have also been obtained by varying the Z coordinate.

References

- [2.1.1.1.8-1] Ruatto, P., "Entwicklung einer Methode zur Berechnung der Elektromagnetischen Kräfte durch Magnetfeldänderungen in ferromagnetischen Strukturen", Karlsruhe, FZK, FZKA 5683, 1996.
- [2.1.1.1.8-2] Boccaccini, L.V. and Ruatto, P., "Effect of the presence of ferromagnetic structural material on the DEMO Helium Cooled Pebble Bed Blanket during plasma disruptions", in Proc. of the 19th SOFT Conference, Lisboa, 1996, pp.1519-1522.
- [2.1.1.1.8-3] "Caracterisation magnetique de l'acier martensitique Z10 CDV Nb 9-1", Report Framatome/Novatome Division, no. NVMK.DC 951541.
- [2.1.1.1.8-4] Roccella, M, Rita, C, ENEA Frascati, personal communication, 1998.
- [2.1.1.1.8-5] Jardin, S.C., Pomphrey, N. and Delucia, J., "Dynamic Modeling of Transport and Positional Control of Tokamaks", J. Comp. Physics 66, 481 (1986).
- [2.1.1.1.8-6] Doinikov, N. et al., "Analysis of the main field disturbance sources and tentative analysis of the correction system. (Design Task D-324-3)", ITER Report, 1996, pp.37-42.

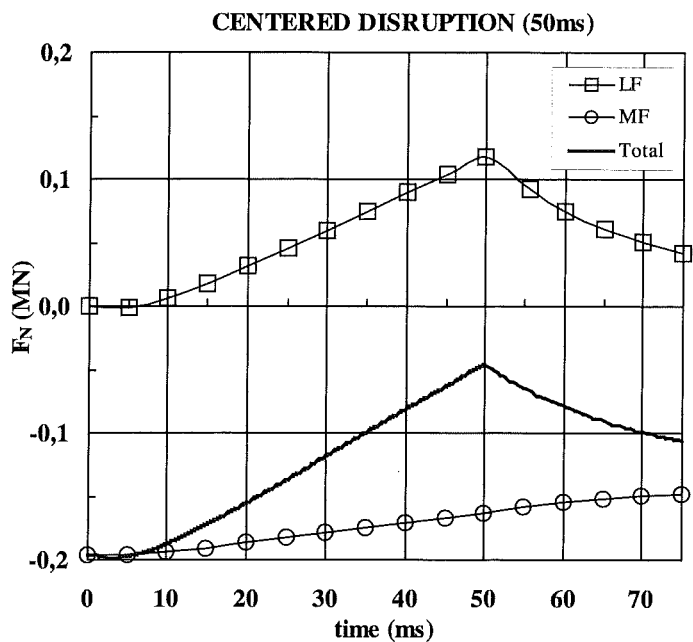


Fig. 2.1.1.1.8-1 – Normal component of the resultant force acting on the TBM support. Magnetization (MF) and Lorentz (LF) contributions are also shown.

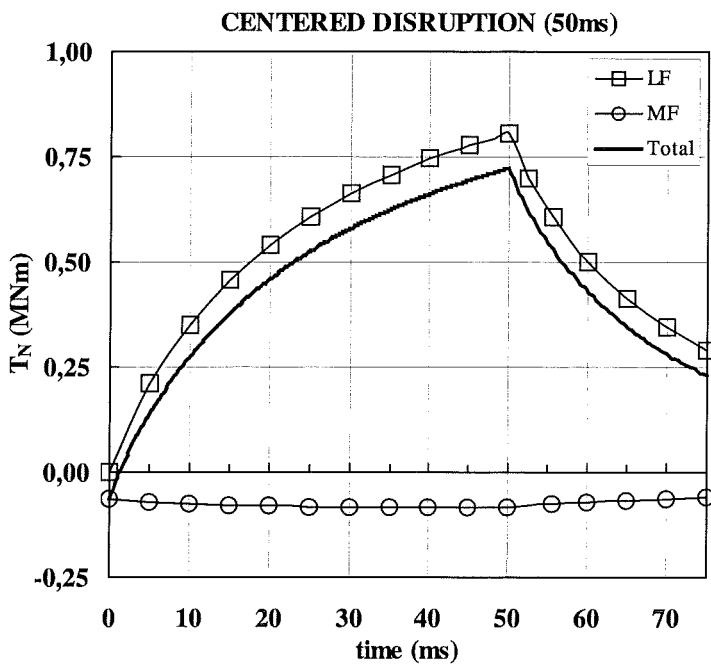


Fig. 2.1.1.1.8-2 – Normal component of the resultant torque acting on the TBM support. Magnetization (MF) and Lorentz (LF) contributions are also shown.

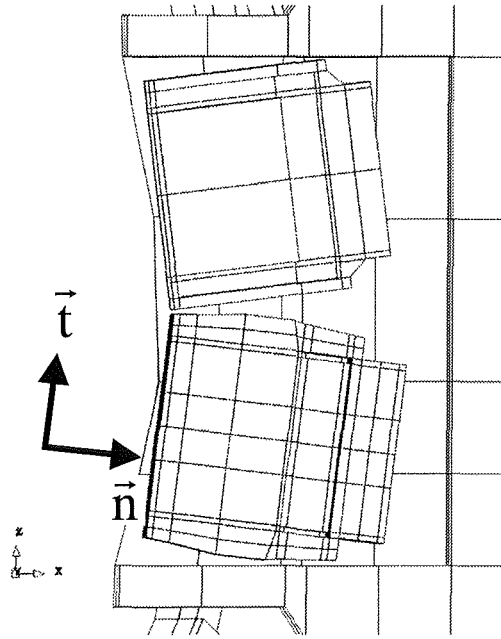


Fig. 2.1.1.1.8-3 – Particular of the finite element model showing the HCPB TBM (below) and the japanese TBM (above). The arrows indicate the normal and tangential directions for the resultant forces and torques calculated at the support of the HCPB TBM.

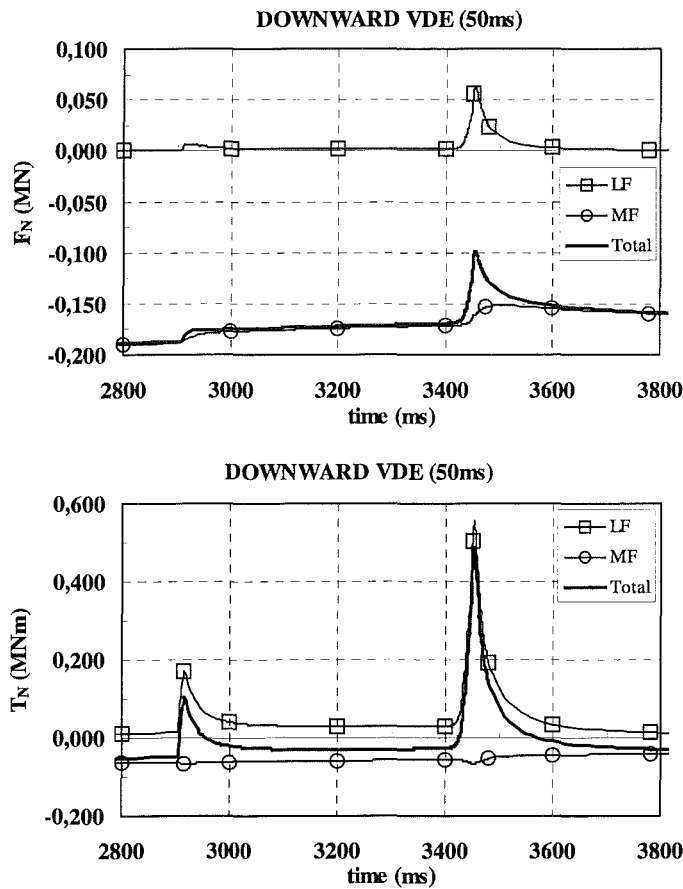


Fig. 2.1.1.1.8-4 – Behaviour for the normal component of the resultant force (F_N) and torque (T_N) acting on the TBM support during a downward VDE are shown. It is evident that the most critical event for the TBM is a centered plasma disruption.

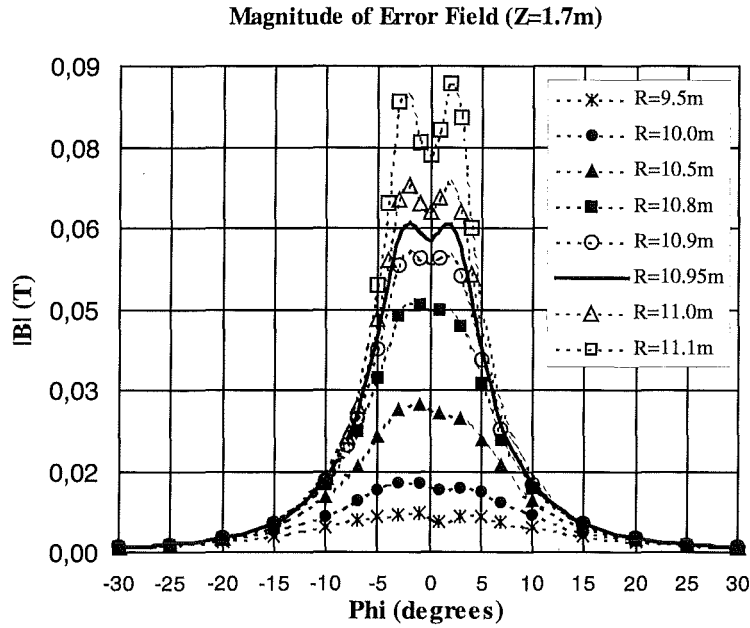


Fig. 2.1.1.8-5 – Magnitude of the error field as a function of the toroidal angle in the plane Z=1.7m and for different R near the TBMs.

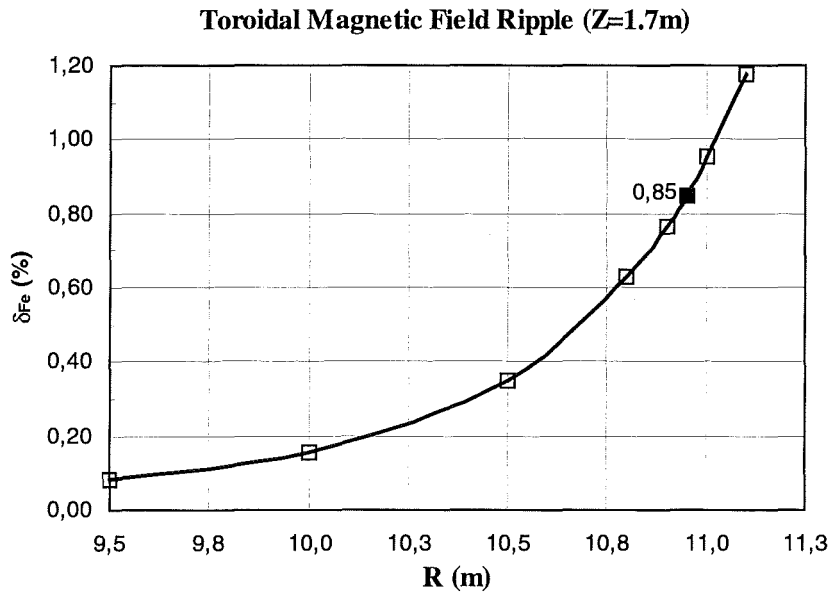


Fig. 2.1.1.8-6 – Toroidal magnetic field ripple for the plane Z=1.7m. At the outer edge of the plasma (R=10.947m) we have $\delta_{Fe} \approx 0.85\%$

2.1.1.1.9 Tritium Control

2.1.1.1.9.1 Tritium permeation

Tritium permeation losses from the First Wall

The permeation through the first wall has been evaluated by means of the one-dimensional computer code TMAP4 [2.1.1.1.9-1].

HCPB-DEMO design calculations [2.1.1.1.9-2].

Main characteristics:

- bare MANET First Wall (5 mm thick layer separating plasma and helium coolant channel);
- constant incident flux of 1.5×10^{20} ions/m²xs;
- FW permeating surface of 730 m² (inboard + outboard);
- average neutron load of 0.4 MW/m²;
- average maximal temperature in the first wall of 745 K.

Corresponding to two different grades of oxidation of the FW downstream side in the helium coolant channels, the permeation rate varies between 8.5 and 12 g/d. The two-dimensional geometry does not reduce the permeation more than 6%.

HCPB TBM-I design calculations [2.1.1.1.9-3].

Main characteristics:

- pulsed operation incident flux equal to 1×10^{20} ions/m²xs with 1000 s pulses and 1200 s plasma dwell time;
- 5 mm thick protective layer of beryllium for a 5 mm thick first wall of MANET;
- neutron load of 0.5 MW/m²;
- maximal temperature in the first wall of 782 K.

A computational model has been implemented in the computer code TMAP4 to reproduce the available experimental data concerning hydrogen ion implantation in beryllium.

Experimental data [2.1.1.1.9-4,5,6,7] have shown that, under ITER-like plasma conditions, the plasma facing surfaces of the beryllium develop high porosity (bubbles) and saturate, leading to a strong uptake of tritium and deuterium ions almost independent of the incident flux. At fluxes typical of ITER, surface erosion of beryllium should be also taken into account.

The 5mm thick coating layer of beryllium was modelled as three segments in series, [2.1.1.1.9-3]: 50 nm of implantation region, i.e. where most of the bubbles are; a 1 µm thick zone of damaged beryllium influenced by the bubbles and the remaining

part of undisturbed beryllium. To accommodate the saturation effects on the plasma side of beryllium, the recombination coefficient has been exponentially modified, thus still allowing a recombination-like boundary condition in the TMAP4 code.

Erosion due to sputtering results in a diffusion in a moving co-ordinate system. It has been taken into account by neglecting the Soret effect for beryllium, i.e. the mass transport due to a temperature gradient. Erosion was included only in the damaged zone. The reduction of the beryllium thickness, leading to a lower inventory and higher permeation, was accounted for by an iterative procedure.

The sputter rate calculated was of 3.25×10^{-10} m/s, i.e. 2 mm eroded beryllium after a total operational time of about 70 days. For the assumed first wall surface of 1.2 m^2 and the whole operating period, a permeation of about 0.007 g has been obtained. This very low permeation is not appreciably influenced by the use, instead of MANET, of a ferritic steel like T91.

Tritium permeation losses from the purge flow system

The major contribution to the permeation is represented by the tritium coming from the lithium orthosilicate beds (Li_4SiO_4), as the permeation from the beryllium bed is negligible.

Identical procedures have been applied to both DEMO and TBM-I designs [2.1.1.1.9-2,3]. In the DEMO design the total permeation from the purge flow system through the total permeating surface (inboard + outboard = 9120 m^2) was of 0.78 g/d. The smaller tritium production and the lower wall temperatures in the TBM-I lead, for a total permeating surface of about 10 m^2 , to a tritium permeation not greater than 0.3 mg/d.

Conclusion

Table 2.1.1.1.9-1 summarise the results of tritium permeation calculation for DEMO and TBM-I design.

Table 2.1.1.1.9-1: tritium permeation in DEMO and TBM-I

Design	First Wall	Purge gas
DEMO	8.5-12 g/d	0.8 g/d
TBM-I	< 0.1 mg/d	0.3 mg/d

With a coating layer of beryllium, the permeation through the first wall is strongly reduced. As far as the permeation is concerned, the choice of the steel to be used together with beryllium does not play an important role.

What remains to be modelled is the influence of carbon on the retention and permeation of beryllium-clad surfaces. There are no many data available about how much of the carbon that will be sputtered from high-heat-flux surfaces in the divertor will be transported to the main plasma chamber and end up on the first wall, where carbon film build-up should not be a problem. The hydrogen implantation in the first wall seems in any case to be significant at depths, that result in development of the described open porosity.

2.1.1.1.9.2 Tritium inventory

The tritium inventory in the TBM has been roughly evaluated either scaling down the inventory in breeder and structural material obtained for the DEMO blanket or using for beryllium multiplier and FW protection layer. The values used in the design are summarised in Tab. 2.7-15 (see also section 2.7.3.1 for further details).

References:

- [2.1.1.1.9-1] G.R. Longhurst et al., TMAP4 User's Manual, INEL, EGG-FSP-10315 (1992).
- [2.1.1.1.9-2] L.Berardinucci, M.Dalle Donne, Proc. of 19th SOFT, Lisbon, Portugal, Sept. 16-20, (1996) 1427-1430.
- [2.1.1.1.9-3] L.Berardinucci, Modeling of Tritium Permeation through Beryllium as Plasma Facing Material, ICFRM-8, Sendai, Japan, to be published on J.Nucl.Mat. (1997)
- [2.1.1.1.9-4] M.I.Guseva, A. Yu Birukov, V.M. Gureev, L.S. Daneljan et al., J. Nucl. Mat., 233-235, (1996) 681-687.
- [2.1.1.1.9-5] V.N. Chernikov, V.Kh. Alimov, A.P. Zakharov et al., J. Nucl. Mat., 233-237, (1996) 860-864.
- [2.1.1.1.9-6] A.A. Haasz and J.W. Davis, Proc. 12th Int. Conf. On Plasma Surface Interactions in Contr. Fusion Devices, St. Raphael (1996).
- [2.1.1.1.9-7] R.A. Causey, K.L. Wilson, Journal of Nuclear Materials, 212-215, (1994) 1436-1442

2.1.1.2 Tritium Extraction Subsystem

The main design data of the Tritium Extraction Subsystem (TES) are given in Table 2.1.1.2-1. For safety reasons, the tubes connecting the TBM with the TES loop have to be designed for a pressure of 8 MPa because leakages from the cooling system can lead to a higher pressure than the nominal working pressure which is 0.1 MPa. Redundant blocking valves are foreseen to protect the loop from a pressure increase beyond 0.2 MPa. For radiological safety reasons, the system must be installed in a glove box as secondary containment.

Table 2.1.1.2-1 : Main Design Data for the Tritium Extraction Subsystem

He Mass Flow	0.85 g/s = 17 Nm ³ /h
Swamping Ratio	He : H ₂ = 1000
Tritium Production Rate	0.2 g / day ^{a)}
Partial Pressures ^{b)}	
p (H ₂)	110 Pa
p (HT+HTO)	0.4 Pa ^{c)}
p (H ₂ O)	≈ 0.3 Pa ^{c)}
Extraction Rates	
H ₂	18.4 mole /day
HT	≈ 0.05 mole /day
H ₂ O / HTO	≈ 1 g / day
Extraction Efficiency	≥ 95 %
Purge Gas Temperature at Test Module Outlet	450 °C
Pressure of Purge Gas	
at Test Module Outlet	0.106 MPa
at Test Module Inlet	0.120 MPa
Pressure Drop in Test Module	0.014 MPa

a) The resulting H/T ratio is 520; it is urgently recommended to apply a swamping ratio He:H₂ = 3000 ... 10 000 which would have advantages with respect to the size of the low temperature adsorber beds and to the amount of gas to be processed by the Isotope Separation System

b) Average values at Test Module outlet (accounting for plasma pulse dwell time)

c) about 80 % of HTO is assumed to be converted to HT + H₂O by isotopic exchange, no HTO / H₂O is considered to be reduced by the steel walls

Process Description

A flow diagram of the tritium extraction system is shown in Figure 2.1.1.2-1. Instrumentation for process control like sensors for temperature, pressure, flow rate, etc. are not included in this figure. The mode of operation shown is the extraction mode where the cold trap and the first molecular sieve bed are in operation.

At the beginning of the loop, there are 5 valves (V1...V5) which are used to enable a safeisolation of the loop from the Test Blanket Module (TBM). This is especially important in the case of a pressure increase in the TBM caused by a leakage in the cooling subsystem. No measures are foreseen in the TES for after heat removal.

Valve V4 is part of a bypass line which allows functional tests of the loop without sending gas through the TBM.

Front-end components of the loop are a cooler (No.1) to reduce the temperature of the incoming gas to room temperature and a filter cartridge (No.2) to remove particulate material which might be carried out from the blanket zone. (It is not indicated in the figure that two of these filters are needed in parallel to cope with larger amounts of particulate material). The filters have to be arranged in such a way that they are easily and fast exchangeable.

Downstream of the filters, there is a bypass line leading to the compressor (No.8) which is foreseen for initial scavenging of the TBM.

The next component is an ionization chamber (No.3a) mounted in a bypass to the main gas stream; an orifice or a throttle valve is needed to provide the required small gas flow through the ionization chamber.

The Q₂O content (Q = H, T) of the gas is frozen out in the cold trap (No.4) operated at $\leq -100^{\circ}\text{C}$. The residual Q₂O concentration at the outlet is < 0.015 vpm. The amount of ice accumulated within 6 days is of the order of a few grams (max. 6 g). It will not be necessary, therefore, to exchange the water collector (Volume ≤ 200 ml) after each test run.

The purge gas is further cooled down by a recuperative heat exchanger (No. 5) and then passed through an adsorber bed (No. 6a) operated at liquid nitrogen (LN₂) temperature (-196°C). The bed is filled with 5A zeolite pellets which adsorb molecular hydrogen as well as gaseous impurities and residual moisture. The bed contains filters on the down-stream and upstream side to prevent particulate material from being transferred during loading or unloading operations. In addition, the bed is equipped with a LN₂ chiller and an electrical heater. The second bed provides additional adsorption capacity; it can be also used when the first bed is being unloaded or regenerated.

The clean gas leaving the adsorber bed is utilized in the heat exchanger mentioned above to precool the gas coming from the cold trap. It is then further warmed up by an electrical heater (No. 7). The next components are the purge gas blower (No.8) coming in contact only with clean gas at room temperature, and the helium make-up unit (No. 9) where hydrogen is added to provide a He : H₂ swamping ratio of 1000 for the gas reentering the test blanket module. In addition, this component is used for the first fill-up of the loop with helium.

Ancillary Installations

The main tasks of the ancillary installations are:

- to facilitate the transfer of the extracted tritium from the main components of the purge gas system to the Isotope Separation System (ISS) and the Water Detritiation System (WDS), respectively;
- to prepare the components of the main purge gas loop for the next tritium extraction campaign.

Unloading of the cold trap:

After closing the inlet and outlet valves the ice is thawed with the help of an electrical heater. The liquefied water is drained into an evacuated water collector (No.10) which is later on transferred to the Water Detritiation System and replaced by an empty collector vessel.

Unloading and regeneration of a low temperature adsorber bed:

It is important to consider the pressure increase during desorption in the warm-up phase; the maximum amount of adsorbed H_2/HT is 110 mole. A relief tank with a volume of 2 m³ is available, therefore, to be connected with the adsorber bed before the temperature increase is started (from -196 °C to about +20°C). The pressure will remain below 0.2 MPa even though the tank is prefilled with 50 kPa helium which is needed as a carrier gas for the hydrogen isotopes during the further un-loading process. With the help of a circulation pump, the desorbed gas is circulated several times through the adsorber and through a Pd/Ag diffuser (No. 14) where the hydrogen isotopes are separated from the helium carrier gas. At the back pressure side of the diffuser, there is a small helium loop containing a circulation pump (No.17) and several uranium getter beds (No. 16) for storage of the hydrogen isotopes. When the loading capacity of these beds is reached they will be transferred to the Isotope Separation System and replaced by fresh beds. This is expected to be needed after 6 days of reactor operation with nominal power.

At the end of the unloading cycle, the relief tank is evacuated (by use pump No.11 which is connected to the Waste Gas System) and refilled with 50 kPa helium.

If the adsorber bed is to be fully regenerated it must be heated to about 300 °C. The desorbing moisture and impurities will also be sent to the Waste Gas System.

Analytical Tools

The processes of tritium extraction and purge gas purification are controlled by continuous measurement of the tritium concentration at several points of the gas loop and by taking gas samples for chemical analysis.

a) Ionization chambers are used at the following points:

- upstream of the cold trap (component No. 3a, see Fig. 2.1.1.2-1);
- downstream of the cold trap; after removal of HTO, the HT concentration is determined and - as the total activity is known - also the HT/HTO ratio;
- downstream of the heater (No. 7) to control the integral tritium removal efficiency of the loop (ionization chamber No. 3a);

- upstream of the relief tank (No. 12) to control the removal of the hydrogen isotopes by the Pd/Ag diffuser and the tritium concentration of the gas sent to the Waste Gas System at the end of the adsorber unloading / regeneration process.
- b) A gas chromatograph (GC) is used to measure the gas composition upstream of the helium make-up unit. A small gas transfer pump is used to transport gas samples to the GC where they are quantitatively analyzed with respect to Q_2 , N_2 , CO, etc. Additional gas samples taken from other points of the TES can be analyzed with the same GC. Hydrogen concentrations in the range of 1000 vpm, however, are preferably determined by specific hydrogen detectors as mentioned below.
- c) Two specific hydrogen detectors to control the hydrogen concentration are used at the inlet of the cold trap and at the outlet of the helium make-up unit.

A moisture detector which would be very difficult to operate at Q_2O concentrations less than 1 ppm appears not to be necessary since the corresponding information can be obtained from the amount of water collected in the cold trap and / or from the results of the measurements carried out with the ionization chambers.

Space Requirements

It is intended to install the Tritium Extraction Subsystem in the Tritium Building. It will be housed in one or two glove boxes requiring a space of at least 15 m². Additional space of about 35 m² is needed for a control station, for electrical cabinets, and for the working area of the operator.

The size of supply and disposal facilities have not been estimated as most of these facilities will be shared with several other subsystems in the Tritium Building.

Table 2.1.1.2-2 gives a summary of the common facilities needed for the operation of the Tritium Extraction Subsystem.

Figure 2.1.1.2-2 gives a preliminary arrangement of the main components in the glove box; the estimated size of the components has been listed in Table 2.1.1.2-3.

Table 2.1.1.2-4 contains a list with the dimensions of the tubes and cables penetrating the walls of the TES glove box.

Table 2.1.1.2 -2: Supply and Disposal Facilities needed for the operation of the TES Loop

Type of Facility
Central Evacuation System Supply Facilities for <ul style="list-style-type: none"> - Gases (He, H₂, Pressurized Air) - Liquid Nitrogen - Cooling Water - Electrical Power (including emergency power and uninterruptible power) Waste Gas and Waste Disposal System Water Detritiation System Radiological Safety Systems

Table 2.1.1.2 - 3: Size of the Main Components of the TES Loop

No.	Component	Size ^{a)}		
1	Cooler	D: 150	H: 700	
2	Filter	D: 60	H: 500	
3a/b	Ionization Chamber	D: 200	H: 400 (each)	
4	Cold Trap	D: 500	H: 1300	
5	Recuperator	D: 800	H: 1600	
6 a/b	Low Temp. Adsorber	D: 1600	H: 2800	
7	Heater	D: 200	H: 500	
8	Compressor	L: 600	W: 600	H: 800
9	Helium Makeup Unit	L: 1000	W: 400	H: 2000
10	Water Collector	D: 100	H: 320	
11/13/17	Blower	L: 500	W: 500	H: 300
12	Relief Tank	D: 1000	H: 2600	
14	Diffusor	D: 130	H: 1200	
15	Getter Bed (2 Units)	D: 350	H: 750 (each)	
16	Helium Buffer Vessel	D: 200	H: 400	
18	LN ₂ -Supply Tank	D: 1000	H: 1100	
19	Gaschromatograph	D: 700	W: 700	H: 700

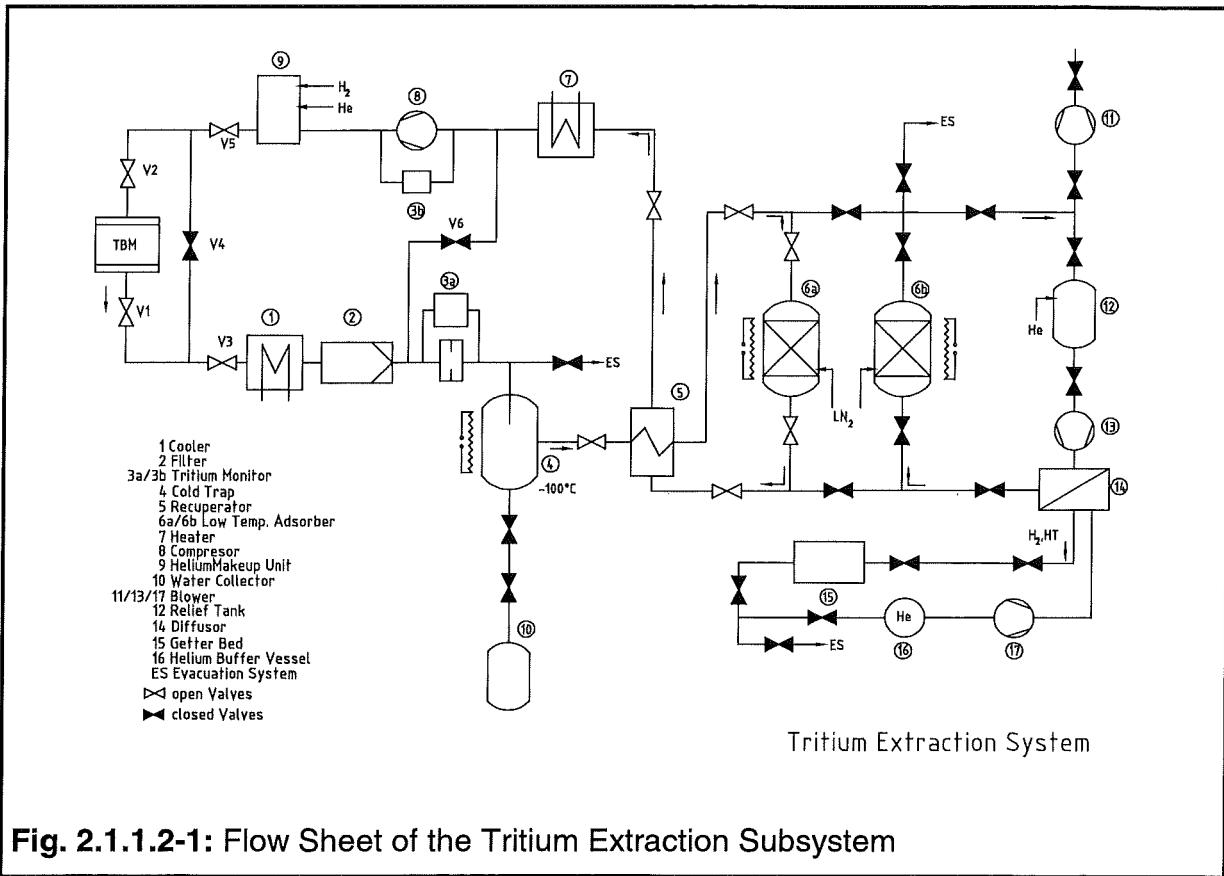
^{a)} D = Diameter, L = Length, W = Width, H = Height. All dimensions in mm and including thermal insulation where needed

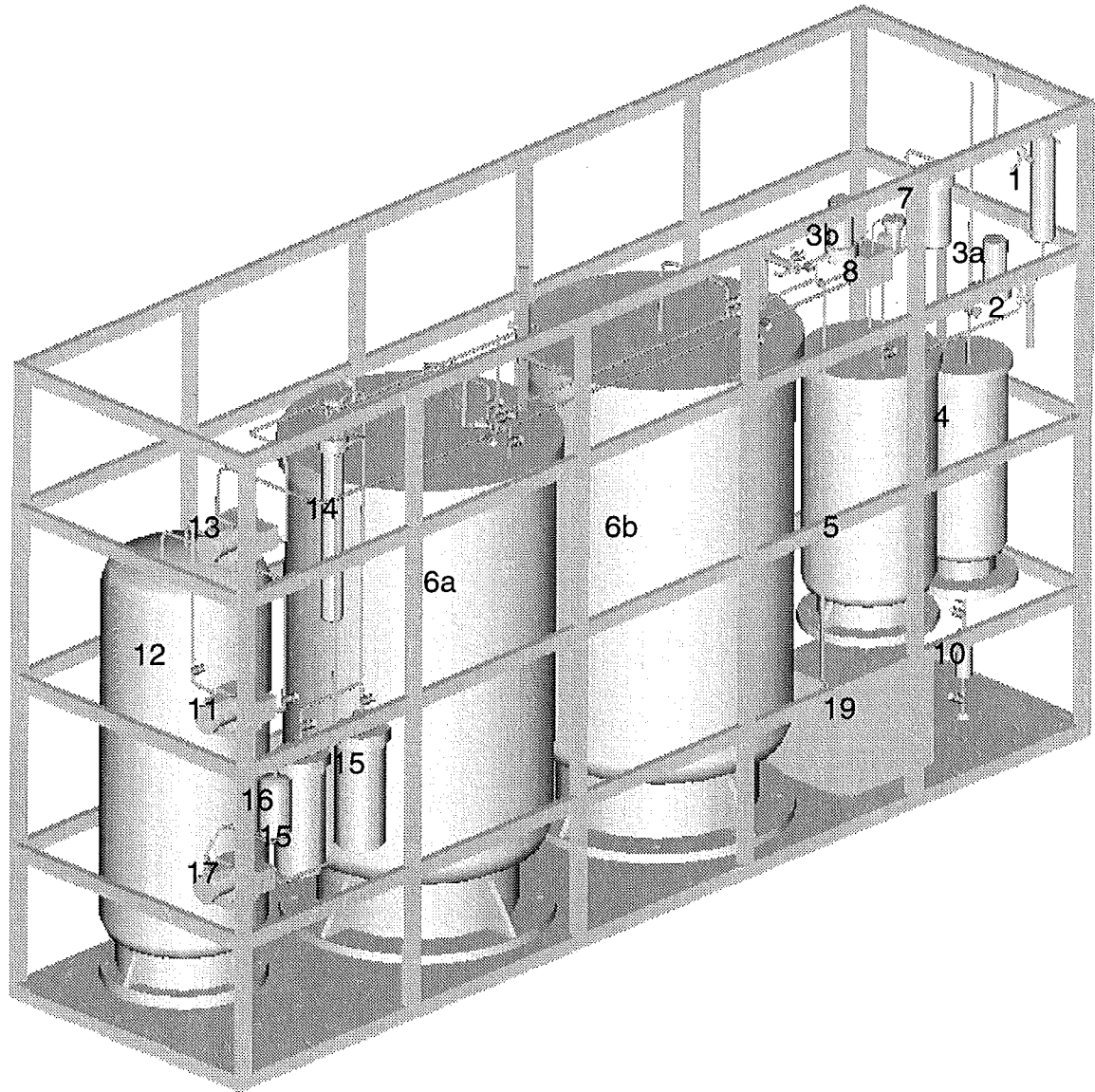
Table 2.1.1.2 - 4: Dimensions of Tubes and Penetrations through the Walls of the TES Glovebox

Medium	Number of Tubes	Diameter (mm) ^{a)}
Purge Gas from / to TBM	2 ^{b)}	120
Cooling Water in / out	2	42.4
Helium	1	17.2
Hydrogen	1	17.2
Liquid Nitrogen	1	84
Central Evacuation System	1	100
Waste Gas	1	60.3
Pressurized Air (for pneumatic valves)	1	17.2
Glovebox Cover Gas (e.g. N ₂)	2	105
Electrical Cables for Process Control and Power Supply	TBD	Feed-Through Box 700 x 500

a) including thermal insulation where needed

b) for radiological safety reasons and for taking advantage of a temperature balancing effect two tubes are installed inside a secondary tube





- | | | | |
|------|--------------------|----------|----------------------|
| 1 | Cooler | 10 | Water Collector |
| 2 | Filter | 11/13/17 | Blower |
| 3a/b | Tritium Monitor | 12 | Relief Tank |
| 4 | Cold Trap | 14 | Diffusor |
| 5 | Recuperator | 15 | Getter Bed |
| 6a/b | Low Temp. Adsorber | 16 | Helium Buffer Vessel |
| 7 | Heater | 19 | Gaschromatograph |
| 8 | Compressor | | |

Fig. 2.1.1.2 - 2: Layout of the Tritium Extraction Subsystem

2.1.1.3 Helium Cooling Subsystem

The cooling subsystem is designed for the European helium-cooled pebble bed (HCPB) test module to be installed in the bottom half of an equatorial test port in ITER, presumably port No. 01. The first wall area of the test module corresponds to the test module frame with an opening 1.15 m wide by 1.075 m high which is separately cooled by water provided by ITER and is thus not considered here. The cooling subsystem includes the primary helium heat removal loops with all components and the secondary heat removal loops. It is assumed that the secondary water loop subsystem is part of the ITER cooling system providing water flow at low temperature of about 35 °C and low pressure of 0.5 MPa. A further interface to the test module are the purge gas lines to the tritium extraction subsystem (TES) which is separate from the cooling stream and with negligible thermal coupling between both subsystems in terms of heat removal.

The cooling subsystem will be housed in the wedge-shaped pit outside of the cryostat at about the same level as the test module (Figure 2.1.1.3-1). The control panel for operation/monitoring of the cooling subsystem will be installed in the Tokamak Service Building requiring a space of approximately 12 m². Further electrical control equipment, like signal transducers, are planned to be placed in the 3m x 2.7m section of the outer gallery close to the loops.

Two separate primary heat removal loops of 2 x 50 % heat capacity are foreseen for redundancy purposes in case of accidents and the need for decay heat removal in accordance with the DEMO blanket design. Figure 2.1.1.3-2 shows a flow diagram of the primary heat removal loops and the interfaces to ancillary equipment. Figure 2.1.1.3-3 and Figure 2.1.1.3-4 show the arrangement of the components in the pit in an extremely compact way due to space constraints, making installation and maintenance very difficult. Please note that a battery of tanks is located on the upper floor of the pit extending into the neighbour wedge with an approximate minimum space required of 0.6 m wide by 6 m long by 2.8 m high.

2.1.1.3.1 Thermal-hydraulic design

Design conditions and assumptions are summarised in Table 2.1.1.3-1. The table contains two columns of values, the nominal values pertaining to the present layout of the first test module for the basic performance phase, and the design values including margin for uncertainties in control and for later options.

The heat to be removed from the test module amounts to 1.9 MW nominal and 2.3 MW design value, based on 0.25 and 0.5 MW/m² of surface heat flux, respectively, nuclear heating due to neutron wall loading of 1.2 MW/m² and the projected area of the module facing the plasma being 1.11 m wide by 1.045 m high. Nominal primary helium coolant conditions are 250 °C and 350 °C (later on 250 and 450 °C) at module inlet and outlet, respectively, and 8 MPa of pressure. The total flow rate of the primary helium is 3.7 kg/s. Two identical loops of 2x50 % of heat capacity are foreseen.

The thermal power of the test module is removed to the ITER secondary cooling water with assumed conditions of 35/75 °C at the heat exchanger inlet/outlet, 0.5 to

1.0 MPa and a mass flow rate of 11.4 kg/s (with a maximum of 13.8 kg/s). Detailed thermal-hydraulic data for loop components are given in the next subsection.

Table 2.1.1.3-1: Nominal and Design Conditions of the Cooling Subsystem for HCPB Test Blanket Module

	Unit	Nominal Value	Design Value
Projected area of module facing the plasma	(m x m)	1.11 x 1.035	1.11 x 1.045
Surface heat flux	(MW/m ²)	0.25	0.5
Neutron wall loading	(MW/m ²)	1.2	1.2
Total heat to be removed	(MW)	1.9	2.3
Primary coolant		helium	helium
Temperature module in/out	(°C)	250/350	250/450
Pressure	(MPa)	8	9.6
Number of circuits		2	2
Mass flow rate (both circuits)	(kg/s)	3.7	3.7
Secondary coolant		water	water
Temperature heat exchanger in/out	(°C)	35/75	35/75
Pressure	(MPa)	0.5	1.0
Number of circuits		2	2
Mass flow rate (both circuits)	(kg/s)	11.4	13.8

2.1.1.3.2 Primary Heat Removal Loops

A flow diagram of one of the two separate cooling loops for the HCPB test module is shown in Figure 2.1.1.3-2. Main components in each loop are, besides the test module, a heat exchanger, circulator, electrical heater, dust filter, and pipework. The primary loop is directly connected to the helium purification subsystem (see 2.1.1.4) via small pipes taking a bypass flow of about 0.1 % of the main mass flow rate. Further interfaces are shown in the flow diagram to the pressure control unit needed for subsystem evacuation, helium supply, and protection against overpressure. Also shown is the minimum required instrumentation for process control.

An overview of thermal-hydraulic data such as pressure loss, helium volume, and helium mass inventory in the different components is displayed in Table 2.1.1.3-2. The total helium mass inventory in one loop amounts to 6.9 kg at nominal operating conditions and the overall pressure loss is about 0.36 MPa about 53 % of which occurring in the test module proper. The heat exchanger layout is characterised in Table 2.1.1.3-3. The primary loop components and heat losses are described below with a summary of the main dimensions and masses involved, as far as thermal inertia due to temperature fluctuations is concerned, being displayed in Table 2.1.1.3-4.

Test Blanket Module: The HCPB blanket test module (TBM) is described in section 2.1.1.1. Similar to the DEMO blanket design the volume fraction of the primary helium relative to the total module volume is about 16 %. With this ratio and a test

module volume of $1.11 \times 1.045 \times 1 \text{ m}^3$ the helium volume amounts to 0.18 m^3 , i.e., 0.09 m^3 pertaining to each loop. The pressure loss is evaluated as 0.19 MPa .

Heat Exchanger: A first layout has been performed assuming a straight tube bundle heat exchanger (HX) with high pressure helium flowing inside the tubes and low pressure water flowing outside. The required tube bundle data along with the primary and secondary loop flow parameters are listed in Table 2.1.1.3-3, again showing the nominal values for the first test module and the design values considering anticipated options with sufficient margin. (The design values are regarded as maximum values for component layout and are, thus, not consistently pertaining to a certain operating mode.) For the design size the helium volume in one HX would be 0.06 m^3 (0.02 m^3 in the tubes and 0.04 m^3 in the end domes). Alternatively a U-tube HX could be envisaged which would not significantly alter the design data.

Table 2.1.1.3-2: HCPB Cooling Loop Pressure Loss and Helium Inventory, nominal conditions

Component	Press. loss (Pa)	Volume per Loop (m^3)	Mass per Loop (kg)
Hot leg pipework	30700	0.143	0.85
Cold leg pipework	27000	0.156	1.15
Main pipe elbows	27000	incl. in pipes	incl. in pipes
Bypass to heat exchanger	(30000)	0.033	0.2
Valves	51400	0.002	0.015
Heat exchanger	4000	0.061	0.4
Circulator	-	0.025	0.18
Electrical heater	500	0.03	0.18
Dust filter	30000	0.02	1.21
Buffer tank	-	0.132	2.76
Test module	190000	0.09	0.6
TOTALS	360500	0.87	7.53

Circulator: One variable speed helium circulator will be installed in the cold leg of each primary loop operating at $250 \text{ }^\circ\text{C}$ in normal operation. Including some margin during heating and baking phases the design temperature is set to $300 \text{ }^\circ\text{C}$ and the design pressure to 9.6 MPa (20 % above nominal for overpressure control). An encapsulated type circulator with vertical shaft is envisaged where the type of bearings (gas lubricated or magnetic) has still to be decided upon. The design specification for the circulator is as follows: temperature $300 \text{ }^\circ\text{C}$, pressure 9.6 MPa , mass flow rate 1.9 kg/s at a pumping head of 0.36 MPa at 80 % of maximum speed and at $250 \text{ }^\circ\text{C}$ inlet temperature, speed variation max/min of at least 4. Under these conditions the electric power of the drive motor would be 130 kW . The helium volume contained in the circulator is estimated as 0.025 m^3 and the overall dimensions of the circulator and drive unit are expected to be 0.5 m diameter times 1.8 m height.

Electrical Heater: This component is needed for baking the test module first wall at $240 \text{ }^\circ\text{C}$ and for heating the whole cooling subsystem, including the test module, to operating temperatures after maintenance or repair periods. It is positioned in a bypass to the HX, assuming that the HX is isolated during heating phases and the circulator is operating at full or reduced speed. The electrical power has been set to 100 kW . This enables to heat the whole TBM subsystem at a rate of about $70 \text{ }^\circ\text{C}$

per hour in case of an ideally uniform heating. The main dimensions of the helium volume are 0.19 m diameter times 1.3 m height, approximately 20 % of which being occupied by the heating rods. This yields a helium volume of 0.03 m³. The estimated pressure loss is small, ~500 Pa. The overall dimensions are assumed to be 0.36 m diameter (at flanges) times 1.7 m height (including the end dome foreseen for electric terminals).

Table 2.1.1.3-3: Heat Exchanger Layout for HCPB Test Module Cooling Subsystem

	Unit	Nominal Value	Design Value
Type		Straight tube bundle	
Number of heat exchangers (HX)		2	2
Heat to be removed per HX	(MW)	0.95	1.15
HX tube size (outer/inner diameter)	(mm)	18/14	18/14
Number of tubes per HX		96	96
Tube bundle diameter x length	(m)	0.27 x 0.9	0.27 x 1.2
Overall HX dimensions diameter x length	(m)	0.35 x 1.8	0.35 x 2.2
Primary coolant		helium inside tube	
Temperature in/out	(°C)	250/350	250/450
Pressure	(MPa)	8	9.6
Mass flow rate per HX	(kg/s)	1.9	<1.9
Flow velocity in/out	(m/s)	20.8/17.5	14.6/10.6
Heat transfer coefficient in/out	(W/(m ² K))	2500/2300	1700/1500
Secondary coolant		water outside tube	
Temperature in/out	(°C)	35/75	35/75
Pressure	(MPa)	0.5	1.0
Mass flow rate per HX	(kg/s)	5.7	6.9
Flow velocity	(m/s)	0.16	0.2
Heat transfer coefficient in/out	(W/(m ² K))	1500/1900	1800/2200

Dust Filter: A filter unit is installed in the hot leg of the main loop, accumulating residual dust and particles from fabrication, and erosion particles down to a size of typically 10-6 m. To some extent even the much smaller sputter products evolving in the neutron field in the TBM may be trapped which otherwise are expected to be deposited mainly in the heat exchanger and at pipe walls. The array of small-diameter filter tubes, or plates in a grid format, forms a removable filter cartridge of 0.35 m diameter and 2.8 m length, giving a helium volume of the filter shell of approximately 0.27 m³. The pressure loss is expected to be less than 0.03 MPa. Details have still to be worked out.

Pipework: For the main pipework, i.e., hot leg and cold leg, an outer diameter of 101.6 mm and a wall thickness of 6.3 mm have been chosen. This results in a flow velocity in normal operation of between 40 and 50 m/s and in small pressure losses. The pipe length is determined on the basis of the component arrangement in the pit shown in Figures 3 and 4. It yields a total length of the main pipework of 48 m (25 m for the cold leg and 23 m for the hot leg). The number of elbows is assumed to be 20. Overall the pipework contributes with 16 % to the pressure losses in the loop (Table 2.1.1.3-2).

The flow rate during baking and heating can be reduced compared to the rated mass flow rate. Thus the bypass to the HX can be smaller than the main pipework. The outer/inner diameter has been set accordingly to 82.5/72.5 mm. In normal operation the bypass is supposed to be almost closed during burn times and open during dwell times (see section 0).

Valves: The number of valves in the main loops has been minimised to avoid inadvertent closure which would mean loss of heat sink in the affected loop. Hence, only one valve is installed before the HX in the main loop and another one in the bypass line before the electrical heater. These two valves are needed for temperature control in normal cyclic operation and must be position controlled.

Pressure Control Unit: This is a combination of equipment needed for evacuation of the cooling subsystem, helium supply, pressure control, and overpressure protection. The components are conventional and of relatively small size, except for the storage and dump tanks. The pressure control unit is essentially isolated from the main cooling loops during normal operation, however in case of a pressure drop, like a loss of coolant accident, the buffer tank will discharge into the main loop.

The evacuation unit is needed for the first start-up as well as after repair of the main cooling loops. It is assumed that a vacuum pipe line is provided as common ITER utility. The pipe line has to be reliably isolated from the loops after evacuation to avoid inadvertent interconnection of the loops or pressurisation of the vacuum system.

The helium supply and storage unit consists of a storage tank, buffer tank, compressor, and pressure regulators. Except for the fresh helium supply and the decommissioning of the used helium, which are supposed to be provided by ITER, the supply and storage unit must be self-sufficient. The storage tank is sized as to take the whole helium inventory of the loop with 10 % margin (excluding the one in the buffer tank), i.e., about 5.7 kg at about 50 °C, 14 MPa, resulting in a tank volume of 0.31 m³. This can be achieved by, e.g., a tank of 0.5 m diameter, 2 m long. A multi-stage compressor and cooler will be needed to load the storage tank for emptying the main loops.

Pressure control in the main loops during normal operation is achieved in the following way: The storage tank is kept at low pressure (≈ 1.5 MPa) so that the main loop can discharge to the storage tank via the pressure regulator if the set point "pressure high" is reached. The buffer tank, on the other hand, has to compensate for the loop pressure if the set point "pressure low" is reached. As it discharges to the loop it will be recharged by a compressor from the storage tank. A buffer tank volume of 10 % of the loop volume is chosen, that is about 0.08 m³, and a maximum operating pressure of 14 MPa. The dimensions of the tank could be, e.g., 0.3 m diameter, 1.5 m length.

The overpressure protection of the cooling loops consists of two redundant safety valves or a combination of one safety valve plus a burst disc. The safety valves discharge into a group of dump tanks which are kept at controlled low pressure (near atmospheric) during normal operation. This avoids releasing contaminated helium into the building and complete depressurising of the main loop in case the valve would fail to close. The dump tanks are sized for the event that the primary loop was inadvertently pressurised to the nominal pressure (8 MPa) at room temperature and the whole subsystem was subsequently heated up to 250 °C, the nominal operating inlet temperature. If in this case the pressure regulator would fail to open, the safety

valve would respond. In order to limit then the pressure to 8 MPa requires a dump volume of about 70 % of the loop volume itself, i.e., 0.56 m³. This is about twice than what is needed as storage volume and can be achieved by, e.g., two tanks of 0.5 m diameter, 1.7 m length.

Most of the equipment of the pressure control unit can be installed on the gallery in the pit next to the battery of tanks as indicated in Figure 2.1.1.3-3.

The heat losses passing the thermal insulation from both cooling circuits (piping and components, but excluding the TBM proper) amount to 17 kW in normal operation, assuming an insulation thickness of mineral wool of between 8 and 12 cm. About 70% of these losses occur from the piping. The surface temperature of the insulation layer assumes 55 to 70 °C at nominal coolant temperature. This is considered to be tolerable, since no access is envisaged during operation.

Table 2.1.1.3-4: Enveloping Dimensions and Masses (for 1 of 2 helium cooling loops, dimensions not including thermal insulation)

Component	Number per loop	Diameter (m)	Length (m)	Mass (kg)
Helium/water heat exchanger	1	0.5	2.2	600
Circulator, vertical shaft (first guess)	1	0.5	0.5	225
Circulator drive motor (first guess)	1	0.6	1	600
Electrical heater	1	0.36	1.7	240
Dust filter (without shield)	1	0.6	3.5	1500
Main pipework (hot leg and cold leg)	1	0.1016	48	700
Helium storage tanks	1	0.5	2.0	580
Helium dump tanks	2	0.5	1.7	500
Buffer tank for pressure control	1	0.3	1.5	210
Elevation of HX above test module	-	-	2.1	-

2.1.1.3.3 Secondary Heat Removal Loops

The secondary heat removal subsystem is considered as part of the ITER cooling system. For the layout a constant water flow with nominal inlet temperature of 35 °C at the secondary side of the heat exchanger (see 2.1.1.3.1) and a flow rate of ~7 kg/s per HX are assumed, leading to pipe dimensions of 50 mm outer diameter, 3 mm wall thickness, at a velocity of ~5 m/s. The outlet temperature will then vary according to the burn and dwell cycles between 75 °C and 35 °C. Flow, pressure, and temperature monitoring are needed. No significant migration of tritium from the primary coolant to the secondary side is expected.

2.1.1.3.4 Maintenance/Remote Handling

Activation of cooling subsystem components installed in the pit is expected to be generally low allowing controlled personnel access after plant shutdown. An exception may be the dust filters which may require extra shielding provisions (perhaps temporary). In-service inspection such as examination of selected welds by different methods (visual, eddy current, ultrasonic), inspection of circulator internals, functional tests of valves, leak tightness of heat exchangers etc. occur during test

module change-out or during planned or unplanned machine shutdown periods. Remote handling is envisaged for connection and disconnection of the TBM. There are isolation flanges with welding lips connecting the module with the rest of the cooling subsystem. One or two such flanges for each of the four main pipes have to be remotely connected (or disconnected in case of test module replacement). Remote handling is also envisaged for replacement of the dust filter. In the case of any defects in heat exchangers or electrical heaters replacement of the whole component may be more appropriate than a repair.

2.1.1.3.5 Assembly

All components of the heat removal subsystem such as heat exchangers, circulators, electrical heaters, dust filters, tanks, and valves will be preassembled at the factory and delivered to the site as functional units. Connection of the components will be performed on site by conventional means. An exception is the installation of the test module. It will be brought in place by the aid of a special transporter being aligned with the test port. It is equipped with all tools needed for positioning, aligning, locking, connecting the module in the 8 m long tunnel of the test port, and perhaps with cooling provisions. The other large components of the cooling subsystem installed in the pit require lifting equipment with a load capacity of about 2 tons (the heaviest component, the dust filter, has a weight of about 1500 kg). Field welded joints will be subjected to surface and/or volumetric inspection, followed by pressure and leak tests. Thermal insulation will be installed after leak testing of the loops.

2.1.1.3.6 System Start-up, Control, and Shutdown

For the first start-up or after a major repair, the cooling subsystem is assumed to be clean and proof tested, components are at room temperature and filled with air. The ITER machine is supposed to be simultaneously conditioned for start-up. The following steps will then be taken with the cooling subsystem:

Subsystem evacuation to <102 Pa within about 24 hours

Subsystem flooding with helium and pressurisation to approximately 4.2 MPa at 25 °C

Heating to 300 °C within a few hours by either the circulator alone at full or reduced speed, or in combination with the electrical heater (see paragraph electrical heater in 2.1.1.3.2); HX closed

Establishing secondary cooling water flow in HX

Establishing temperature control at desired baking temperature (about 240 °C at circulator outlet) by controlling the flow through HX, heater power still on

Keeping subsystem stable for baking period

Driving circulator to nominal speed (if needed)

Establishing temperature and pressure control at stand-by level: 250 °C, 8 ± 0.3 MPa at circulator outlet, heater power on. Subsystem is now ready for operation.

For cooling subsystem control in normal operation the typical ITER load cycle is envisaged, i.e., pulse duration of 1000 s and repetition time of 2200 s with specified power ramp-up and ramp-down. The power removed by the cooling loops thus varies

between about 2.2 MW and 0.3 to 0.5 MW, the latter coming mainly from circulators and heaters (with less than 30 kW from decay), that is a ratio of 7:1 (respectively 4:1). Because of the given large mean temperature difference in the HX between the primary and secondary side the heat removed in the HX can most effectively be influenced by primary helium flow control. Hence, the following preliminary subsystem control scheme is proposed for pulsed operation, based on first thermodynamic analysis with consideration of the thermal inertia of all components.

The principal objective is to keep the test module inlet temperature at 250 °C.

The secondary cooling water inlet temperature should be kept at 35 °C.

The circulator should be operated at rated speed.

The electrical heaters are turned off.

Flow partition through the HX and heater bypass is controlled as to maintain the inlet temperature to the TBM as close as possible to 250 °C.

If for some reason much longer dwell times or shutdown periods have to be bridged, decay heat removal at reduced circulator speed, or even by natural convection, is envisaged.

Complete shutdown of the HCPB-TBM including removal or replacement of the TBM will be accomplished by the aid of the transporter. In this case one of the cooling loops will be emptied and disconnected, while the other loop maintains decay heat removal. The disconnected piping of the TBM will then be connected to the transporter's cooling system which overtakes decay heat removal. Subsequently, the second cooling loop will be treated in the same way as the first one, before the TBM is removed. It is assumed that during the whole procedure an inert gas atmosphere with a pressure of about 0.1 MPa and a temperature of less than 200 °C be introduced into the vacuum vessel. Under these conditions it is expected from analyses performed for DEMO that the decay heat of the TBM can be dissipated to the surrounding without extra active cooling, constituting a back-up means to the transporter's temporary decay heat removal mission.

2.1.1.3.7 Materials

All of the piping and components in the primary cooling subsystem will be constructed of austenitic steel. The test module will be made of ferritic steel (section 2.1.1.1.7 of [1]) with the interface being at the isolation flanges next to the test module. All of the piping and components will be equipped with 8 to 12 cm of a mineral thermal insulation.

2.1.1.3.8 Safety

The main safety concerns with the cooling subsystem are the loss of coolant accident with regard to tritium and activation products release, and the loss of flow or loss of heat sink accident in both loops with respect to decay heat removal. They are assessed in section 2.1.1.1.8.

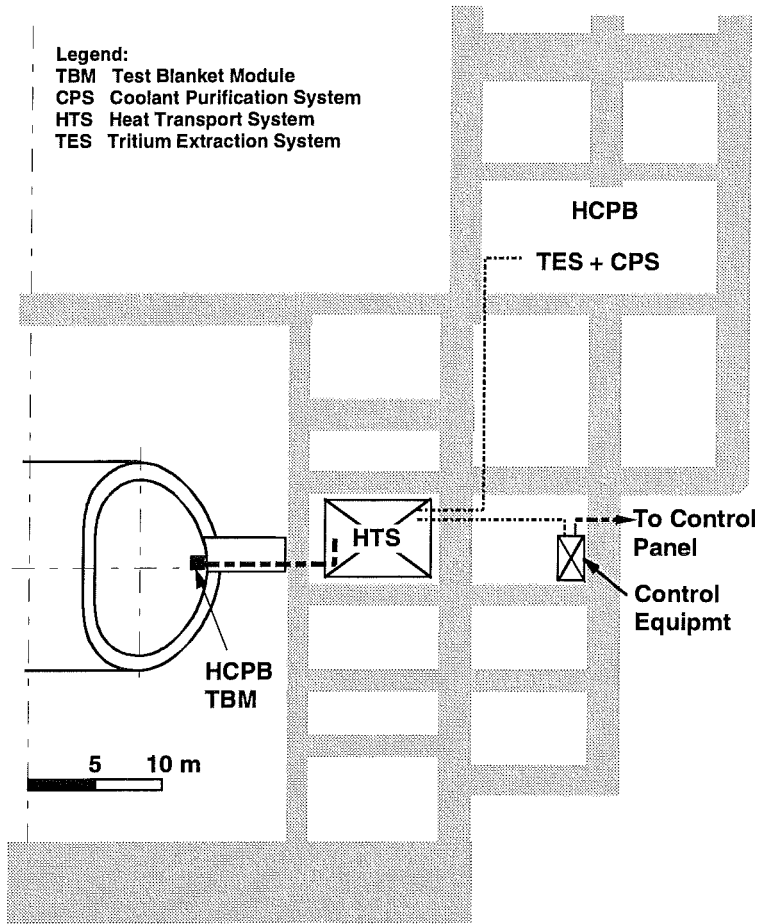
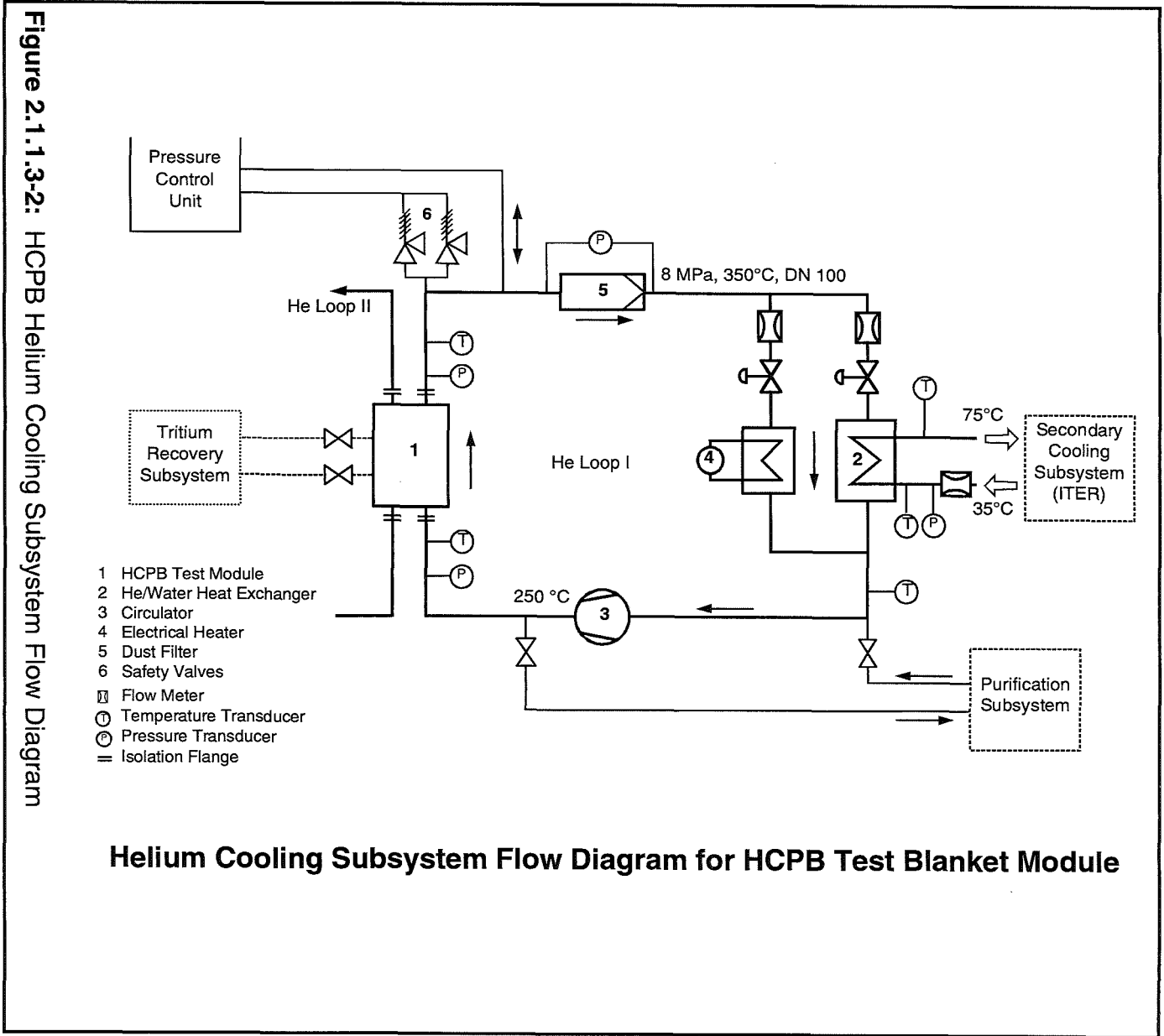
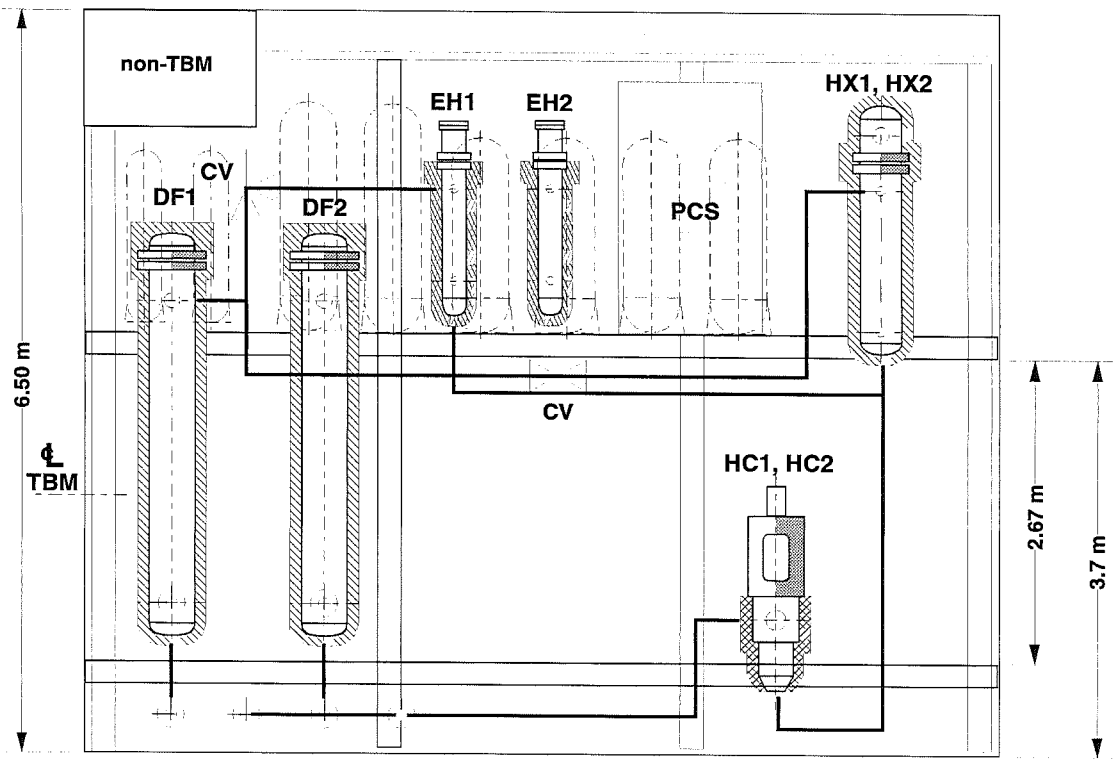


Fig. 2.1.1.3-1 Location of HCPB Helium Cooling Subsystem in ITER

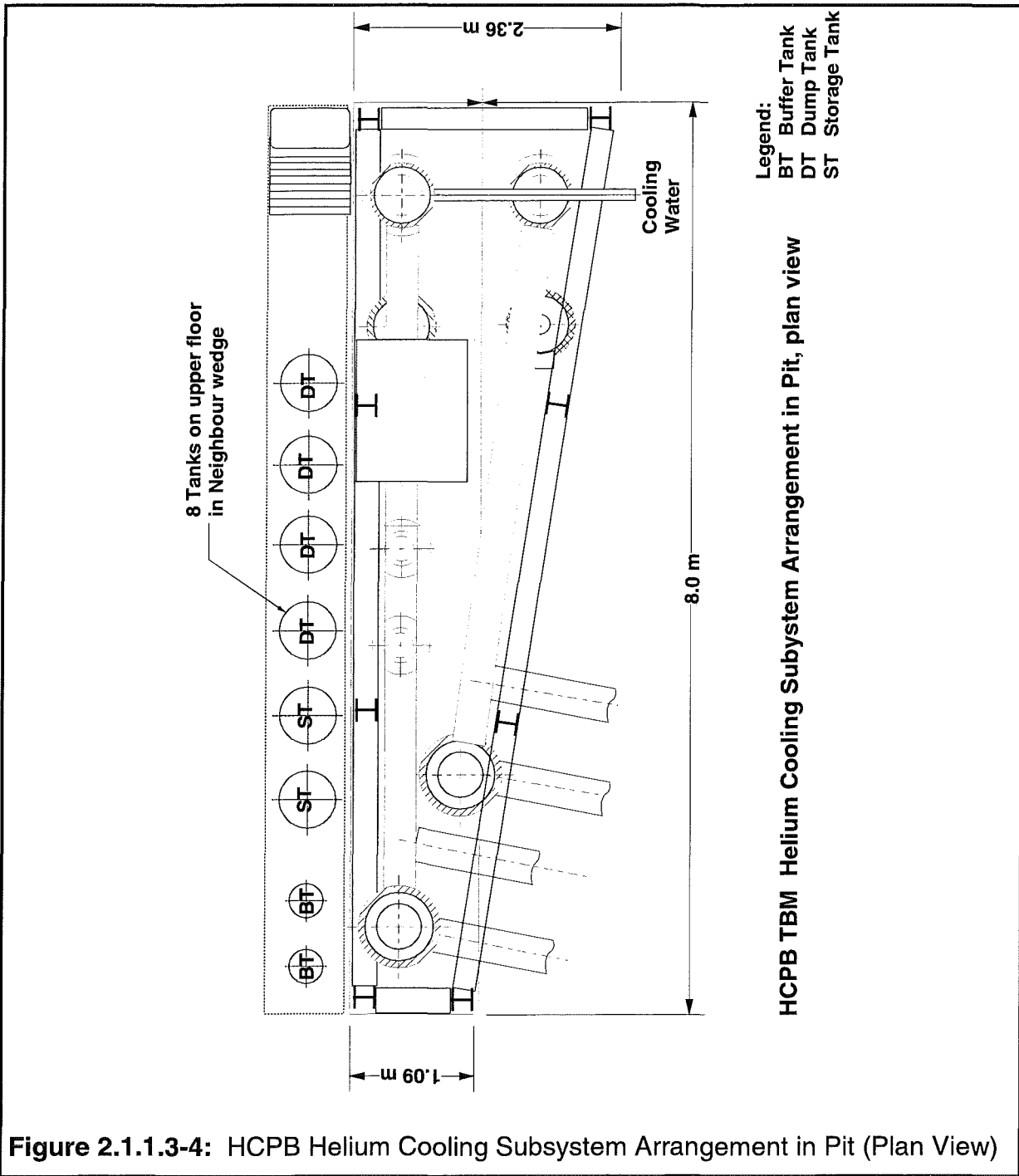




- Legend:
- CV Control Valve
 - DF Dust filter
 - EH Electrical Heater
 - HC Helium Circulator
 - HX Heat Exchanger
 - PCS Pressure Control System

HCPB TBM Helium Cooling Subsystem Arrangement in pit, elevation view

Figure 2.1.1.3-3: HCPB Helium Cooling Subsystem Arrangement in Pit (Elevation View)



2.1.1.4 Coolant Purification Subsystem

For each of the two coolant systems of the blanket test module one purification system is provided to purify a fraction of 0.1% of the helium coolant stream, i.e. to extract hydrogen isotopes as well as solid, liquid or gaseous impurities. The main design data of the purification systems are given in Table 2.1.1.4-1.

Table 2.1.1.4-1: Main Design Data for each of the Coolant Purification Systems

He Mass Flow in Purification System	1.85 g/s = 37.3 Nm ³ /h
Pressure	8 MPa
Total Amount of He Coolant	7.5 kg
Partial Pressures ^{a)}	
p (H ₂)	< 10 Pa
p (HT)	< 0.1 Pa
p (DT)	< 0.1 Pa
p (Q ₂ O)	35 Pa
p (N ₂)	8 Pa
Extraction Rates	
Q ₂ O	0.2 mole / day ^{b)}
N ₂	0.04 mole / day
O ₂	0.03 mole / day ^{c)}
Tritium Extraction Efficiency	≥ 95 %
Temperature of the Coolant at Coolant Purification Inlet / Outlet	250 °C / 50 °C

a) under equilibrium conditions (obtained within 4 hours) in the coolant

b) due to catalytic oxidation, H₂, HD, and HT are extracted as Q₂O (Q = H, D, T)

c) excess oxygen from the oxidizer

The thermal power removed in each coolant system is 0.95 MW, the corresponding mass flow rate is 1.85 kg He/sec. The tritium content in the coolant is caused by permeation from the First Wall and from the purge gas of the Tritium Extraction Subsystem. According to the calculations described in paragraph 2.1.1.1.9 an average value for the tritium permeation rate into the coolant is

$$m_p = 0.0042 \cdot 10^{-3} \text{ mole T / h}$$

As 0.1 % of the coolant is continuously purified with an efficiency of 95 %, the tritium concentration in the coolant will increase to an equilibrium concentration c_e which is reached when the Removal rate $m_r = 0.001 \cdot 0.95 \cdot m_T$ is equal to the Permeation

rate $m_p = 0.004 \cdot 10^{-3}$ mole T/h, where m_T is mass flow rate of tritium in the cooling loop under equilibrium conditions.

This leads to $m_T = 0.0044$ mole T/h

and $c_e = m_T/m_{He} = 2.6 \cdot 10^{-9}$ ($m_{He} = 1.665 \cdot 10^6$ mole/h)

This is equivalent to a HT partial pressure of 0.02 Pa. The concentration of H₂ in the coolant is calculated from the HT partial pressure by taking into account the much higher concentration of H₂ in the purge gas (about a factor 600 in comparison to HT), the fractional contribution of the tritium permeation from the purge gas system (about 25% of the total permeation), and the higher permeation rate of H in comparison to T (factor 1.73). The resulting partial pressure of H₂ is 5.4 Pa.

The partial pressures and extraction rates of HTO / H₂O given in Table 2.1.1.4-1 have been calculated assuming a leakage of 3 g water per day from the heat exchanger into the coolant loop. The corresponding values for N₂ were obtained for a concentration of 1 ppm in the coolant.

Process Description

A flow sheet of the coolant purification system (CPS) is shown in Fig. 2.1.1.4 - 1. The instrumentation for process control like sensors for temperature, pressure, flow rate etc. is not included in the figure.

The slip stream entering the CPS is extracted from the main cooling loop downstream of the circulator (see Fig. 2.0.4 - 1). The first component is a water separator to remove condensed water. It is installed in a bypass and will not be used under normal conditions, i.e. as long as the coolant does not contain water droplets.

The gas is then warmed up to 450 °C by an electrical heater and transferred to an oxidizer unit containing a precious metal catalyst (Pd or Pt on alumina). An over-stoichiometric amount of oxygen is added to obtain a quantitative conversion of Q₂ to Q₂O (Q = H, D, T). The high temperature of the gas is favorable for the kinetics of the oxidation process.

The next component is a water cooler where the gas temperature is reduced to room temperature. The Q₂O content is frozen out in a cold trap operated at -100°C.

Finally, the gas is passed through a recuperator and then to a 5A molecular sieve bed which is cooled with liquid nitrogen (LN₂) to adsorb gaseous impurities like N₂ and the excess oxygen not used up in the oxidizer. Any hydrogen isotopes that have not been oxidized are also adsorbed. The second bed provides additional adsorption capacity; it may be used when the first bed has not been unloaded or regenerated.

The pure helium is carried back through the recuperator, further warmed up by an electrical heater, and then returned into the main cooling loop upstream of the circulation pump. As the gas flow rate reentering the cooling loop is only 0.1 % of the coolant flow rate, it is of minor importance that both gas streams do not have the same temperature (50°C and 250°C, respectively).

By utilizing the pressure difference of the main coolant pump it should be possible to operate the purification system without an additional compressor or circulation pump. Nevertheless, a corresponding pump (No.5) will be available on demand.

At the end of an experimental cycle, the operation of the cooling system and of the CPS should be continued for about 12 hours to arrive at a reasonably low concentration of hydrogen isotopes and impurities in the coolant.

Before the initial operation of the CPS, a test run can be carried out without the inter-connection to the coolant loop. For this purpose, the loop is filled with a test gas of appropriate pressure; the valves at the loop inlet and outlet are closed, the bypass valve V1 is opened, and the gas flow is started with the help of the circulator.

Regeneration

Some components must be regenerated before their retention capacity has been reached. The cold trap loaded with ice is depressurized (via relief valve 10) and warmed up to room temperature to liquefy the water which is then drained into a water container and sent to the Water Detritiation System.

The adsorber beds are first depressurized like the cold trap (via relief valve 11). During a normal unloading operation they are warmed up to room temperature, and the desorbing impurities are sent to the Waste Gas System. A complete regeneration is achieved by heating to 300 °C and purging with clean helium.

Analytical Tools

The tritium extraction is controlled by continuous measurement of the tritium concentration at several points of the loop. Four ionization chambers are used for this reason:

- No.1: At the loop inlet upstream of the electrical heater,
- No.2: Downstream of the cold trap (supplying information about satisfactory function of the oxidizer and the cold trap),
- No.3: At the loop outlet (under proper conditions, the reading should be the same as of No.2),
- No.4: Downstream of valve 11 (to monitor the effluent gases).

In addition, the composition of the coolant gas is analyzed with the help of a gas chromatograph by taking gas samples at the inlet and the outlet of the loop.

Space Requirements

The two Coolant Purification Subsystems will be installed in the Tritium Building in close neighbourhood to the Tritium Extraction Subsystem. The size of the main components has been estimated and listed in Table 2.1.1.4-2. The geometrical layout is shown in Figure 2.1.1.4-2. The space requirement for two CPS loops is about 16 m². Additional space of at least 30 m² in front of the facility will be needed for electrical cabinets, for a control station, and for the working area of an operator. Fig.2.1.1.4.-3 gives a proposal for the installation of the two subsystems for the HCPB Test Blanket Module. The integral space requirement is about 100 m².

It is expected that supply and disposal facilities are essentially the same as those needed for the Tritium Extraction Subsystem (see Table 2.1.2-2).

Table 2.1.1.4-2: Size of the Main Components

No.	Component	Size ^{a)}
1	Water Separator	D: 60 H: 700
2	Electrical Heater	D: 350 H: 900
3	Catalytic Oxidizer	D: 500 H: 1000
4	Cooler	D: 250 H: 700
5	Blower	L: 600 W: 600 H: 800
6	Cold Trap	D: 500 H: 1300
7	Recuperator	D: 500 H: 1200
8 a/b	Low Temp. Adsorber	D: 600 H: 800
9	Electrical Heater	D: 250 H: 900
12	Relief Tank	D: 2000 H: 4000

^{a)} D = Diameter, H = Height, L = Length, W = Width; all dimensions in mm and including thermal insulation where necessary

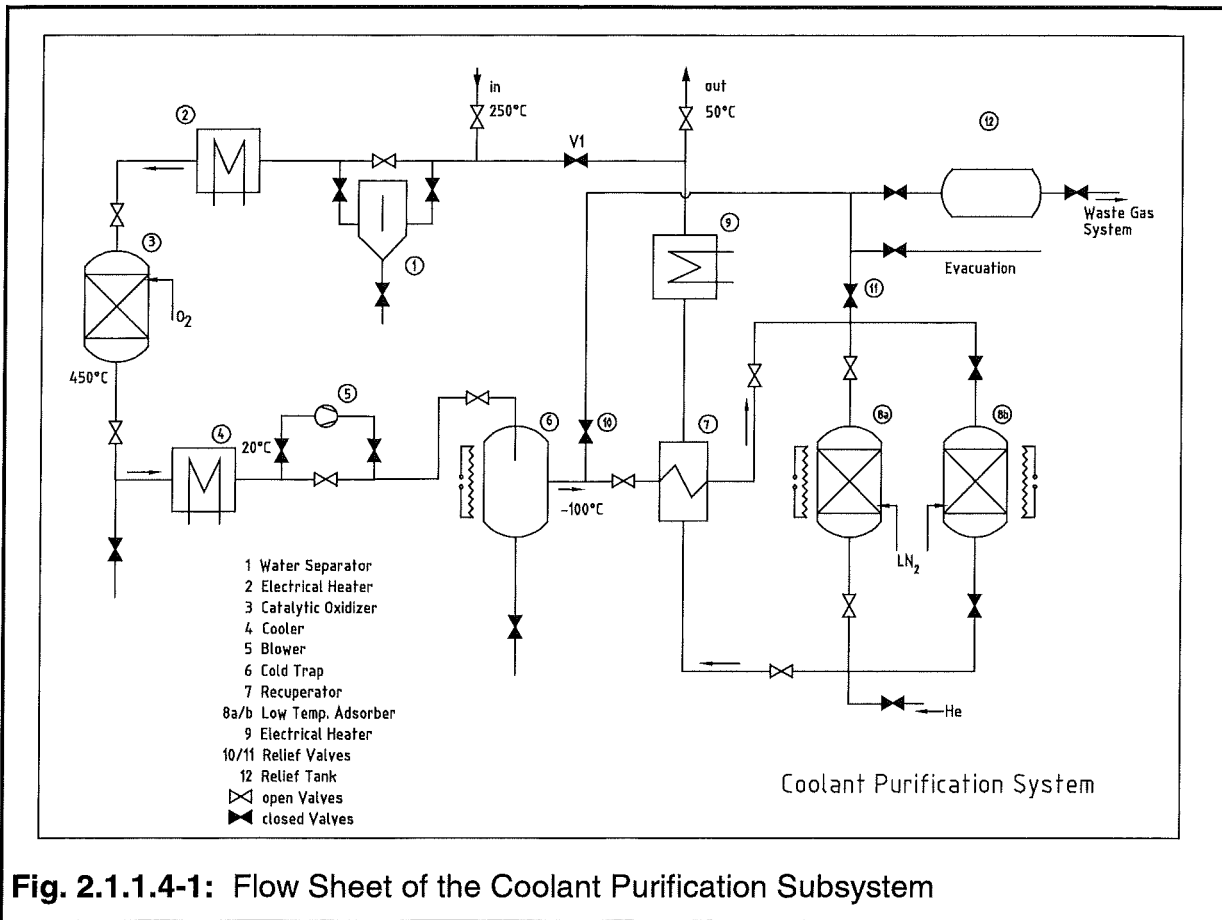
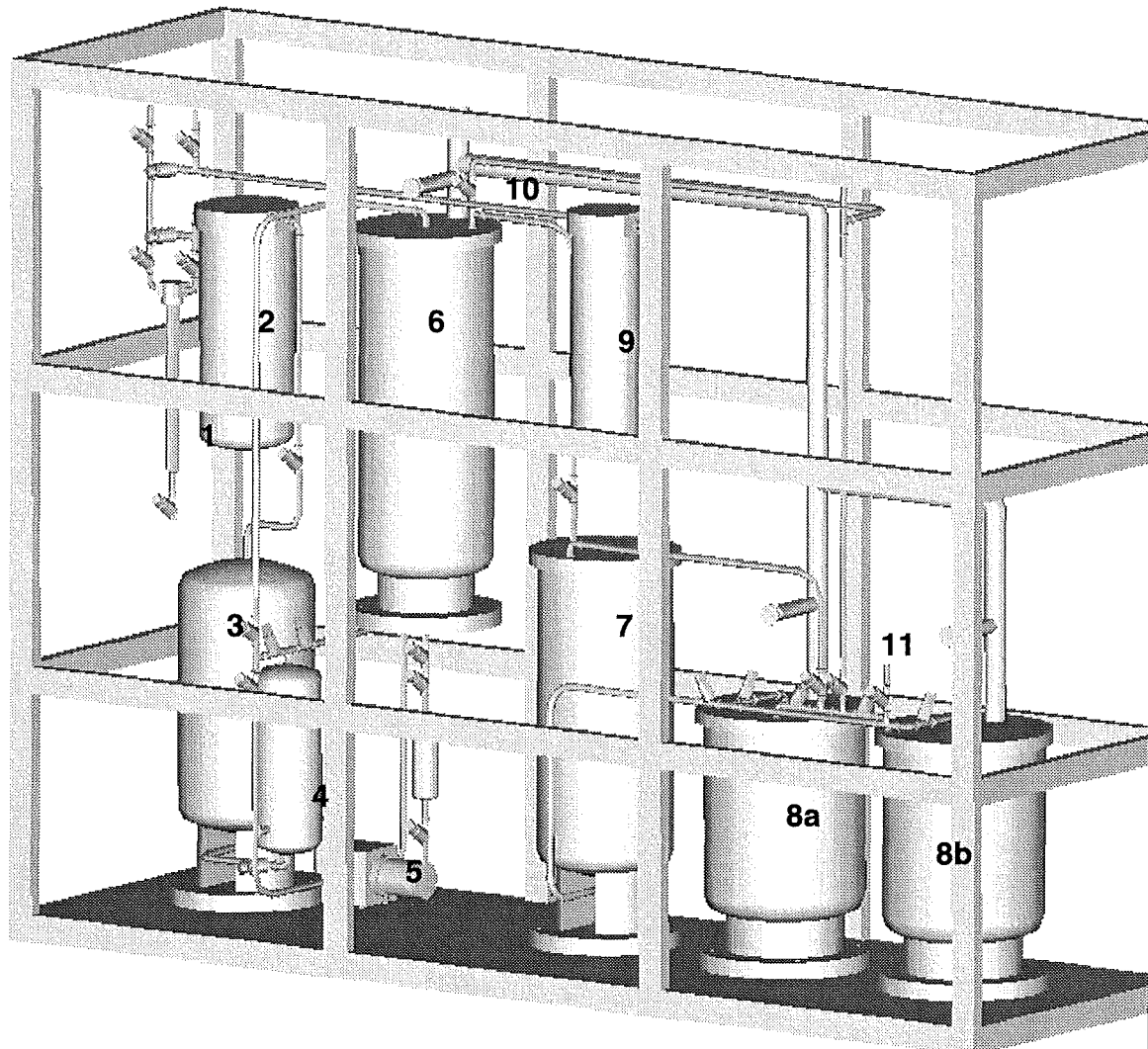


Fig. 2.1.1.4-1: Flow Sheet of the Coolant Purification Subsystem



1	Water Separator	6	Cold Trap
2	Electrical Heater	7	Recuperator
3	Catalytic Oxidizer	8a/b	Low Temp. Adsorber
4	Cooler	9	Electric Heater
5	Blower	10/11	Relief Valves

Fig.2.1.1.4-2: Layout of the Coolant Purification Subsystem.

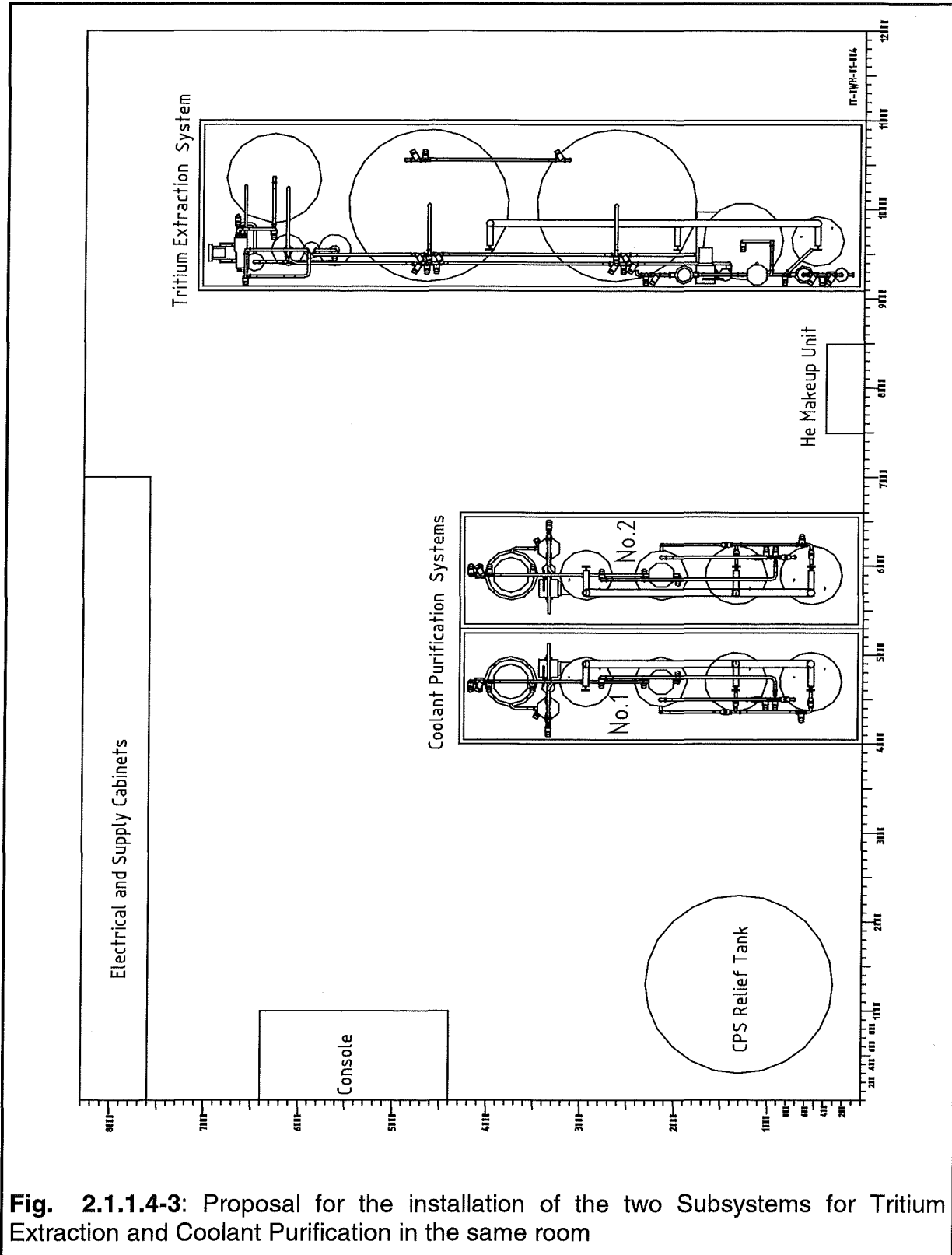


Fig. 2.1.1.4-3: Proposal for the installation of the two Subsystems for Tritium Extraction and Coolant Purification in the same room

2.1.1.5 Test Blanket Remote Handling Subsystem

All equipment to be used in the horizontal ports should be designed for radial installation and removal of components through the port extensions. Since the equipment will be inside the Bioshield and will be highly activated after reactor operation, it will be necessary to use remote handling systems for all operations within the Bioshield boundaries. This requirement will apply to the Test Blanket Subsystem. The design of the remote handling system of the test blanket modules is dependent upon the piping system layout within the port extension. One of the project recommendations is to minimize the amount of remote operations inside the port extension. A concept was developed which combines the TBM's, the Frame, the Shield, the VV plug and the related plumbing as one superassembly, ("Test Blanket Assembly" or TBA) as already shown in section 2.1.1.1. This allows full functional testing of the assembly prior to installation within the port. As a result, the remote handling system was adapted to handle this assembly. The overall length of this assembly is less than 4.1 meters. The weight of the assembly is in the range of 50-60 tonnes.

The remote handling system for the Blanket Test Modules will take full advantage of the equipment designed by the JCT to minimize duplication of efforts and to standardize system operations. As a result, the current design of the remote handling system will utilize a series of transporters each is designed to perform a certain task. The transporter is the standard JCT design with overall dimensions of 8 m long, 3.8 m wide and 5 m high. All operations that are identical to other ITER operations will use the same ITER system to perform, such as removing the bioshield plugs and the cryostat closure plate. As a result the piping system for the test blanket modules will be designed to meet the requirements of this tool, such as minimum bend radii. Operations that are specific to the test blanket system will be integrated into the overall system design.

Removing and installing a test blanket assembly will involve a number of steps. Prior to removing the blanket test modules, procedures will be established to prepare the modules for removal such as breaking the vacuum in the vessel, releasing the coolant helium to the helium storage, draining the coolant water from the TBM shielding and frame and purging the system to reduce the amount of residual tritium inside the modules. The next step would be to disconnect the tritium extraction system from the blanket modules and clear the way for the blanket removal operations to start. A top level procedure of the remote handling process is outlined below. Using this procedure will help in identifying the special equipment needed for the test blanket handling system. Also this procedure starts after an inert gas atmosphere (nitrogen) has been introduced to the vacuum vessel.

TBA replacement procedure [2.1.1.5-1]

The basic removal steps for the TBA are listed below (see Fig. 2.1.1.5-1, 2.1.1.5-2 and 2.1.1.5-3). Installation is performed by reverse order.

Hands-on preparation

1. Draining and flush all coolant and purge circuits.
2. Cut end caps on pipes.
3. Cut pipes at shown location to clear the Bio-shield plug.
4. Cut pipes between Bio-shield and Cryostat using internal cutting tool. Remove each pipe and store.
5. Remove Bio-shield plug.
6. Cut bellows between pipe and Cryostat Door.
7. Using internal bore tool, cut each pipe close to the V.V. Plug and remove

Remote steps for TBA removal

8. Using Remote Handling manipulator, disconnect power and diagnostic cables at one end and move them to a special stow position.
9. Cut seal weld of V.V. Plug and remove fasteners.
10. Using ITER's Remote Handling Equipment, remove the Test Blanket Assembly.

Remarks

This remote handling process is based on removing the full test blanket assembly as a whole unit. Removing an individual submodule within the port is not possible under this scenario. Implementing such a capability into the remote handling system will further complicate the operation and will increase the time required for removal and installation. Since one of the requirements of the test program is to perform maintenance operations during scheduled reactor shutdowns, every effort is taken to minimize the number of operations required for blanket removal and installation. As noted earlier, the test blanket remote handling system will take full advantage of the ITER designed equipment.

The outline of the remote handling process mentions some special operations that are specific to the test blanket modules. This operations will utilize special tools designed specifically to perform this task. Description and function of the special equipment will be presented in the Section 2.1.1.5.1.

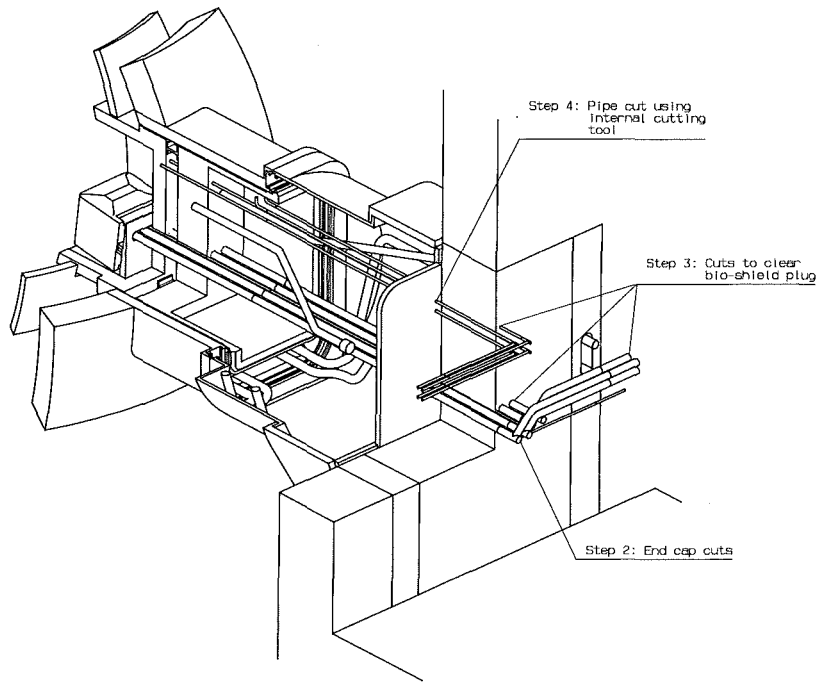


Fig. 2.1.1.5-1: Step 2 to 4 of the TBA replacement procedure.

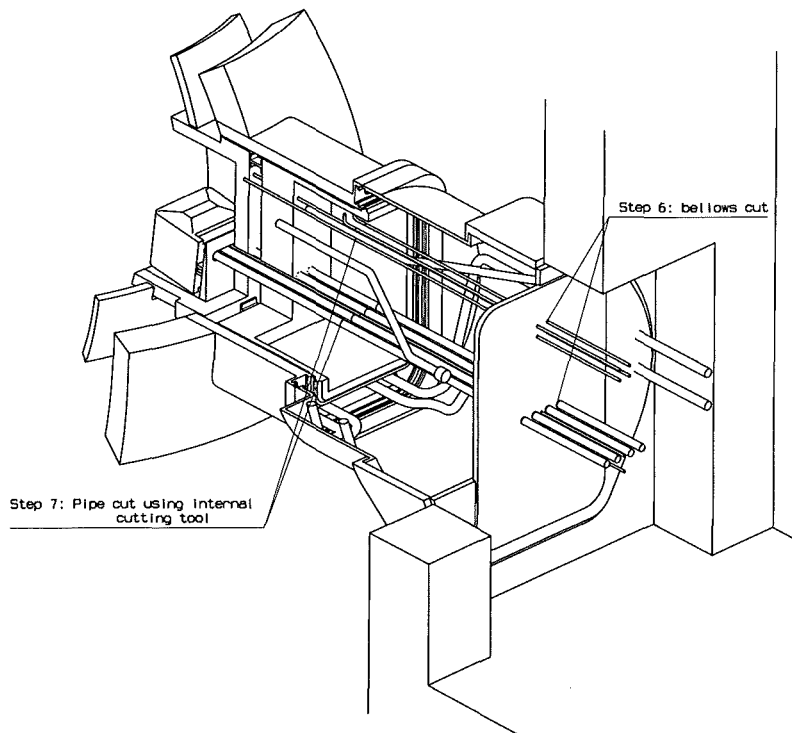


Fig.2.1.1.5-2: Step 6 and 7 of the TBA replacement procedure.

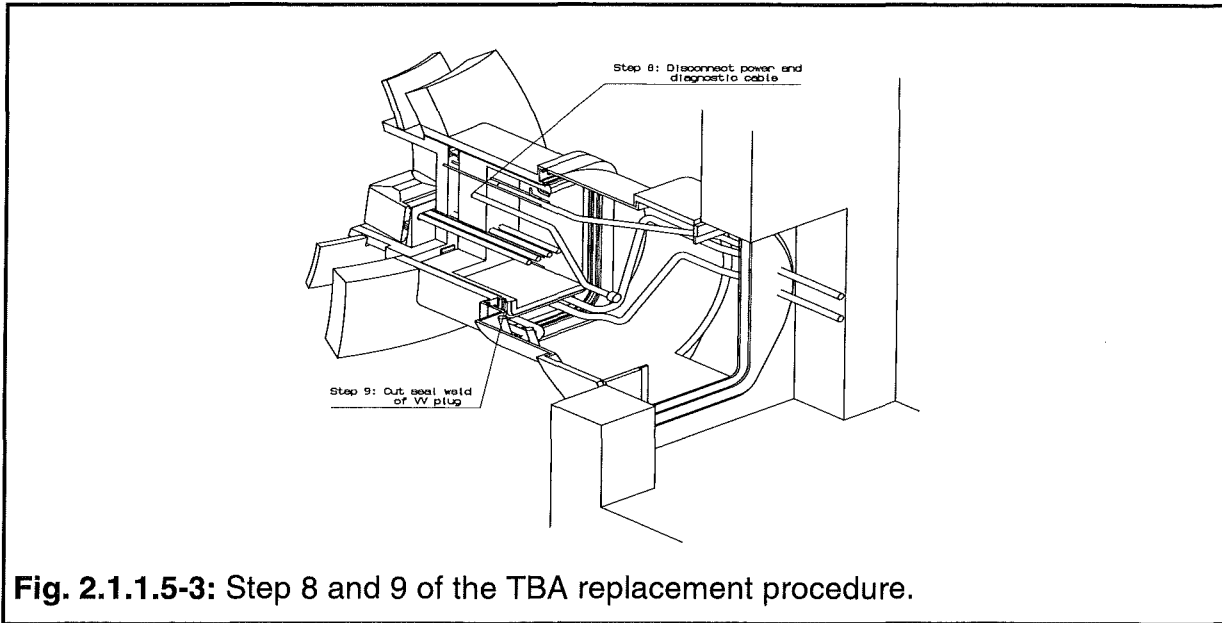


Fig. 2.1.1.5-3: Step 8 and 9 of the TBA replacement procedure.

2.1.1.5.1 Mechanical Design

The remote handling (RH) system for the test blanket modules will consist of a number of components designed to perform certain tasks. A number of the tasks required for the removal and installation of the test blanket modules are identical to ITER tasks, such as bioshield plug installation, cryostat plug interface and the internal pipe cutting and welding operation. For those tasks, ITER equipment will be used. Special equipment such as Test blanket RH transporter, RH vehicle, Port Assembly Carrier will be designed by the test blanket group with interface data inputs from ITER. A brief description of each of the special equipment is included below [2.1.1.5-2].

Test blanket RH transporter (transfer cask) - This transporter will be based on the standard transporter design as it is developed by ITER. This transporter will be designed to handle a number of tasks. As noted in the remote handling process procedure in the previous section, the transporter should be equipped with special tools to perform a number of specific operations. A manipulator is needed to plug and unplug the power and diagnostics cable bundles without damaging them. This manipulator will serve other tasks by exchanging the end effector tools to fit a specific task. Some of those tools include a fastening tool to handle the vacuum vessel plug bolts. Another tool is needed to cut and weld the lip seal weld of the vacuum vessel plug. Deployment of the temporary tracks between the cryostat door and the vacuum vessel is also handled with this manipulator. Other tools include inspection equipment and possibly viewing equipment such as a camera to perform remote visual inspection.

The transporter is also designed to contain the test blanket assembly. Internal tracks are installed to allow the blanket support vehicle to travel into and out of this transporter. Room should be provided within the transporter to store the temporary

tracks when not in use. Monitoring equipment designed to monitor the status of the test blanket modules during transport to/from the test port should be built into the transporter with capabilities to transmit important or emergency status data to the control room. Emergency recovery operations should be designed and built into this transporter to enable it to recover from certain emergency conditions without interrupting the operation of ITER. Other equipment stored inside the transporter include the remote bolting tool and the blanket support vehicle.

RH vehicle - The RH vehicle provides the necessary force along the radial axis to withdraw or insert the port assembly. It also transports and positions the dexterous manipulator, viewing systems and tools necessary for performing operations on the primary closure plate attachment. It requires at least a radial axis drive along the port assembly carrier and a coupling to the port assembly. Others may be required depending on the degree of misalignment between the port and carrier. The radial drive is envisioned as a rack and pinion arrangement with the carrier. The coupling connection to the port assembly has not been designed in detail. The type of connection is dependent on the possible misalignments. A single coupling that is misalignment-tolerant, such as a spherical ball coupling or pinned joint, will be used if possible.

Port Assembly Carrier - The port assembly carrier is attached to the RH transfer cask and extends along the radial axis of port up to the primary closure plate in order to position the RH vehicle, manipulator, viewing equipment and tools. It supports the port assembly when it is removed from the port and delivers it to the cask. When extended out of the cask, the carrier is supported by a bridge/beam in the lower region of the port interspace. The bridge is in turn supported by the cryostat and VV port and is connected to the port only during maintenance. Whether the interspace bridge will remain in place or be deployed as part of the maintenance operations is TBD. Included within the carrier structure are 3 platforms that progressively raise to support the port assembly as it is withdrawn from the port. Raised platforms are required since the flange at the end of the port (primary closure plate) must overlap with the port wall. Multiple platforms ensure the weight of the assembly is taken by the carrier and not the vehicle.

2.1.1.5.2 Decay Heat Removal During Remote Handling

Preliminary Remark

The analyses described in this section have been carried out using the results of the nuclear calculation carried out for MANET as structural material [2.1.1.5-3]. The replacement by EUROFER leads to changes in the afterheat generation in the time period of interest for remote handling. Furthermore, some recent design changes (caps of the modules, shape of the frame) have not yet been taken into account. Hence, the results given below have to be revised as soon as definite input data area available.

Results

To allow the remote handling of the TBM, the helium of the cooling systems has to be released to the storage system, and the helium pipes have to be cut. After this operation, active cooling of the TBM is no longer possible, and the decay heat has to be removed by inherent mechanisms like radiation and natural convection and/or to be stored in the TBM. During this phase the VV is filled with an inert gas (nitrogen) at about atmospheric pressure. In the subsequent analysis of the decay heat removal it has been assumed that the decoupling of the TBM from the active cooling systems is carried out at the earliest one day after termination of the power generation. At this time the total power produced in the TBM is 1.11×10^{-3} MW, and in the frame 7.25×10^{-3} MW. The maximum power generation rate in the steel amounts to 2.04×10^{-2} MW/m³. These data apply to a neutron fluence of 1 MWa/m². Two situations have been considered: In case a) it is assumed that the TBM is at any location between the VV and the transporter, but the cryostat and transporter closure plates are still open. Under these conditions, heat can be removed from the FW to the opposite cooled surfaces (inboard shield/blanket, port extension). After closure of the cover plates, this heat transfer path may be inhibited, in particular as long as the transporter is still docked to the cryostat flange. Under these conditions, heat must be removed via the side walls of the TBM to the frame and then to the wall of the transporter (case b.). The ambient temperatures (gas and surfaces) have been assumed to be 200 °C.

Case a)

For the analysis of case a) the same 1-D model was used as in some of the safety studies. The model represents a radial single-cell cylinder cut out of the TBM from the FW all the way through the breeding zone (BZ), manifold region, support structure, up to and including the radial shield. More details on the model are given in Sect. 2.7.

In the analysis the following assumptions were made:

- The transient starts one day after shutdown.
- The decay heat generation rates are as calculated with FISPACT (see Sect. 2.7).
- The initial temperature of the TBM is 250 °C.
- Heat is dissipated only by radiation from the FW to the hemispherical environment; the emissivity is $\epsilon = 0.3$. The other surfaces of the TBM are assumed to be adiabatic.
- In the breeding zone the TBM is assumed to be composed of 80 % steel and 20 % helium. This is representative for the thick-walled poloidal caps. The straight part of the TBM consisting of the layered structures of pebble beds and cooling plates has a lower ratio of power generation to thermal conductivity which leads to lower temperatures than in the caps. For the back region of the TBM, steel fractions have been assumed according to the actual design.

The calculated temperature histories at selected points of the TBM are shown in Fig.2.1.1.5.2-1. The initial temperature rise rate of the FW is about 70 K/day; at the back side it is by about a factor of 5 lower. The maximum temperatures are reached after about 24 days and amount to 359 °C at the FW and 374 °C at the shield. This is far below the specified temperature limit of Be coated structures.

A similar calculation has been carried out for the frame which is a continuous massive steel structure from the FW to the shield region. The calculated temperature histories are not significantly different from those given above for the cap of the TBM.

Case b)

For case b) a steady state temperature calculation has been carried out using the following assumptions:

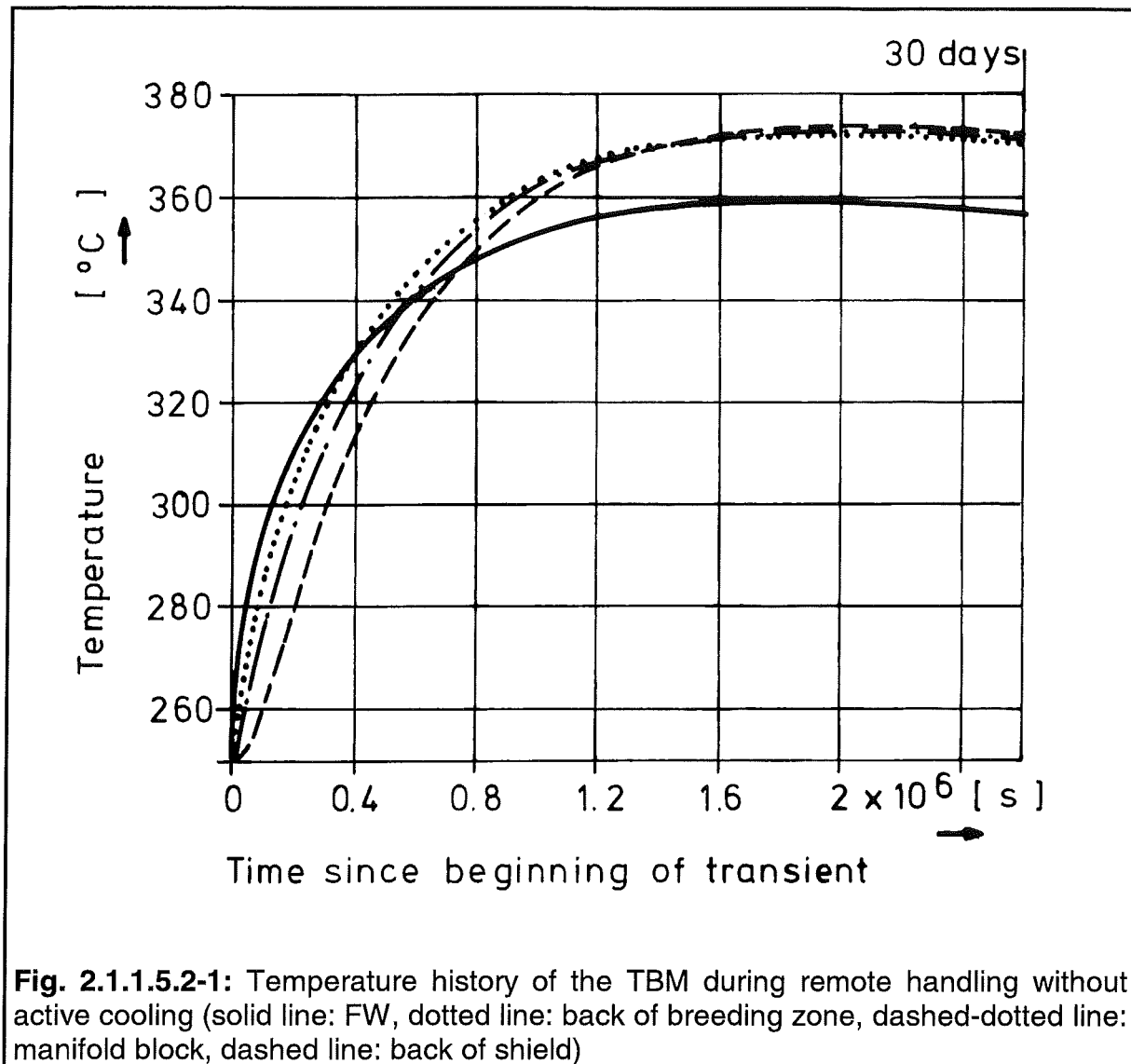
- The power generation is constant according to the values given above for one day after shutdown.
- Heat transfer occurs only across the lateral surfaces, i.e. in the toroidal direction.
- Temperature differences in the structures are calculated assuming one-dimensional toroidal heat conduction taking into account the internal heat sources. Heat conduction in the other directions is accounted for by using average surface heat fluxes.
- Heat from the surfaces is removed by radiation ($\epsilon = 0.3$) and natural convection (using standard correlations for vertical surfaces).

The analysis has shown that 70 % of the heat from the frame is removed by free convection and 30 % by radiation. With respect to the heat transfer across the narrow gap between the module and the frame, radiation is dominating, and the convective contribution can be ignored.

The following temperatures have been obtained:

- outer surface of the frame: 320 °C
- outer surface of the module: 516 °C
- maximum in the module: 540 °C

The quality of the results is mainly determined by three simplifying assumptions: the averaging of the heat flux, the neglect of the radial and poloidal surfaces, and the use of the 1-day heat generation densities. Two of these assumptions lead to an over-estimation of the temperature, the third one (heat flux averaging) leads to an underestimation. Although a quantitative statement on the uncertainties of the analysis is difficult, it is expected that a more detailed analysis (2-D or even 3-D) will yield maximum TBM temperatures below the limit of 500 °C. Furthermore, it should be noted that the temperature maximum is reached after a time of more than 20 days. This is much longer than expected for normal remote handling procedures. Hence, in an emergency situation, sufficient time would be available for suitable counter measures.



References

- [2.1.1.5-1] Mo. Dagher, Review of ITER Test Blanket System Design, ST-VNS User Meeting, May 6-7, 1997, Rancho Santa Fe, Ca.
- [2.1.1.5-2] Tom Burgess, "Equatorial Port RH", e-mail of 31.10.97 to Lester Waganer.
- [2.1.1.5-3] M. Dalle Donne and L.V. Boccaccini (Ed.): Europead Helium Cooled Pebble Bed (HCPB) Test Blanket; ITER Design Description Document, Status 1.12.1996, FZKA 5891 (April 1997).

2.1.1.6 Reliability Analysis

The availability of the HCPB-TBM including the supply pipes and the He-cooling loops (*Primary heat removal loops*) has been analyzed in order to get preliminary quantitative estimates. No experience is available on the reliability of equipments like the TBM; therefore, the failure rate has to be determined "synthetically" using the failure rates of the basic components of the TBM like welds, tubes, and pipe bends. Data for these components are available from other technologies, combined with assumptions based on expert opinion.

The TBM is designed such that certain types of failures like small internal leaks can be tolerated and will not necessarily lead to shut down of the facility. This can be taken into account by two failure modes: the "leak" failure mode and the "loss of integrity" failure mode. The failure rates given in Table 2.1.1.6-1 represent the leak mode, which is normally one order of magnitude higher than the loss of integrity failure mode. The design pressure of the purge gas system is not finally fixed, yet. The pressure depends, beside others, from the result of the stress calculation of the test module vessel. Therefore, in availability analyses, in most cases the higher failure rates according to Tab. 2.1.1.6-1 are conservatively taken.

Table 2.1.1.6-1: Failure rates for the components of the test module and the He-cooling loops

Failure component	Failure rate
Pipe failure [1/mh]	3.0×10^{-9}
SG failure 1.15 MW [1/h]	1.7×10^{-8}
Valve failure [1/h]	1.0×10^{-6}
Blower failure [1/h]	1.0×10^{-5}
Filter [1/h]	2.7×10^{-6}
Collector failure [1/h]	1.0×10^{-8}
EB weld [1/mh]	1.0×10^{-9}
TIG weld [1/mh]	1.0×10^{-9}
Diffusion weld [1/mh]	1.0×10^{-9}
Longitudinal weld [1/mh]	1.0×10^{-9}
Butt weld [1/h]	1.0×10^{-9}
Pipe bend (180°) [1/h]	1.0×10^{-8}
Pipe bend (90°) [1/h]	5.0×10^{-9}

A repair of the TBM inside the vacuum vessel is not envisaged. The question of repair in case of a leakage of the coolant flow system outside the torus must be left open and the answer depends mainly on the location of leak. It is postulated in Chapter 1.2.9 that replacement of the test module will take 8 weeks. Additionally, it is assumed that a leakage induced failure outside the torus can be repaired within 6 weeks. The general test module description, mentions also time periods for

exchange or repair of two and of four weeks. To cope with this differences in the analysis, the mean time to repair (MTTR) was taken as parameter and varied between two and eight weeks. This "repair time" (MTTR) determines - together with the failure rates - the unavailability of the TBM, which is defined as the probability for the inoperability of the TBM when it should be operable.

Concerning the TBM without the He-cooling loops, the FMEA has shown that four failure effects have to be considered: helium ingress into the VV, distortions of the TBM coolability, distortions of the purge gas flow to the pebble beds inside the TBM, and loss of the structural integrity of the TBM. The quantitative evaluation of the failure rates and unavailabilities has been carried out using standard methods of fault tree analysis. The results are compiled in Table 2.1.1.6-2. The TBM reliability

Table 2.1.1.6-2: Results of the reliability analysis for the test module without the cooling loops

Failure effects	Failure rate [1/h]	Percent [%]
He ingress into VV	4.1×10^{-7}	67
Distortions of the TBM coolability	1.5×10^{-7}	25
Distortions of purge gas flow inside TBM	6.1×10^{-9}	1
Loss of structural integrity of TBM	4.3×10^{-8}	7
Total	6.1×10^{-7}	100

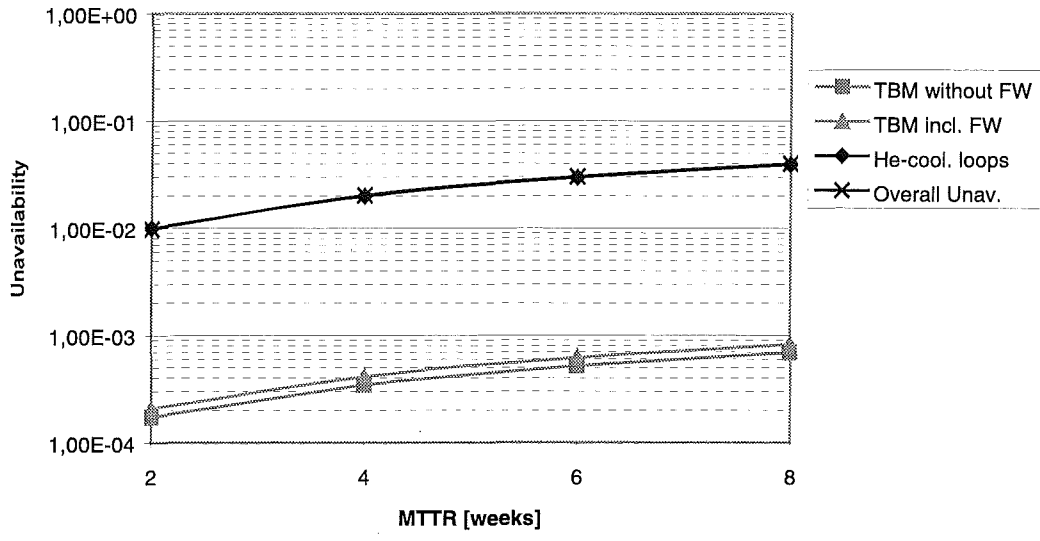
is dominantly determined by the failure effect "helium ingress into the VV" with a contribution of 67% to the unavailability. The main cause are leaks of the supply pipes inside the VV. The low contribution of the TBM itself to this case is due to the high degree of fault tolerance against internal leaks. The contribution of the failure effect "loss of TBM structural integrity" to the overall unavailability amounts to only 7%. The total failure rate of the TBM is $6.13 \times 10^{-7} \text{ h}^{-1}$ which is less than 0.01 a^{-1} . The corresponding unavailability is between 2×10^{-4} and 8.2×10^{-4} , dependent on the MTTR between two and eight weeks. The increase of reliability compared to the DEMO blanket system is a consequence of the size of the TBM which represents only a very small fraction of the DEMO blanket. The results are also given in Fig. 2.1.1.6-1. The lowest curve shows the test module without the FW part, while the next higher curve includes the FW part. A parameter variation for the TBM without the cooling loops has shown that an increase of the failure rates given in Table 2.1.1.6-1 by one order of magnitude would lead to an overall unavailability of about 1%. This shows that a significant margin is available to accommodate effects which are not yet included in the analysis, e.g. irradiation effects.

Tab. 2.1.1.6-3: Calculated failure rates for the main components and percentage of the overall unavailability of the test module including the He-cooling loops

Description	Calculated component failure rate [1/h]	Percentage of the overall unavailability [%]
Test module	6.2×10^{-7}	2
Pipes, bends, heat exchangers, welds	6.1×10^{-7}	2
Valves	4.0×10^{-6}	13
Circulators	2.0×10^{-5}	65
Dust-filter	5.6×10^{-6}	18
Total	3.1×10^{-5}	100

The unavailability of the He-cooling loops dominate the overall unavailability. Dependent on the MTTR this value varies between 1.0×10^{-2} and 3.9×10^{-2} , whilst the overall unavailability varies between 1.02×10^{-2} and 4.0×10^{-2} . This equals an availability between 99 and 96%. This result is also included in Fig. 2.1.1.6-1. The unavailability of the test module is nearly two orders of magnitude lower than that of for the He-cooling loops. The calculated failure rates and the contribution to the overall unavailability the test module including He-cooling loops are given in Tab. 2.1.1.6-3. The highest influence to the overall unavailability comes from the circulators (65%), the next higher from the dust-filter (18%) and from the valves (13%). Compared to the He-cooling loops, the contribution of the test module of 2% can almost be neglected.

Fig. 2.1.1.6-1: Unavailability of the HCPB Test Module



2.1.1.7 Test Program

ITER offers the unique possibility to test simultaneously all aspects of a DEMO relevant blanket concept in the real geometrical configuration, with the relevant magnetic field, and with an incident neutron flux having the real neutron spectrum and spatial distribution. The main differences to DEMO are the lower wall load (1.0 MW/m² instead of 2 MW/m² or more), the shorter burn time and the lower neutron fluence.

2.1.1.7.1 Test objectives

The test objectives are:

1. Experimental evidence of the possibility of obtain a sufficiently high tritium breeding ratio that would lead to tritium self-sufficiency in a DEMO reactor.
2. Demonstration of the on-line tritium extraction and recovery system.
3. Production of high-grade heat that is removed with a suitable coolant medium to demonstrate the possibility of electricity generation in a reactor.
4. Code validation: the previous tests (out-of-pile, in fission reactor) allow to develop codes capable to calculate temperatures, flow distributions, pressure, stresses in the material and so on. These codes can be validated and improved by comparison with the tests in ITER.
5. Basic feasibility: the tests will show if synergistic effects will cause failure not foreseen by the extrapolation of the previous tests (out-of-pile, in fission reactors).

2.1.1.7.2 ITER requirements

Table 2.1.1.7-1 shows an estimation of the time to reach equilibrium conditions for the main blanket processes to be tested in ITER.

Table 2.1.1.7-1: Time to reach equilibrium conditions in the TBM

Parameter	time
Temperature: blanket front	100 s
Blanket back	300 s
Tritium inventory: 50% equil.	1000 s
67% equil.	3000 s
Tritium permeation to coolant	≈ 1 day
Tritium extraction system	6 - 10 h

The time constants of the blanket to be tested impose the following requirements on ITER:

1. A plasma continuous operation with back-to-back pulses for periods of 3 to 6 days.

2. A burn time sufficiently longer than the temperature time constant of a major portion of the blanket. A burn time ≥ 1000 s is considered adequate.
3. The off-burn time should not be too long, so that the process which requires long operation periods can effectively smooth out the pulses. An off-burn-time $\leq 1000 - 1500$ s is considered adequate.
4. A few interruptions of up to 1 day can be tolerated, as during this time at low temperature the tritium remains frozen in the breeder material. A longer interruption may lead to chemical modifications which make the measurement interpretation difficult.

2.1.1.7.3 Test Plan

During the Basic Performance Phase (BPP) of ITER two test modules will be tested. The first (BMT-I) will have the same configuration of the DEMO blanket, however with a higher Li^6 -enrichment (90 % instead of 40 % of the DEMO). The second (BMT-II) will also have a Li^6 -enrichment of 90 %, however the geometry of the blanket will be slightly modified to achieve higher, and thus more relevant, temperatures at the coolant helium outlet and in the ceramic breeder pebbles.

The test program foresees the following test phases during the BPP

Phase A: "lower power operation"

Neutronic, electromagnetic, remote handling tests and system check out will be performed for the TBM-I and/or TBM-II.

Phase B: "preliminary testing phase"

Screening tests will be performed for the TBM-I and TBM-II.

Phase C : "testing phase"

Performance tests will be performed for the TBM-I and/or TBM-II according to the results of the screening tests.

Table 2.1.1.7-2 presents a TBM test schedule for the BPP.

Table 2.1.1.7-2: TBM test schedule (Basic Performance Phase).

Operation year	1	2	3	4	5	6	7	8	9	10
ITER:										
Average burn length (s)		-		500	1000			1000		
Number of pulses		3200		1600	1000			6000		
Average repetition time (s)		-		1700	2200			2200		
Total plasma operation time (h)		-		222	280			1670 ⁽¹⁾		
TBM:	Phase A			Phase B			Phase C			
Performed tests	Remote handling system operation Neutronic tests Electromagnetic tests System check out			Screening tests			Performance tests			
Testing operation time:	-			≈ 300 h			≈ 800h			
TBM tested:	TBM-I and/or TBM-II			TBM-I and TBM-II			TBM-I and/or TBM-II (2)			

(1) Including 50% availability for continuous test campaigns of 3-6 days with nominal pulse operation scenario [2.1.1.7-1].

(2) According to the results of the screening tests.

References:

[2.1.1.7-1] Fax of Dr. Parker of 14 October 1997 to the TBWG-members.

2.1.2 Supporting Design Documents

Supporting design documents are listed in the Appendix A-C.

Appendix A 9Cr RCC-MR properties data

Appendix B Li_4SiO_4 pebble bed

Appendix C Beryllium pebble bed

2.2 System Performance Characteristics

2.2.1 Operating State Description

The Test Blanket System has TBD operational states. At the moment only nominal data for the 3 versions of the TBM are summarized

2.2.2 Operating State Data

Normal Plasma Operating Data (steady state during 1000 s pulse)

Test Module	TBM-I	TBM-II	TBM-III
Total power (surf. flux included) [MW]	1.81	1.82	1.85
Total helium Mass flow [Kg/s]	3.5	2.1	3.5
Helium Pressure [MPa]	8	8	8
Helium Pressure drop in TBM [MPa]	0.18	0.20	0.18
Helium inlet/outlet temperature [°C]	250 / 350	250 / 420	250 / 352
Max. power density [MW/m ³] in			
Structural material	11	11	10
Beryllium pebble bed	5	5	5
Ceramic pebble bed	20	16	24
Max. temperatures [°C] in			
Structural material	500	509	499
Beryllium pebble bed	444	503	446
Ceramic pebble bed	581	837	632
Max von Mises primary stresses [MPa]	56	62	56
Max von Mises primary plus secondary stresses [MPa]	332	329	331
Frame	TBM-I	TBM-II	TBM-III
Total power [MW]	3.3	3.3	3.6
Water mass flow [Kg/s]	TBD	TBD	TBD
Water Pressure [MPa]	4	4	4
Water Pressure drop [MPa]	TBD	TBD	TBD

Water inlet/outlet temperature [°C]	140 / TBD	140 / TBD	140 / TBD
-------------------------------------	-----------	-----------	-----------

Shield	TBM-I	TBM-II	TBM-III
Total power [KW]	35	35	36.5
Water mass flow [Kg/s]	TBD	TBD	TBD
Water Pressure [MPa]	4	4	4
Water Pressure drop [MPa]	TBD	TBD	TBD
Water inlet/outlet temperature [°C]	140 / TBD	140 / TBD	140 / TBD

Helium Cooling Subsystem	TBM-I	TBM-II	TBM-III
Primary coolant	helium		
number of circuits	2		
pressure [MPa]	8		
hot leg temperature [°C]	350		
cold leg temperature [°C]	250		
mass flow rate (both circuits) [kg/s]	3.7		
flow velocity [m/s] hot/cold leg	20.8 / 17.5		
loop pressure drop (TBM included) [MPa]	0.36		
total mass of coolant (both loops) [kg]	15		
Secondary coolant	water		
number of circuits	2		
pressure [MPa]	0.5		
temperature in/out [°C]	35 / 75		
mass flow rate (both circuits) [kg/s]	11.4		
flow velocity [m/s]	0.16		

Tritium Extration Subsystem	TBM-I	TBM-II	TBM-III
Purge flow:			
pressure at TBM outlet [MPa]			0.106
pressure at TBM inlet [MPa]			0.120
temperature at TBM outlet [°C]			450
temperature at TBM inlet [°C]			20
mass flow rate [g/s]			0.85
Tritium production rate g/day			0.2

Swamping Ratio (He/H ₂)	1000
Partial Pressure [Pa]	
p(H ₂)	110
p(HT+HTO)	0.4
p(H ₂ O)	0.3
Extraction Rates:	
H ₂ [mole/day]	18.4
HT [mole/day]	0.05
H ₂ O / HTO [g/day]	≈ 1.0

Coolant Purification Subsystem	TBM-I	TBM-II	TBM-III
Coolant Purification Circuit:			
pressure [MPa]	8		
temperature inlet / outlet [°C]	250/50		
mass flow rate [g/s]	1.85		
Partial Pressure [Pa]			
p(H ₂)	<10		
p(HT)	<0.1		
p(DT)	<0.1		
p(Q ₂ O)	35		
p(N ₂)	8		
Extraction Rates [mole/day]:			
Q ₂ O	0.2		
N ₂	0.04		
O ₂	0.03		
Tritium Extration Efficiency	≥95 %		

2.3 System Arrangement

The Test Blanket Subsystem consist of five main subsystems:

1. the Test Blanket Subsystem (first wall, breeding blanket, shield, and structure);
2. the Tritium Extraction Subsystem (tritium removal, handling, and processing);
3. the Helium Cooling Subsystem (heat transfer and transport);
4. the Coolant Purification Subsystem;
5. the Test Blanket Remote Handling Subsystem (remote handling as related to the test blanket systems).

The system arrangement has been already described in section 2.1. In the following, subsystem location, related drawings and subsection in which each subsystem is described, are summarized.

Subsystem	Location	Drawings	Section
Test Blanket	VV Horizontal Port	2.0.2-4	2.1.1.1
Tritium Extraction	Tritium Building	2.1.1.2-2	2.1.1.2
Helium Cooling	pit adjacent to the test port	2.1.1.3-3, -4	2.1.1.3
Coolant Purification	Tritium Building	2.1.1.4-2	2.1.1.4
Blanket Remote Handling		2.1.1.5-1, -2, -3	2.1.1.5

2.4 Component Design Description

2.4.1 List of Components

In order to provide the required functions, the European HCPB Test Blanket System is composed of the following subsystem and their components:

1. Test Blanket Subsystem
 - Test Blanket Module
 - Frame
 - Shield
 - Vacuum Vessel Plug
 - Plumbing

2. Tritium Extraction Subsystem
 - Cooler
 - Filter
 - Tritium Monitor
 - Cold Trap
 - Recuperator
 - Low Temperature Adsorber
 - Heater
 - Compressor
 - Helium Make-up Unit
 - Water Collector
 - Relief Tank
 - Blower
 - Diffusor
 - Getter Bed
 - Helium Buffer Vessel
 - LN₂Tank
 - Gaschromatograph
 - Glove Box

3. Helium Cooling Subsystem
 - Heat Exchangers
 - Circulator
 - Electrical Heater
 - Dust Filter
 - Pipework
 - Valves
 - Pressure Control Subsystem
 - Helium Storage Tank

- Helium Dump Tank
- Buffer Tank
- Compressor
- Pressure Regulators
- Safety Valves

4. Coolant Purification Subsystem

- Water Separator
- Electrical Heater
- Catalytic Oxidizer
- Cooler
- Blower
- Cold Trap
- Recuperator
- Low Temperature Adsorber
- Relief Tank

5. Test Blanket Remote Handling (RH) Subsystem

- Test Blanket RH Transporter
- RH Vehicle
- Port Assembly Carrier

The components and systems are extensively described in section 2.1. This section contains only a short description of all the components with some additional information.

2.4.2 Test Blanket Subsystem

Blanket Test Module

The HCPB-TBM is already described in Section 2.1.1.1.

Support Frame

The Support Frame is made of the same structural material (316LN-IG) as the back plate and maintained by the cooling water at about the same temperature of the back plate at their contact surfaces. The part of the frame facing the plasma is covered by a layer of beryllium as armour material and an heat sink of 316LN-IG stainless steel tubes embedded in a copper alloy layer. The design will be similar to the ITER shielding Blanket.

Shield

The Shield is cooled by water and maintained at the same temperature of the Support Frame at its contact surfaces. It is made of 316LN-IG.

Vacuum Vessel Plug

TBD

Plumbing

In Table 2.4.2-1 number, size, description and material of the pipes are summarized. A set of two supply and two return pipes provides the HCPB Blanket Test Module with high pressure helium coolant. A set of one supply and one return pipe provides the 0.1 MPa helium for the purging of the tritium produced in the TBM.

A simple set of water pipes is used to cool the Support Frame and the Shield. A conduit is reserved for the diagnostics.

The plumbing system has to be completed by the helium coolant and purge pipes for the Japanese TBM

Table 2.4.2-1: Plumbing Description

Pipe description (1)	No.	Size (2)	Material	Pipe Carrier (Oper. Cond.)
Helium Coolant Supply	2	101.6	EUROFER	Helium (8 MPa, 250°C)
Helium Coolant Return	2	101.6	EUROFER	Helium (8 MPa, 350-420°C)
Purge Gas Supply (3)	1	25	EUROFER	Helium (0.1 MPa, 20°C)
Purge Gas Return (3)	1	25	EUROFER	Helium (0.1 MPa, 450°C)
Diagnostics Conduct	1	250	316LN-IG	
Frame Cool. Supply	1	50	316LN-IG	Water (4 MPa, 140°C)
Frame Cool. Return	1	50	316LN-IG	Water (4 MPa, 190°C)
Shield Cool. Supply	1	50	316LN-IG	Water (4 MPa, 140°C)
Shield Cool. Return	1	50	316LN-IG	Water (4 MPa, 190°C)

- (1) The helium coolant and purge pipes for the Japanese TBM are not included in the table.
- (2) Outer Diameter (in mm) not accounting for thermal insulation (5 - 10 cm).
- (3) Two concentric tubes with detection gap.

2.4.3 Tritium Extraction Subsystem

The main design data of the Tritium Extraction Subsystem (TES) are given in Table 2.1.1.2-1. For safety reasons, the tubes connecting the TBM with the TES loop has to be designed for a pressure of 8 MPa because leakages from the cooling system can lead to a higher pressure than the nominal working pressure which is 0.1 MPa. Redundant blocking valves are foreseen to protect the loop from a pressure increase beyond 0.2 MPa. For radiological safety reasons, the system must be installed in a secondary containment.

In the following table (Table 2.4.3-1) the components of the Subsystem are listed with remarks on their development status.

Table 2.4.3-1: Component development and design

Component	Available from Industry	Remarks
Cold Trap	Yes	a)
Molecular Sieve Beds	Yes	a)
Diffuser	Yes	a)
Cooler, Heater	Yes	b)
Filter	Yes	b)
Recuperator	Yes	b)
Getter Beds	Yes	a)
Circulator	Yes	b)

a) These components can be purchased from the industry; however, as they will be operated under conditions characterized by high gas flow rates and extremely low concentrations of Q_2O and Q_2 ($Q = H, T$) which are not at all typical for industrial applications, it appears indispensable to carry out an experimental test program to optimize/modify the design of the components, i.e. to avoid over-dimensioning and to demonstrate the desired removal factors. In addition, such tests are needed to develop appropriate means for process control and analytical measurements.

b) The most appropriate type of machine is not yet clear; it will be necessary to prepare and test a special design with respect to oil freeness, leak tightness, etc. (see also Section 2.4.3, Compressor No. 8).

The next paragraphs describe the technical specifications of the components; the numbers given in brackets refer to Fig. 2.1.1.2-1.

Cooler (No.1)

The long distance between the TMB and TES and the fact that the tubes with the incoming and the outgoing gas are installed side by side inside a common insulation will lead to a partial temperature equilibration of both gas streams.

The cooler is designed as a heat exchanger containing cold water in the shell and the purge gas (helium) in the inner tube bundle.

Gas temperature at inlet	max. 450°C
Gas temperature at outlet	30°C
Helium mass flow	$0.85 \cdot 10^{-3}$ kg/s
Helium pressure	0.11 MPa
Cooling power	4 KW
Water temperature at inlet	20°C
Size (D x H)	150 mm x 700 mm

Particle Filter (No. 2)

It is the task of the particle filter to remove particulate material which might be carried out from the blanket zone. The filters must be easily exchangeable within 1-2 hours.

Type of filter	Filter cartridges containing sintered stainless steel fiber mats Fiber thickness: 2 - 4 μ m
Removal efficiency	> 99 % (critical particle diameter is assumed to be 0.15 μ m)
Pressure drop	< 15 mbar
Number of filters	2
Size (D x H)	60 mm x 500 mm
Weight	about 15 kg

The pressure drop Δp has to be measured continuously. An exchange of a filter cartridge is recommended at a $\Delta p > 30$ mbar. It is expected that the filters will contain beryllium dust and radioactive activation products. Thus, the cartridges must be handled as radioactive waste.

Tritium Monitors (No. 3a/b)

The Tritium Monitor 3a is installed in a bypass, in parallel to an orifice in the main loop which is necessary to maintain a gas flow of some l / min in the bypass. The tritium concentration under equilibrium condition at a TBM power of 2.3 MW is $1.3 \cdot 10^5$ Bq / ml which is sufficiently high for applying an ionization chamber.

In addition, the bypass line contains two manually operated valves which can be closed for exchange of the monitor.

Type	Ionization Chamber
Sensitive volume	10 ml
Range	$10^3 - 5 \cdot 10^5$ Bq / ml

It has to be considered that some gaseous radioactive products (e.g. S-35, Xe-135, Xe-133, C-14, Kr-85) will be detected besides H-3. It should be tried to carry out a quantitative estimate of the additional nuclide activity on the basis of an impurity analysis of the breeder and the beryllium pebbles.

The Tritium Monitor 3b is used to measure the efficiency of the tritium removal by the TES which is designed to be ≥ 90 %. Thus, the tritium concentration to be detected will be 10 - 100 times smaller than in the case discussed above. This requires a larger ionization chamber.

Type	Ionization Chamber
Sensitive volume	200 - 1000 ml
Range	$10 - 10^5$ Bq / ml

Some of the radioactive products mentioned above (mainly Xe and Kr isotopes) will still be present in the purge gas at the location of the Tritium Monitor 3b.

Cold Trap (No. 4)

The Q₂O content (Q = H,T) of the gas is frozen out in the cold trap which is operated at $< -100^\circ\text{C}$. The residual Q₂O concentration is < 0.015 vpm. The amount of ice accumulated within 6 days is of the order of a few grams (max. 6 g). The trap is cooled with LN₂. Filling level and temperature are continuously controlled. A heating plate in the center of the trap is used for recovery of liquefied water which is drained into a water collector. When a volume of 100 - 200 ml is chosen for this collector, it will not be necessary to exchange the collector after each test run.

Humidity at inlet / outlet	2.7 / 0.015 vpm
Gas temperature at inlet / outlet	$20^\circ\text{C} / \leq -100^\circ\text{C}$
Size (D x H)	500 mm x 1300 mm

Recuperator (No. 5)

The recuperator has the task to further reduce the temperature of the gas leaving the cold trap (gas 1) by utilizing the clean gas leaving the adsorber (gas 2).

Inlet temperature of gas 1	$\leq -100^\circ\text{C}$
Inlet temperature of gas 2	$\approx -190^\circ\text{C}$
Outlet temperature of gas 1	$\leq -170^\circ\text{C}$

Outlet temperature of gas 2	$\geq -140^{\circ}\text{C}$
Size (D x H)	800 mm x 1600 mm

Low Temperature Adsorber (No. 6a/b)

The adsorber beds are filled with 5A zeolite pellets which adsorb molecular hydrogen as well as gaseous impurities and residual moisture. The beds contain filters on the down-stream and upstream side to prevent particulate material from being transferred during loading or unloading operations. In addition, each bed is equipped with a LN₂ chiller and an electrical heater.

Mass of adsorber material	500 kg (per bed)
Operation temperature	-195°C
Size (D x H)	1100 mm x 2800 mm
Unloading	Warm-up to -150°C to unload helium and hydrogen isotopes which are circulated through units 12, 13, 14; Q ₂ (Q = H, T) is separated by the diffusor; warm-up to room temperature to desorb impurities which are sent to the Waste Gas System (via pump 12).
Regeneration	Heat-up to 300 °C and purge with clean helium

Heater (No. 7)

The heater is used to warm up the gas coming from the recuperator (No. 5).

Gas temperature at inlet / outlet	$\geq -140^{\circ}\text{C} / 20^{\circ}\text{C}$
Electrical power	1 KW
Size (D x H)	200 mm x 500 mm

Compressor (No. 8)

The task of the compressor is to transport the purge gas through the closed loop consisting of the TMB and the components 1 - 9 of the Tritium Extraction Subsystem. Due to its position in the TES loop, the compressor comes in contact only with clean gas at room temperature.

Helium mass flow	0.85 g / s
Pressure at suction side	0.090 MPa
Pressure increase	0.032 MPa (including 0.014 MPa in TBM)
Size (L x W x H)	600 mm x 600 mm x 800 mm

According to information supplied by James Howden & Company Ltd./Scotland, the following types of machines can be used:

- a small multi-stage centrifugal machine with magnetic bearings,
- a small reciprocating device having a bellows-sealed crankcase, or
- a diaphragm compressor.

Helium Make-up Unit (No. 9)

In the helium make-up unit hydrogen is added to provide a He : H₂ swamping ratio of 1000 for the gas reentering the blanket test module. In addition, this component is used for the first fill-up of the loop with helium and for compensating smaller He losses due to leakages. The unit comprises the following components:

- He and H₂ supply,
- Pressure control and hydrogen sensor (sensitivity ≤ 0.05 ppm) at the inlet,
- Mass flow control for hydrogen,
- Small compressor to inject 17 NI H₂/h into the TES loop.

Size (L x W x H) : 1000 mm x 400 mm x 2000 mm

Water Collector (No. 10)

The liquefied water from the cold trap is drained into an evacuated water collector which is later on transferred to the Water Detritiation System and replaced by an empty collector vessel.

Volume ≤ 200 ml

It is expected that at least 50 % of the tritium generated in the TBM will be collected in the form of HTO. At the end of a test campaign of 6 days, the max. tritium activity in the water collector will remain below 10 000 Ci (i.e. below $3.7 \cdot 10^{14}$ Bq). Thus, it will not be necessary to exchange the collector after each test campaign.

Relief Tank (No. 12)

A relief tank with a volume of 2 m³ is available to restrict the pressure increase during desorption in the warm-up phase of the adsorber to a value below 0.2 MPa as described in 2.1.1.2. The relief tank is prefilled with 50 kPa helium which is needed to carry the desorbed hydrogen isotopes to the diffusor.

At the end of the unloading cycle, the gas of the relief tank is sent to the Waste Gas System (via circulator No. 11). Then the tank is evacuated and refilled with 50 kPa.

Blower (No. 13)

The blower is installed in the secondary loop of the adsorber beds like the relief tank mentioned above. It is used to transport the desorbed hydrogen isotopes to the diffusor.

Gas flow rate	60 NI / min
Gas composition	He \approx 35 %, Q ₂ \approx 65%
Pressure at suction side	0.06 - 0.19 MPa
Pressure increase	0.01 - 0.02 MPa
Size (L x W x H)	500 mm x 500 mm x 300 mm

Diffusor (No. 14)

The Pd/Ag diffusor separates the hydrogen isotopes from the helium carrier gas.

Gas flow rate	60 NI / min
Inlet pressure	0.07 - 0.20 MPa
Temperature	300 - 400 °C
Size (D x L)	130 mm x 1200 mm

The helium gas loop at the secondary side of the diffusor has the task to transport the permeated hydrogen isotopes to the getter beds for storage. It will be sufficient to employ a gas flow rate in this loop of about 3 NI /min.

Getter Beds (No. 15)

Two uranium getter beds are provided for storage of the hydrogen isotopes. When the loading capacity of these beds is reached they will be transferred to the Isotope Separation System and replaced by fresh beds.

Mass of uranium	10 kg (each bed)
Size	350 mm x 750 mm

Helium Buffer Vessel (No. 16)

The buffer vessel is used to supply the transport gas (helium) for the gas loop at the secondary side of the diffusor.

Volume	10 l
Gas pressure	0.1 MPa

LN₂ Supply Tank (No. 18)

This tank is the reservoir for the LN₂ supply of the cold trap and the adsorber beds. A preliminary design is made for a volume of 500 l LN₂.

Size (D x H) 1000 mm x 1100 mm

Gaschromatograph (No. 19)

The gas chromatograph (GC) is used to analyze gaseous impurities in the purge gas, such as N₂, CO, O₂. In addition, the residual amount of H₂ has to be measured to control the efficiency of the low temperature adsorber beds. In all cases, a high sensitivity of the GC is required as the expected concentration of the gas components will be in the range of 0.1 ... 10 ppm.

Size (D x W x H) 700 mm x 700 mm x 700 mm

Glove Box

Gas loops containing a tritium activity of several thousand Curies ($> 10^{13}$ Bq) must be installed in a glove box to prevent a contamination of the room air in the case of a leakage in the loop system. In addition, the atmosphere in the box should be either dry air or nitrogen to prevent the formation of HTO whose radiological danger is ten thousand times higher than that of HT.

The integral tritium activity of the TES after 6 days of reactor operation at nominal power is about 8600 Ci ($3.2 \cdot 10^{14}$ Bq).

Size of the Glove Box (L x W x H) 7 m x 2 m x 3 m
4 m x 2 m x 3 m

2.4.4 Helium Cooling Subsystem

The cooling subsystem is designed for the European helium-cooled pebble bed (HCPB) test module to be installed in the bottom half of an equatorial test port in ITER, presumably port No. 01 Two separate primary heat removal loops of 2 x 50 % heat capacity are foreseen for redundancy purposes in accordance with the DEMO blanket design. Figure 2.1.1.3-2 shows a flow diagram of the primary heat removal loops and the interfaces to ancillary equipment. Figure 2.1.1.3-3 and Fig. 2.1.1.3-4 shows the arrangement of the components in the pit.

In the following table (Table 2.4.4-1) the components of the Subsystem are listed with remarks on their development status.

Table 2.4.4-1 Component development and design

Component	Remarks
Heat Exchangers	special design (tritium leaktightness)
Circulator	special design (operating temperature, leaktightness and bearing)
Electrical Heater	special quality assurance program (tritium leaktightness)
Dust Filter	special design (efficiency and grain size)
Pipework	Conventional
Valves	special design (flow control performance)
Pressure Control Sys.	Conventional (presence of tritium)

The single components are already described in Section 2.1.1.3.

2.4.5 Coolant Purification Subsystem

For each of the two cooling systems of the test blanket module one coolant purification system (CPS) is provided to purify a fraction of 0.1% of the helium coolant stream, i.e. to extract hydrogen isotopes as well as solid, liquid or gaseous impurities from the main coolant. The main design data of the purification systems are given in Section 2.1.1.4.

In the following table (Table 2.4.5-1) the components of the subsystem are listed with remarks on their development status.

Table 2.4.5-1 Component development and design

Component	Available from Industry	Remarks
Oxidizer	Yes	a)
Cold Trap	Yes	a)
Molecular Sieve Beds	Yes	a)
Heater	Yes	b)
Recuperator	Yes	b)
Water Separator	Yes	b)
Blower	Yes	b)

- a) These components can be purchased from the industry; however, as they will be operated under conditions characterized by high gas flow rates and extremely low concentrations of Q_2O and Q_2 ($Q = H, T$) which are not at all typical for industrial applications, it appears indispensable to carry out an experimental test program to optimize/modify the design of the components, i.e. to avoid over-dimensioning and to demonstrate the desired removal factors. In addition, such tests are needed to develop appropriate means for process control and analytical measurements.
- b) These components can be purchased from the industry or from special suppliers without the need of experimental testing as described above.
- c) The most appropriate type of machine is not yet clear; it will be necessary to prepare and test a special design with respect to oil freeness, leak tightness, etc. (see also Section 2.4.5, Blower No. 5).

The next paragraphs describe the technical specifications of the components; the numbers given in brackets refer to Fig. 2.1.1.4 - 1.

Water Separator (Component No. 1)

The water separator is foreseen to remove condensed water. It is installed in a bypass of the CPS and will not be used under normal conditions, i.e. as long as no liquid water is contained in the gas of the cooling system. Due to the relatively low pressure of the cooling water in the secondary cooling loop (0.5 MPa) in comparison

to the gas pressure of the primary coolant (8 MPa), an ingress of water is very unlikely.

If, nevertheless, water droplets should be present in the coolant they are removed by the water separator. A filter cartridge containing stainless steel fiber mats can be used for this purpose. The cartridge must be installed in an upright position to allow the water to drain off.

Size (D x H) 60 mm x 700 mm
(including a volume of 500 ml for the separated water)

Electrical Heater (No. 2)

The electrical heater has the task to increase the temperature of the helium stream to 450° C, i. e. to the operation temperature of the next component.

Electrical power 4 KW
Size (D x H) 350 mm x 900mm (including thermal insulation)

Catalytic Oxidizer (No. 3)

The catalytic oxidizer is used to convert the hydrogen isotopes Q_2 to Q_2O ($Q=H,D,T$). The unit contains a precious metal catalyst (Pd or Pt on alumina). An overstoichiometric amount of oxygen is added to obtain a quantitative conversion.

Due to the hygroscopic property of the catalyst, some of the water will be retained in the oxidizer bed at the beginning of the operation.

Size (D x H) 500 mm x 1000 mm (including thermal insulation)
Amount of O_2 to be added $0.4 \cdot 10^{-3}$ NI O_2 /min (excess of 100 %)

Cooler (No. 4)

The water cooler reduces the temperature of the gas to room temperature. It is designed as a double-pipe heat exchanger containing cold water in the jacket and the helium stream in the inner tube.

Gas temperature at inlet 450 °C
Gas temperature at outlet 30 ° C
Helium mass flow 1.85 g / s
Helium pressure 8 MPa
Cooling power 9 KW
Size (D x H) 250 mm x 700 mm

Blower (No. 5)

Although it should be possible to operate the purification system without an additional compressor or circulation pump, a corresponding pump will be available on demand.

Helium mass flow	1.85 g / s
Pressure at suction side	8 MPa
Pressure increase	0.03 MPa
Size (L x W x H)	600 mm x 600 mm x 800 mm

According to information supplied by James Howden & Company Ltd./Scotland, the following types of machines can be used: a) a small reciprocating unit having a bellows-sealed crankcase, b) a diaphragm compressor, or c) a single stage rotary regenerative device.

Cold Trap (No. 6)

The cold trap is used to freeze out the Q_2O content of the gas. The amount of water extracted under the conditions described in Table 2.1.1.4-1 is 3.5 g/day. The trap is cooled with LN_2 . Filling level and temperature are continuously controlled. A heating plate in the center of the trap is used for the recovery of liquefied water which is drained into a water vessel. Before the recovery process is started the trap is depressurized via relief valve No. 10.

The liquid water is processed in the Water Detritiation System.

Humidity at inlet / outlet	$\leq 15 \text{ vpm} / \leq 0.015 \text{ vpm}$
Gas temperature at inlet / outlet	$30 \text{ }^\circ\text{C} / \leq - 100 \text{ }^\circ\text{C}$
Size (D x H)	500 mm x 1300 mm (including thermal insulation)
Volume of water vessel	200 ml

Recuperator (No. 7)

The recuperator has the task to further reduce the temperature of the gas leaving the cold trap (gas 1) by utilizing the clean gas leaving the adsorber (gas 2).

Inlet temperature of gas 1	$\leq - 100^\circ\text{C}$
Inlet temperature of gas 2	$\approx - 190^\circ\text{C}$
Outlet temperature of gas 1	$\leq - 170^\circ\text{C}$
Outlet temperature of gas 2	$\geq - 140^\circ\text{C}$
Size (D x H)	500 mm x 1200 mm

Low Temperature Adsorber (No. 8a/b)

The adsorber beds are filled with 5A zeolite pellets which adsorb gaseous impurities like N₂ and the excess oxygen not used by the oxidizer. Any hydrogen isotopes that have not been oxidized are also adsorbed. The beds contain filters on the downstream and upstream side to prevent particulate material from being transferred during loading or unloading operations. In addition, each bed is equipped with a LN₂ chiller and an electrical heater. The second bed provides additional adsorption capacity; it may be used when the first bed has not been unloaded or regenerated.

Mass of adsorber material	50 kg (per bed)
Operation temperature	- 195°C
Size (D x H)	600 mm x 800 mm

Unloading:

1. Step: Depressurization into the relief tank No. 12a;
2. Step: Discharge of the gas from the relief tank to the Waste Gas System
3. Step: Warm-up to room temperature to desorb impurities which are also sent to the Waste Gas System.

Regeneration: Heat-up to 300 °C and purge with clean helium.

Electrical Heater (No. 9)

The heater is used to warm up the gas coming from the recuperator (No. 7).

Gas temperature at inlet / outlet	≥ -140°C / 50 °C
Electrical Power	4 KW
Size (D x H)	250 mm x 900 mm

Relief Tank (No. 12)

The relief tank has two tasks:

- a) To act as a buffer tank during depressurization of single components; in particular, it is used for the cold trap and the molecular sieve beds prior the warm-up operation.
- b) To store the desorbing impurities, which are released from the adsorber bed during unloading and regeneration operations. These impurities are later on sent to the Waste Gas System.

Because the depressurization is normally carried out at temperatures $\leq -100^{\circ}\text{C}$ the relief tank has to be insulated to prevent the formation of condensation water (from the ambient atmosphere).

Size (D x H)	2000 mm x 4000 mm (including insulation)
----------------	--

If there is no sufficient space available, it would be possible to use only one relief tank for both Coolant Purification Subsystems. The only disadvantage of this proposal would be that depressurization and unloading operations cannot be carried out simultaneously for both loops.

2.4.6 Test Blanket Remote Handling Subsystem

The components of the remote handling subsystem for the test blanket modules are already described in Section 2.1.1.5.

2.5 Instrumentation and Control

During ITER operation, the blanket test modules are monitored and controlled separately through a dedicated control system. The monitoring and control systems are designed to insure proper blanket operation, and provide warning in case of malfunction. In addition, it is used as a data acquisition for recording relevant information for analysis purposes.

Monitoring of the blanket modules and the shielding assembly involves reading temperature, pressure and flow rates of all fluids used. Temperature monitoring of critical surfaces, such as the first wall surface, is required for safety purposes. Controlling the operating parameters of the blanket assembly requires active control systems to maintain pressures and flow rates to keep the blankets and shield operating within their specified design conditions. Control devices such as flow meters, control valves and pressure regulators are anticipated to be outside the bioshield in the pit area. This allows manned access to these devices for maintenance or replacement. Measuring instruments within the blanket assembly are considered a part of the overall assembly. They are installed and maintained in the hot cell during blanket maintenance. Additional instruments are installed on the piping system between the blanket module and the door. Additional pipe monitoring instruments include leak detection devices. Those devices will serve the whole blanket assembly as they are designed to monitor leaks within the port extension. Another area where leak detection is required is between the cryostat and the bioshield. Since cutting and welding of pipes will take place in this area, monitoring devices are a critical item in the safe operation of the blanket modules.

Data acquisition for analysis purposes consists of reading temperatures, pressures, flow rates and tritium content. The instruments used for this purpose can be used as a backup to the control system to provide redundancy and enhance safety. Power and control cable are connected to the blanket assembly in their respective locations. They are then bundled together and routed to a vacuum sealed bulkhead connection at the vacuum vessel door. This is considered part of the blanket assembly. Another plug and a wire bundle is used on the other side of the vacuum vessel door to connect the instruments to the outside monitoring system. A manipulator is used to disconnect the wire bundles prior to removing the blanket assembly.

Data acquisition and control systems are located in the pit area near the port opening, or they could be located inside the tritium processing transporter should this concept be adopted. Another required link will be provided by ITER is the communication line between the data acquisition system and the ITER control room.

Test Blanket Subsystem

The Test Blanket Subsystem requires instrumentation to monitor temperature, pressure, pressure drop and mass flow of the coolants, temperature of the pebble beds, and temperature and local stresses of the structural materials. Additionally the measurement of the tritium concentration at the test module outlet and inlet of the helium coolant and of the purge gas loops should be performed to allow to make a tritium balance and assess the tritium permeation losses.

TBM

cooling plates	Temperature, local stresses
first wall	Temperature, local stresses
pebble beds	Temperature
helium coolant	Temperature, pressure, pressure drop
purge gas	Temperature, pressure, pressure drop

Frame TBD

Shield/ VV Plug TBD

Plumbing Temperature, pressure, pressure drop, tritium and protium concentrations

Specific Instrumentation for the TBM is listed in Table 2.5-1.

2.6 System Interfaces

In order to successfully complete all the test objectives, the Test Blanket System must work in cooperation with many of the other ITER systems and facilities.

2.6.1 Plasma Interface

The first wall of the Test Blanket Module and of the Frame is recessed from the shield blanket contour by a minimum amount of 60 mm. The first wall of the test module is planar, without curvature, but is conform as closely as possible to the first wall of the adjacent shield blanket modules. The plasma side of the first wall of the Test Blanket Module and the Frame is protected by a 5 mm beryllium layer in order to avoid that high atomic weight particles can reach the plasma.

The HCPB Test Blanket System has a leak rate of coolant Helium lower than 10^{-8} Pa m³ s⁻¹.

The first wall of the Test Blanket Module and the Frame has been design in order to remove the surface heat flux and the nuclear heating within the allowable temperature and stress limits.

The presence of a large amount of ferromagnetic material - as structural material for the Blanket Test Module - in the proximity of the plasma magnetic boundary causes a local slight distortion of the toroidal magnetic field. However this distortion remains below the allowable limits [2.6.1-1].

References:

- [2.6.1-1] Statement of R.Aymar at the Test Blanket Working Group Meeting of 16-17th Januar 1996.

2.6.2 Blanket System Interface

The Test Blanket Subsystem has no mechanical interface with the ITER Blanket System; there is a gap allowance of 50 mm completely around the perimeter accounting for differential movement between Blanket System and Vacuum Vessel. The adjacent surfaces of the Test Blanket System (Frame) are cooled to approximately the same temperature of the ITER Blanket System (150°C).

The first wall of the Test Blanket System is recessed below the general surface level of the surrounding Shield Blanket First Wall. This imposes additional surface heating requirements on the adjacent Shield Blanket First Wall components.

2.6.3 Vacuum Vessel Interface

The Test Blanket plumbing extends through the VV plug (see Section 2.1.1.1). This approach eliminates any penetrations through the vacuum vessel wall.. For number, size and description of the pipes at the vacuum vessel boundary see Table 2.4.2.5-1.

Note that all penetrations through the vacuum vessel boundaries will require vacuum tight flexible connections such as bellows (Fig. 2.1.1.1-3). The design of such connections will be similar to those approved by the JCT.

The VV Port Extension is responsible for supporting the static and the dynamic loads generated by Test Blanket Subsystem and provides the proper dimensional control for alignment of the TBS inside the port.

2.6.4 Remote Handling Interface

The remote handling system for the Test Blanket System will take full advantage of the equipment designed by the JCT to minimize duplication of efforts and to standardize system operations. All operations that are identical to other ITER operations will use the same ITER system to perform, such as removing the bioshield plugs and the cryostat plugs. Also internal pipe cutting and welding operation will use the JCT's bore tool design.

Operations that are specific to the Test Blanket System will be integrated into the overall system design. Some of the interface requirements are listed below:

- Maximum supported weight TBD
- position accuracy TBD
- kinematic requirements TBD
- inspection requirements TBD
- accomodation of special end effectors TBD
- accomodation of special material and coolants TBD

2.6.5 Cryostat Interface

The plumbing system from the Vacuum Vessel boundary penetrates the Cryostat boundary as shown in Fig. 2.1.1.1-1. Dimensions, size and description of the pipes are listed in Table 2.6.5-1.

All the penetrations through the cryostat boundaries will require vacuum tight flexible connections such as bellows. The design of such connection will be similar to those approved by the JRC.

Table 2.6.5-1 Cryostat Penetration List

Pipe description ^(*)	No.	Size ^(**)	Material	Pipe Carrier (Oper. Cond.)
Helium Coolant Supply ⁽¹⁾	2	101.6	316LN-IG	Helium (8 MPa, 250°C)
Helium Coolant Return ⁽¹⁾	2	101.6	316LN-IG	Helium (8 MPa, 350-420°C)
Purge Gas Supply ⁽²⁾	1	25	316LN-IG	Helium (0.1 MPa, 20°C)
Purge Gas Return ⁽²⁾	1	25	316LN-IG	Helium (0.1 MPa, 450°C)
Diagnostic Conduct ^{(1) (2)}	1	250	316LN-IG	
Frame Coolant Supply ⁽³⁾	1	50	316LN-IG	Water (4 MPa, 140°C)
Frame Coolant Return ⁽³⁾	1	50	316LN-IG	Water (4 MPa, 190°C)
Shield Coolant Supply ⁽³⁾	1	50	316LN-IG	Water (4 MPa, 140°C)
Shield Coolant Return ⁽³⁾	1	50	316LN-IG	Water (4 MPa, 190°C)

^(*) The helium cooling and purge pipes for the Japanese TBM are not included in the table.

^(**) Outer Diameter (in mm) not accounting for eventual thermal insulation (5-10 cm).

⁽¹⁾ Helium Cooling Subsystem

⁽²⁾ Tritium Extration Subsystem

⁽³⁾ ITER Primary Heat Transfer System

2.6.6 Primary and Secondary Heat Transfer Interface

The Frame and the Shield of the Test Blanket Subsystem are cooled by water provided by the Primary Heat Transfer System of ITER. The design requirements are listed in Table 2.6.6-1.

The secondary heat removal system of the Helium Cooling Subsystem is considered as part of the ITER cooling system. For the layout a constant water flow with nominal inlet temperature of 35 °C at the secondary side of the two heat exchangers (see 2.1.1.3.1) and a flow rate of ~7 kg/s per heat exchanger are assumed, leading to pipe dimensions of 50 mm diameter, 3 mm wall thickness, at a velocity of ~5 m/s. The outlet temperature will then vary according to the burn and dwell cycles between 75°C and 35°C. Flow, pressure, and temperature monitoring are needed. No significant migration of tritium from the primary coolant to the secondary side is expected.

2.6.6-1 Design requirements for the ITER Primary Heat Transfer Interface

Parameters	Frame	Shield
Power [Mw]: BPP/EPP	3.3 / 3.6	TBD
Loop no.	1	1
Pressure [MPa]	4	4
Coolant temperature:		
Inlet	150°C	150°C
Outlet	190°C	190
Flow rate [kg/s]: BPP/EPP	15.8 / 17.2	TBD
Outer Pipe diameter (without insulation)		
Inlet	50 mm	50 mm
Outlet	50 mm	50 mm
Tritium generation	TBD	TBD

The secondary loop of the two water cooler of the Coolant Purification Subsystem is considered as part of the ITER cooling system. For the layout a constant water flow with nominal inlet temperature of 35 °C and a flow rate of TBD kg/s per cooler are assumed, leading to pipe dimensions of TBD mm diameter, TBD mm wall thickness, at a velocity of TBD m/s. The outlet temperature will then vary according to the burn and dwell cycles between 60 °C and 35 °C. No significant migration of tritium from the primary coolant to the secondary side is expected.

The secondary loop of the two water cooler of the Tritium Extraction Subsystem is considered as part of the ITER cooling system. For the layout a constant water flow with nominal inlet temperature of 35 °C and a flow rate of TBD kg/s per cooler are assumed, leading to pipe dimensions of TBD mm diameter, TBD mm wall thickness, at a velocity of TBD m/s. The outlet temperature will then vary according to the burn and dwell cycles between 60 °C and 35 °C. No significant migration of tritium from the primary coolant to the secondary side is expected. Only in case of leakage through the heat changer a not negligible amount of tritium can reach the secondary side.

2.6.7 Vacuum Pumping and Leak Detection Interface

The test Blanket System has a leak rate of coolant Helium lower than 10^{-8} Pa m³ s⁻¹.

In case of loss of all the Helium coolant present in the Test Blanket System (46 Kg, in two independent loops) the pressure in the Vacuum Vessel will remain less of 5 bar.

2.6.8 Tritium Plant Interface

Molecular hydrogen isotopes (HT,H₂) are stored in uranium getter beds (see Section 2.4.3) of the Tritium Extraction Subsystem. When the loading capacity of these beds

is reached they will be transfer to the Isotope Separation System. This is expected to be needed after 6 days of nominal operation with back-to-back pulses. The rate of HT and H₂ extracted is given in Table 2.1.1.2-1.

The cold trap (see Section 2.4.3) of the Tritium Extraction Subsystem is periodically depressurized and warmed up to room temperature to liquefy the water which is then drained into a water container and sent to the Water Detritiation System. The rate of water extracted is given in Table 2.1.1.2-1.

The adsorber beds (See Section 2.4.3) of the Tritium Extraction Subsystem are periodically depressurized and warmed up to room temperature. The desorbing impurities are sent to the Waste Gas System.

The cold traps (see Section 2.4.5) of the Colant Purification Subsystems are periodically depressurized and warmed up to room temperature to liquefy the water which is then drained into a water container and sent to the Water Detritiation System. The rate of water extracted under Design Conditions is given in Table 2.1.1.4-1.

The adsorber beds (see Section 2.4.5) of the Colant Purification Subsystem are periodically depressurized and warmed up to room temperature. The desorbing impurities are sent to the Waste Gas System.

2.6.9 Tokamak Operations and Control Interface

The TBM will remain inside the Test Port for few years.

An interruption of at least 2 days of the plasma operation is required to exchange the uranium Getter Beds of the Tritium Extraction Subsystem (see 2.1.1.2). This operation is, in the present design, required after 6 days of nominal operation with back-to-back pulses. The period of operation could be longer but this would require to increase the number of Getter Beds.

2.6.10 Building and Transporter Interface

It is intended to install the Tritium Extraction Subsystem in the Tritium Building. The size of the main components has been estimated and listed in Table 2.1.1.2 - 3. The integral space requirement is about 40 m². It is expected that supply and disposal facilities are available. This facilities are listed in Table 2.1.1.2-2. Figure 2.1.1.2. - 2 gives a preliminary arrangement of the components of the Tritium Extraction Subsystem.

The Coolant Purification Subsystem is also installed in the Tritium Building. The size of the main components has been estimated and listed in Table 2.1.1.4-2. A first proposal for the geometrical arrangement is given in Figure 2.1.1.4.-2. The integral space requirement of the facility is about 40 m². The supply and disposal facilities listed in Table 2.1.1.4-2 are also needed for the Coolant Purification Subsystem.

The Helium Cooling Subsystem will be housed in a wedge-shaped pit outside of the cryostat at about the same level as the test module. Figure 2.1.1.3-2 shows the arrangement in the pit.

During the operations of removing and installing of the Test Blanket Subsystem the ITER transporters are used to perform the operations that are identical to other ITER operations, such as the removing of the cryostat and bioshield plug. A special transporter (Test Blanket Remote Handling Transporter, see Section 2.1.1.5.1) has to be designed for the operation involving the management of the Test Blanket Subsystem. This transporter will be based on the standard transport design of ITER.

2.6.11 Hot Cell Interface

The hot cells have to handle the Blanket Remote Handling Transporter which contains the Test Blanket Subsystem from its location in the ITER reactor. This Transporter fulfills the standard JCT design with overall dimensions of 8 m long, 3.8 m wide and 5 m high.

The following operations have to be performed in hot cell to separate the components of the Test Blanket Subsystem:

- remove the Test Blanket Subsystem from its location in the Transporter;
- cut the tubes at designed planes;
- unfasten the bolts between the Shield and the Frame;
- unfasten the bolts of the mechanical connection between the TBM and the Shield.

At the end of the irradiation time foreseen for the HCPB TBM, the following operations have to be performed on the component:

- cut the TBM and remove the beryllium and orthosilicate pebble from the beds for investigation:
 - tritium release test
 - mechanical investigation
 - crush test
 - thermal cycling test
- cut probes of the structure for investigations.
 - tritium release test
 - swelling test
 - embrittlement test
 - tritium inventory determination

The following repairs have to be performed too:

- weld small leakages in the components;
- replace tubes;
- replace damaged instrumentation.

2.6.12 Other Interfaces

The particulate filters will be transferred to the waste disposal system after exchange.

2.7 Safety analysis of reference events

The safety considerations of the Test Blanket Module (TBM) focus on the accidental safety aspects to the extent that conceivable failures of the TBM system can impede the safe operation of ITER. On the other side, occupational safety and waste generation issues have not been elaborated so far, since they are small compared to those associated with the basic ITER machine.

Two event families were found to be the most demanding occurrences with respect to potential damage in ITER, associated with the release of radioactive material (in particular tritium) into the containment, i.e., in-vessel TBM coolant leaks and ex-vessel TBM coolant leaks. These two postulated initiating events (PIE) were investigated in different variants or in combination with a set of postulated aggravating occurrences that could be triggered by the PIE. An attempt was made by the ITER Joint Central Team to harmonise the spectrum of events to be analysed for each type of test blanket modules.

The following event sequences were studied for the HCPB TBM, considering cases 1a and 2a as the reference initiating events and the cases 1b, 1c, 1d, and 2b, 2c, 2d, respectively, as parameter studies thereof.

- 1) Large in-vessel TBM coolant leaks
 - a) FW cooling channel failure
 - b) FW failure plus pebble bed beryllium/steam chemical reaction
 - c) Large leak inside module
 - d) Small leak inside module
- 2) Large ex-vessel TBM coolant leaks
 - a) Main pipe break in the vault
 - b) Main pipe break plus subsequent failure of FW
 - c) Main pipe break plus large leak inside TBM
 - d) Main pipe break (or loss of flow) plus FW failure at beryllium melting

The structure of the safety section is organised in accordance with the breakdown chosen in the NSSR-2 report. Each of the eight events is described in successive paragraphs entitled (i) Identification of causes, (ii) Method of analysis, (iii) Transient analysis results, (iv) Evaluation of radiological release, (v) Uncertainties in results, and (vi) Summary. The data base for the safety analysis is compiled in section 2.7.3. An overview of the assumptions made in the cases investigated is given in the following two-page Table 2.7-0.

The analysis is limited to the TBM-I type test module design as described in section 2.1.1.1 with EUROFER as structural material and for a lifetime planned to be achieved in the basic performance phase of ITER. This corresponds to a fluence level at the first wall of 0.36 MWa/m^2 , including 20% margin. The thermal-hydraulics analysis is based on the cooling subsystem layout according to section 2.1.1.3.

Table 2.7-0 (Part 1): Large In-Vessel TBM Coolant Leaks, List of Parameters

Case → And Parameter ↓	1a FW failure as PIE	1b PIE plus Be/steam Reaction	1c Large Leak inside Module	1d Small Leak inside Module
Event category	IV	V	IV	III
Fusion power at beginning of PIE	1.65 GW	1.65 GW	1.65 GW	1.65 GW
Fluence level for decay heat history	0.36 MWa/m ²	0.36 MWa/m ²	0.36 MWa/m ²	0.36 MWa/m ²
Shutdown delay time	0 s	0 s	1000 s	1000 s
Power ramp-down time	1 s	1 s	1 s	1 s
Circulator begin-to-trip time	0 s	0 s	1000 s	1000 s
Circulator trip half time ¹	4 s	4 s	4 s	4 s
HX elevation above TBM	2.1 m	2.1 m	2.1 m	2.1 m
HX bypass control	no response	no response	on	On
Temperature control system	Off	Off	on	On
Buffer tank surge line	Open	Open	open → closed	open → closed
Number of loops affected	Both	Both	both	One
Break size	4 FW channels	4 FW channels	78.5 cm ²	0.25 cm ²
Break location	FW	FW	Internal manifold	cooling plate
FW/multiplier interface failure	No	Yes	no	No
Breeder/multiplier release into VV	No	no and yes	no	No
Discharge volume	3800 m ³ (VV)	3800 m ³ (VV)	0.4 m ³ (box)	0.4 m ³ (box)
Surface of VV internals	1223 m ²	1223 m ²	n.a.	n.a.
Other ITER components affected	all 10 FW/IBB and 4 OBB/LIM	all 10 FW/IBB and 4 OBB/LIM	no in-vessel cooling	no in-vessel cooling
Purge gas system affected	No	Isolated	1 m ³ , isolated at 2 bar	1 m ³ , isolated at 2 bar
Purge gas system	no credit	No	no	No

¹ Reasonable fit to curve from [2.7-4], p. 23

heat removal				
Secondary cooling flow	off for 1 h	off for 1 h	off (1000-4600s)	off (1000-4600s)
VV coolant temperature	200°C	200°C	200°C	200°C
ITER FW temperature	200-465°C	200-465°C	200-465°C	200-465°C
Support frame cooling system	Ignored	Ignored	ignored	Ignored
Pebble bed Be chem. Reaction	n. a.	Be/steam, SF=1	n. a.	n. a.
FW Be chem. Reaction	Be/steam, SF=2	Be/steam, SF=1	n. a.	n. a.
Concerns related to TBM	a) VV pressure b) T-release c) Temp. Bursts d) Decay heat e) H ₂ from FW-Be/steam	a) to e) as in case 1a b) H ₂ and heat from pebble-Be/steam c) TES pressure	a) Box pressure b) TES pressure c) Temp. bursts d) Decay heat	a) Box pressure b) TES pressure c) Temp. Bursts
Analyses method and problem time	RELAP 400s, 1D model 10 days H ₂ – production see case 1d	RELAP results from 1a, Estimates on Be/steam react.	RELAP 2400s	RELAP 2400s

Table 2.7-0 (Part 2): Large Ex-Vessel TBM Coolant Leaks, List of Parameters

Case → And Parameter ↓	2a Main pipe break in the vault as PIE	2b PIE plus Subsequent Failure of FW	2c PIE plus Large Break inside TBM	2d PIE plus Subsequent Failure of FW at 1290°C
Event category	IV	IV	IV	V
Fusion power at beginning of PIE	1.65 GW	1.65 GW	1.65 GW	1.65 GW
Fluence level for decay heat history	0.36 Mwa/m ²	0.36 Mwa/m ²	0.36 Mwa/m ²	0.36 Mwa/m ²
Shutdown delay time	10 (and 4 s)	10 s	10 s	ca 120 s
Power ramp-down time	1 s	1 s	1 s	1 s
Circulator begin-to-trip time	0 s	0 s	0 s	0 s
Circulator trip half time	4 s	4 s	4 s	4 s
HX elevation above TBM	2.1 m	2.1 m	2.1 m	2.1 m
HX bypass control	no response	no response	no response	closed
Temperature control system	Off	Off	off	off
Buffer tank surge line	Open	Open	open	open
Number of loops affected	One	Both	both	both
Break size	78.7 cm ²	78.5 cm ² and 4 FW channels	78.5 cm ² ex-VV, 78.5 cm ² in TBM	78.5 cm ² ex-VV, 4 FW channels
Break location	main pipe at circulator inlet	main pipe at circulator inlet and FW	main pipe at circulator inlet and int. manifold	main pipe at circulator inlet and FW
FW/multiplier interface failure	No	No	No	no
Breeder/multiplier release into VV	No	No	No	no
Discharge volume	2150 m ³ (vault)	2150 m ³ (vault) 3800 m ³ (VV)	2150 m ³ (vault)	3800 m ³ (VV)

Surface of VV internals	n.a.	1223 m ²	n.a.	1223 m ²
Other ITER components affected	no in-VV cooling	no in-VV cooling	no in-VV cooling	no in-VV cooling
Purge gas system affected	No	No	Isolated	no
Secondary cooling flow	off for 1 h	off for 1 h	off for 1 h	off for 1 h
VV coolant system	200°C	200°C	200°C	200°C
ITER FW temperature	200-465°C	200-465°C	200-465°C	200-465°C
Support frame cooling system	Ignored	Ignored	ignored	ignored
Pebble bed Be chem. Reaction	No	No	Be/air, SF=5	n. a.
FW Be chem. Reaction	No	Be/air, SF=5	no	Be/steam, SF=1
Concerns related to TBM	a) Vault pressure b) Temp. Bursts c) H-3 release d) Decay heat e) Design temp. Limits	a) Vault pressure b) VV pressure c) Decay heat d) FW Be/air e) H-3 release	a) Vault pressure b) Box and TES pressure c) Decay heat d) pebble Be/air e) H-3 release	a) VV pressure b) H-3 release c) Vault pressure d) Decay heat e) FW Be/steam
Analyses method and problem time	RELAP 100s, FIDAP 60s, 1D model 1 day, Stress evaluation	RELAP 2000s, 1D model 10 days Estimates on Be/air reaction	RELAP from 2a, 1D model 1 day, Estimates on be/air reaction	RELAP from 1a, FIDAP ≈120 s, 1D model 10 days Estimates on Be/steam react.

2.7.1 Large in-vessel TBM coolant leaks

2.7.1.1 Case 1a: Failure of first wall (Cat. IV)

i) Identification of causes and accident description

The postulated accident is a multiple break of the TBM FW cooling channels with the blowdown of the high pressure primary helium coolant into the vacuum vessel (VV). For break size a double ended rupture of 4 FW coolant channels pertaining to both cooling loops is assumed, with the coolant/multiplier interface remaining intact. This type of failure is conceivable to evolve from a relatively small leak which triggers an intense disruption, which in turn produces high local stress and/or runaway electron damage to the extent described, and propagating to other in-vessel components, as for instance, described in section VII.2.2.1 of [2.7-1]. Consequently, the additional failure of all ITER blanket cooling loops is postulated, flushing water and steam into the VV. It is to be noted that only the implications associated with the TBM system are considered here. Pressurisation of the VV by steam, and effluent release from other than TBM systems are assumed to be covered elsewhere.

The following time sequence of events is assumed in the analysis (Table 2.7-1). The ITER machine is operating at 10% over-power (1.65 GW). A peak surface heat flux of 50 W/cm^2 due to temporal and local peaking at the TBM is assumed prior to the PIE. At time zero the TBM FW fails (PIE). For simplicity instantaneous break of 4 cooling channels is postulated and helium ingress into the VV triggers an intense disruption. At the same time circulators in both cooling loops start to trip with a speed half time of 4 seconds. The plasma quench is terminated within one second. At this time (1 s) all ITER shield blankets are affected, some of them flushing steam into the VV. In a conservative way it is postulated that a loss of off-site power coincides with the disruption, which is interpreted as a loss of secondary coolant flow in the heat exchangers of the TBM cooling circuits, equivalent to a loss of heat sink. The loss of off-site power also means that the VV cooling system is in the natural convection mode, maintaining the VV inner surface temperature below 200°C . The loss of coolant in the shield blanket causes the ITER FW to heat up to a level of at most 465°C after 1 day, falling off afterwards according to the curve specified in [2.7-1] and reproduced in Table 2.7-24.

The principal concerns for this accident scenario are listed below. Table 2.7-1 gives the time sequence of events.

- Vacuum vessel pressurisation
- Activation products release into the VV
- Temperature evolution in the TBM
- Decay heat removal via conduction and radiation along radial path ways
- H_2 production from FW-Be/steam reaction

Table 2.7-1: Case 1a - Time sequence of events for large in-vessel TBM coolant leak caused by FW failure

Event Sequence	Time
Total fusion power 1.65 GW, 50 W/cm ² surface heat flux	<0
Break of 4 TBM FW cooling channels, 2 in each loop	0 s
Helium coolant blowdown into VV triggers disruption	0 s
Pumps in affected loops start to trip with half time of 4 s	0 s
End of plasma energy quench with extra wall loading of 4.2 MW/m ²	1 s
All 10 FW/IBB and 4 OBB/LIM loops affected	1 s
Loss of heat sink (HX) in both loops	1 s
ITER FW temperature starts to ramp-up from 200 to 465°C (Table 2.7-24)	1 s
VV temperature <200°C (coolant in natural circulation mode)	All times

ii) Method of analysis

The RELAP5/MOD3.2 code was used to calculate the flow rates, pressure, and temperatures in the TBM cooling circuits during the transients. A single coolant loop was used to represent the two identical loops (Figure 2.7-1) [2.7-2]. The model includes the TBM proper, circulator, dust filter, helium/water heat exchanger, a buffer tank for pressure control, and the interconnecting piping, including a bypass to the heat exchanger according to the flow diagram shown in Figure 2.1.1.3-2 of [2.7-3]. All components are modelled as heat structures to account for the thermal inertia of the system. The secondary cooling system is represented to the extent as to define the boundary conditions at the heat exchanger.

The TBM itself is modelled according to the schematic given in Figure 2.7-2. All the FW cooling channels and 20 cooling plates with their pertaining beryllium and breeder pebble beds are lumped together to give one unit consisting of the representative FW cooling channels (No. 20 in the schematic) and six breeding zones (No. 22-27) being interconnected via manifolds (No. 21 and 28). The main inlet and outlet manifolds at the back of the TBM are represented as single heat structures. There is a calibrated bypass flow from the inlet manifold to the outlet manifold to cool the poloidal caps (No 30). The RELAP analysis started from the nominal power level (as opposed to the TBM specific temperature analysis described below) as it has little influence on the cooling system dynamics. It also ignored the extra disruption load.

A 1D heat transport model has been set up to analyse the decay heat transport in the HCPB TBM in the post blowdown phase. It represents a radial unit cell column cut out of the TBM from the first wall all the way through the breeding zone, manifold region, support structure, up to and including the 0.48 m thick radial shield (Figure 2.7-3). The model is divided into 22 elements according to the radial nodes used in the neutronics analysis in [2.7-3]. A typical volumetric material composition of the elements as occurring in a unit cell of the TBM-1 (comprising, e.g., in the breeding zone one layer of breeder pebbles, one layer of beryllium pebbles and two cooling plates) is presented in Table 2.7-22. This radial build is the standard composition used in the analysis. Energy conservation in each element between the time and space dependent decay heat power, internal energy, and longitudinal thermal losses

yields the equation to compute the temperature evolution in each element for a given set of initial and boundary conditions. The longitudinal heat transport model includes thermal conduction, radiation across elements with high void (or helium) fractions, and radiation from the bounding surfaces to the environment at both ends of the model. The material data assigned to each element are lumped values representing the material mixture, i.e., the specific heat is derived as the mass-weighted mean, and the thermal conductivity is derived as the volume-weighted mean pertaining to each element. The temperature dependent source data of the materials involved (EUROFER, beryllium pebbles, Li_4SiO_4 pebbles, and helium) are specified in section 2.7.3.3. As initial conditions in the 1D decay heat removal analysis a typical radial temperature profile in the TBM as obtained in steady state operation at 10% over-power has been assumed (Figure 2.7-22), adding an extra temperature burst in the FW nodes caused by the disruption (compare Table 2.7-23 and section 2.7.3.4, paragraph iv).

The main parameters and assumptions used in the analysis are summarised below.

- Time sequence of events as specified in Table 2.7-1.
- Cooling system layout according to section 2.1.1.3 of [2.7-3] (compare Figure 2.7-1 for RELAP nodalization)
- Discharge volume for both coolant loops is 3800 m³ (free volume of VV)
- Buffer tank surge line (item 7 in Figure 2.7-1) opens to main loop
- Purge gas system not affected, but no credit given to its heat removal capability
- No FW/multiplier interface failure, hence no steam ingress into the pebble bed

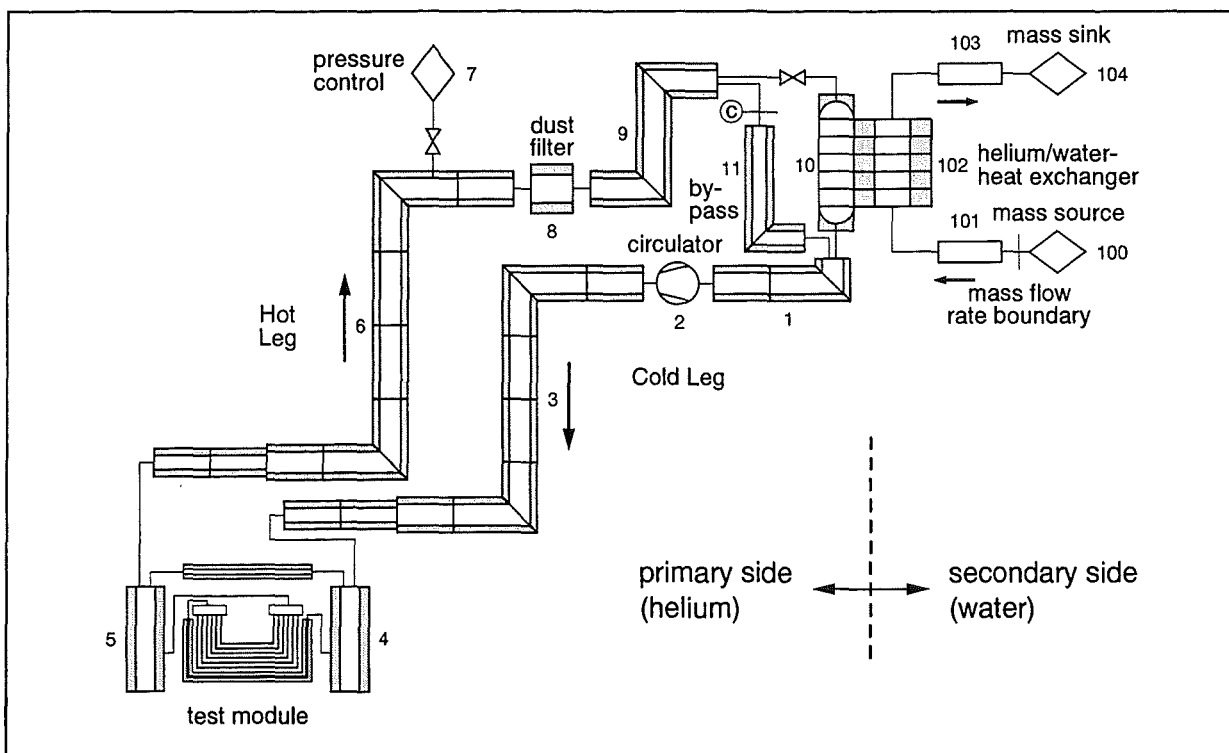


Figure 2.7-1: RELAP Nodalization of the HCPB TBM cooling circuits

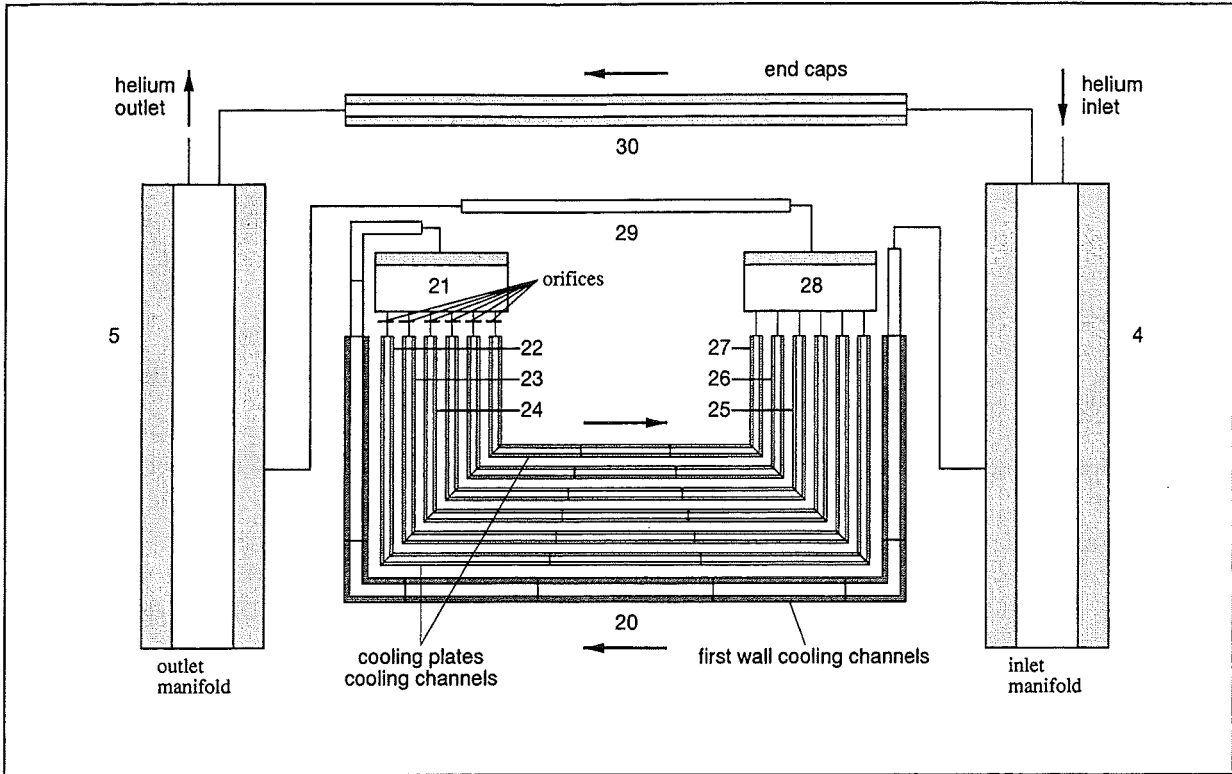


Figure 2.7-2: Detailed RELAP nodalization of the HCPB TBM

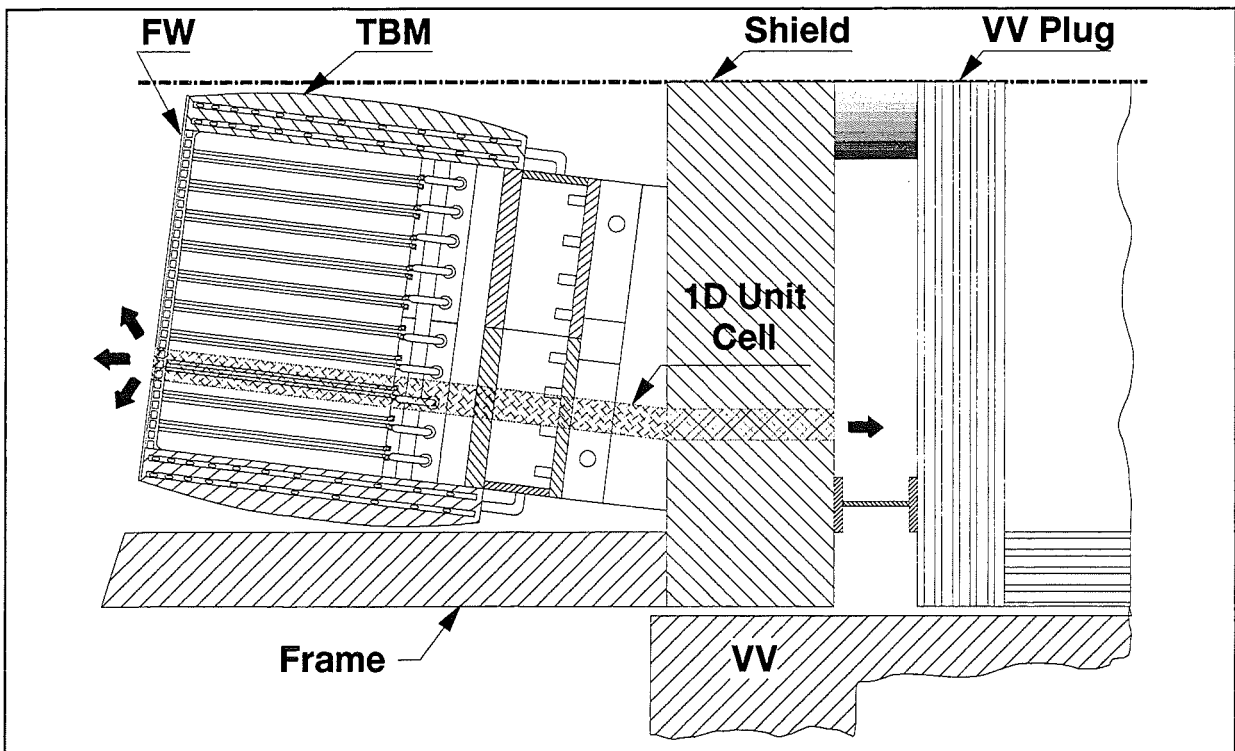


Figure 2.7-3: Schematic of the 1D heat transport model

(The cross hatched stripe represents a typical unit cell.)

iii) Transient analysis results

RELAP results: Transients of the blowdown phase are illustrated in Figures 2.7-4 and 2.7-5. The discharge of the helium coolant inventory from both cooling loops through the broken FW channels lasts for about 20 s.

The diagram at the top of Figure 2.7-4 shows the loop pressure decay in the cold leg and hot leg, which are practically identical, decreasing from the initial 8 MPa to the level of the VV pressure within 12 s. Accordingly, the VV pressure builds up from zero to the small value of about 3500 Pa (second diagram from top). Since in the analysis any pressure build-up from other ITER in-vessel components has been ignored, the VV pressure presented here has to be taken as partial pressure contributed by the HCPB TBM subsystem.

The next two diagrams in Figure 2.7-4 show the mass flow rate and helium velocity in different sections of the TBM cooling system. While the flow rates decrease at about the same time scale as the pressure does, the velocities remain almost stable for a period of 18 seconds because of the gas expansion. There remains a small velocity of a few m/s which is attributed to further heat-up and expansion of the helium. It is to be noted that the flow direction at the entrance to the dust filter stays in normal flow direction at all times, avoiding the risk of flushing accumulated dust from the filter by back streaming. The gas speed in the simulated break cross section assumes the velocity of sound of about 760 m/s for 18 s (not shown).

The gas temperatures experience moderate fluctuations during the blowdown phase due to expansion and heat-up, with the trend for small increases with time. A marked temporal temperature drop of 150 K occurs in the hot leg as a result of the cold (50°C) gas fed from the buffer tank.

The temperature evolution in selected points of the TBM RELAP model is presented in Figure 2.7-5. Shown are sets of temperature curves obtained for the cooling plates (top frame), the beryllium pebble beds, and the breeder pebble beds (all taken at the poloidal mid plane), each set representing the six radial breeding zones. The diagram at the bottom shows, as orientation in this context, the temperature history in the FW when the over-power and disruption loads are ignored. A better FW temperature representation will be given in the 1D heat transport results below.

The peak temperatures in the beryllium and breeder pebble layers relax within about 100 s, approaching equal values as the cooling plates in each radial zone thereafter. The remaining temperature drift in the breeding zone caused by decay heat amounts to typically 0.007 K/s in this first phase of the loss of coolant.

There is a radial temperature gradient across the six breeding zones both during steady state (at $t=0$) and in the course of the transient, given that the division of the coolant flow was trimmed as to achieve an almost equal coolant temperature level of 350°C in all channels at the outlet. This effect becomes of interest with view to the chemical reaction of beryllium discussed with case 1b.

Since in the RELAP model of the TBM (Figure 2.7-2) thermal coupling between radial zones is not included, the long term temperature development driven by conduction in radial direction was analysed by applying the 1D heat transport model described next.

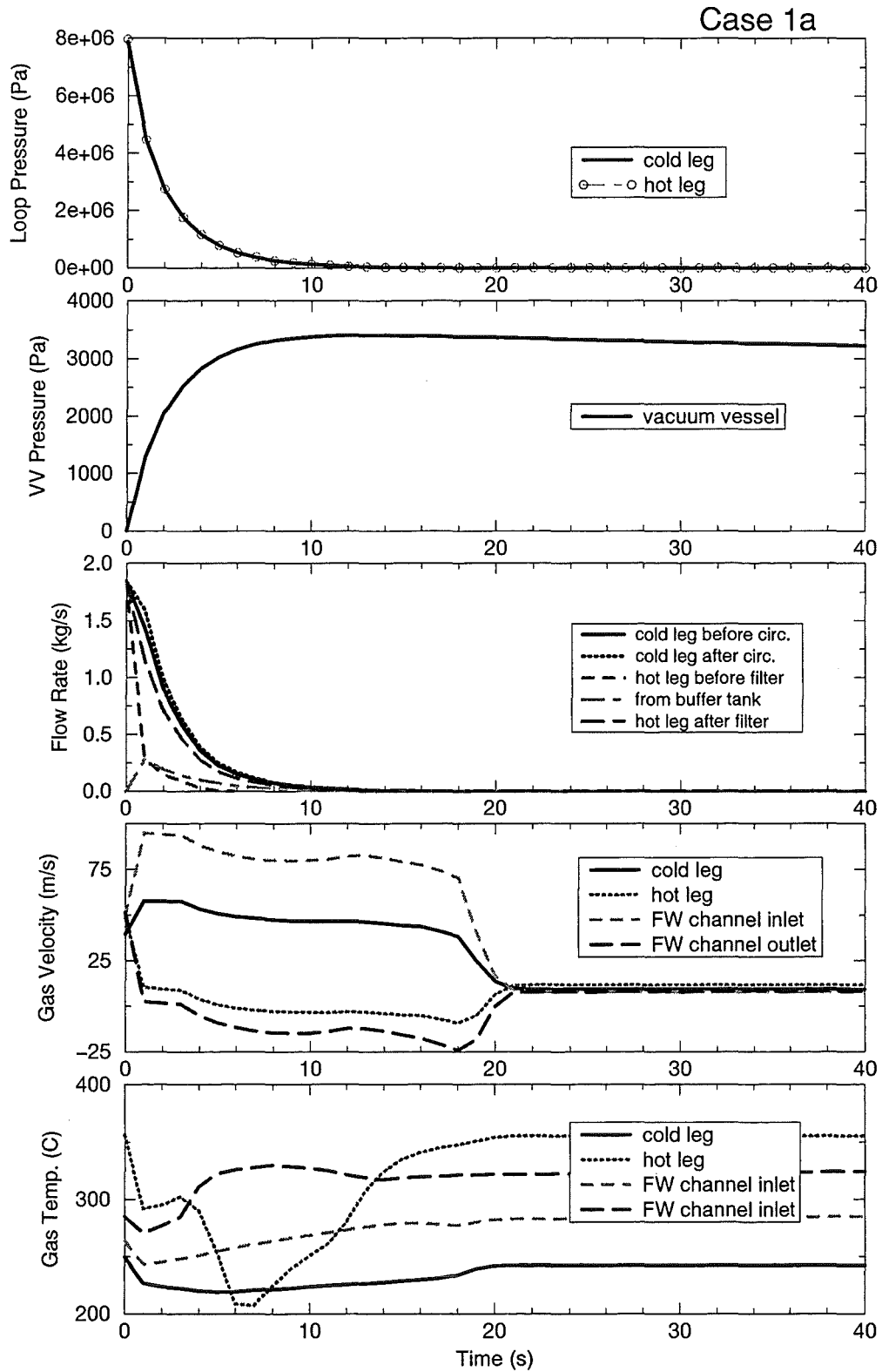


Figure 2.7-4: Case 1a - Large in-vessel coolant leak by FW failure, RELAP results

(loop pressure, vacuum vessel pressure, flow rates, velocities, and gas temperatures in different parts of the cooling system)

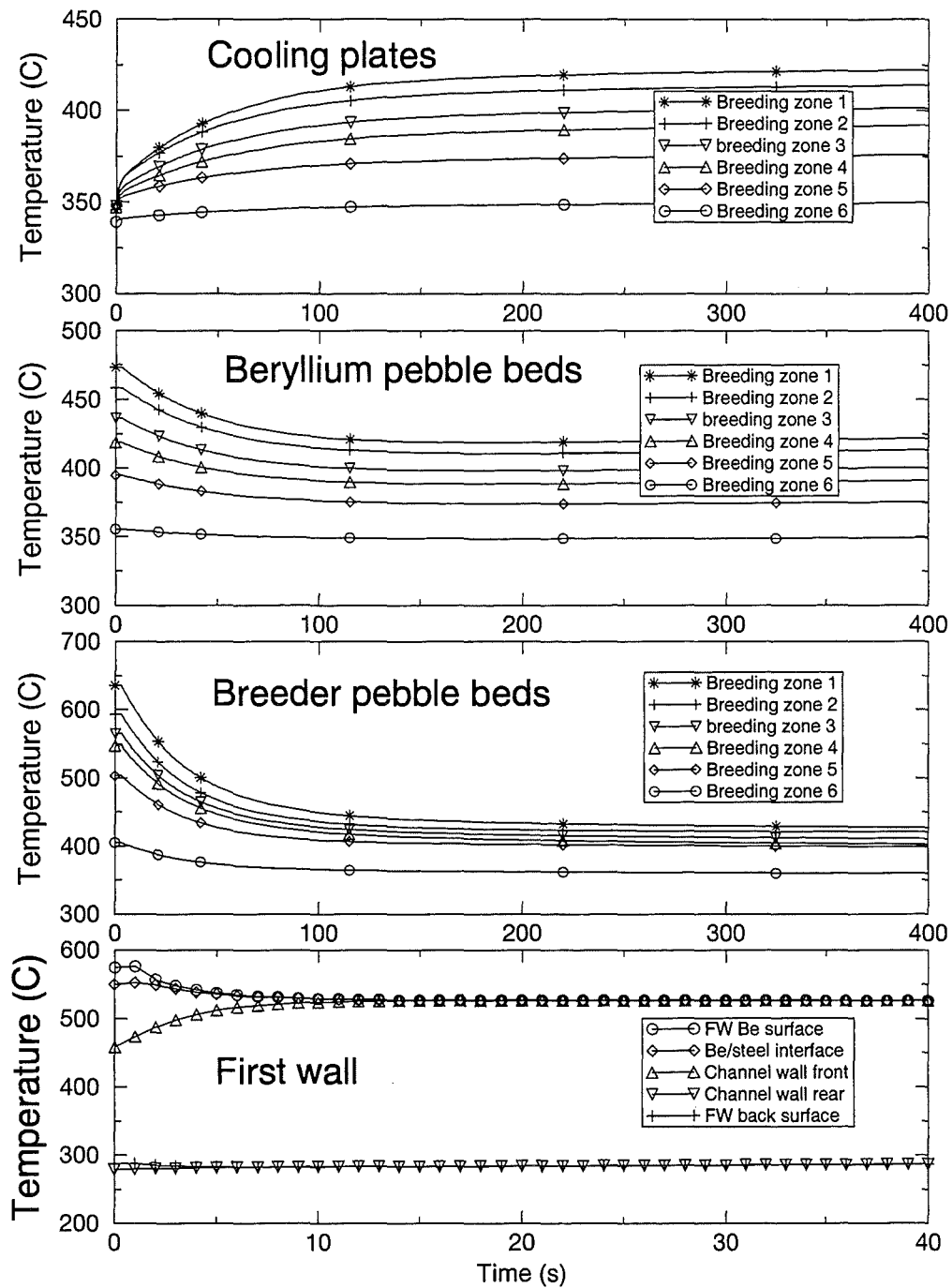


Figure 2.7-5: Case 1a - Large in-vessel coolant leak by FW failure, RELAP results

(Temperature evolution in selected zones of the TBM)

1D heat transport results: The typical long-term temperature evolution of the TBM is presented in Figure 2.7-6 for a period of 10 days after the LOCA, where the bottom graph is a zoomed-in portion of the top graph. Shown is the history of the mean temperature in each of the 22 radial elements of the 1D model. The curves are obtained by applying the initial temperature profile defined in Table 2.7-23 for this case 1a. The heat is dissipated from the front and back surface solely by radiation,

assuming the reference ITER FW temperature evolution specified in Table 2.7-24 as indicated by the dashed line in Figure 2.7-6, and a vacuum vessel wall temperature of 200°C. The latter includes some margin with respect to the VV coolant temperature of 100°C. For comparison, the effect of other FW temperatures and of an adiabatic condition at the back side have been investigated separately as parameter study.

The safety relevant results of the 1D analysis can be summarised as follows: The temperature in the FW nodes including the beryllium protection layer equalises within 80 s at about 430°C, i.e., at a low level (visible in the bottom frame of Figure 2.7-6). It then rises at a rate of 50 K/hour reaching the maximum of 480°C after 4 hours. Similarly, the front nodes in the breeding zone (that means in the beryllium pebble beds) heat up to 480°C for a few hours and then decline as the temperature goes down after 1 day. The rear parts of the TBM reach 370-400°C and the shield back surface assumes 350°C. A marked cool-down is observed after 7 days, when the ITER FW temperature as boundary condition was reduced more rapidly to 200°C.

A sensitivity study of how the ITER FW temperature and the heat transfer at the back would affect the peak temperature in the TBM, occurring at about 4 hours after start of the transient, yielded the results given in Table 2.7-2. The impact on the peak is small, although the long term evolutions are different. The peak beryllium temperature in the breeding zone (peak TBM BZ) never exceeds the 500°C level.

Table 2.7- 2: Case 1a – Characteristic temperatures (in °C) in the TBM for various boundary conditions

Parameter $T_{ITER, FW}$	Parameter T_{VV}	Peak TBM FW Temperature (at \approx 4h)	Peak TBM BZ Temperature range
Reference curve	200	480	380-480
Reference curve	Adiabatic	480	380-480
200	200	470	380-470
300	200	480	380-480
400	200	495	380-495

iv) Evaluation of radiological release

The only radiological release into the VV is the amount of tritium and activation products carried by the helium coolant. The maximum tritium content in the coolant of 1 mg only (Table 2.7-15) is insignificant. The mobile activation products in the cooling loops (especially in the dust filters) have not been quantified but are negligible compared to the amounts of dust envisaged to be mobilised in the VV.

Activation products release from the TBM FW is conceived to be at most of the order of the proportion TBM surface to ITER FW surface, i.e., less than 1%.

v) *Uncertainties in results*

Uncertainties in the analysis and data base are irrelevant with view to the small contribution of the TBM to the overall consequences assessed in section VII.2.2 of [2.7-1] for this severe accident.

vi) *Summary*

The principal concerns formulated in the accident description for this severe accident revealed to be uncritical. Contribution to the VV pressurisation by the TBM helium coolant is small (3500 Pa). Tritium and activation products release from the TBM into the VV is insignificant compared to the total amount mobilised from non-TBM components. The TBM FW temperature can be kept below 500°C by solely radiation and conduction. The hydrogen production from FW-Be/steam reaction is thus very small (compare case 2d in section 2.7.2.4), passive decay heat removal is assured at moderate TBM temperatures (typically <460°C). Nevertheless, the accident would be disastrous to ITER and the TBM must be designed to not be the initiator.

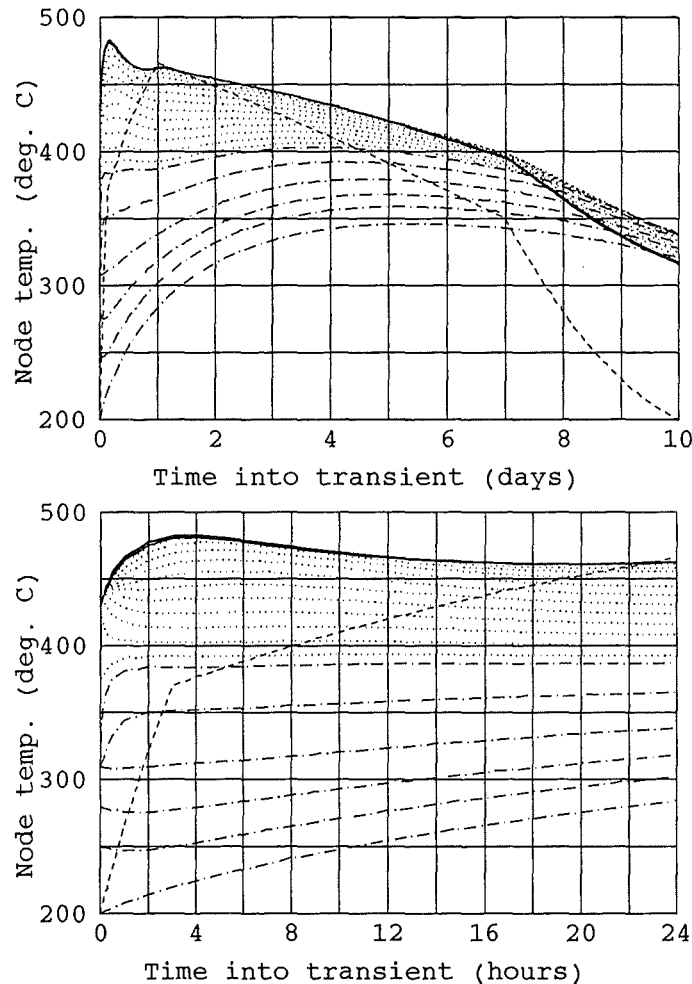


Figure 2.7-6: Case 1a - 1D model TBM temperature evolution

(solid: FW nodes, dotted: breeding zone nodes, dash-dotted: manifold and shield nodes, dashed: ITER FW reference curve)

2.7.1.2 Case 1b: Failure of FW plus Be/steam reaction (Cat. V)

i) Identification of causes and accident description

As a parameter variation to the base case 1a it is postulated that the intense disruption causes a breach of the TBM FW box allowing steam ingress into the beryllium pebble beds and, hence, into the purge gas system. Since the steam pressure in the VV will temporarily rise to 0.11 MPa within about 200 s (Figure VII.2.2-2 of [2.7-1]) the steam can replace part or all of the purge gas in both breeder and multiplier pebble beds and will pressurise the tritium extraction subsystem (TES) until the TES isolation valves will respond or pressure equilibrium is reached. At that time forced convection steam flow through the pebble beds is stopped and steam transport into the beryllium layers will be dominated by diffusion processes.

The time sequence of events postulated is given in Table 2.7-3. It is essentially the same as that discussed under case 1a except for the two additional steps considered here, i.e., the failure of the FW/multiplier interface occurring simultaneously with the disruption at 1 s, and the purge gas system isolation from the TBM, for which 5 minutes have been assumed rather arbitrarily but in a pessimistic way.

The principal concerns for this accident scenario are listed below.

- FW/multiplier interface failure leading to beryllium/steam reaction (H₂ production, heat generation, tritium release)
- Purge gas system temporarily pressurised up to 0.11 MPa absolute by steam (perhaps with a certain breathing effect) before the isolation valves are closed.

Table 2.7-3: Case 1b - Time sequence of events for large in-vessel TBM coolant leak caused by FW failure plus Be/steam reaction

Event Sequence	Time
Total fusion power 1.65 GW, 50 W/cm ² surface heat flux	<0
Break of 4 TBM FW cooling channels, 2 in each loop	0 s
Helium coolant blowdown into VV triggers disruption	0 s
Pumps in affected loops start to trip with half time of 4 s	0 s
End of plasma energy quench with extra wall loading of 4.2 MW/m ²	1 s
All 10 FW/IBB and 4 OBB/LIM loops affected	1 s
Failure of FW/multiplier interface allowing steam ingress	1 s
Loss of heat sink (HX) in both loops	1 s
ITER FW temperature starts to ramp-up from 200 to 465°C (Table 2.7-24)	1 s
VV temperature <200°C (coolant in natural circulation mode)	All times
Purge gas system isolated from TBM	300 s

An alternative scenario to this in-situ chemical reaction of beryllium is that the pebbles would be ejected and spread into the VV, where they would settle at some bottom in-vessel components by gravity. In this case, the dispersion of the beryllium

from at most 2 layers (approximately 90 kg) would be a reasonable assumption. This extremely unlikely event will only be briefly addressed in the evaluation of radiological release in paragraph iv below.

ii) Method of analysis

The RELAP5/Mod3.2 model for the thermal-hydraulic blowdown process is identical to the one described under case 1a, hence the same analysis applies.

The 1D heat transport model to assess the decay heat driven temperature history in the TBM in the post blowdown phase is also the same as in case 1a, as long as the power production from chemical reaction is small which will be shown.

The beryllium/steam chemical reaction in the pebble bed has been assessed as follows. The temperature history of the beryllium pebbles obtained from the 1D heat transport analysis for the post blowdown phase is used to compute the time dependent H_2 production rate and exothermic heat. As an enveloping approach, an unlimited steam access to the entire pebble surface area of $8.3 \text{ m}^2/\text{kg}$ of pebbles has been assumed. The estimate is based on experimental data and correlations specified in the safety analysis data list [4]. In particular, the equations given in Table 2.7-21 were used with a safety factor $SF_S=1$ for this Cat V event.

The main parameters and assumptions used in the analysis are summarised below.

- Time sequence of events as specified in Table 2.7-3
- RELAP thermal-hydraulics as in case 1a
- TBM post accident temperature evolution as in case 1a, Figure 2.7-6
- Steam has full access to all beryllium pebbles of $\approx 450 \text{ kg}$, $8.3 \text{ m}^3/\text{kg}$
- Chemical reaction equation according to Table 2.7-1, $SF_S=1$

iii) Transient analysis results

The RELAP transient results in terms of the blowdown phase are identical to those described for the base case 1a.

The 1D model long-term temperature evolution is also identical to those described for the base case 1a. In fact, the temperature history from Figure 2.7-6 is taken as input to the chemical assessment.

The pebble bed beryllium/steam chemical reaction assessment in terms of hydrogen and heat generation yielded the following results.

Figure 2.7-7 (left frame) shows the cumulative hydrogen production from an unlimited Be/steam reaction of the entire TBM beryllium pebble bed in the course of the 10 day period. It is evident from the temperature history given in Figure 2.7-6 that the largest production rate occurs during the first few days. When the pebble bed temperature declines and eventually falls below 400°C the production rate is very small, vanishing completely after 7 days. The total accumulated hydrogen produced is 100 g.

The exercise has also been performed for the parameter variation discussed in section 2.7.1.1 for $T_{ITER,FW}=200^\circ\text{C}$ and 400°C . The resulting hydrogen production is then 13 g and 83 g, respectively (Table 2.7-4).

The chemical heat was ignored in the temperature evaluation. The peak heat generation is indeed small compared to the total decay heat produced in the TBM as demonstrated in Figure 2.7-7 (right frame). It peaks at 125 W with the reference FW temperature curve and stays below 200 W even at $T_{ITER,FE}=400^{\circ}\text{C}$ (Table 2.7-4). The margin to the decay heat is at least 1.5 orders of magnitude. Hence, neglecting the chemical heat in the temperature assessment is justified in this case.

Table 2.7-4: Case 1b - TBM pebble bed beryllium/steam reaction results for various boundary conditions

Parameter $T_{ITER,FW}$	10 day cumulative hydrogen production (g)	Peak chemical heat production (W)
Reference curve	100	125
200	13	82
400	83	190

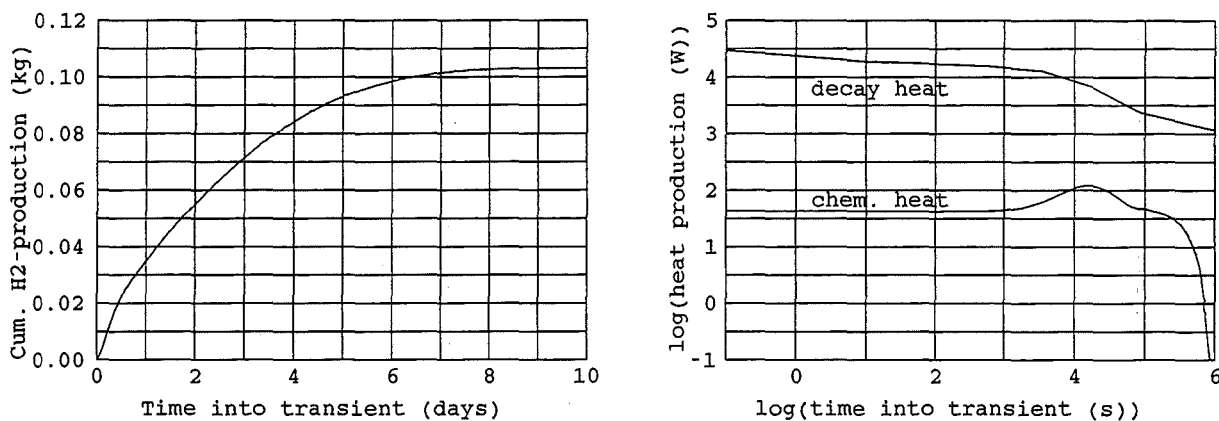


Figure 2.7-7: Case 1b - Cumulative hydrogen (left) and chemical heat (right) production in TBM from pebble bed Be/steam reaction

iv) Evaluation of radiological release

In addition to the small amount of tritium carried by the helium coolant as described in section 2.7.1.1, tritium can in principal also be released from the beryllium pebble beds and from the tritium extraction subsystem.

The pebble beds contain at the end of the basic performance phase at maximum 0.14 g of tritium (Table 2.7-15). Modelling of the tritium release upon heat-up of the pebble beds predict significant release only for large temperature rises and for long times [2.7-5]. Since the temperature in the TBM during the post accident phase hardly exceeds operating temperature levels (Figure 2.7-6) the release is expected to be only a small fraction of the inventory and, thus, is negligible in the context of this scenario. The same is true for the proportion of pebbles that might be ejected from the TBM and settles down on some in-vessel components.

The amount of tritium mobilisable in the tritium extraction subsystem upon steam ingress has not been assessed. With view to the fact that it could be transported into the VV mainly by diffusion processes through small piping until the subsystem is

isolated, also this amount cannot contribute significantly to the overall activation products release mechanism established for this type of event in [2.7-1].

v) Uncertainties in results

Uncertainties in the analysis and data base are irrelevant with view to the small contribution of the TBM to the overall consequences assessed in section VII.2.2 of [2.7-1] for this severe accident.

vi) Summary

The principal concerns formulated in the accident description for this aggravating effect of failure of the FW/multiplier interface, occurring in addition to the base case 1a, revealed to be uncritical. The pebble bed beryllium/steam reaction produces about 100 g of hydrogen and negligible quantities of heat compared to the decay heat. The tritium release into the VV, bounded by the total inventory in the TBM multiplier of 0.14 g, is also relatively small. The tritium transported from the tritium extraction subsystem into the VV before the isolation valves close has not been quantified, but is not seen as an issue.

2.7.1.3 Case 1c: Large leak inside module (Cat. IV)

i) Identification of causes and accident description

The postulated accident is a break inside the TBM, for instance, rupture of the welded helium header or, very unlikely, rupture of the main inlet/outlet manifold block. For break size the full cross section of an inlet/outlet pipe nozzle (78.5 cm²) is assumed. The failure would lead to pressurisation of the TBM box, including all pebble beds, and of the tritium extraction subsystem via the purge gas piping. The helium pressure in the affected cooling loops would stabilise at some level, depending on the size of the additional volumes. A shutdown delay time of 1000 s is arbitrarily postulated, followed by an instantaneous plasma shutdown with disruption.

The whole scenario is based on the design rule that the blanket box and the whole tritium extraction subsystem sustain the full pressure of the TBM cooling system. Meanwhile, this proposition has changed: (a) there must be a pressure relief for the blanket box, and (b) there must be a fast isolation of the tritium extraction subsystem to keep its pressure low. Pending the technical solution (the options will be briefly addressed in paragraph iii below) the scenario considered here will be that there is no pressure relief for the TBM box and the tritium extraction subsystem is isolated as soon as its pressure reaches 0.2 MPa absolute.

This leads to the following time sequence of events as the basis for RELAP analyses (Table 2.7-5): The ITER machine is operating at 10% over-power (1.65 GW). A peak surface heat flux of 50 W/cm² due to temporal and spatial peaking at the TBM is assumed prior to the PIE, which is a large leak from both loops in the manifold region of the TBM. (The case of a failure in a single loop cannot properly be handled by the present RELAP model.) The pressure in the tritium extraction subsystem rises until it is isolated from the TBM upon reaching 0.2 MPa. 1000 s after the PIE the plasma disrupts. At the same time a loss of off-site power is assumed (ITER specification), leading to pump trip in both primary and secondary loops. So in essence, this scenario means a rather abrupt pressure fluctuation in the TBM primary cooling loops, succeeded by a loss of flow after about 1000 s, without major impact on ITER in-vessel components. Nevertheless no credit is given to any in-vessel cooling for the base ITER machine according to a decision reported in [2.7-6].

The principal concerns for this accident scenario are listed below. Table 2.7-5 gives the time sequence of events.

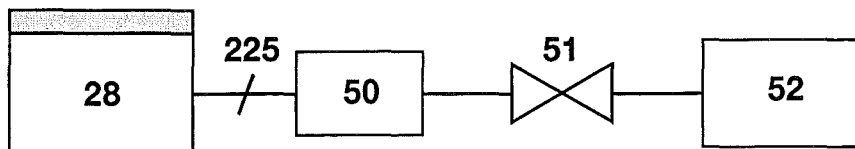
- Pressure transients after the PIE
- Equilibrium pressure in loops and TBM box in the 1000 s full power phase
- Pressure build-up in the tritium extraction subsystem
- TBM structure temperature evolution during the 1000 s full power phase
- Temperature evolution (decay heat removal) during the 1 hour period after shutdown with loss of off-site power.

Table 2.7-5: Case 1c - Time sequence of events for large leak inside TBM

Event Sequence	Time
Total fusion power 1.65 GW, 50 W/cm ² surface heat flux	<0
Large leak (78 cm ²) in manifold region of TBM from both loops	0 s
Purge gas system isolated from TBM	see results
Plasma disrupts	1000 s
End of plasma energy quench with extra wall loading of 4.2 MW/m ²	1001 s
Pumps in both loops start to trip with half time of 4 s	1001 s
Loss of heat sink (HX) in both loops	1001 s
ITER FW temperature starts to ramp-up from 200 to 465°C (Table 2.7-24)	1001 s
VV temperature <200°C (coolant in natural circulation mode)	All times

ii) Method of analysis

The RELAP5/MOD3.2 code was used to calculate the pressure, flow rates and temperatures during the transient phases and up to 2400 s into the accident. The same RELAP model as described under case 1a (Figures 2.7-1 and 2.7-2) was applied with the following modifications to account for the discharge volumes (see sketch below). Two extra volumes (No. 50 for the purge gas volume in the TBM and No. 52 to represent the tritium extraction subsystem) were connected to the TBM header (No. 28, compare Figure 2.7-2) at time zero via junction No. 225. The valve (51) was closed as the pressure in volume (52) reached 0.2 MPa.



Discharge volumes in case 1c: large leak inside TBM

The long-term temperature evolution and decay heat removal aspects have also been obtained from the RELAP analysis.

The main parameters and assumptions used in the analysis are summarised below:

- Time sequence of events as specified in Table 2.7-5.
- Power ramp-down time: ~1 s
- Leak size of the failed helium header: 78.5 cm²
- Free TBM internal volume (No. 50 in the sketch): 0.2 m³ per loop
- Free volume in the tritium extraction subsystem (No. 52) prior to isolation: 1 m³
- Buffer tank surge line: open for $t > 0$
- Heat exchanger elevation above TBM: 2.1 m

iii) Transient analysis results

RELAP results: The relevant transient variables like pressure, flow rates, and structural temperatures with view to the concerns stated in the accident description are depicted in Figure 2.7-8.

After rupture of the header in the TBM the coolant pressure in the main loops collapses for a fraction of a second, recovering as soon as the additional volume in the TBM box gets filled and the tritium extraction subsystem is isolated. Recovery to 90 % of the nominal pressure level takes only about one second, since the additional volume is small and the buffer tank automatically recharges the system (Figure 2.7-8, top diagram). As a result, heat removal from the TBM remains practically unaffected, until the disruption occurs at 1000 s, accompanied by the loss of power. Even after shutdown the system pressure is almost stable for the next one hour period (second frame from top).

The pressure build-up in the tritium extraction subsystem is very fast (3rd frame from top). In the present analysis no flow resistor has been modelled in the junction connecting the free TBM box volume and the tritium extraction subsystem. Therefore, the pressure build-up to the set point of 0.2 MPa occurred within less than 0.5 s. Even after introducing some realistic piping between both volumes the transient is very fast as an earlier study showed [2.7-2]. This requires fast pressure controlled shutters, perhaps in combination with dedicated flow resistors in the purge gas piping.

The remaining gravity driven mass flow rate in the main loops of 1.7 % from nominal after pump trip (4th frame from top) is sufficient to transfer the decay heat from the TBM to the loop system, in particular to the heat exchangers, which on the water side have enough heat capacity to take up the whole TBM decay heat for more than one hour.

The large thermal inertia of the system, in combination with the maintained high pressure, does not allow significant temperature changes during the power-on period (bottom frame). After shutdown the hot leg temperature increases slowly, getting stable around 400°C.

In conclusion, there is no critical situation in this large internal leak event. The design has to assure fast isolation of the tritium extraction subsystem. If the TBM box cannot sustain the full system pressure, pressure relief from the box must be provided (see remark below).

Remark: Three options are seen to limit the TBM box pressure in case of this large internal leak event: (a) discharge the helium via a rupture disc directly to the VV, (b) discharge the helium via properly sized piping and a rupture disc or relief valve directly to the vault, (c) discharge the helium via properly sized piping and relief device to extra discharge tanks (requiring, for instance, 5 m³ per loop at an end pressure of 1 MPa). Solutions (b) and (c) need further analysis. The most straightforward solution is the discharge to the VV, option (a).

iv) Evaluation of radiological release

There is no release of tritium or activation products since the TBM system boundary (box, piping, components, tritium extraction subsystem) remain tight by definition.

v) Uncertainties in results

Assessment of the pressure transients is straightforward and any uncertainties cannot alter the summary results. The results concerning the decay heat removal by natural circulation during the loss of off-site power period have not been verified. Nevertheless, the decaying temperatures are uncritical. In addition, they are conservative in the sense that no credit has been taken of any insulation losses from the system components.

vi) Summary

There is no critical situation in this large internal TBM leak event with respect to the concerns stated in the accident description. The pressure fluctuations in the main cooling system are of very short duration (of a few seconds), and the nominal pressure will almost be maintained in the post accident phase. The design has to assure fast (fraction of a second) pressure controlled isolation of the tritium extraction subsystem. If the TBM box cannot sustain the full system pressure, pressure relief must be provided. A few options are proposed. The temperatures in the TBM remain stable during the 1000 s burn phase after the leak and decrease rapidly afterwards due to natural circulation heat removal and the large heat capacity in the heat exchangers. There is no release of activation products from the TBM system boundary.

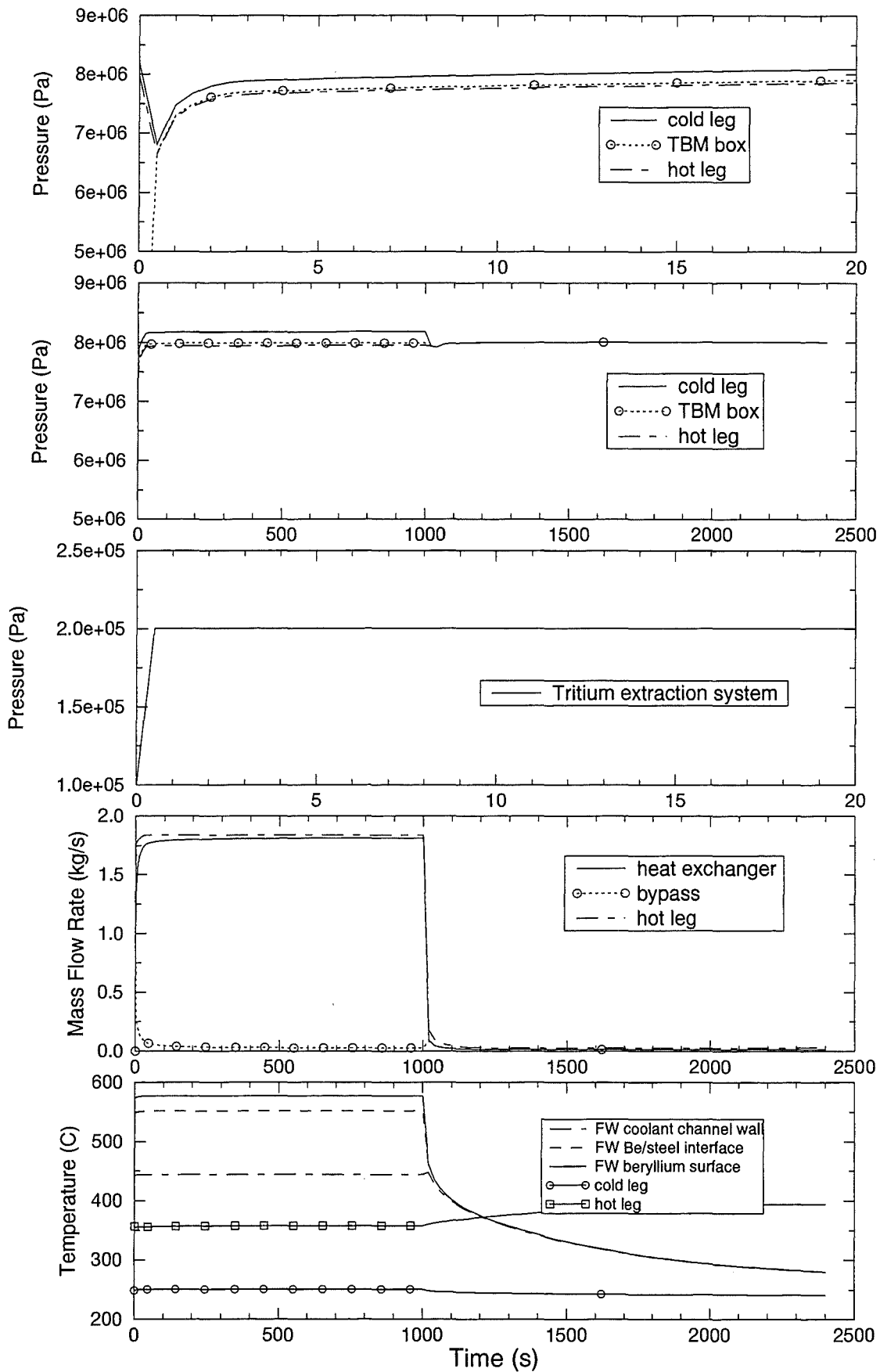


Figure 2.7- 8: Case 1c - Large leak inside module - RELAP transient analysis results

2.7.1.4 Case 1d: Small leak inside module (Cat. III)

i) Identification of causes and accident description

The accident is very much the same as described for the large leak (case 1c), except for leak size and leak location. Breach of a cooling plate or break of one of the numerous small pipe nozzles is postulated, giving way for the high pressure helium to flow into the purge gas chambers of the TBM and into the tritium extraction subsystem. Again, it is postulated that there is no pressure relief of the TBM box and that the tritium extraction subsystem is isolated as soon as its pressure reaches 0.2 MPa absolute. Consequently, pressurisation of the additional volumes will be slower compared to case 1c. It should be mentioned that the small leak scenario was not invented for HCPB, it is merely a concern with liquid metal concepts involving the potential for undetected chemical reactions. Nevertheless, the time scale for pressurisation of affected components is of interest for further development.

The following time sequence of events has been used for the RELAP analysis (Table 2.7-6): ITER is operating at 10% over-power (1.65 GW). A peak surface heat flux of 50 W/cm² due to temporal and spatial peaking at the TBM is assumed prior to the PIE, which is a small leak in one of the cooling plates, i.e., only one cooling loop be affected. The pressure in the purge gas chambers of the TBM and in the tritium extraction subsystem rises until the latter is isolated from the TBM upon reaching 0.2 MPa. 1000 s after the PIE the plasma is shutdown and triggers a disruption, which in turn causes loss of off-site power and pump trip in both primary and secondary loops.

The principal concerns for this accident scenario are listed below. Table 2.7-6 gives the time sequence of events.

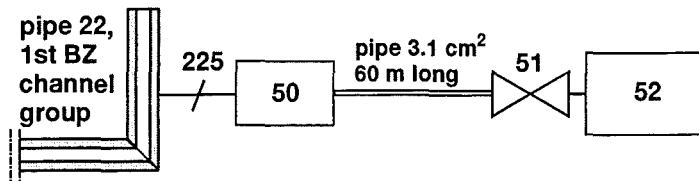
- Pressure transients after the leak inside the module
- Equilibrium pressure in loops and TBM box in the 1000 s full power phase
- Pressure build-up in the tritium extraction subsystem

Table 2.7-6: Case 1d - Time sequence of events for small leak inside TBM

Event Sequence	Time
Total fusion power 1.65 GW, 50 W/cm ² surface heat flux	<0
Small leak (0.25 cm ²), e.g., in a cooling plate of TBM from one loop	0 s
Purge gas system isolated from TBM	see results
Plasma shutdown triggers disruption	1000 s
End of plasma energy quench with extra wall loading of 4.2 MW/m ²	1001 s
Pumps in both loops start to trip with half time of 4 s	1001 s
Loss of heat sink (HX) in both loops	1001 s
ITER FW temperature starts to ramp-up from 200 to 465°C (Table 2.7-24)	1001 s
VV temperature <200°C (in natural circulation mode)	All times

ii) Method of analysis

The RELAP5/MOD3.2 code was used to calculate the pressure, flow rates and temperatures during the transient phases and up to 2400 s into the accident. The same RELAP model as described under case 1a (Figures 2.7-1 and 2.7-2) was applied with the following modifications to account for break location and discharge volumes (see sketch below). The purge gas volume in the TBM (50) was connected to the first breeding zone channel group (pipe 22, 5th node) via the junction (225) representing the 0.25 cm² breach. A long pipe was placed between volumes (50) and (52), the latter representing the tritium extraction subsystem.



Discharge volumes in case 1d: Small leak inside TBM

The long-term temperature evolution and decay heat removal aspects have also been obtained from the RELAP analysis.

The main parameters and assumptions used in the analysis are summarised below:

- Time sequence of events as specified in Table 2.7-6.
- Power ramp-down time: ~1 s
- leak size of the cooling plate: 0.25 cm²
- Free TBM internal purge gas volume (No. 50 in the sketch): 0.4 m³
- Free purge gas volume (No. 52) in tritium extraction subsystem before isolation: 1 m³
- Buffer tank surge line: open for $t > 0$
- Heat exchanger elevation above TBM: 2.1 m

iii) Transient analysis results

RELAP results: Selected pressure, flow rate, and velocity transients are displayed in Figure 2.7-9. Of most interest is the first phase after the PIE, when the pressure builds up in the TBM box. This lasts for 13 s (top frame). Velocity of sound is reached in the breach during this phase, yielding a flow rate of 0.135 kg/s (bottom frames). The pressure in the tritium extraction subsystem increases at a rate of ≈ 0.13 MPa/s (not shown), i.e., isolation valves close after ≈ 0.8 s at 0.2 MPa absolute. The pressure in the main loop does not see significant fluctuations, neither in the initial phase, nor after plasma shutdown at 1000 s (2nd frame from top). Thus, the heat removal is not disturbed and the same temperature evolution applies as described with case 1c. Temperatures and decay heat removal are uncritical.

iv) Evaluation of radiological release

There is no release of tritium or activation products since the TBM system boundary (box, piping, components, tritium extraction subsystem) remain tight by definition.

v) Uncertainties in results

There is no concern with uncertainties. See the arguments in section 2.7.1.3.

vi) Summary

There is no critical situation in the small internal TBM leak event with respect to the concerns stated in the accident description. The pressure fluctuations in the main cooling system caused by this small leak of 0.25 cm^2 size are hardly to detect and are not suited as a trip signal. The pressure build-up in the box is linear in time and lasts for 13 seconds. The design has to assure fast (order of a second) pressure controlled isolation of the tritium extraction subsystem, which can serve as a trip signal. The aspects of TBM box pressure and temperature evolution are covered by the large leak scenario, case 2c.

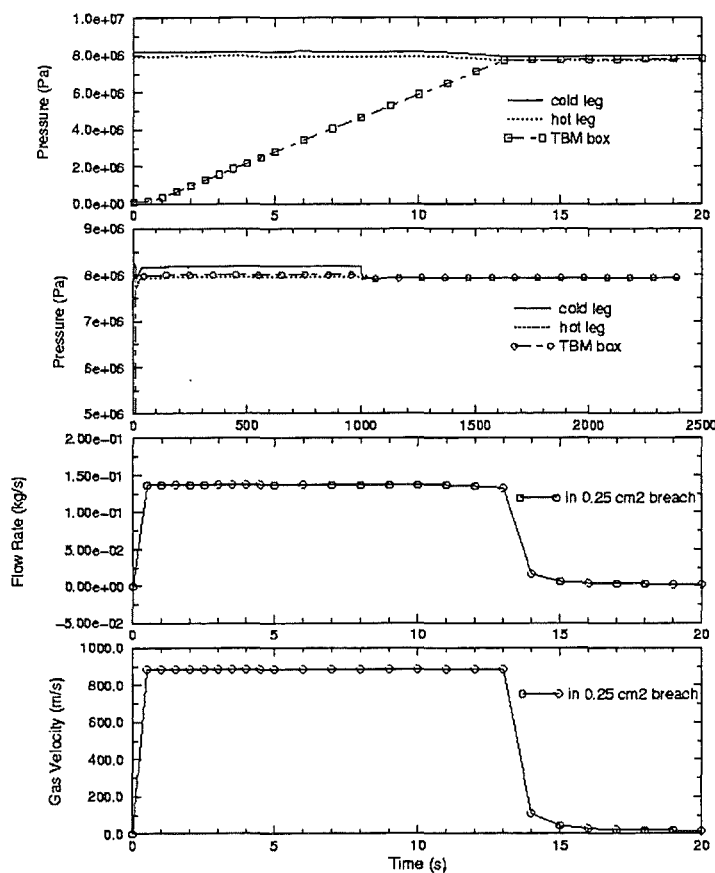


Figure 2.7- 9: Case 1d - Small leak inside module - RELAP transient analysis results

2.7.2 Large ex-vessel TBM coolant leaks

2.7.2.1 Case 2a: Main pipe break in the vault (Cat. IV)

i) Identification of causes and accident description

The postulated accident is a guillotine break of the main coolant pipe with blowdown of the high pressure helium from one out of two cooling loops into the vault. For break size and location a double-ended rupture of the 0.1 m diameter cold leg pipe at circulator inlet is assumed. This type of failure is very unlikely to occur but is a frequently adopted enveloping assumption in accident analysis. The accident is intended to be detected by the plant safety system, for instance, by a signal "pressure high" in the vault. If this turns out to be too slow, a signal "pressure low" in the TBM cooling system could be used to trigger a plasma shutdown. In any case, there will be some delay in the power shutdown and the present analysis is to show the severeness of the transients and the margin to shutdown the plant without any aggravating damage. (The latter will be discussed later.)

The following time sequence of events is assumed in the analysis (Table 2.7-7). ITER is operating at 10% over-power (1.65 GW). A peak surface heat flux of 50 W/cm² due to temporal and local peaking at the TBM is assumed before the plasma is shutdown. At time zero, the double-ended pipe break occurs in one cooling loop and the circulator in the affected loop begins to trip with a half time of 4 s. After a delay of 10 seconds a fast plasma shutdown will be triggered, entailing a disruption with the plasma energy quench lasting for 1 s. In a conservative way it is postulated that a loss of off-site power coincides with the fast shutdown, which is interpreted as loss of pump power to the intact loop and as a loss of secondary coolant flow in the heat exchangers. The loss of off-site power also means that the VV cooling system is in the natural circulation mode, maintaining the VV inner surface temperature below 200°C. The loss of coolant in the shield blanket causes the ITER FW to heat up to a level of at most 465°C after one day, falling off afterwards according to the curve specified in [2.7-1] and reproduced in Table 2.7-24.

The safety relevant concerns in this accident scenario are:

- Vault pressure evolution, signal generation
- Temperature bursts (design limits) at the TBM first wall
- Design temperature limits
- Tritium and activation products release from coolant
- Decay heat removal during the loss of off-site power phase.

Table 2.7- 7: Case 2a - Time sequence of events for large ex-vessel TBM coolant leak

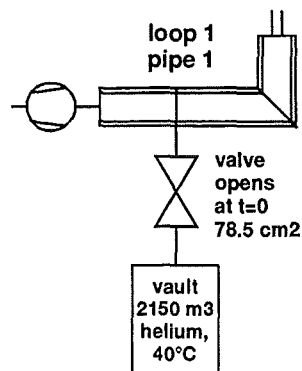
Event Sequence	Time
Total fusion power 1.65 GW, 50 W/cm ² surface heat flux	<0
Double-ended main pipe break in one cooling loop	0 s
Pump in affected loop starts to trip with half time of 4 s	0 s
Plasma burn is terminated by signal "pressure low", disruption	10 s (a)
End of plasma energy quench with extra wall loading of 4.2 MW/m ²	11 s
Pump in intact loop starts to trip with half time of 4 s	11 s
Loss of heat sink (secondary coolant flow) in both loops	11 s
ITER FW temperature starts to ramp-up from 200 to 465°C (Table 2.7-24)	11 s
VV temperature <200°C (in natural circulation mode)	All times

(a) alternatively 4 s are assumed, shifting all following times by 6 s ahead.

ii) Method of analysis

Flow rates and pressure transients during the blowdown phase have been analysed with the RELAP code. Since the RELAP model used cannot properly calculate the temperature distribution in the TBM if only one loop is affected, an additional 3D temperature analysis of the TBM front part has been performed by use of the FIDAP code [2.7-7]. The temperature bursts caused by the disruption and the decay heat removal aspects were assessed by applying 1D heat transport models.

RELAP/MOD3.2 analysis: The same model as described in section 2.7.1.1 was used, in particular the nodalization of the cooling circuits (Figure 2.7-1) and the detailed RELAP nodalization of the TBM proper (Figure 2.7-2). Modelling of the leak size and location is shown in the schematic below. Please note that this does not really represent a double-ended pipe break. However, it comes close to it, since the discharge from the loop would occur mainly through one open end (the one coming from the heat exchanger) while the flow in the other branch coming from the TBM is impeded by the strong flow resistance in the TBM.



RELAP model addition for break size and discharge volumes in case 2a

FIDAP analysis: The 3D finite element model for the FIDAP temperature analysis of the TBM front part is shown in Figure 2.7-10. It is a poloidal-radial cut through the TBM and represents the blanket box with 7 cooling channels and part of the neighbouring breeding zone (essentially breeding zone No. 1 out of 6). Cooling channels denoted as I pertain to cooling loop 1 and cooling channels denoted as II are served by cooling loop 2 which is assumed to be the failed loop. Flow direction is alternating between channels according to the flow pattern of TBM-I. Thus, the chosen section is the smallest unit cell with repetitive flow pattern from one cell to the next. In toroidal direction the whole U-shaped first wall box was modelled with the proper radial power distribution using 10 meshes in each side wall including the bends, and 10 meshes in the plasma facing front part. The mass flow rates and heat transfer coefficient during the pump trip were taken from RELAP analysis as input to FIDAP. The decay heat power was neglected.

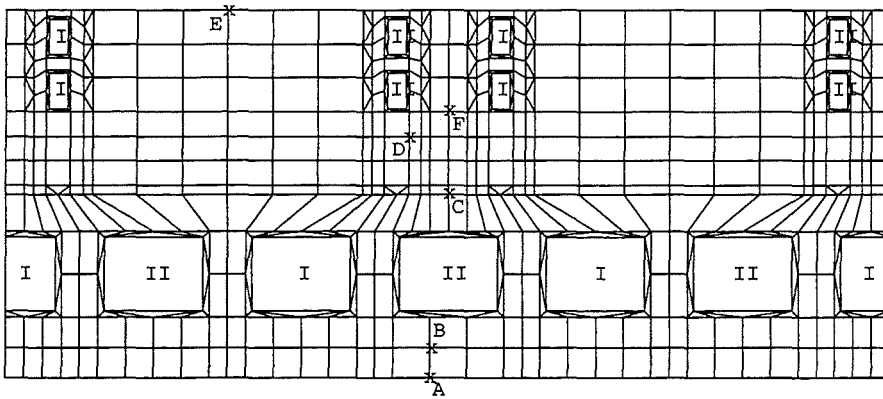


Figure 2.7- 10: FIDAP nodalization of the TBM-I front part.

(Shown are the nodes (A) beryllium protection layer surface, (B) Be/structure interface, (C) structure/breeder interface, (D) cooling plate, (E) poloidal centre of the beryllium pebble bed, (F) poloidal centre of the breeder pebble bed)

1D heat transport analysis: The model to assess the decay heat transport is described in section 2.7.1.1 with details given in section 2.7.3.4. The initial radial temperature distribution has been adapted to the peak temperature results obtained from the FIDAP analysis with 10 s shutdown delay from Figure 2.7-12 (compare section 2.7.3.4, paragraph iii).

An extra localised 1D sub-model has been used to calculate the temperature bursts in the FW caused by the disruption. This sub-model and its results, which were utilised in the definition of the initial temperature in the 1D long-term heat transport analysis, are described in section 2.7.3.4, paragraph iv.

The main parameters, and assumptions used in the analysis are summarise below:

- Time sequence of events as specified in Table 2.7-7
- Fusion power shutdown delay time: 10 s (alternatively 4 s)
- Power ramp-down time: 1 s
- Free volume in vault: 2150 m³

- Buffer tank surge line: open for $t > 0$
- Initial node temperatures for 1D model see Table 2.7-23, this case 2a

iii) Transient analysis results

RELAP results: Transients of the blowdown phase are illustrated in Figure 2.7-11. The discharge of the helium coolant from one loop lasts for about 5 s.

The diagram at the top of Figure 2.7-11 shows the loop pressure decay in the cold leg close to the break and in the hot leg upstream and downstream of the dust filter. The pressure decreases from the initial 8 MPa to the level of the vault pressure within about 5 s. Accordingly, the vault pressure builds up from atmospheric (0.1 MPa) to 0.1045 MPa (second frame from top). This is a pressure increase by 4.5 % and hence, is not suitable to trigger a plasma shutdown. Surveillance of the loop pressure itself will be much more efficient for this purpose.

The third frame indicates the mass flow rate in a somewhat chopped way (the frequency of the output printing was chosen too low). The mass flow rate in the dust filter can almost double relative to the stationary value of 1.85 kg/s for a short time, but the flow direction remains normal, avoiding the risk of flushing accumulated dust by back streaming.

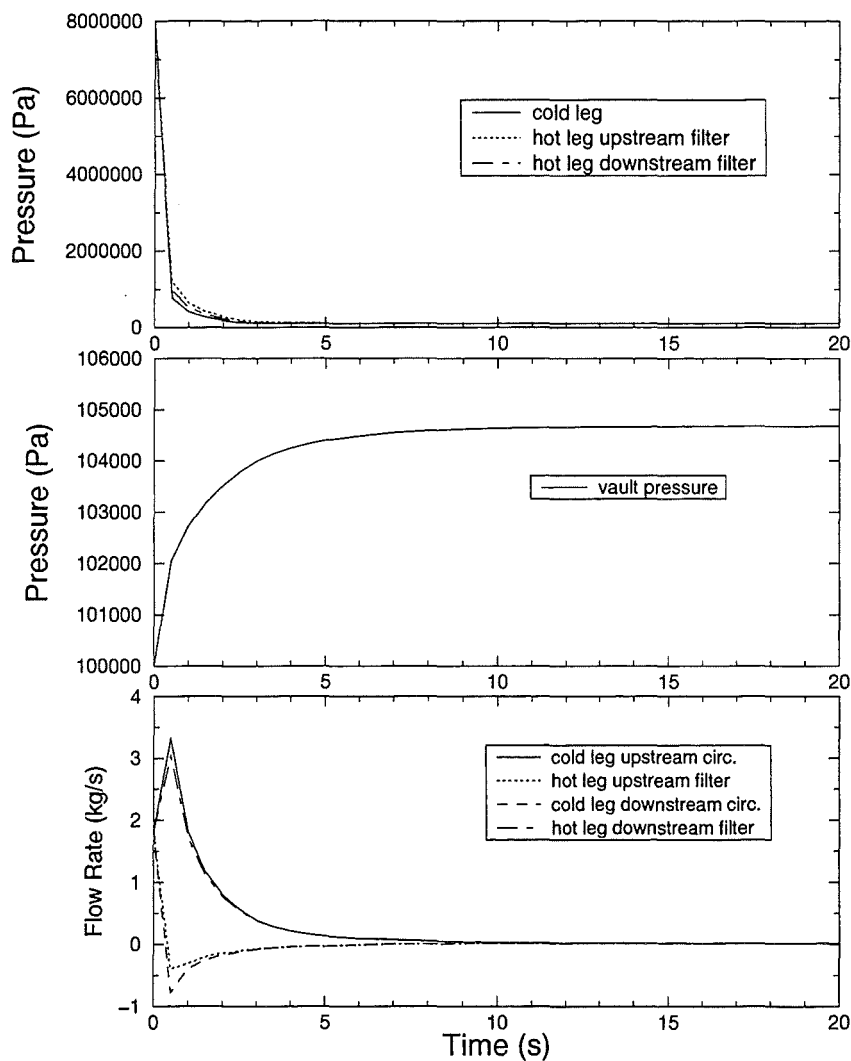


Figure 2.7- 11: Case 2a – pressure and flow rate transients in a cold leg pipe

break, RELAP results

FIDAP results: The temperature evolution at selected points of the TBM front part is plotted in Figure 2.7-12 for the 10 s shutdown delay. Location of points A to F are indicated in Figure 2.7-10. The initial heat-up rate in the FW before the disruption occurs is about 6 K/s. The disruption causes a sharp temperature burst at the FW surface (point A) of an additional 210 K which is strongly dampened with the distance from the FW. Thus the beryllium/steel interface (point B) experiences only a ΔT of 100 K and the back of the FW (point C) sees hardly any temperature increase. The maximum temperatures reached in the 60 s time period analysed are listed in Table 2.7-8 along with the initial steady state values attained at 10% over-power. Also shown are the maximum temperatures that would be reached if the shutdown occurred sooner, i.e., after 4 s, which is more realistic.

Table 2.7- 8: Case 2a - Peak temperatures reached in the TBM front part after loss of coolant in one loop (starting from 10% over-power with disruption)

Point and location (see Figure 2.7-10)	Initial steady state temp. (°C)	Maximum temperature (°C) with shutdown delay time of	
		10 s	4 s
(A) Be protective layer surface	525	790	750
(B) Be/structure interface	505	650	620
(C) structure/breeder interface	345	380	360
(D) cooling plate	385	410	390
(E) beryllium pebble bed	470	470	470
(F) breeder pebble bed	620	620	620

1D heat transport model results: The long-term temperature evolution in the TBM is practically identical to the one discussed with case 2c in section 2.7.2.3. Please refer to Figure 2.7-16 for details. The FW temperature has a second peak after 4 hours at 485°C. After 3 days temperatures in all radial nodes fall below 400°C. In the long run (10 days) temperatures in the shield region are influenced by the boundary conditions assumed (here $T_{VV}=200^\circ\text{C}$). Even with an adiabatic boundary at the back the shield would stay below 450°C (not shown).

iv) Evaluation of radiological release

The radiological release into the vault is the amount of tritium and activation products carried by the helium coolant. The maximum tritium content in the coolant is of the order 1 mg (Table 2.7-15). The mobile activation products in the cooling loops (especially in the dust filters) is unknown, but can be kept small by routinely replacing the filters if needed. The purge gas system remains tight and causes no release.

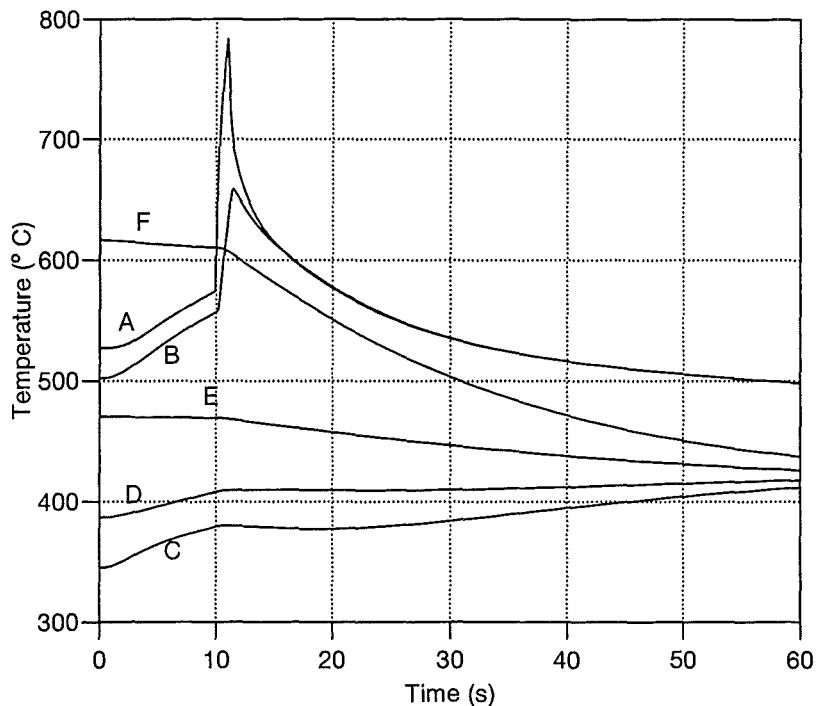


Figure 2.7- 12: Case 2a - Main pipe failure in the vault, short-term temperature evolution in the front part of the TBM, FIDAP results

(10 s shutdown delay followed by disruption, refer to Figure 2.7-10 for location of points A to F)

v) Uncertainties in results

The vault pressure build-up is small and, hence, it is not a suitable parameter for shutdown signal generation when considering uncertainties. The FIDAP temperature assessment is elaborated so that most of the uncertainties are due to the uncertainties in the shutdown delay, which could be much shorter than the 10 s assumed. An achievable delay time is approximately 4 s. Uncertainties related to tritium release and decay heat removal are not an issue.

vi) Summary

The concerns formulated in the accident description for this ex-vessel pipe break event are assessed as follows: The peak vault pressure increase is inherently low (4500 Pa) and is not suited to generate a shutdown signal. A better solution would be a signal "pressure low" in the cooling system, e.g., at a set point of 6.4 MPa. The temperature bursts caused by the disruption load are substantial leading to peak surface temperatures close to 800°C but of very short duration (few seconds). The FW structure heats up to 650°C. The integrity of the box with one cooling loop at full pressure needs to be verified. Minimising the shutdown delay to about 4 s can alleviate the problem but not very efficiently. If the FW should yet fail, the event becomes equal to case 2b discussed in section 2.7.2.2. Activation products release into the vault is small and decay heat removal is assured by passive means.

2.7.2.2 Case 2b: Main pipe break in vault plus failure of FW (Cat. IV)

i) Identification of causes and accident description

The postulated event is a guillotine break of the main coolant pipe with blowdown of the high pressure helium from one loop into the vault (so far, same as case 2a). The subsequent disruption will cause failure of the TBM FW cooling channels with blowdown of the helium from the second loop into the VV. For break size a double-ended rupture of 4 FW cooling channels pertaining to both cooling loops is assumed with the coolant/multiplier interface remaining intact. In combination with the ex-vessel pipe break, connection between the vault and the VV is created. Hence, the VV becomes flooded with air, constituting a loss of vacuum accident (LOVA) similar to the event sequence described in section VII.4.6 of [2.7-1]. Again, loss of off-site power is assumed to coincide with the initiating event. The ITER in-vessel components remain tight, but no credit is given to ITER in-vessel cooling according to an ITER project decision [2.7-6]. The scenario will be treated here as far as the TBM system is concerned. Accidental effluents release from the VV and the vault are not part of the scope of this analysis, since it is assumed that these aspects are well covered by the shielding blanket analysis.

The following time sequence of events is assumed in this accident scenario (Table 2.7-9). ITER is operating at 10% over-power. A peak surface heat flux of 50 W/cm^2 due to temporal and local peaking at the TBM is assumed before the plasma disrupts. At time zero the double-ended pipe break occurs in loop 1 and the circulator begins to trip. After a delay time of 10 s plasma burn is terminated causing disruption. This in turn, leads to an instantaneous rupture of the TBM FW and to a loss of off-site power (circulator trip in loop 2 and loss of secondary coolant flow). At the same time the VV starts to be flooded with helium from loop 2, and subsequently with air coming from the vault. The VV cooling system transits to the natural circulation mode keeping the VV inner wall temperature below 200°C . The ITER FW is assumed to experience the reference temperature evolution as predicted in section VII.4.6 of [2.7-1] for the "loss of vacuum through one VV penetration" scenario and as specified in Table 2.7-24.

Table 2.7- 9: Case 2b - Time sequence of events for large ex-vessel TBM coolant leak with subsequent failure of TBM FW

Event Sequence	Time
Total fusion power 1.65 GW, 50 W/cm ² surface heat flux	<0
Double-ended main pipe break in cooling loop 1	0 s
Circulator in affected loop starts to trip with half time of 4 s	0 s
Plasma burn is terminated by signal "pressure low", disruption	10 s
End of plasma energy quench with extra wall loading of 4.2 MW/m ²	11 s
Rupture of TBM FW, break of 4 TBM cooling channels, 2 per loop	11 s
Loss of heat sink (secondary coolant flow) in both loops	11 s
ITER FW temperature starts to ramp-up from 200 to 465°C (Table 2.7-24)	11 s
Air ingress from vault into VV, sub-atmospheric pressure balance	See results
VV temperature <200°C (in natural circulation mode)	All times

The safety relevant concerns (excluding aspects of effluents release as mentioned earlier) in this accident scenario are:

- Vault pressure evolution, signal generation by vault pressure
- VV pressure balance after LOVA
- Decay heat driven temperature evolution in the TBM
- Beryllium/air reaction of the TBM protective layer
- Tritium and activation products release from the coolant.

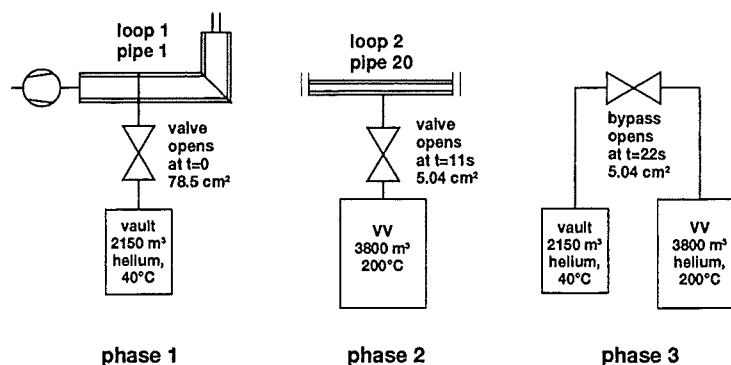
ii) Method of analysis

Pressure transients during the blowdown phase have been analysed with the RELAP code. The decay heat driven temperature evolution in the TBM was assessed applying the 1D heat transport model, and the beryllium/air reaction of the protective layer has been estimated, using the temperature history from the 1D results. The modelling assumptions and parameters are described below.

RELAP/MOD3.2 analysis: The same basic model as described in section 2.7.1.1 was used, in particular the nodalization of the cooling circuits (Figure 2.7-1) and the detailed nodalization of the TBM proper (Figure 2.7-2). The problem with the current model is that interaction of two separate loops cannot be treated properly. Therefore, the pressure transient is regarded in three independent phases, namely

- phase 1: loop 1 breaks and discharges into the vault (0 - 11 s)
- phase 2: TBM FW fails and loop 2 discharges into the VV (11 - 22 s)
- phase 3: the vault/VV bypass opens and the pressure equalises in both volumes (>22 s)

This division is acceptable, since the process of the third phase runs on a much longer time scale than phases 1 and 2. The case specific RELAP model amendment is visualised in the following schematic, where dummy valves, denoted as valves or bypass, simulate the opening of the specified cross sections at specified times.



RELAP model addition for break size and discharge volumes

(see Figure 2.7-2 for full loop model.)

1D heat transport model: The temperature evolution in the TBM was calculated with the model and radial build as described in section 2.7.1.1. To account for the increased temperature profile caused by the 10 s delay the reference steady state

profile from Figure 2.7-22 has been modified according to the FIDAP results obtained for case 2a. Also added is the temperature burst in the FW nodes caused by the disruption as described in section 2.7.3.4, paragraph iv. The revised initial temperature profile is listed in Table 2.7-23. Furthermore, the reference FW temperature evolution of the ITER shielding blanket as specified in section 2.7.3.4, paragraph v, was used as boundary condition.

Be/air reaction of the protective layer: The equation for the reaction rate specified in SADL-2 [2.7-4] and reproduced in Table 2.7-20 are used for bounding estimates.

The main parameters and assumptions used in the analysis are listed below:

- Time sequence of events as specified in Table 2.7-9
- Vault and VV initial conditions according to the sketch shown above
- Fusion power shutdown delay time: 10 s
- Leak size in cold leg of loop 1: 78.5 cm²
- Leak size in FW cooling channels: 5.04 cm²
- Leak size in bypass vault/VV: 5.04 cm²
- Safety factor for use in Be/air reaction assessment: 5

iii) Transient analysis results

RELAP results: The pressure transients developing at first in the vault and then in the VV are shown in Figure 2.7-13. The vault pressure rises within 5 s to the maximum value of 104 kPa, i.e., 4 % above nominal, and hence, does not reach the envisaged set point of 105 kPa to shutdown the plasma (as was already mentioned with case 2a).

The pressure in the VV increases fast from zero to 1.7 kPa upon TBM FW failure at $t=11$ s by discharging the helium from the cooling loop 2. When the vault/VV bypass opens at $t=22$ s (instead of 11 s as explained above) venting occurs at a rate of about 15 Pa/s, levelling off to the equilibrium pressure of ~50 kPa. This value has been estimated neglecting heat exchange at the walls and assuming that there would be no vacuum breaker in the vault boundary.

In summary, peak pressure in the vault stays below the set point. The pressure balance with the VV becomes sub-atmospheric (~50 kPa) and even with a certain gas heat-up at in-vessel components the pressure cannot reach the set point of the VV over-pressure protection.

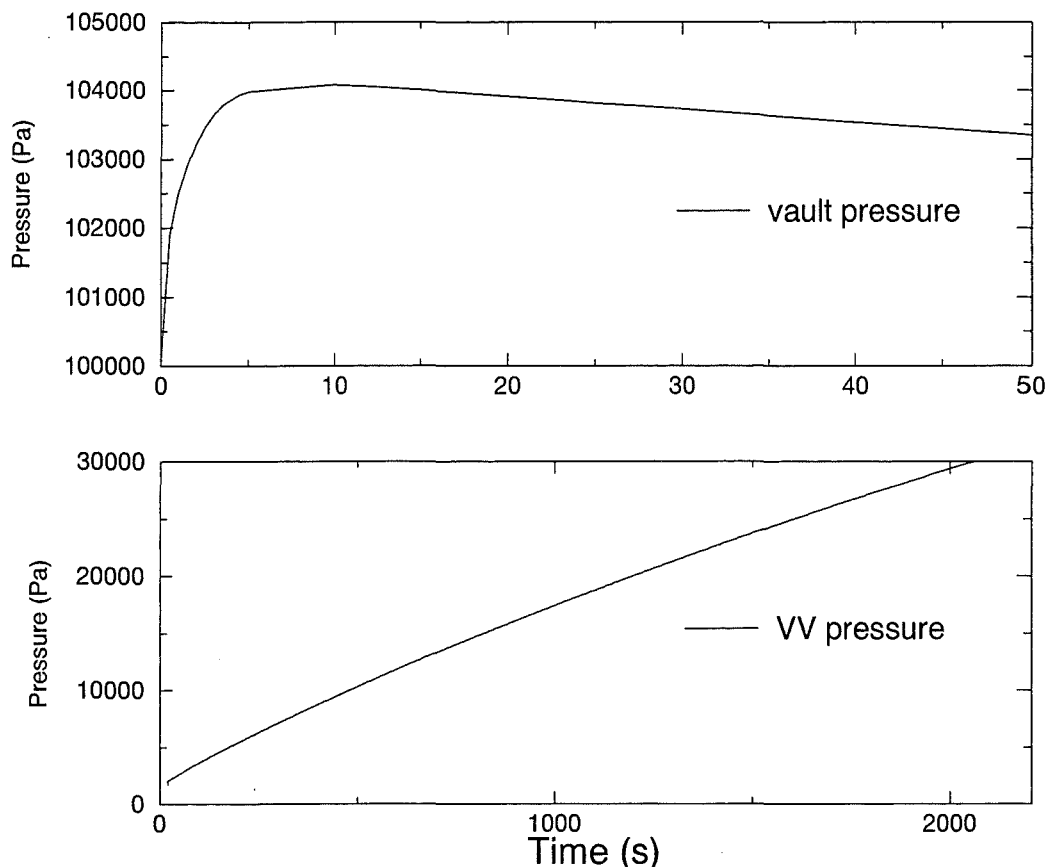


Figure 2.7- 13: Case 2b - RELAP results of vault and vacuum vessel pressure

1D heat transport results: The temperature evolution in the TBM during a 10 days post accident period is plotted in Figure 2.7-14 (where the rapidly relaxing initial values are not visible). The FW temperature peaks at about 4 hours after PIE, reaching 480°C and cooling down thereafter. For comparison, the input ITER FW temperature history is shown as dashed line, which has its peak one day after the PIE. Its strong influence on the TBM temperature evolution is evident. The mixed mean temperature in the breeding zone nodes, and thus in the beryllium pebble beds, represented by the dotted lines stays essentially below the normal operating peak temperature of about 490°C (compare Figure 2.7-22).

Remark: The temperature evolution is very much alike the one reported for case 1a in Figure 2.7-6 despite the higher initial temperature profile specified in Table 2.7-23. Differences to case 1a larger than 5K are only visible within the first hour (not shown).

Beryllium/air reaction of the protective layer: Since the peak FW temperature stays below 500°C, the chemical reaction is not critical. For instance, at 500°C the chemical heat produced from Be/air reaction at the surface is by more than three orders of magnitude smaller than the heat radiated from that same surface (at $\Delta T > 20$ K relative to the surrounding) and, therefore, it is negligible.

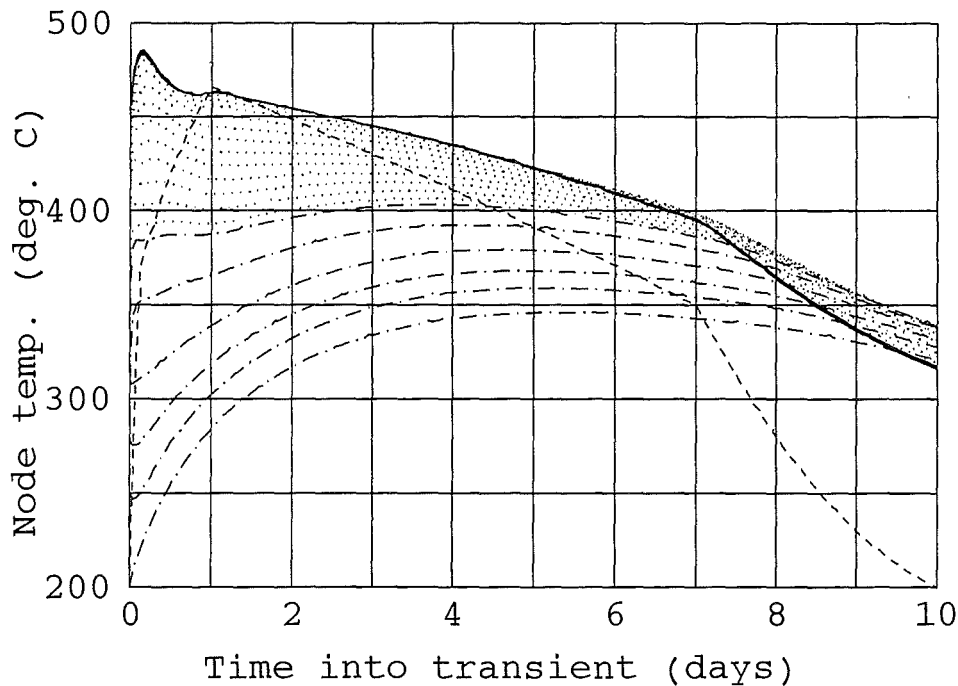


Figure 2.7- 14: Case 2b - Temperature evolution in the TBM, 1D heat transport model

(solid: FW nodes, dotted: breeding zone nodes, dash-dotted: manifold and shield nodes, dashed line: ITER FW temperature as input)

iv) Evaluation of radiological release

The only radiological release from the TBM system boundary is the amount of tritium and activation products carried by the helium coolant, which is split, one half (coming from loop 1) going into the vault, and the other half entering the VV. The total amount is inherently small (<1 mg of tritium) and negligible compared to the quantities of tritium and dust present in the VV. There is no threat for release to outside the VV/vault boundary.

v) Uncertainties in results

Uncertainties in the analysis are uncritical, since the effects are inherently small. Details in results are dominated by the event sequence and boundary conditions postulated.

vi) Summary

The concerns addressed in this unlikely event of a double-ended pipe break accompanied by a large failure of the FW do not pose extra safety issues on the ITER basic machine. The peak vault pressure increase is inherently low (~4000 Pa). The VV and vault pressure will balance at about 50 kPa after more than one hour, if no vacuum breaker is assumed. The decay heat can be removed by conduction and radiation at moderate temperatures. The FW temperature peaks after 4 hours at 480°C. The temperature in the breeding zone stays essentially below 480°C. The heat produced by the beryllium/air reaction at the protective layer is negligible. The radiological release to the vault and VV is no issue.

2.7.2.3 Case 2c: Main pipe break in the vault plus large leak inside module (Cat IV)

j) Identification of causes and accident description

The postulated accident is a guillotine break of the main cooling pipe with blowdown of the high pressure helium from a single loop into the vault. The subsequent disruption will cause a break inside the TBM, for instance, rupture of the welded helium header or of the inlet/outlet block, in a way that both loops become interconnected. As a result, also the second loop releases the coolant to the vault, and air can enter the beryllium and ceramic pebble beds via the loop which failed in the first place. As in the preceding cases, loss of off-site power is assumed to coincide with the disruption. The ITER in-vessel components remain intact, but no credit is given to in-vessel cooling.

The following time sequence of events is assumed in this accident scenario (compare Table 2.7-10). ITER is operating at 10% over-power (1.65 GW). A peak surface heat flux of 50 W/cm² due to temporal and local peaking at the TBM is assumed before the plasma disrupts. At time zero the double-ended pipe break occurs in loop 1 and the circulator begins to trip. After a delay time of 10 s plasma burn is terminated causing disruption. This in turn, leads to an instantaneous large leak inside the module creating at the same time a connection between both loops and a bypass between the loops and the TBM box, i.e., the purge gas system. The VV cooling system transits to the natural circulation mode, keeping the VV wall temperature below 200°C throughout the post accident period. The loss of coolant in the shield blanket causes the ITER FW to heat up to a level of at most 465°C after one day, falling off afterwards according to the curve specified in [2.7-1] and reproduced in Table 2.7-24.

Table 2.7- 10: Case 2c - Time sequence of events for large ex-vessel TBM coolant leak plus large break inside TBM

Event Sequence	Time
Total fusion power 1.65 GW (nominal), 50 W/cm ² surface heat flux	<0
Double ended main pipe break in one cooling loop	0 s
Circulator in affected loop starts to trip with half time of 4 s	0 s
Plasma burn is terminated by signal "pressure low" causing disruption	10 s
End of plasma energy quench with extra wall loading of 4.2 MW/m ²	11 s
Large leak (78 cm ²) in manifold region of TBM from loop 2	11 s
Loss of heat sink (secondary coolant flow) in both loops	11 s
ITER FW temperature starts to ramp-up from 200 to 465°C (Table 2.7-24)	11 s
Air ingress from vault into TBM pebble beds	11 s
VV temperature <120°C (in natural circulation mode)	All times

The concerns in this accident scenario are:

- vault pressure evolution, signal generation
- TBM box and tritium extraction subsystem pressurisation
- Decay heat driven temperature evolution in the TBM in connection with tritium release from beryllium
- beryllium/air reaction in pebble beds
- Tritium and activation products release from the coolant and pebble bed.

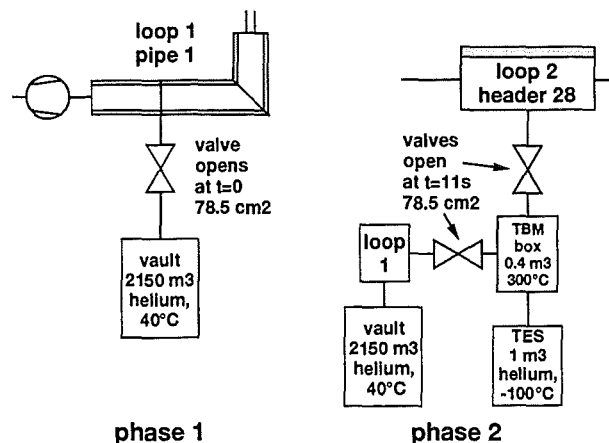
ii) Method of analysis

Pressure transients in the vault during the blowdown phase have been deduced from RELAP results obtained from case 2b. The decay heat driven temperature evolution in the TBM was assessed with the 1D heat transport model. The beryllium/air reaction in the pebble beds was estimated by use of an extra computational routine that couples the temperature distribution history from the 1D model with reaction equations specified in section 2.7.3.3 and pebble bed geometry parameters. The initial and boundary conditions are described below.

RELAP analysis: No extra RELAP calculations have been performed. Instead, estimates on the pressure transients in the vault were made based on the results from case 2b and on the failure sequence illustrated in the following schematic.

As mentioned earlier, the current model cannot properly treat the interaction of two individual loops. Therefore, the pressure transient is regarded in two independent phases, namely

- phase 1: loop 1 breaks and discharges into the vault (0 - 11 s)
- phase 2: loop 2 pressure boundary fails to discharges helium into the purge gas system and vault (>11 s).



RELAP model addition for break size and discharge volumes of case 2c.

(see Figure 2.7-1 for full loop model.)

The valves shown in the sketch are dummy valves serving to simulate the openings (breaks) of specified cross section at specified times. As already explained with case 2a the valve controlling the breaks in loop 1 is only an approximate representation of a double-ended pipe break.

1D heat transfer model: The temperature evolution in the TBM was calculated with the model and radial build as described in section 2.7.1.1 with details given in section 2.7.3.4. In order to account for the increased temperature profile caused by the 10 s delay in plasma shutdown (while one cooling loop has failed) the reference steady state profile from Figure 2.7-22 has been modified based on the FIDAP results obtained for case 2a, Figure 2.7-12. Furthermore, a temperature burst caused by the disruption load at the FW nodes has been added. The revised initial temperature profile is listed in Table 2.7-23.

The Be/air reaction of pebble beds has been assessed qualitatively by using the maximum temperatures obtained in the post accident phase in the equations for beryllium/air reaction given in Table 2.7-20, applying a safety factor of 5.

The main parameters and assumptions used in the analysis are summarised below.

- Time sequence of events as specified in Table 2.7-10
- Vault and VV initial conditions according to the sketch shown above
- Fusion power shutdown delay time: 10 s
- Power ramp-down time: 1 s
- Free volume in vault: 2150 m³
- Buffer tank surge line: open for $t > 0$ in loop 1 and for $t > 11$ s in loop 2
- Initial temperature distribution for 1D model see Table 2.7-23
- Beryllium pebbles total surface (geometrical surface): 3730 m².

iii) Transient analysis results

RELAP results: The pressure rise in the vault is illustrated in Figure 2.7-15. The first phase of discharging the helium from loop 1 is identical to the transient obtained in case 2a, i.e., the vault pressure builds up from atmospheric to 0.1045 MPa in 5 s. When the second loop is emptied at $t=11$ s, the same partial pressure is added to the vault pressure, reaching finally a total pressure of 0.109 MPa which is about 9 % above normal.

The pressure history in the TBM box and in the tritium extraction subsystem have not been evaluated. In fact, this process depends strongly from the actual formation of the internal break (where it would occur, how it would open to the TBM box and how it would establish a connection between loop 2 and loop 1). All this is physically hard to imagine and cannot be treated with the present tools. One can speculate, based on the investigations of the other cases, that there will be a short pressure pulse in the box with peak values close to the nominal system pressure (if no pressure relief is provided), lasting for a fraction of a second. The tritium extraction subsystem (TES) may see a dampened pressure pulse which can be avoided or alleviated by flow resistors and fast shutting isolation valves.

1D heat transport model results: The temperature evolution in the TBM is shown in Figure 2.7-16 for a 24 hours period after the accident. In this context only the temperature in the beryllium pebble beds (dotted lines) is of interest. It assumes a range of 390°C to 485°C in the first few hours and falls below 450°C after about 3 days as was shown already in Figure 2.7-14 for case 2b. Thus, there is only a temperature increase of a few tens of °C above the steady state temperature range

at 10% over-power (compare Figure 2.7-22). The consequences in terms of tritium release are discussed in paragraph iv.

The 1D heat transport model does not account for the chemical heat in case of Be/air reaction. Figure 2.7-17 gives a general overview of the order of magnitude on heat production as function of the inverse absolute temperature. In this model it has been assumed that air (or steam, where applicable) has unlimited access to all pebbles in the TBM which expose a surface of typically 8.3 m² per kg of pebbles or 3730 m² in total. Safety factors of 5 for Be/air and 2 for Be/steam reactions, respectively, were applied. In the present case with a peak beryllium temperature of 485°C the chemical heat in the TBM would be of the order of 600 W, which is less than 10% of the integrated decay heat (which is about 6500 W after four days of decay, when the temperature is at its peak), justifying the neglect of the chemical heat in the temperature assessment.

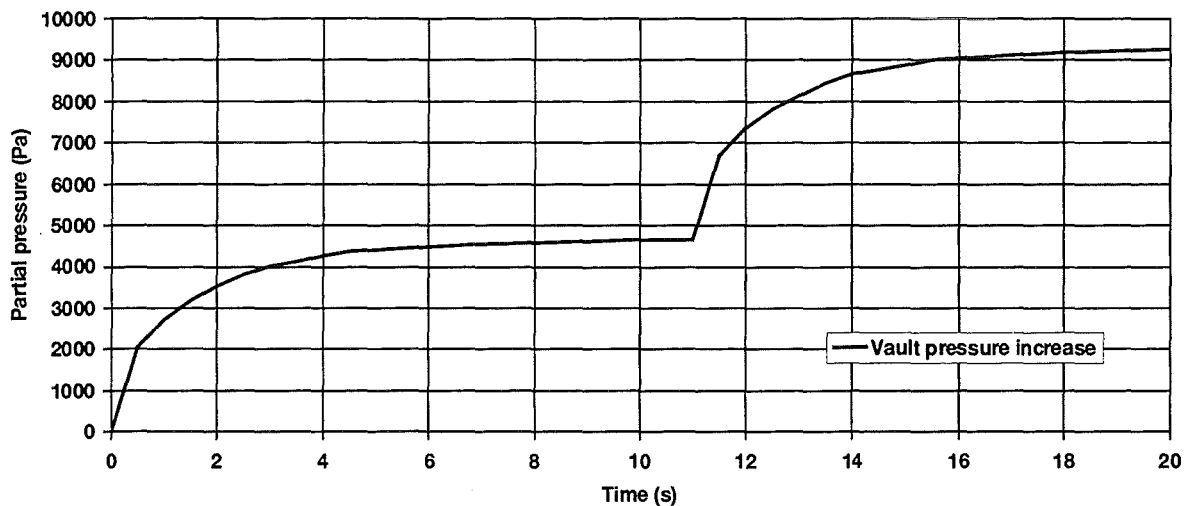


Figure 2.7- 15: Case 2c - RELAP results of pressure increase in the vault upon break of loop 1 at t=0 and break of loop 2 at t=11 s.

iv) Evaluation of radiological release

The spontaneous release of tritium into the vault is equal to the total tritium inventory from both cooling loops, i.e., of the order of 1 mg (Table 2.7-15). One has also to account for a certain release from beryllium pebbles. The estimated release rates reported in [2.7-5] upon a sudden temperature increase suggest that there is a spontaneous release and a temperature and time dependent release. The first fraction could be of the order of 60 mg when the results obtained for DEMO are scaled down by the beryllium masses to the size of the TBM. The second part would be negligible due to the small temperature rise and duration presented in paragraph iii. There is no tritium expected to come out from the tritium extraction subsystem, since the TES is assumed to be isolated by shutoff valves.

The activation products accumulated in the helium cooling loops, especially in the dust filters, have not been quantified. They are expected to be small anyway. Since the flow in the filters remains in normal flow direction as mentioned in cases 1a and 2a, the fraction being carried into the vault should not raise big problems.

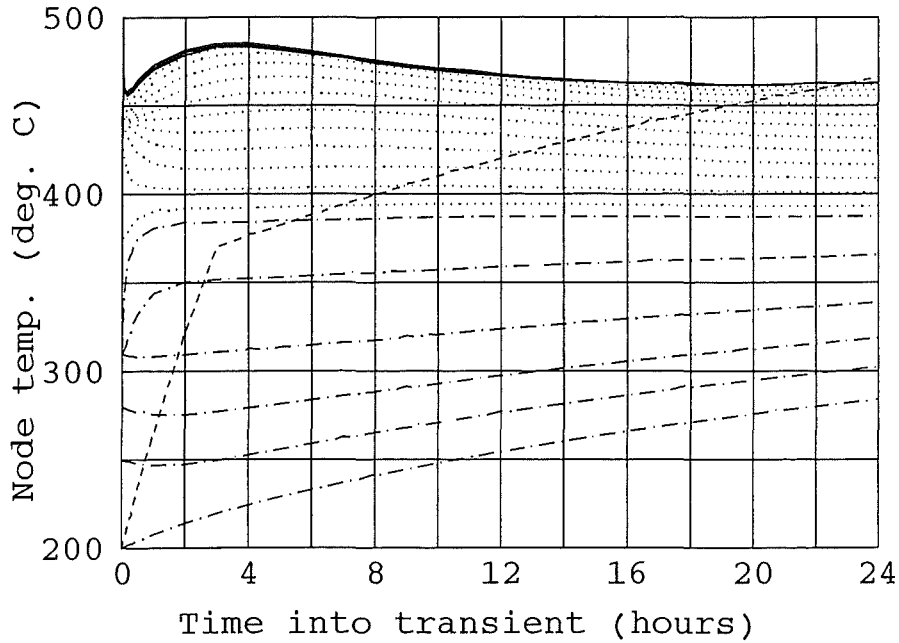


Figure 2.7- 16: Case 2c - 1D model TBM temperature evolution

(solid: FW nodes, dotted: breeding zone nodes, dash-dotted: manifold and shield nodes, dashed: ITER FW reference curve)

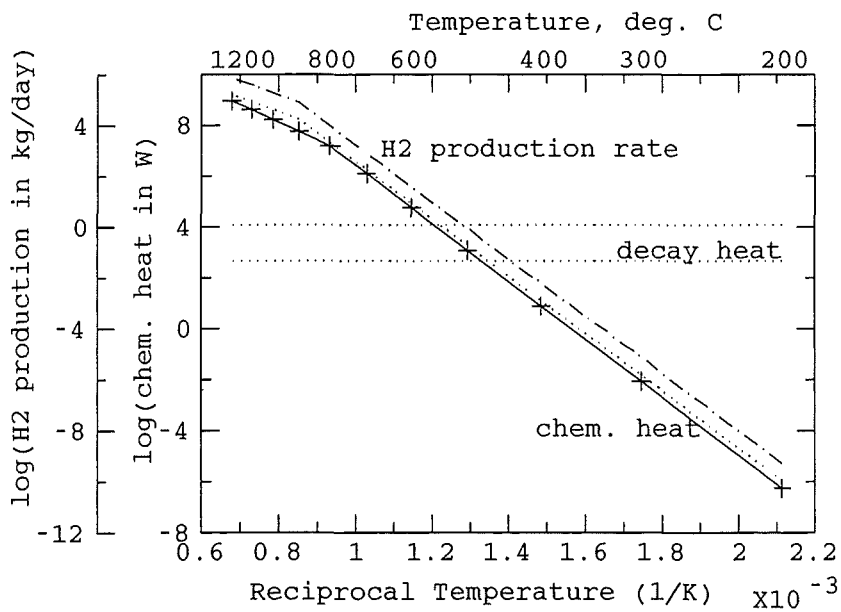


Figure 2.7- 17: Chemical reaction rates of TBM beryllium pebbles

(solid: heat for Be/air, dotted: heat for Be/steam, dash-dotted: hydrogen for Be/steam, horizontal band: TBM decay heat decreasing with decay time)

v) Uncertainties in results

Uncertainties in the vault pressure assessment are irrelevant. There remain questions with the pressure pulse originating in the TBM box and perhaps propagating to the tritium extraction subsystem. The temperature evaluation is straightforward and uncritical. Large uncertainties exist in the chemical reaction assessment, but the applied safety factors and the basic assumption of unlimited access of air to the entire pebble bed surface are extremely conservative.

vi) Summary

The concerns formulated in the accident description for this category IV event with a guillotine break in the main pipe and a large leak inside the TBM do not severely impair the ITER safety. The vault pressure after break of the first loop is too low as to serve as shutdown signal. The TBM box and the TES may see pressure pulses which have to be taken care of by design, i.e., by pressure relief for the box and by flow resistors and fast shutters for the TES. The decay heat removal is assured by radial heat transport at slightly increased beryllium temperatures relative to nominal temperature levels, keeping the beryllium/air reaction in the pebble beds low. Tritium transport into the vault is dominated by some spontaneous release expected to come from the beryllium pebble beds. A bounding estimate being ~60 mg.

2.7.2.4 Case 2d: Loss of flow plus FW failure at beryllium melting (Cat. V)

i) Identification of causes and accident description

The rationale for this case is that there is a strong cooling disturbance in the TBM which remains undetected until the plasma is passively shutdown by melting of the protective layer, i.e., at 1290°C for beryllium.

The causes for such an undiscovered initiating event could, in principle, be

- a) ex-vessel loss of coolant in one loop
- b) ex-vessel loss of coolant in both loops
- c) loss of flow in one loop
- d) loss of flow in both loops
- e) loss of heat sink (secondary flow) in both loops

The events a) and c) with a single loop failing can be ruled out, since melting will never be reached. (A FIDAP calculation has shown that the temperature stabilised below 800°C.) Event b) with simultaneous failure of two loops (without any external event that would trigger a shutdown) is unrealistic. Event d) is conceivable if the flow control valves in both loops close inadvertently either by false signals or by human error. Event e) is hard to judge at present since secondary cooling water supply is in the responsibility of the ITER team. Nevertheless, it would be covered by the event d) anyway.

Thus, the only considerable initiating event is seen in a coherent closure of the control valves in both loops. This would mean, however, that the full system pressure would be maintained. Under these circumstances it is very unlikely that the FW integrity would be preserved at temperatures close to the melting point of steel. Nevertheless, due to the lack of proven evidence that the FW would fail significantly before surface melting occurs, the melting assumption has to be applied as bounding case.

Please note that this is no longer a large ex-vessel TBM coolant leak of the second group (as it was expected to be beforehand) but an externally initiated large in-vessel TBM coolant leak, belonging to the first group of events.

The following time sequence of events is postulated (Table 2.7-11). ITER is operating at 10% over-power (1.65 GW). A peak surface heat flux of 50 W/cm² due to temporal and local peaking at the TBM is assumed before the plasma disrupts. At time zero the flow control valves in both loops inadvertently close (PIE). The plasma burn is terminated by melting of the protective beryllium layer upon reaching 1290°C at the surface. This has been calculated to occur at $t \approx 118$ s. At this time the plasma disrupts and the FW of the TBM fails, discharging helium from both cooling loops into the VV. The plasma quench is terminated after another second. At this point (119 s) all ITER shield blankets are affected, some of them flushing steam into the VV. Loss of off-site power coincides with the disruption. This means that the VV cooling system is in the natural convection mode, maintaining the VV inner surface

temperature below 200°C. The loss of coolant in the shield blanket causes the ITER FW to heat up to a level of at most 465°C after one day, falling off afterwards according to the curve specified in [2.7-1] and reproduced in Table 2.7-24.

The principal concerns for this hypothetical accident scenario are essentially the same as in case 1a, but under aggravating conditions. They are listed below.

- Vacuum vessel pressurisation
- Activation products release into the VV
- Temperature evolution in the TBM
- Decay heat removal via conduction and radiation along radial path ways only
- H₂ and heat production from FW-Be/steam reaction

Table 2.7- 11: Case 2d - Time sequence of events for loss of flow plus FW failure at beryllium melting

Event Sequence	Time
Total fusion power 1.65 GW, 50 W/cm ² surface heat flux	<0
Inadvertent valve closure in both loops	0 s
Plasma burn is terminated by melting of the protective layer	≈118 s
End of plasma energy quench with extra wall loading of 4.2 MW/m ²	119 s
Rupture of TBM FW, i.e., break of 4 TBM cooling channels, 2 per loop	119 s
Loss of heat sink (secondary coolant flow) in both loops	119 s
ITER FW temperature starts to ramp-up from 200 to 465°C (Table 2.7-24)	119 s
VV temperature <200°C (in natural circulation mode)	All times

ii) Method of analysis

RELAP analysis: No RELAP analysis has been performed for this case because the blowdown process is very similar to the one described under case 1a, from which the results are adopted.

FIDAP analysis: The temperature evolution in the front part of the TBM has been analysed with the 3D FIDAP model briefly described under case 2a, section 2.7.2.1, paragraph ii, and in Figure 2.7-10. Actually, a loss of coolant was assumed in the analysis, which however, has almost the same consequences in terms of temperatures as a sudden loss of flow. The calculation was performed up to 120 s, when melting at the FW surface was reached. It is to be noted that the material data in the high temperature regime are uncertain.

1D heat transport analysis: The model is described in section 2.7.1.1. The initial radial temperature distribution has been adapted to the extrapolated temperature results from FIDAP analysis to occur at the time of shutdown and is listed in Table 2.7-23. In this case no extra temperature burst in the FW nodes due to the disruption load has been added, because the model and the material data are inadequate at melting of the beryllium layer.

The beryllium/steam chemical reaction at the FW surface has been assessed as follows. The temperature history of the TBM obtained from the 1D heat transport analysis is used to compute the time dependent hydrogen production rate and exothermic heat. The assessment is based on the correlations specified in [2.7-4] for FW beryllium for different temperature regimes with the safety factor set to unity for this category V event.

The main parameters and assumptions used in the analysis are summarised below.

- Time sequence of events as specified in Table 2.7-11
- Discharge volume for both coolant loops: 3800 m³ (free volume of VV)
- Buffer tank surge line: open for $t > 119$ s
- Purge gas system not affected, but no credit given to its heat removal capability
- No FW/multiplier interface failure, hence no steam ingress into the pebble beds
- Initial TBM radial temperature distribution: see Table 2.7-23
- Size of TBM FW covered by beryllium protective layer: 1.07 m²

iii) Transient analysis results

RELAP results: Pressure and flow transients obtained for case 1a (Figure 2.7-4) can be used as orientation (when adding on the time scale the shutdown delay of 118 s). The closed valves postulated here will not significantly change the loop pressure and the VV pressure evolution. The loop pressure decreases from the initial 8 MPa to the level of the VV pressure within 12 s. Accordingly, the partial pressure in the VV builds up from zero to the small value of 3500 Pa. The steam pressure in the VV will dominate the further development which is beyond the scope of this work.

FIDAP results: The temperature evolution at selected points of the TBM front part is plotted in Figure 2.7-18 for 120 s after the PIE. The curves belong to the hottest spots within the 3D model, that is, (A) on the beryllium protection layer surface, (B) on the Be/structure interface, (C) on the structure/breeder interface, (D) in the cooling plate, (E) in the poloidal centre of the beryllium pebble bed, and (F) in the centre of the breeder pebble bed (compare Figure 2.7-10). The surface temperature of 1290°C will be reached at $t=118$ s. Temperatures at nodes A to F at that time and their time derivatives are listed in Table 2.7-12. One can see that the front of the FW structure (point B with 1265°C) is beyond any technical limits for ferritic steel. The beryllium pebbles are at a moderate temperature level, about 100°C above the normal peak, decreasing in radial direction.

Table 2.7- 12: Case 2d - Temperatures and their transients at selected points of the TBM at passive plasma shutdown

Point and location (see Figure 2.7-10)	Temp. at steady state (°C)	Temp. at shutdown (°C)	Temperature transient (K/s)
(A) Be protection layer	530	1290	5
(B) Be/structure interface	500	1265	5
(C) Struct./breeder interface	345	760	3
(D) Cooling plate	390	710	2.8
(E) Beryllium pebble bed	470	620	2.5
(F) Breeder pebble bed	615	840	2.3

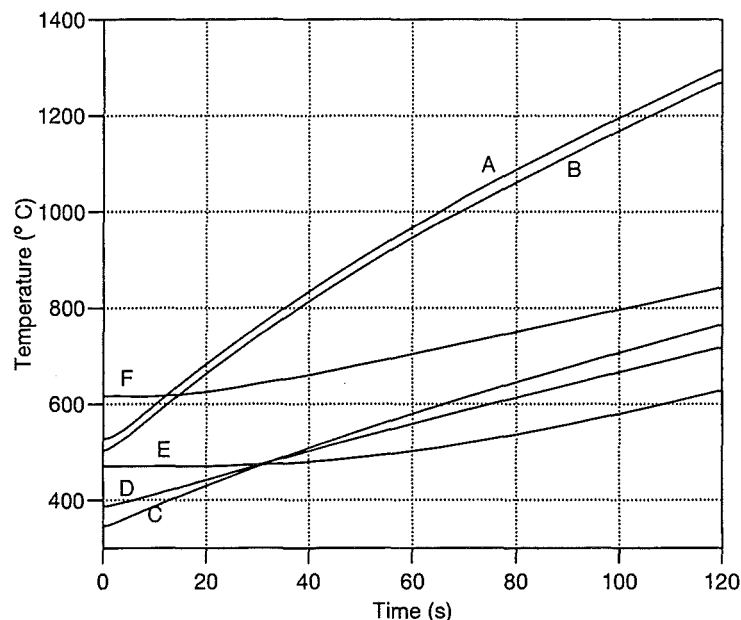


Figure 2.7- 18: Case 2d - Temperature evolution in the front part of the TBM, FIDAP results

(compare Figure 2.7-10 for location of nodes A to F)

1D heat transport results: The long-term temperature evolution in the TBM is shown in Figure 2.7-19 for a 10 days period. At the beginning it is dictated by the initial temperature distribution specified, which relaxes in a few minutes (left frame). Thereafter the ITER FW temperature used as boundary condition for radiated heat dominates the behaviour. The peak temperatures both in the beryllium pebble beds and in the protective layer fall below the 500°C level after about 15 hours.

An almost identical temperature history was obtained for the first two days after the PIE when the boundary conditions were changed at the VV side from the radiation model to adiabatic conditions. Again, the peak temperatures both in the beryllium pebble beds and in the protective layer fall below the 500°C level after about 15 hours and remained there for all times (not shown).

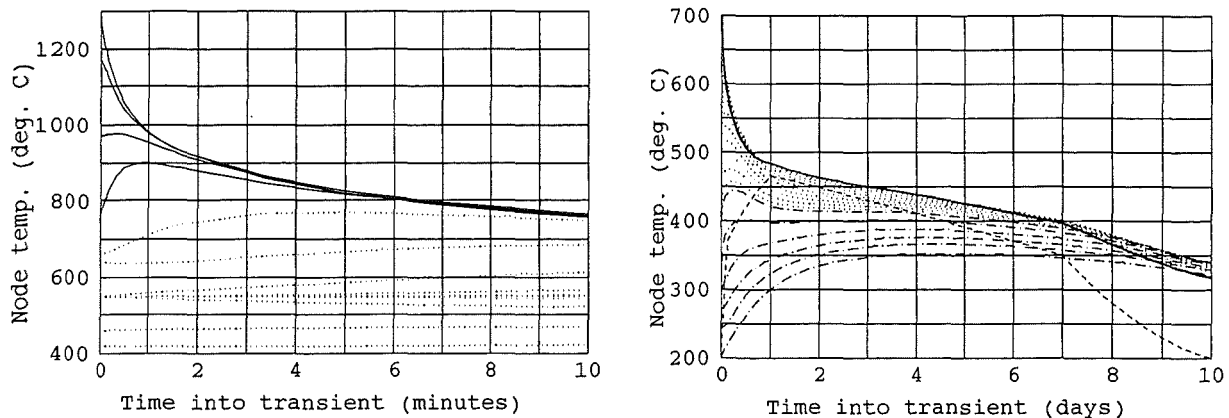


Figure 2.7- 19: Case 2d - Temperature evolution in the TBM, 1D heat transport model

(solid: FW nodes, dotted: breeding zone nodes, dash-dotted: manifold and shield nodes, dashed line: ITER reference FW temperature as input)

Be/steam chemical reaction results: The estimate of the exothermic heat at the TBM FW yielded high values after plasma shutdown, when steam ingress is postulated and the temperature is very high. Table 2.7-13 gives a few typical results for the FW temperature, the chemical heat produced, the heat that is radiated into the VV (assuming the ITER FW temperature to be 200°C at that time, emissivity=0.3), and the cumulative hydrogen production at the TBM FW. One can see that the chemical heat at the beginning exceeds the radiated heat by a factor of 4.7 and, therefore, can no longer be neglected in the temperature evaluation. The cumulative hydrogen produced amounts to 119 g after 1 hour. Further hydrogen production in this assessment ceases after about 6 hours at a total value of 125 g.

Table 2.7- 13: Case 2d - FW Be/steam chemical reaction results for the TBM

(safety factor for chemical heat and hydrogen production set to 1)

Time (s)	TBM surface Temp. (°C)	Chemical heat (kW/m ²)	Radiated heat (kW/m ²)	Cumulative H ₂ production (g)
119+0	1290	468	100	0
119+10	1167	247	74	20
119+50	1002	79	45	51
119+100	929	43	35	68
119+600	758	3.4	18.7	104
119+3600	630	0.24	10.6	119

iv) Evaluation of radiological release

The radiological release into the VV is the amount of tritium and activation products carried by the helium coolant, and the tritium that might be liberated from the

beryllium protective layer during the high temperature phase. The maximum tritium content in the coolant of 1 mg only (Table 2.7-15) is insignificant. The mobile activation products in the cooling loops (especially in the dust filters) have not been quantified but are negligible compared to the amounts of dust envisaged to be mobilised in the VV. The tritium stored in the beryllium protective layer was estimated as 0.11 g (Table 2.7-15). Even if all of it would come out, it would be still a relatively small amount in this hypothetical accident.

v) Uncertainties in results

Uncertainties in pressure transient calculations cannot change the result significantly. The temperature assessment suffers from a lack of thermo-physical material data in the high temperature regime. Since the most critical temperature in this context is the one at the FW (the peak of which is given here by definition), uncertainties play a minor role. The TBM Be/steam reaction results should serve as orientation mark only.

vi) Summary

The principal concerns formulated in the description for this hypothetical accident revealed to be relatively uncritical despite the hypothetical (Cat V) character of the event sequence. Contribution to the VV pressurisation by the TBM helium coolant is small (3500 Pa). Tritium and activation products release from the TBM into the VV is insignificant compared to the total amount mobilised in the ITER basic machine. The temperature evolution in the TBM is uncritical (except for the FW), and the decay heat removal is assured by passive means. For the FW a heavy chemical reaction has been predicted during a 100 s period after shutdowns which could be self-sustaining. This point would need more detailed but very complex studies. The estimated hydrogen production of 125 g, on the other hand, is small. It is bounded in any case at 2.2 kg if all beryllium from the TBM FW was burnt.

2.7.3 Safety analysis data base

2.7.3.1 Materials and toxic materials inventory

To give an overview of the types of materials and masses involved, and their coarse distribution in the TBM system the inventories are summarised in this section. It is distinguished between material masses in technical terms (e.g., structural material, breeder, multiplier, coolant) and two radio-toxic categories, i.e., tritium and activation products (AP). Only those inventories are considered which may influence in some way the sequence of an accident, for instance, via chemical reaction, mechanical energy release, thermal inertia, or liberation of radioactivity.

In Table 2.7-14 are given the mass inventories in the HCPB-TBM subsystems relevant in accident analysis. The test module proper (excluding the shield) includes 4000 kg of structural material, 450 kg of beryllium pebbles, and 120 kg of breeder pebbles. The cooling subsystem (2 loops plus components) contains an additional steel mass of 6000 kg, constituting a relatively large heat capacity. Note that also the shield and attachment have a large steel mass of about 6000 kg, assuming shield dimensions of $1.3 \times 1.5 \times 0.48 \text{ m}^3$ and a steel fraction of 80% (this tends to be reduced with the new attachment design). The helium enclosed in the main loops amounts to 14 kg under operating conditions (8 MPa, 300°C average temperature).

The tritium inventory in the TBM has not yet been evaluated in detail. A preliminary assessment for the structure and breeder material is made by scaling down the inventory obtained for the outboard of the DEMO blanket after 2.5 years of full power operation, corresponding to a total neutron fluence at the outboard first wall at torus mid plane of about $10^{23}/\text{cm}^2$. A scaling factor of 1/480 (one tenth of one out of 48 outboard segments) is used, resulting in the tritium inventories given in Table 2.7-15. As can be seen, the tritium content in the TBM is in the 20 mg range in structural and breeder materials each. For the beryllium multiplier a tritium inventory at the end of BPP and EPP of 0.14 g and 4 g, respectively, has been estimated.

The primary coolant (both loops) contains only 1 mg (10 Ci) of tritium when the purification process is in equilibrium, otherwise even less, provided that the purification system is operating while the ITER power is on. In this estimate an average value for the tritium permeation rate into the coolant of $0.1 \times 10^{-3} \text{ mole-T/h}$ has been assumed. This is equal to the tritium removal rate in the helium purification subsystem (section 2.1.1.4 of [2.7-3]) where the tritium is frozen out in cold traps. These traps will, consequently, accumulate up to approximately 44 mg of tritium within six days. After this period they will be regenerated.

The tritium inventory in the plasma facing beryllium layer has been calculated for ITER geometry (here assumed three continuous full power years) as 0.088 g tritium per kg of beryllium. Assuming zero release, this would yield 0.88 g of tritium in the 10 kg beryllium contained in the TBM plasma facing layer. Since the first wall beryllium will not last for three full power years the tritium content will only be a proportion of that amount, e.g., ~0.11 g at the end of the BPP with 0.36 full power years.

Activation products inventories in the TBM materials (breeder, multiplier, and structural material, and in the primary cooling loops) are to be determined.

Table 2.7- 14: Mass Inventory in the TBM System Relevant to Accident Analysis

Subsystem and type of material	Inventory (kg)
Inventories in the TBM proper	
Structural material (EUROFER)	
First wall (FW)	120
Breeding zone (BZ)	550
Manifold zone (MZ)	1300
Poloidal caps	2000
Shield (SH)	6000
Plasma facing material (beryllium, 5 mm)	10
Breeder (Li_4SiO_4) in BZ	120
Multiplier (beryllium pebbles) in BZ	450
Coolant (helium, operating conditions)	1.2
Purge gas (helium, operating conditions)	0.01
Inventories in cooling subsystem (2 main loops)	
Structural material (type 316L)	6000
Coolant (helium, operating conditions)	14
Inventories in helium purification subsystem	
Structural material	TBD
Helium	TBD
Inventories in tritium extraction subsystem	
Structural material	TBD
Helium (purge gas, main loop only)	1.1

Table 2.7- 15: Estimates of Tritium Inventory in TBM subsystems (see text for neutron fluence or operating time)

Tritium containing material	Tritium Inventory (g)
TBM including primary coolant	
Structural material	
First wall	8×10^{-3}
Breeding zone	10×10^{-3}
Manifold zone	0.6×10^{-6}
Plasma facing material, BPP (Be, 5 mm)	0.11
Breeder material (Li_4SiO_4)	15×10^{-3}
Multiplier (beryllium pebbles) BPP / EPP	0.14 / 4
Primary coolant (helium, 2 loops)	1×10^{-3}
Helium purification subsystem (in cold traps of both loops, (maximum))	44×10^{-3}
Tritium extraction subsystem	TBD

2.7.3.2 Energy sources

Energy sources in upset or accidental conditions are seen in (a) plasma disruptions, (b) delayed plasma shutdown after a cooling disturbance, (c) decay heat, (d) work potential of pressurised coolants, and (e) exothermic chemical reaction. This section

summarises the energy sources for the HCPB TBM based on the inventories described in section 2.7.3.1. An overview of the energy quantities (a) to (e) is given in Table 2.7-15. The values are explained in the paragraphs to follow.

Table 2.7- 16: Energy sources in the HCPB TBM

Energy source	Energy (MJ)
a) Plasma disruptions	4.5
b) Delayed plasma shutdown Normal: 3 s delay, 100 s ramp-down	101
c) Decay heat integrated over:	
1 minute	1.1
1 hour	48
1 day	304
1 month	2480
d) Work potential of helium coolant (both loops)	20
e) Chemical energy	
Beryllium/water reaction	18000
Beryllium/air reaction	30000

- (a) For short and severe disruptions due to alpha-particle induced instabilities a surface wall loading of 4.2 MJ/m^2 is assumed to be deposited within 1 s [2.7-6]. Given a TBM plasma facing surface of 1.07 m^2 yields a deposited energy of 4.5 MJ.
- (b) The energy due to delayed plasma shutdown is the time integral of surface power and internal power for a given shutdown scenario. For a normal shutdown sequence (3 s delay , 100 s ramp-down) this energy deposited in the TBM is 101 MJ. Any second in shutdown delay would add 1.9 MJ. Please note that the delayed plasma shutdown considered here serves as example only. In the current ITER design no safety relevant ramp-down is foreseen.
- (c) The decay heat power generation is described in section 2.1.1.1.1 of [2.7-3]. The spatial distribution has been evaluated by use of a 3D model for various conditions as function of decay time. This safety assessment is based on the results obtained for the TBM-I (with 9 mm thick breeder layers), a fusion power of 1500 MW, a fluence level of 0.36 MWa/m^2 (continuous operation) corresponding to the end of life fluence after the basic performance phase. The fluence level includes a poloidal peaking factor of 1.2 to account for the TBM position at torus mid-plane.

The time, space, and material dependent decay heat power density in the TBM is illustrated in Figure 2.7-20. It shows the ranges of decay heat in the different components of the TBM, i.e., in structural material (EUROFER, solid lines), beryllium pebbles (dotted lines), and in the Li_4SiO_4 breeder pebbles (long-dashed lines). The upper bound for a given material refers to the front side (next to or identical with the FW) and the lower bound refers to the back side (with the depth from the FW indicated in the figure legend). Also shown is the decay heat density in the beryllium FW protection layer (dashed-dotted line). The radial profiles at certain times are almost linear in a semi-logarithmic scale (log(decay heat) vs. time).

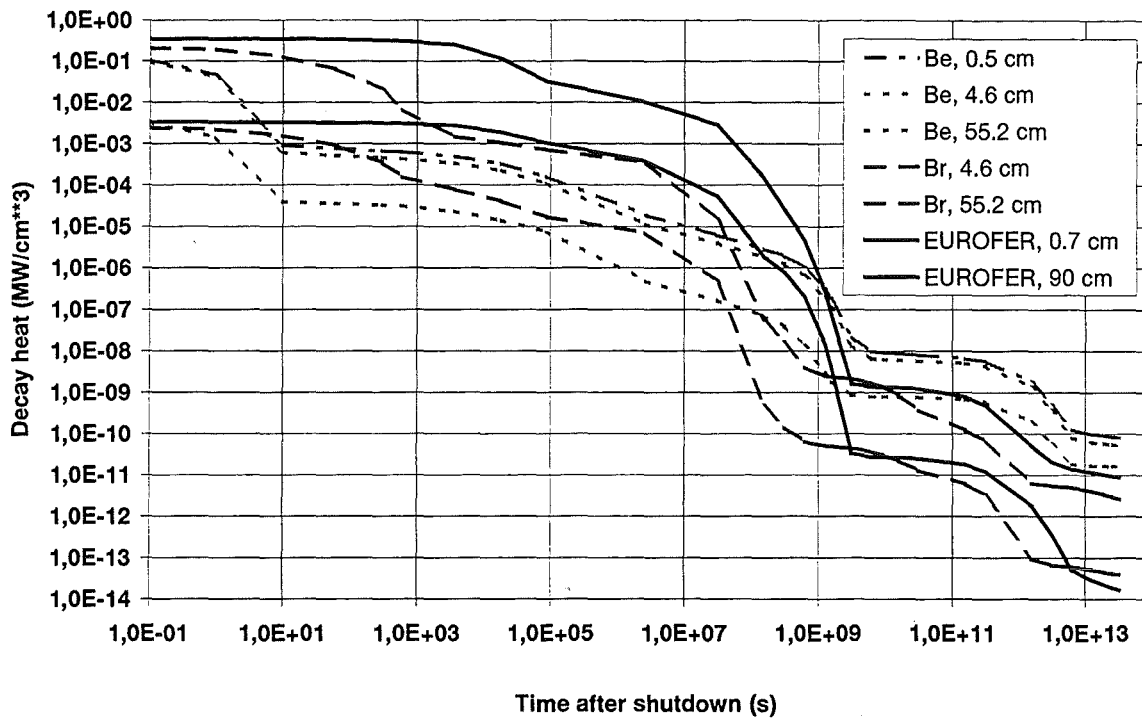


Figure 2.7- 20: Decay heat power density in TBM materials vs. decay time.

The integrated decay heat power generation in the TBM for the same conditions as described above is plotted in Figure A-2.7-21 together with the curves obtained for the shield and the entire support frame. The middle curve refers to the TBM-I module including the manifold (up to the radial position of 1.0128 m) and the poloidal caps. The total decay heat of the module amounts to 30 kW at $t=0$ s, declining to 2.4 kW after 1 day. Right after shutdown 58% of the decay heat is generated in EUROFER whereas, for instance, after one day the EUROFER produces 99% of the heat. Hence, the decay heat generated in beryllium and breeder pebbles can be neglected for times longer than one day after shutdown.

It is interesting to note that the heavy shield at the back of the module (0.48 m thick) produces much less decay heat (by about one order of magnitude) than the module proper. On the other hand the decay heat in the stainless steel frame is very large. In the TBM safety analysis the support frame has always been ignored.

Again, the total integrated decay heat power for the TBM after 1 minute, 1 hour, 1 day, 1 month yields values of 17.9, 12.9, 2.4, 0.87 kW, respectively. This leads to the time integrated energy as displayed in Table 2.7-16.

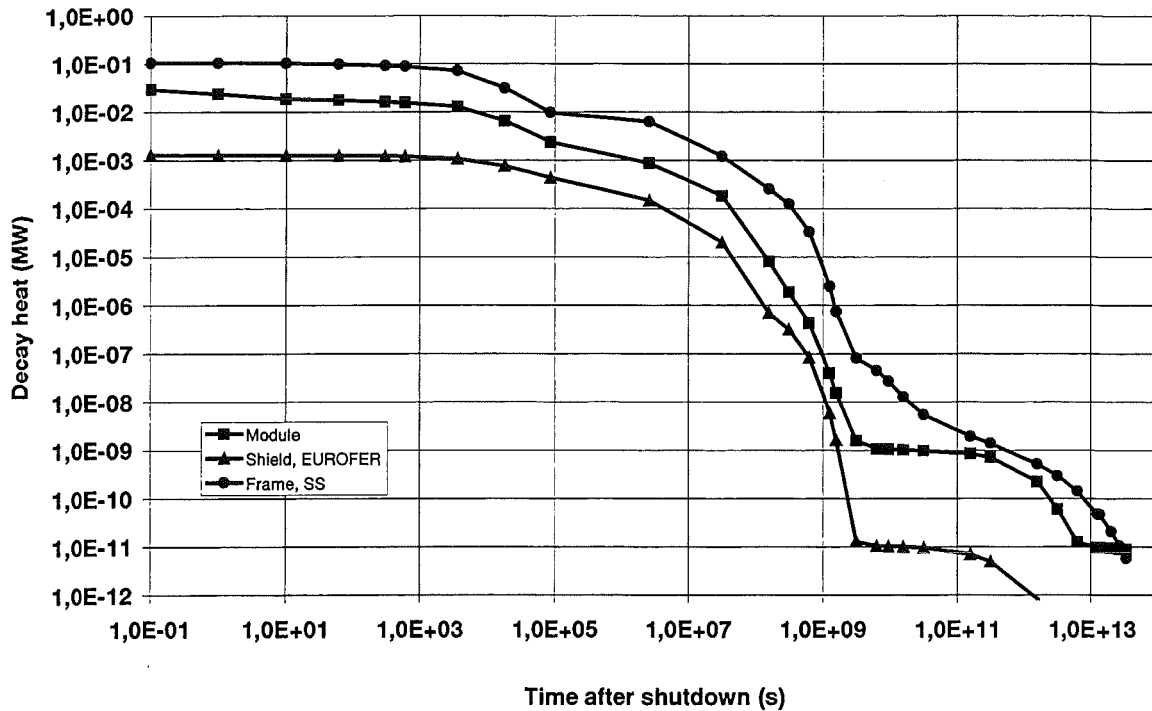


Figure 2.7- 21: Integrated decay heat of TBM with shield and frame

- d) The main helium cooling subsystem contains about 14 kg of helium at 8 MPa and a mean temperature of 300°C. The work potential relative to ambient conditions amounts to about 20 MJ.
- e) The exothermic reaction per kg of beryllium with water or oxygen generates 40 MJ or 67.4 MJ, respectively, resulting in a total chemical energy potential of the beryllium pebble beds (450 kg) of 18000 MJ for a beryllium/water reaction and 30000 MJ for a beryllium/air reaction. This is large compared to the other energies.

2.7.3.3 Material data used in safety analysis

Specific heat of materials present in the TBM

The following equations have been used to compute the specific heat of structural material, beryllium, breeder material (Li_4SiO_4), and helium. For the mixture in the breeding zone a mass weighted mean value is used as specified below. Table 2.7-17 shows the values in the temperature range 0 to 1500°C.

Specific heat is in $\text{Ws}/(\text{kgK})$, T in K , and $T_0=273.15 K$

Steel (EUROFER)

The correlation for MANET [2.7-8] was used since the difference to EUROFER is small and the data base for the structural material is not yet finalised:

$$c_p = 432.8 + 0.7038 \cdot (T - T_0) - 2.2113 \cdot 10^{-3} \cdot (T - T_0)^2 + 5.316 \cdot 10^{-6} \cdot (T - T_0)^3 - 3.105 \cdot 10^{-9} \cdot (T - T_0)^4$$

for $293K < T < 900K$

Beryllium (pure metal) [2.7-8]:

$$c_p = (2.353 + 0.632 \cdot 10^{-3} \cdot T + 0.107 \cdot 10^{-6} \cdot T^2 - 0.652 \cdot 10^5 \cdot T^{-2}) \cdot 10^{-3}$$

for $300K < T < 1530K$

Breeder material Li_4SiO_4 [2.7-8]:

$$c_p = (0.940 + 1.46 \cdot 10^{-3} \cdot T + 4.01 \cdot 10^3 \cdot T^{-2}) \cdot 10^{-3}$$

for $273K < T < 773K$

Helium gas [2.7-9]:

$$c_p = 5196 - 1043 \cdot (1/T^{1.3333} - 28300/T^3) \cdot 10^{-5} \cdot p$$

for $273K < T < 1473K$ and p in Pa for $10^5 Pa < p < 10^8 Pa$

Mixture (steel, beryllium, breeder and helium) in breeding zone:

$$C_{p,Mixture} = 0.470 \cdot C_{p,EUROFER} + 0.444 \cdot C_{p,Be} + 0.086 \cdot C_{p,Br} + 8.9 \cdot 10^{-6} \cdot C_{p,He}$$

Table 2.7- 17: Specific Heat of TBM Materials vs. Temperature

Temp. (°C)	Temp. (K)	CP- Steel (Ws/(kgK))	CP- Beryllium (Ws/(kgK))	CP- Breeder (Ws/(kgK))	CP-Helium (Ws/(kgK))	CP-Mixture (Ws/(kgK))
0	273	432.8	1660	1393	5197	1060
100	373	486.1	2135	1514	5196	1307
200	473	522.7	2385	1649	5196	1446
300	573	563.3	2552	1789	5196	1552
400	673	621.2	2683	1932	5196	1649
500	773	702.3	2797	2076	5196	1751
600	873	804.9	2901	2076	5196	1845
700	973	805.0	3001	2076	5196	1889
800	1073	805.0	3098	2076	5196	1932
900	1173	805.0	3194	2076	5196	1975
1000	1273	805.0	3291	2076	5196	2018
1100	1373	805.0	3388	2076	5196	2061
1200	1473	805.0	3486	2076	5196	2105
1300	1573	805.0	3543	2076	5196	2130
1400	1673	805.0	3543	2076	5196	2130
1500	1773	805.0	3543	2076	5196	2120

Caution: Data have been extrapolated over a wide range, where they might not be valid (shaded areas in Table 2.7-17). This is for numerical reasons in the 1D analysis. Be careful with results for temperatures beyond approximately 800°C.

CP-Steel is given for MANET up to 600°C only [2.7-8. Above 600°C it is assumed to be constant at 805 Ws/(kgK).

CP-Beryllium is given up to 800°C. From 800 to 1250°C it has been extrapolated. Above 1250°C it is assumed to be constant at 3543 Ws/(kgK).

CP-Breeder is given up to 500°C. Above 500°C it is assume to be constant at 2076 Ws/(kgK).

CP-Helium is practically a constant at 0.1 MPa. Pressure dependence is insensitive too.

Thermal conductivity of materials present in the TBM

The following equations have been used to compute the thermal conductivity of structural material steel (EUROFER), beryllium, breeder material (Li_4SiO_4), and helium. For the mixture in the breeding zone a volume weighted mean value is used as specified below. Table 2.7-18 shows the values in the temperature range 0 to 1500°C.

Equations used for thermal conductivity k in W/(mK), T in K, and $T_0=273\text{K}$:

Steel (EUROFER)

The correlation for MANET [2.7-8] was used since the difference to EUROFER is small and the data base for the structural material in not yet finalised:

$$k = 24.25 + 6.251 \cdot 10^{-3} \cdot (T - 300) - 6.284 \cdot 10^{-6} \cdot (T - 300)^2 + 3.627 \cdot 10^{-9} \cdot (T - 300)^3$$

for 293K < T < 873K

Beryllium pebbles [2.7-10]:

$$k = 6.235 \cdot \left\{ 1 + 353 \cdot \left[(\alpha_{Be} - \alpha_{Ma}) \cdot (T - 300) + \left[\left[1 + \frac{\Delta V}{V} \right]^{\frac{1}{3}} - 1 \right] \right] \right\}$$

for 293K < T < 873K

where the thermal expansion coefficient of beryllium is approximated by [2.7-8]

$$\alpha_{Be} = 8.43 \cdot 10^{-6} \cdot (1 + 1.36 \cdot 10^{-3} \cdot T - 3.53 \cdot 10^{-7} \cdot T^2)$$

$\Delta V/V$ volume swelling of beryllium under neutron irradiation (here $\Delta V/V=0$) and the thermal expansion coefficient of EUROFER is approximated by:

$$\alpha_{EUROFER} = 9.604 \cdot 10^{-6} + 4.96 \cdot 10^{-9} \cdot (T - T_0)$$

Breeder pebbles Li_4SiO_4 [2.7-5]:

$$k = 0.708 + 4.51 \cdot 10^{-4} \cdot (T - T_0) + 5.66 \cdot 10^{-7} \cdot (T - T_0)^2$$

for 293K < T < 873K

Helium as function of temperature and pressure, p in Pa, [2.7-9]:

$$k = 0.144 \cdot \left(\frac{T}{273.15} \right)^{0.7} \cdot (1 + 2 \cdot 10^{-9} \cdot p)$$

for 273K < T < 1473K, $10^5 \text{ Pa} < p < 10^7 \text{ Pa}$

Mixture (steel, beryllium, breeder and helium) in breeding zone:

$$k_{\text{Mixture}} = 0.133 \cdot k_{\text{EUROFER}} + 0.527 \cdot k_{\text{Be}} + 0.0788 \cdot k_{\text{Br}} + 0.261 \cdot k_{\text{He}}$$

Table 2.7- 18: Thermal Conductivity of TBM Materials vs. Temperature

Temp. (°C)	Temp. (K)	k-steel (W/(mK))	k-Beryllium (W/(mK))	k-Breeder (W/(mK))	k-Helium (W/(mK))	k-Mixture (W/(mK))
0	273.15	24.08	6.13	0.71	0.14	6.53
100	373.15	24.68	6.59	0.76	0.18	6.86
200	473.15	25.16	7.22	0.82	0.21	7.27
300	573.15	25.56	8.00	0.89	0.24	7.75
400	673.15	25.90	8.87	0.98	0.27	8.27
500	773.15	26.19	9.81	1.08	0.30	8.82
600	873.15	26.45	10.77	1.18	0.33	9.37
700	973.15	26.50	11.09	1.20	0.35	9.55
800	1073.15	26.50	11.09	1.20	0.38	9.56
900	1173.15	26.50	11.09	1.20	0.40	9.57
1000	1273.15	26.50	11.09	1.20	0.42	9.57
1100	1373.15	26.50	11.09	1.20	0.45	9.58
1200	1473.15	26.50	11.09	1.20	0.47	9.59
1300	1573.15	26.50	11.09	1.20	0.49	9.59
1400	1673.15	26.50	11.09	1.20	0.51	9.60
1500	1773.15	26.50	11.09	1.20	0.53	9.60

Remarks:

Caution: Data have been extrapolated over a wide range, where they might not be valid. This is for numerical reasons in the 1D analysis. Be careful with results for temperatures beyond approximately 800°C.

k-values for steel (MANET) after [2.7-8], p. III/2, above 600°C assumed to be constant.

Thermal expansion values for steel and beryllium are needed in the equation for the thermal conductivity of beryllium pebbles. They are computed as follows:

Alpha-values for steel is a linear fit to values from an unknown source, they are app. 4% less than curve given by [2.7-8].

Alpha values for beryllium after [2.7-8], p. VIII/4, extrapolated with same equation beyond 1000°C.

k-value for beryllium after [2.7-10], p 52 with alpha values for steel and beryllium as indicated above.

k-values for breeder material after [2.7-10], p. 20. Above 600°C k is assumed to be constant. (Note that this correlation is not consistent with data given in [2.7-8] on p. V/11.

k-values for helium after [2.7-9], p 147, here listed for pressure = 10⁵ Pa.

k-Mixture is the volume weighted average thermal conductivity of the mixture in the breeding zone with the following volume fractions: steel 0.133, beryllium 0.527, breeder 0.0788, and helium 0.261.

Density of materials present in the TBM

The densities and void fractions presented in Table 2.7-19 have been used.

Table 2.7- 19: Density and porosity of materials present in the TBM

Material	Density of solid material (kg/m ³)	Void fraction in pebble bed or cooling plates
Steel (EUROFER)	7750	-
Cooling plates (EUROFER)	7750	0.4
Beryllium	1850	0.192
Breeder (Li ₄ SiO ₄)	2400	0.36

Chemical reaction rates of beryllium [2.7-4]

Table 2.7- 20: Beryllium/air chemical reaction

T<800°C	$RA = 5.37 \cdot 10^7 \cdot \exp\left(\frac{-26200}{T(K)}\right)$	mole-Be reacted/(m ² s)
T>800°C	$RA = 3.87 \cdot 10^3 \cdot \exp\left(\frac{-15900}{T(K)}\right)$	mole-Be reacted/(m ² s)
Basic equ.	$Be + \frac{1}{2}O_2 \Rightarrow BeO - 610 \cdot kJ/mole$	

A safety factor SF_A=5 is recommended for Cat II – IV events and SF_A=1 for Cat V events to account for data uncertainties.

Table 2.7- 21: Beryllium/steam chemical reaction

T<900°C	$RS = 4.8 \cdot 10^9 \cdot \exp\left(\frac{-25850}{T(K)}\right)$	liter-H ₂ (stp)/(m ² s)
T>900°C	$RS = 7.9 \cdot 10^4 \cdot \exp\left(\frac{-12830}{T(K)}\right)$	liter-H ₂ (stp)/(m ² s)
Basic equ.	$Be + H_2O \Rightarrow BeO + H_2 - 370 \cdot kJ/mole$	

A safety factor SF_S=2 is recommended for Cat II – IV events and SF_S=1 for Cat V events to account for data uncertainties.

2.7.3.4 The 1D heat transport model

The 1D heat transport model to analyse the decay heat transport in the HCPB TBM in the post blowdown phase represents a radial unit cell column cut out of the TBM from the first wall all the way through the shield (Figure 2.7-3). The model is divided into 22 elements (nodes) as specified in Table 2.7-22. Further description of the model is given in section 2.7.1.1, paragraph ii.

i) Radial build of the 1D model

Table 2.7- 22: Radial Build of HCPB TBM - 1D Model

Node No.	Zone Identifier	Zone Name	Zone Material (vol.-%)	R _{in} (mm)	ΔR (mm)
	PLASMA	Plasma chamber	void	5156	6129
1	FWBEM	FW Be (module)	Be (100%)	11285	5
2	FWM(1)	FW EUROFER (Zone 1)	EUROFER (100%)	11290	5
3	FWM(2)	FW EUROFER (Zone 2)	EUROFER (75%), He (25%)	11295	14
4	FWM(3)	FW EUROFER (Zone 3)	EUROFER (100%)	11309	7
5	BRZM(1)	Breeding zone module (Zone1)	EUROFER (13.3%), Be (52.7%), Li ₄ SiO ₄ (7.88%), He (26.1%)	11316	29
6	BRZM(2)	Breeding zone module (Zone2)	EUROFER (13.3%), Be (52.7%), Li ₄ SiO ₄ (7.88%), He (26.1%)	11345	30
7	BRZM(3)	Breeding zone module (Zone3)	EUROFER (13.3%), Be (52.7%), Li ₄ SiO ₄ (7.88%), He (26.1%)	11375	40
8	BRZM(4)	Breeding zone module (Zone4)	EUROFER (13.3%), Be (52.7%), Li ₄ SiO ₄ (7.88%), He (26.1%)	11415	50
9	BRZM(5)	Breeding zone module (Zone5)	EUROFER (13.3%), Be (52.7%), Li ₄ SiO ₄ (7.88%), He (26.1%)	11465	50
10	BRZM(6)	Breeding zone module (Zone6)	EUROFER (13.3%), Be (52.7%), Li ₄ SiO ₄ (7.88%), He (26.1%)	11515	50
11	BRZM(7)	Breeding zone module (Zone7)	EUROFER (13.3%), Be (52.7%), Li ₄ SiO ₄ (7.88%), He (26.1%)	11565	50
12	BRZM(8)	Breeding zone module (Zone8)	EUROFER (13.3%), Be (52.7%), Li ₄ SiO ₄ (7.88%), He (26.1%)	11615	50
13	BRZM(9)	Breeding zone module (Zone9)	EUROFER (13.3%), Be (52.7%), Li ₄ SiO ₄ (7.88%), He (26.1%)	11665	50
14	BRZM(10)	Breeding zone module (Zone10)	EUROFER (13.3%), Be (52.7%), Li ₄ SiO ₄ (7.88%), He (26.1%)	11715	50
15	BRZM(11)	Breeding zone module (Zone10)	EUROFER (13.3%), Be (52.7%), Li ₄ SiO ₄ (7.88%), He (26.1%)	11765	50
16	BRZM(12)	Breeding zone module (Zone12)	EUROFER (13.3%), Be (52.7%), Li ₄ SiO ₄ (7.88%), He (26.1%)	11815	43
17	MANIM(1)	Manifold block (Zone 1)	EUROFER (50%), He (50%)	11858	40
18	MANIM(2)	Manifold block (Zone 2)	EUROFER (13.5%), He (86.5%)	11898	170
19	MANIM(3)	Manifold block (Zone 3)	EUROFER (65%), He (35%)	12068	230
20	COVM(1)	Cover plate (Zone 1)	EUROFER (20%), He (80%)	12298	130
21	COVM(2)	Cover plate (Zone 2)	EUROFER (80%), He (20%)	12428	140
22	SHDM	Shield	EUROFER (80%), He (20%)	12568	480
	GSPM	Gap shield plug	void	13048	

Notes:

- Surface of zone FWBEM radiates into black hemisphere with temperature T_{ITER,FW} equivalent to the ITER FW temperature
- Surface of zone SHDM radiates to the VV plug with temperature T_{VV} equivalent to the VV wall temperature (radiation heat transfer model for two parallel planes)
- The volumetric composition in the breeding zone corresponds to a unit cell composed of 1 breeder layer, 1 Be layer, and 2 cooling plates (ignoring side walls and top/bottom caps)
- Li₄SiO₄ pebble bed porosity is 0.36, beryllium pebble bed porosity is 0.192.

ii) Radiation heat transfer model

Longitudinal radiation heat transfer is modelled between internal elements where appropriate and from/to the end surfaces of the 1D model.

Radiation heat transfer between internal elements: If there are elements with a high void (or helium) fraction, the heat transport across these elements is mainly achieved by thermal radiation. Given element i as the void element, radiation heat flux per unit cross sectional area between the adjacent elements $i-1$ and $i+1$ is modelled for the configuration of two parallel planes according to the following equation

$$q_{i-1,i+1}^{rad} = \sigma_{i-1,i+1} \cdot (T_{i-1}^4 - T_{i+1}^4)$$

where

$$\sigma_{i-1,i+1} = \frac{\sigma}{\frac{1}{\epsilon_{i-1}} + \frac{1}{\epsilon_{i+1}} - 1}$$

$\sigma = 5.77 \cdot 10^{-8} \text{ W}/(\text{m}^2\text{K}^4)$ Stefan-Boltzmann constant

ϵ_{i-1} and ϵ_{i+1} are the emissivity of opposing surfaces of elements $i-1$ and $i+1$

T_{i-1} and T_{i+1} are the actual mean temperatures of elements $i-1$ and $i+1$

Radiation heat transfer from/to the end surfaces: The end surfaces of the 1D model, i.e., the FW of the TBM and the back face of the 0.48 m thick shield lose or receive radiated heat to/from the surrounding components. This is modelled based on a configuration of a finite plane radiating into a hemisphere according to the equation

$$q_i^{rad} = \sigma \cdot \epsilon_i \cdot (T_i^4 - T_\infty^4)$$

where σ , ϵ_i and T_i are equivalent to the definitions given above,

$i=1$ or 22 are the extreme elements of the 1D model,

T_∞ is the assumed uniform temperature of the surrounding components, i.e., the ITER FW if $i=1$ and the VV if $i=22$.

Alternatively, the model for two opposing parallel planes can be used at one or both ends. In this study the hemispherical radiation model was applied to the FW and the model for parallel planes was used at the back. Emissivity values of $\epsilon_i = 0.3$ were assumed throughout.

iii) Initial temperature profile in the TBM used in the 1D model

The radial temperature profile indicated by the solid line in Figure 2.7-22 is taken as an approximate representation of the steady state mixed mean temperature distribution in the TBM to be used in the 1D decay heat removal analysis. It has been derived in part from FIDAP results for the revised TBM-I with 9 mm breeder layers at steady state operation with 10% over-power applied to the nominal volumetric heat. The surface heat flux at the TBM was set to $50 \text{ W}/\text{cm}^2$ in the FIDAP analysis which is considered as the peak heat flux including both spatial and temporal overloads. The coolant inlet temperature and the mass flow rate were chosen as in normal

operation, implying that the outlet temperature was slightly increased compared to normal ($\approx 357^\circ\text{C}$ instead of 350°C).

In the breeding zone the temperature was assumed to be constant in radial direction in a pessimistic way. At radii larger than 57.3 cm from the FW (i.e., node numbers 17 and higher in Table 2.7-22) the temperature profile was estimated based on the coolant temperatures expected in those nodes.

In cases with significant shutdown delay after the cooling disturbance (like cases 2a, 2b, 2c) the decay heat transport analysis has to start from a higher level. Hence, an increase of 40 to 50 K in the FW nodes 1 to 4 relative to steady state has been applied, which is derived from FIDAP results presented in Figure 2.7-12 (compare Table 2.7-23). The bulk of the TBM is not significantly affected by the 10 s shutdown delay. In the case 2d with shutdown occurring at melting of the protection layer the initial temperature profile has been deduced from Figure 2.7-18. An extra temperature burst caused by the disruption is discussed next.

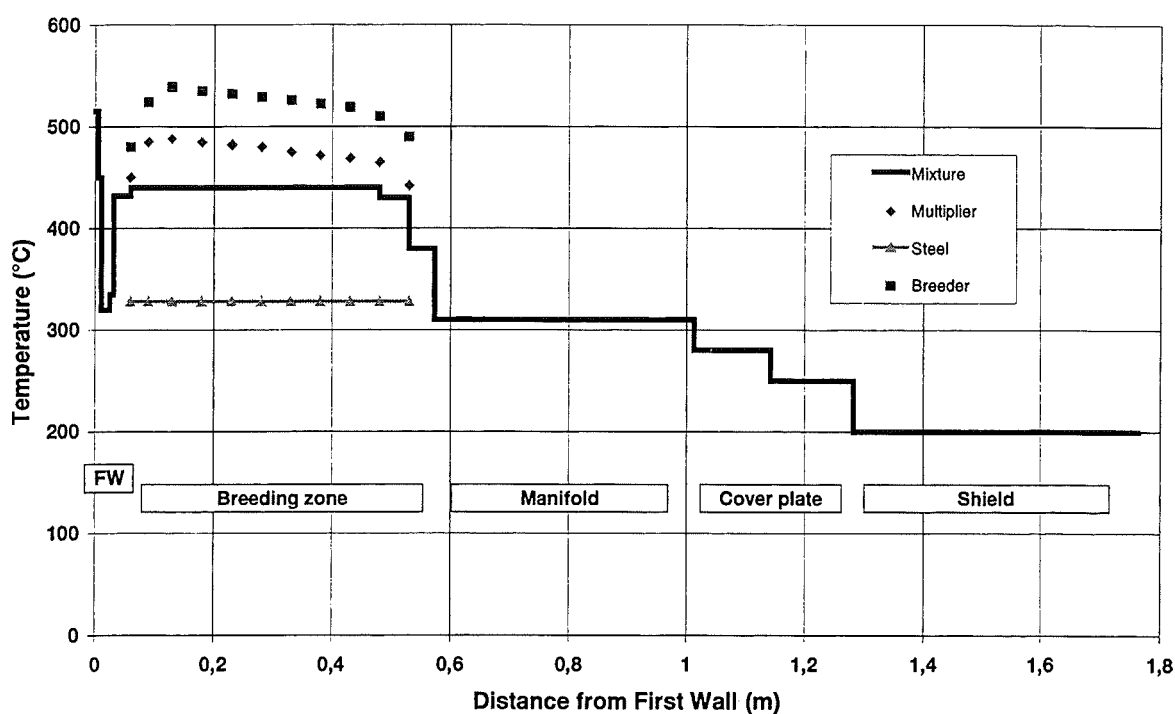


Figure 2.7- 22: Reference steady state temperature profile in TBM at 10% over-power for accident analysis

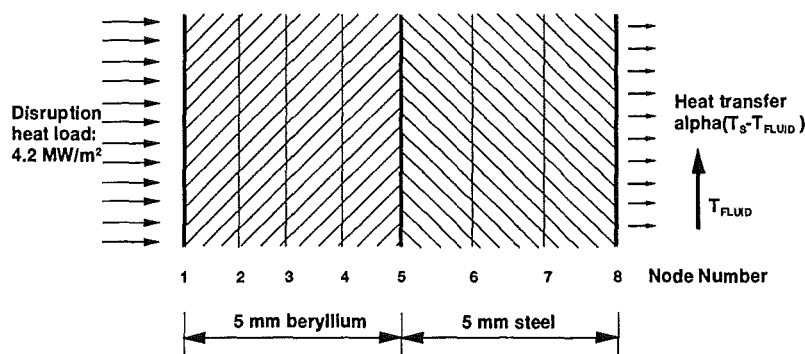
(Dotted lines indicate the poloidal peak in pebble beds for comparison only)

Table 2.7- 23: Initial node temperatures in °C used in the 1D model in different cases (The second term in a sum accounts for the jump caused by disruption)

Node No.	Case 1a	Case 2a	Case 2b	Case 2c	Case 2d
1	515+130	565+130	565+130	565+130	1280
2	450+55	500+55	500+55	500+55	1170
3	320+10	360+10	360+10	360+10	970
4	335+5	375+5	375+5	375+5	760
5	432	432	432	432	660
6	440	440	440	440	640
7 to 14	440	440	440	440	550
15	430	430	430	430	460
16	380	380	380	380	420
17	310	310	310	310	370
18	310	310	310	310	310
19	310	310	310	310	300
20	280	280	280	280	271
21	250	250	250	250	250
22	200	200	200	200	200

iv) Temperature bursts caused by disruption

An extra temperature burst has to be taken into account in the FW nodes. The effect of a uniform 4.2 MW/m^2 surface heat load lasting for 1 second (which is the current model for the disruption load) has been calculated with a SPEAKEASY routine. It calculates the 1D transient temperature distribution in a multi-layer plate (slab) with temperature dependent thermal conductivity and heat capacity. This 1D sub-model (not to confuse with the 1D model described in previous paragraphs) represents only the front plate of the FW consisting of the 5 mm beryllium layer and the 5 mm steel layer as depicted in the sketch below.



1D sub-model to calculate temperature bursts in the FW caused by disruption

The boundary conditions are simplified: constant surface heat load at the plasma facing side for 1 second and constant (like in normal operation) wall/fluid heat transfer at the back at all times.

The 8-node sub-model yields the node temperature evolution presented in Figure 2.7-23 (solid lines). The mean temperature in the 5 mm beryllium layer and in the 5 mm steel layer (which are congruent with the nodes 1 and 2, respectively, of the 1D model defined in Tables 2.7-22 and 2.7-23) are drawn as dashed-dotted lines. As can be seen, at the end of the 1 s disruption heat pulse the mean temperature in the beryllium layer has risen by 130 K and in the steel layer by 55 K. These temperature increments are added in Table 2.7-23 to obtain the initial temperature distribution for the 1D decay heat transport analysis. The small increments added at nodes 3 and 4 in Table 2.7-23 account for the simplified boundary condition at the back side of this sub-model.

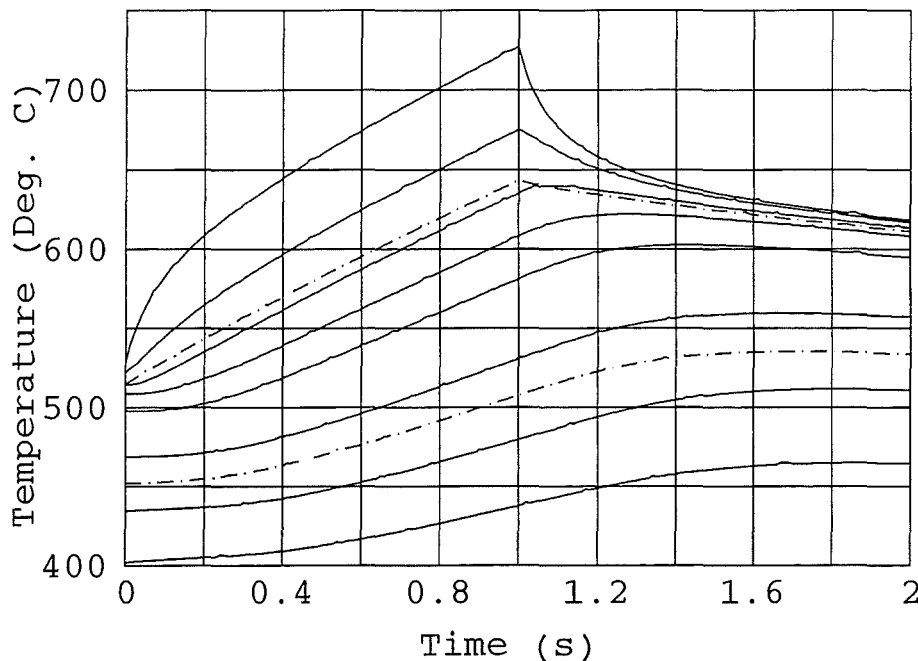


Figure 2.7- 23: Temperature evolution in the FW nodes 1-8 of the sub-model caused by disruption load of 4.2 MW/m^2 , lasting for 1 second.

(Dashed-dotted lines show mean values in Be and steel layer)

v) ITER shielding blanket FW temperature evolution

ITER shielding blanket FW temperature is used as thermal radiation boundary condition in the 1D heat transfer model. In the cases analysed, where no credit can be given to in-vessel cooling, the ITER FW is predicted to heat up from 200 to 465°C during the first day falling off afterwards. This curve denoted in this report as reference ITER FW temperature evolution is specified in [2.7-1] as follows:

Table 2.7- 24: Reference ITER FW temperature evolution

Time after shutdown	FW temperature (°C)
0 s	200
1 hour	265
3 hours	370
10 hours	410
1 day	465
2 days	450
4 days	410
7 days	350
8 days	280
9 days	230
10 days	200

References

- [2.7-1] ITER Non-Site specific Safety Report (NSSR-2), Volume VII (Draft).
- [2.7-2] K. Gabel, K. Kleefeldt: Thermal-hydraulic analysis of the helium cooled pebble bed test blanket module for ITER during normal operation and accidents, FZKA 6059, May 1998.
- [2.7-3] L. V. Boccaccini, M. Dalle Donne et al.: Design Description Document (Status: 5.12.97), 5.6.B European Helium Cooled Pebble Bed (HCPB) Test Blanket, Internal Report submitted to ITER (1997).
- [2.7-4] H. W. Bartels et al.: Safety Analysis Data List-2 (SADL-2), Version 2 (May 1997)
- [2.7-5] M. Dalle Donne et al.: European DEMO BOT Solid Breeder Blanket, KfK 5429, (1994).
- [2.7-6] Private communication with H.-W. Bartels, ITER JCT, February 1998.
- [2.7-7] Users Manual, Fluid Dynamics International Inc., Revision 7.0, 1. Edition, April 1993.
- [2.7-8] M. Kühle: Material data base for the NET test blanket design studies, FZK internal report (1990).
- [2.7-9] R. Schuster, W. Zimmerer: Darstellung der Stoffdaten des Systems MAPLIB in tabellarischer und graphischer Form, KfK-Ext. 8/77-1 (1977).
- [2.7-10] M. Dalle Donne, L. V. Boccaccini et al.: European helium cooled pebble bed (HCPB) test blanket, ITER Design Description Document, FZKA 5891 (1997).

Appendix A 9Cr RCC-MR properties data



Energieonderzoek Centrum Nederland
Netherlands Energy Research Foundation ECN

ECN NUCLEAR ENERGY

Forschungszentrum karlsruhe
Prof. M. Dalle Donne
Postfach 3640
D-76021 KARLSRUHE

Direct line: +31 224 56 4665
Telefax : +31 224 56 3490
Our ref. : 71099/BvdS/mh/1996/003187
Your ref. : -
Subject : 9Cr RCC-MR properties data

Petten, 2 August 1996

Dear Mario,

For your information I have attached the data on 9Cr steel mechanical properties as given in the RCC-MR. Before using the data a short explanation is needed. In the 1987 version of the code three product forms of 9Cr steel have been included in the Part Procurement Specifications:

- RM 2422: Z10 CDVNb 9-1 alloy steel forgings for steam generator tube plates.
- RM 2431: Z10 CDVNb 9-1 alloy steel thick plates for steam generator tube plates.
- RM 2442: Z10 CDNV 9-1 beamless chromium-molybdenum alloy steel tubes for FBR steam generator bundles.

The chemical specification for these materials is given in the 1987 issue of the RCC-MR as follows:

C	0.08	-	0.12
Mn	0.3	-	0.5
P _{max}	0.02		
S _{max}	0.01		
Si	0.2	-	0.6
Ni _{max}	0.2		
Cr	8.00	-	9.00
Mo	0.85	-	1.05
V	0.18	-	0.25
Cu _{max}	0.1		
Nb	0.06	-	0.10
Al _{max}	0.04		
N	0.03	-	0.07



- 2 -

These three forms shall comply with the Properties Group 18 s as given in RCC-MR '87. This properties group 18 s I have attached to this letter. Additionally I have added the fatigue data of properties group 17 s. The reason is that in the 18 s version the fatigue limits are not issued. Originally this 9Cr steel complied with Properties Group 17 s. There fatigue data are included. In order to give you an idea of the fatigue trend I have included the relevant part of 17 s, but formally it is not given in 18 s.

The Properties Group 18 s data have been compared with large data bases of similar 9Cr steels under CEC study contract RAI-0199-VK by Curbishley et al. in January 1995. Some discrepancies have been observed for long term creep exposures at 823 K. Since this is not a relevant temperature domain for the ITER test object I do still support the use of the 18 s Properties Group. The new low activation Cr steel have the potential of improving the "classical" properties given in the RCC-MR, which is another reason not to bother with the findings of the study contract.

I fear that the fax processing affects the quality of the figures. The information is therefore sent to you by surface mail to make sure it can be read. I apologize for the resulting delay.

If you require additional information or explanations, please do not hesitate to contact me.

Yours sincerely,

A handwritten signature in black ink, appearing to read 'B. van der Schaaf', written over a horizontal line.

ir. B. van der Schaaf
Member Management Team
ECN Nuclear Energy

TABLE OF CONTENTS

A3.18S.1	INTRODUCTION
A3.18S.2	PHYSICAL PROPERTIES
A3.18S.2.1	Coefficient of thermal expansion
A3.18S.2.2	Young's modulus
A3.18S.2.3	Poisson's ratio
A3.18S.3	TENSILE STRENGTH PROPERTIES
A3.18S.3.1	Minimum and average yield strength at 0,2% offset
A3.18S.3.2	Minimum and average tensile strength
A3.18S.4	NEGLECTIBLE CREEP CURVE (to be issued)
A3.18S.5	ANALYSIS DATA
A3.18S.5.1	Value of S_m
A3.18S.5.2	Values of S_t
A3.18S.5.3	Creep rupture stress: S_r
A3.18S.5.4	Saturation fatigue curves (to be issued)
A3.18S.5.5	Isochronous curves, creep strain (to be issued)
A3.18S.5.6	Stresses S_{Rh} and S_{Rc} (to be issued)
A3.18S.5.7	Symmetrization coefficient K_s (to be issued)
A3.18S.5.8	Fatigue - Creep interaction diagram
A3.18S.5.9	Cyclic curves, values of K_e and K_v (to be issued)
A3.18S.6	ANALYSIS DATA
A3.18S.6.1	Monotonic tensile hardening rule
A3.18S.6.2	Bilinear curves (to be issued)
A3.18S.6.3	Creep-strain law
A3.18S.6.4	Fatigue curve (to be issued)
A3.18S.6.5	Maximum allowable strain: D_{max}

A3.18S.1 INTRODUCTION

A3.18S.2 PHYSICAL PROPERTIES

A3.18S.2.1 COEFFICIENT OF THERMAL EXPANSION

This is the average coefficient of linear thermal expansion α between 20 °C and the temperature indicated θ .

α is given as a function of θ by the following:

Table 2.1.1

θ (°C)	20	100	200	300	400	500	600	700
$\alpha \cdot 10^{-6} \cdot (°C)^{-1}$	10,4	10,8	11,2	11,6	11,9	12,2	12,5	12,7

Figure 2.1.2

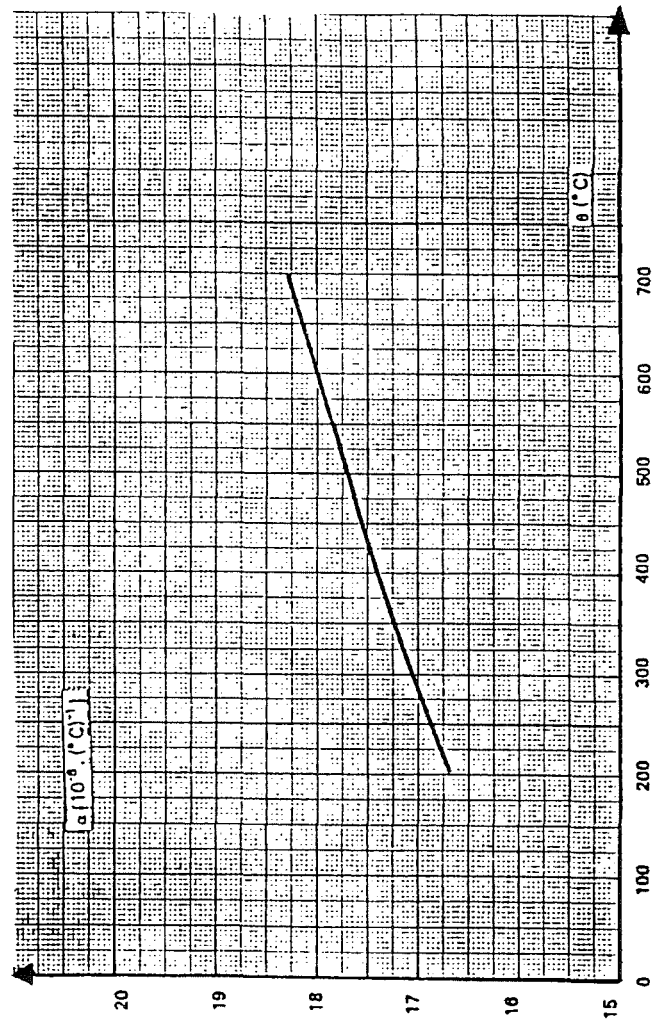


Figure A3.18S.2.1.2
AVERAGE COEFFICIENT OF LINEAR
THERMAL EXPANSION

A3.18S.2.2 YOUNG'S MODULUS

Young's modulus, E (MPa) is given as a function of the temperature θ by the following:

. Formula 2.2.1

$$E = 207300 - 64,58 \theta \quad 20 \leq \theta^{\circ}\text{C} \leq 500$$

$$E = 235000 - 120 \theta \quad 500 \leq \theta^{\circ}\text{C} \leq 600$$

. Table 2.2.2

θ °C	20	100	200	300	350	400	450	500	550	600
E (10 ³)N/mm ²	206	201	194	188	185	181,5	178	175	163	151

. Figure 2.2.3

A3.18S.2.3 POISSON'S RATIO

This is taken as 0,3 within the elastic range.

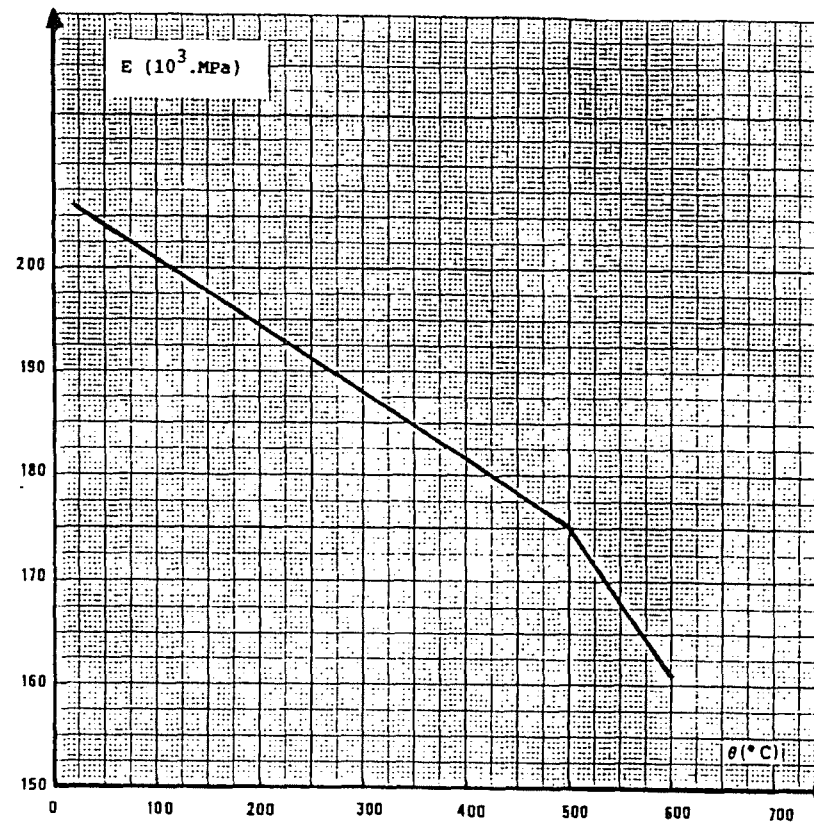


Figure A3.18S.2.2.3
YOUNG'S MODULUS

A3.185.3 TENSILE STRENGTH PREPERTIES

A3.185.3.1 MINIMUM AND AVERAGE YIELD STRENGTH AT 0,2% OFFSET

The minimum yield strength at 0,2% offset ($R_{0,002}$)_{min} is given as a function of temperature θ by the following:

. Formula 3.1.1

$$(R_{0,002})_{\min} = 409,56 - 0,51595 \theta + 1,9521 \cdot 10^{-3} \theta^2 - 2,7776 \cdot 10^{-6} \theta^3$$

This formula is applicable for $20 \leq \theta \text{ } ^\circ\text{C} \leq 700$

. Table 3.1.2

θ ($^\circ\text{C}$)	20	50	100	150	200	250	300	350
($R_{0,002}$) _{min} MPa								
Tubes	420	400	375	367	362	359	355	349
Plates	400	390	375	367	362	359	355	349

θ ($^\circ\text{C}$)	400	450	500	550	600
($R_{0,002}$) _{min} MPa					
Tubes	338	320	292	254	203
Plates	338	320	292	254	203

. Figure 3.1.3

The average yield strength at 0,2% offset is given as a function of temperature θ by:

. Formula 3.1.4

$$(R_{0,002})_{\text{avg}} = 564,25 - 0,7108 \theta + 2,6894 \cdot 10^{-3} \theta^2 - 3,8267 \cdot 10^{-6} \theta^3$$

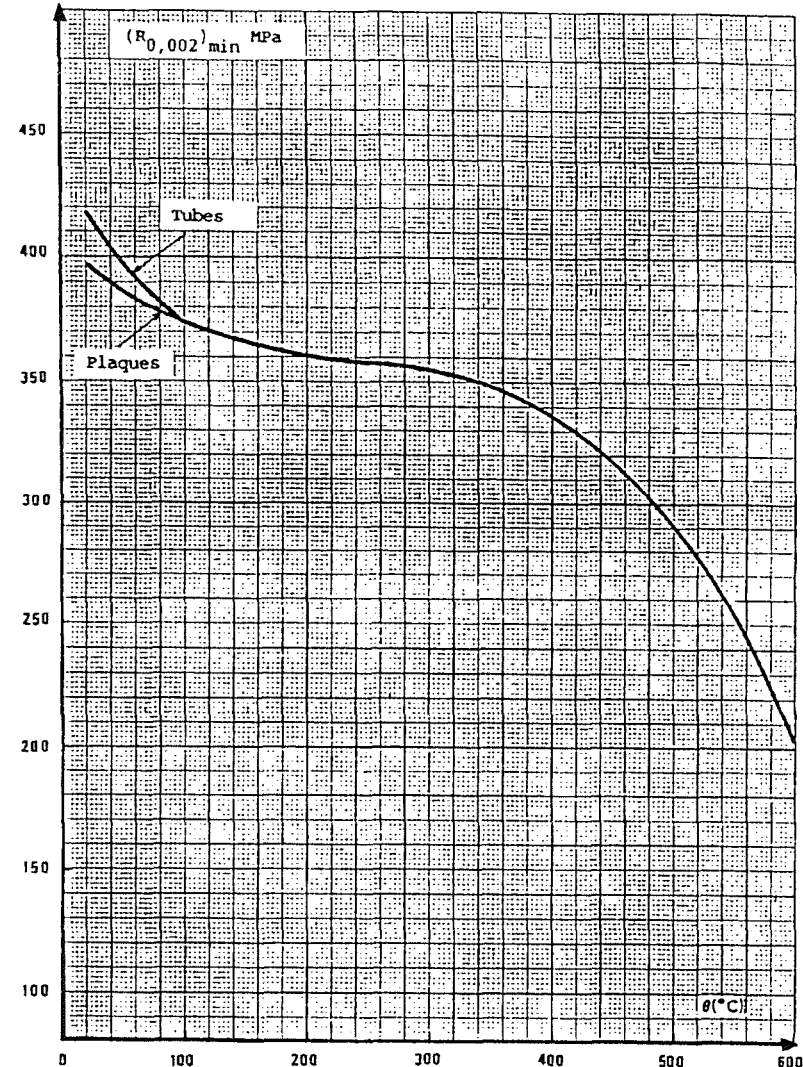


Figure A3.185.3.1.3
YIELD STRENGTH AT 0,2% OFFSET

A3.18S.3.2 MINIMUM AND AVERAGE TENSILE STRENGTH

The minimum tensile strength $(R_m)_{min}$ is given as a function of temperature θ by the following:

. Formula 3.2.1

$$(R_m)_{min} = 598,06 - 0,9922 \theta + 4,6386 \cdot 10^{-3} \theta^2 - 9,199 \cdot 10^{-6} \theta^3 + 4,535 \cdot 10^{-9} \theta^4$$

This formula is applicable for $20 < \theta < 600$

. Table 3.2.2

θ (°C)	20	50	100	150	200	250	300	350	400
$(R_m)_{min}$ MPa	580	559	536,5	525	519	514	506	493	471

θ (°C)	450	500	550	600
$(R_m)_{min}$ MPa	439	395	340	273

. Figure 3.2.3

The average tensile strength $(R_m)_{avg}$ is given as a function of temperature θ by:

. Formula 3.2.4

$$(R_m)_{avg} = 722,02 - 1,198 \theta + 5,60 \cdot 10^{-3} \theta^2 - 11,06 \cdot 10^{-6} \theta^3 + 5,475 \cdot 10^{-9} \theta^4$$

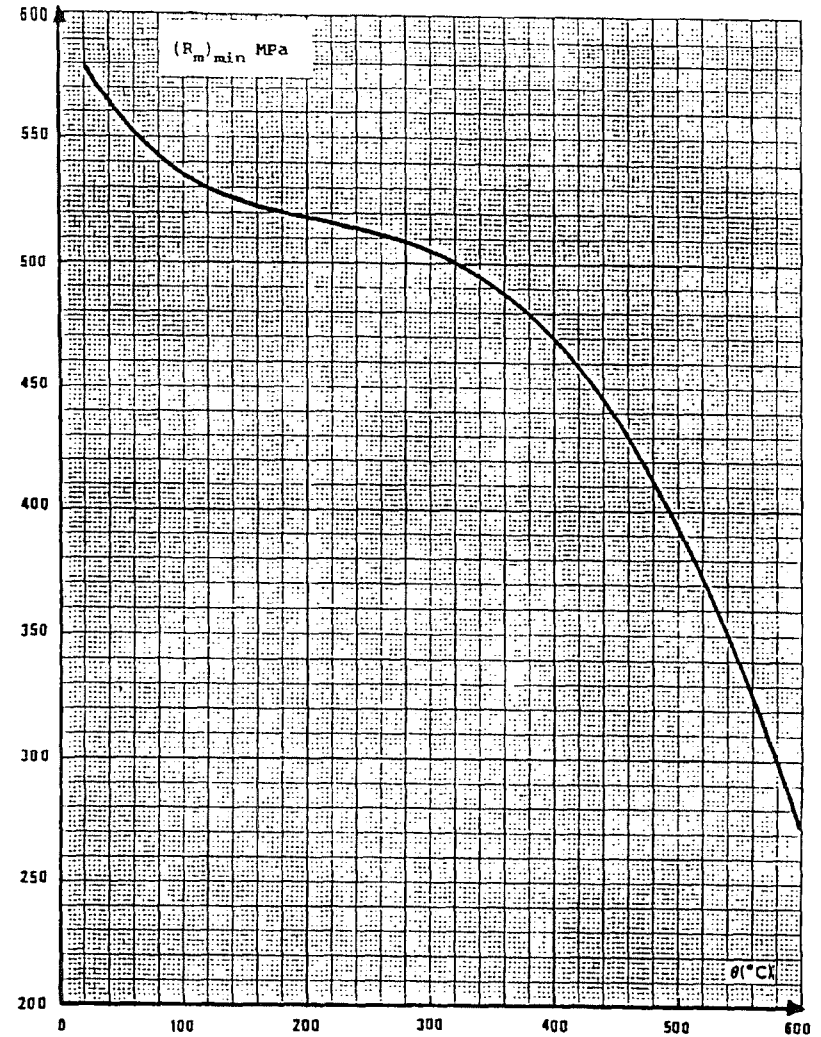


Figure A3.18S.3.2.3
MINIMUM TENSILE STRENGTH

A3.18S.4 NEGLIGIBLE CREEP CURVE (To be issued)

A3.18S.5 ANALYSIS DATA

A3.18S.5.1 VALUES OF S_m

The maximum allowable stress S_m is given as a function of temperature θ by the following:

Table 5.1.1

θ (°C)	20	50	100	150	200	250	300	350	400	450	500	550	600
S_m (MPa)	193	193	193	193	192	190	187	183	174	163	146	126	101

Figure 5.1.2

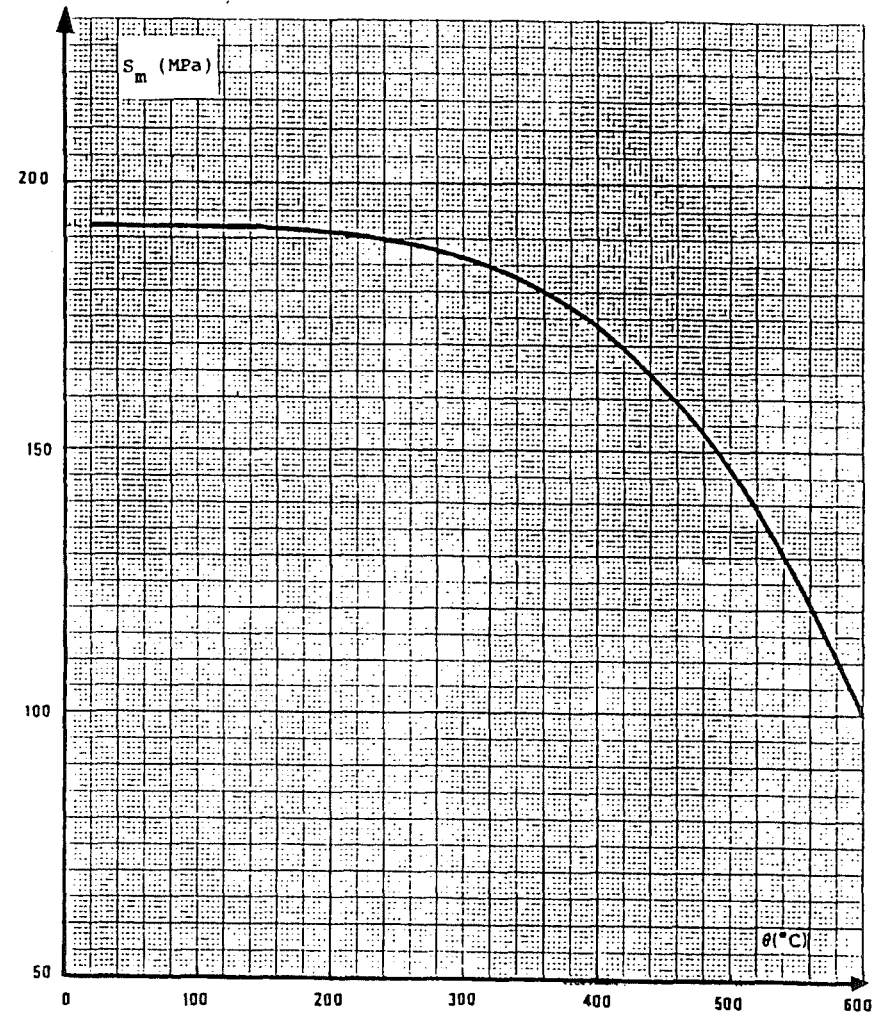


Figure A3.18S.5.1.2
ALLOWABLE STRESSES S_m

A3.18S.5.2 VALUES OF S_t

The maximum allowable stress S_t is given as a function of the temperature θ and time t by the following table or figure in which S_t is expressed in MPa, θ in °C and t in h:

- . Table 5.2.1
- . Figure 5.2.2

$t(h)$ $\theta(^{\circ}C)$	1	10	30	102	3×10^2	103	3×10^3	104	3×10^4	10^5	3×10^5
425		293	293	287	271	255	241	227	216	204	194
450		277	261	245	232	219	207	196	186	176	167
475		238	225	212	201	189	180	169	161	151	143
500		207	196	185	175	166	157	146	138	129	121
525		181	171	161	152	142	134	125	117	108	101
550		157	149	139	131	121	113	105	97	89	81
575		137	129	119	111	102	94	86	78	70	63
600		118	110	101	93	84	76	68	61	53	47
625		100	92	83	75	67	59	52	45	39	33
650		83	75	66	57	51	45	38	33	27	23
675		67	59	51	45	37	32	27	22		

Table A3.18S.5.2.1

MAXIMUM ALLOWABLE STRESS S_t IN MPa

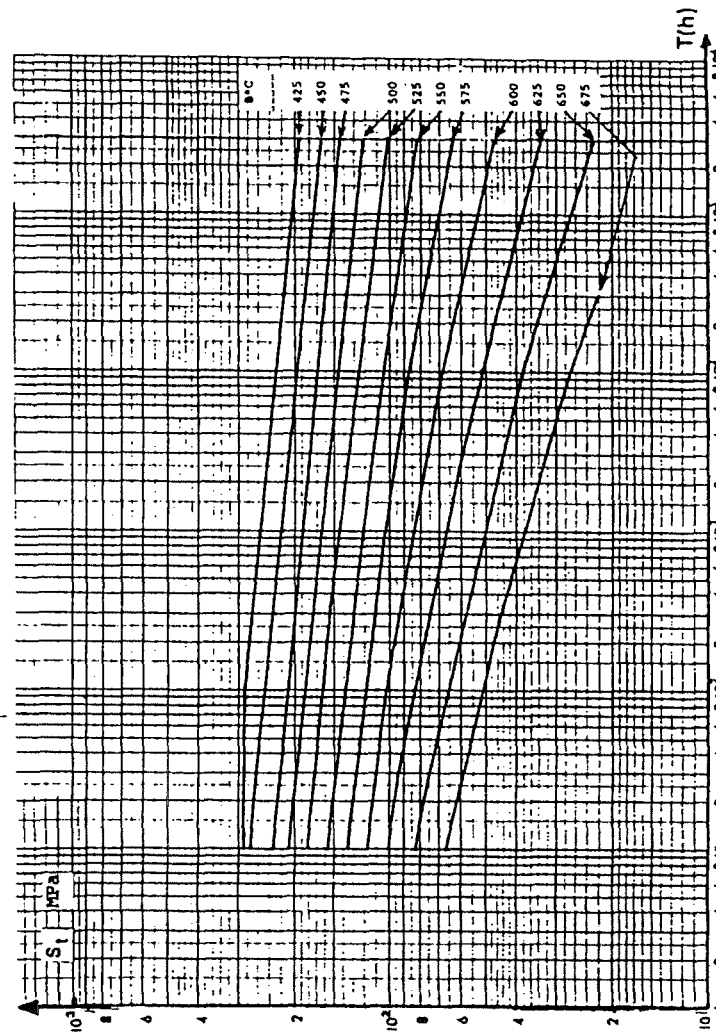


Figure A3.18S.5.2.2

MAXIMUM ALLOWABLE STRESSES S_t IN MPa

A3.6S.5.3 CREEP RUPTURE STRESS : S_r

The minimum value of the creep rupture stress S_r is given as a function of temperature θ and time t by the following:

- . Table 5.3.1
- . Figure 5.3.2

t(h) θ°C	1	10	30	102	3×10 ²	103	3×10 ³	104	3×10 ⁴	105	3×10 ⁵
425		439	439	430	406	382	362	341	324	307	292
450		415	392	368	348	328	311	294	279	264	251
475		357	338	318	301	284	270	254	241	227	215
500		311	294	277	262	247	233	219	207	194	182
525		272	257	241	228	213	201	187	175	162	151
550		238	224	209	196	182	170	157	145	133	122
575		206	193	179	167	153	141	129	117	105	95
600		177	165	151	139	126	114	102	91	80	71
625		150	138	124	112	100	89	78	68	59	50
650		124	112	99	88	77	67	57	49	40	34
675		100	89	77	67	56	48	40	33		

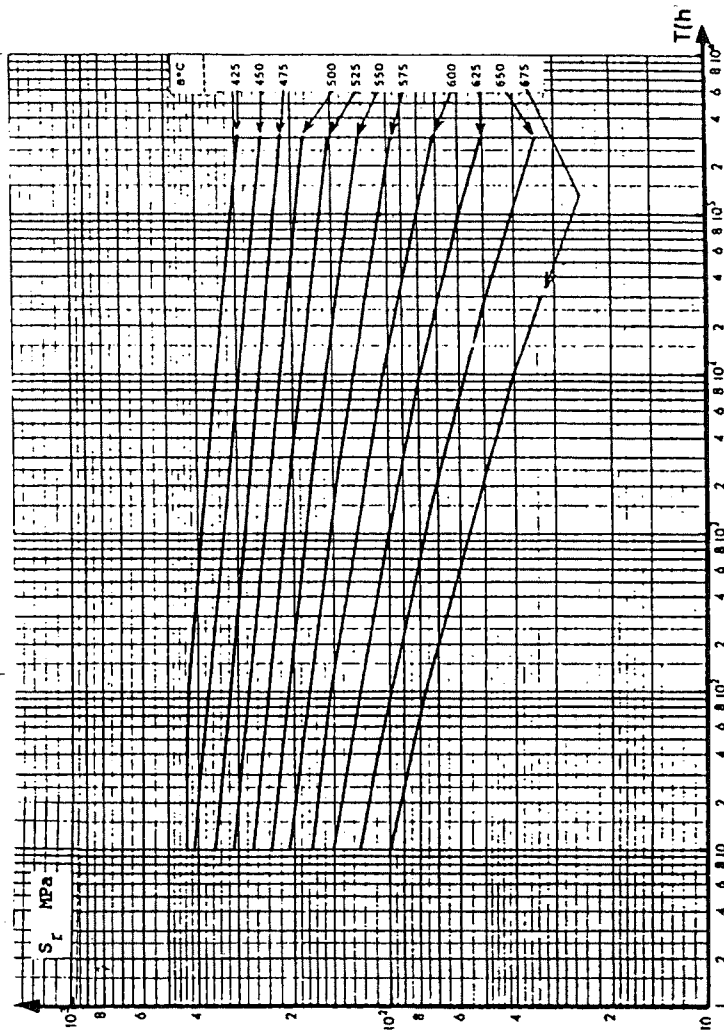


Table A3.18S.5.3.1

MINIMUM VALUES OF CREEP RUPTURE STRESS S_r (MPa)

Figure A3.18S.5.3.2

MINIMUM VALUES OF CREEP RUPTURE STRESS S_r (MPa)

A3.18S.5.4 SATURATION FATIGUE CURVES

To be issued.

A3.18S.5.5 ISOCHRONOUS CURVES, CREEP STRAIN

To be issued.

A3.18S.5.6 STRESSES S_{rh} AND S_{rc}

To be issued.

A3.18S.5.7 SYMMETRIZATION COEFFICIENT K_s

To be issued.

A3.18S.5.8 FATIGUE - CREEP INTERACTION DIAGRAM

To be issued.

A3.18S.5.9 CYCLE CURVES, VALUES OF K_1 and K_2

To be issued.

A3.6S.6 ANALYSIS DATA

A3.6S.6.1 MONOTONIC TENSILE HARDENING RULE

A3.6S.6.1.1 For plastic strain limited to 1,7%

The average tensile hardening rule is given by the following:

. Formula 6.1.1.1

$$(\sigma)_{avg} = (R_{0,002})_{avg} \times C(\theta) \times \epsilon_p^n$$

with:

$$(R_{0,002})_{avg} = 564,25 - 0,7108\theta + 2,6894 \cdot 10^{-3}\theta^2 - 3,8267 \cdot 10^{-6}\theta^3$$

In this formula, ϵ_p (%) designates the plastic strain induced by stress σ (MPa) at temperature θ ($^{\circ}C$).

This formula is applicable for:

θ	20	200	300	400	450	500	525	550	550
C	1,0855	1,088	1,0985	1,1085	1,119	1,0985	1,0985	1,0605	1,0435
n	0,0511	0,0525	0,0585	0,0640	0,0690	0,0582	0,0451	0,0367	0,0264

The formula expressing the minimum hardening rule is obtained by replacing $(R_{0,002})_{avg}$ by $(R_{0,002})_{min}$ in the above formula.

. Table 6.1.1.2

. Figures 6.1.1.3

A3.18S.6.1.2 For total strain reaching the distributed elongation

To be issued.

$\theta = 20\text{ }^{\circ}\text{C}$			$\theta = 200\text{ }^{\circ}\text{C}$			$\theta = 300\text{ }^{\circ}\text{C}$		
σ (MPa)	ϵ_p (%)	ϵ_t (%)	σ (MPa)	ϵ_p (%)	ϵ_t (%)	σ (MPa)	ϵ_p (%)	ϵ_t (%)
400	0,00038	0,19455	350	0,00023	0,18030	350	0,00065	0,18690
425	0,00124	0,20755	375	0,00087	0,19379	375	0,00210	0,20165
450	0,00381	0,22225	400	0,00297	0,20876	400	0,00632	0,21918
475	0,01097	0,24155	425	0,00942	0,22807	425	0,01781	0,24398
500	0,02993	0,27265	450	0,02798	0,25949	450	0,04731	0,28678
510	0,04409	0,29166	480	0,04252	0,27917	480	0,06888	0,31366
520	0,06448	0,31690	470	0,06404	0,30584	470	0,09946	0,34957
530	0,09360	0,35088	480	0,09563	0,34257	480	0,14253	0,39796
540	0,13494	0,39708	490	0,14162	0,39371	490	0,20274	0,46343
550	0,19324	0,48023	500	0,20807	0,46531	500	0,28633	0,55240
560	0,27493	0,54678	510	0,30339	0,56577	510	0,40163	0,67302
570	0,38874	0,66544	520	0,43914	0,70666	520	0,55967	0,83639
580	0,54635	0,82790	530	0,63113	0,90383	530	0,77499	1,05703
590	0,76340	1,04981	540	0,90103	1,17884	540	1,06663	1,35399
600	1,06070	1,35197	550	1,27790	1,56086	550	1,45845	1,75213
610	1,46580	1,76192	560	1,80104	2,08914	555	1,70353	1,99688
615	1,71971	2,01825						

Table A3.1B5.6.1.1.2

MEAN STRESS σ INDUCING PLASTIC STRAIN ϵ_p AND TOTAL STRAIN ϵ_t AT TEMPERATURE θ

$\theta = 400\text{ }^{\circ}\text{C}$			$\theta = 450\text{ }^{\circ}\text{C}$			$\theta = 500\text{ }^{\circ}\text{C}$		
σ (MPa)	ϵ_p (%)	ϵ_t (%)	σ (MPa)	ϵ_p (%)	ϵ_t (%)	σ (MPa)	ϵ_p (%)	ϵ_t (%)
300	0,00021	0,16654	300	0,00075	0,16907	275	0,00028	0,16743
325	0,00074	0,17984	325	0,00240	0,18475	300	0,00126	0,17269
350	0,00235	0,19523	350	0,00703	0,20341	320	0,00382	0,18668
375	0,00689	0,21355	370	0,01574	0,22334	330	0,00648	0,19506
400	0,01888	0,23931	390	0,03377	0,25259	340	0,01082	0,20511
420	0,04044	0,27190	410	0,06973	0,29977	350	0,01780	0,21780
440	0,08361	0,32609	420	0,09889	0,33454	360	0,02888	0,23459
450	0,11875	0,36674	430	0,13910	0,38036	370	0,04623	0,25766
460	0,16736	0,42086	440	0,19413	0,44100	380	0,07308	0,29023
470	0,23414	0,49315	450	0,26890	0,52139	390	0,11417	0,33703
480	0,32526	0,58978	460	0,36982	0,62792	400	0,17635	0,40492
490	0,44879	0,71882	470	0,50515	0,76885	410	0,26948	0,50377
500	0,61522	0,89076	480	0,68547	0,95478	420	0,40763	0,64763
510	0,83811	1,11917	490	0,92433	1,19925	430	0,61061	0,85632
520	1,13493	1,42149	500	1,23891	1,51944	440	0,90620	1,15763
530	1,52801	1,82008	510	1,65095	1,93709	450	1,33301	1,58015
535	1,76927	2,06410	512	1,74734	2,03461	455	1,61156	1,87156

Table A3.1B5.6.1.1.2 (cont. 1)

MEAN STRESS σ INDUCING PLASTIC STRAIN ϵ_p AND TOTAL STRAIN ϵ_t AT TEMPERATURE θ

$\theta = 525\text{ }^{\circ}\text{C}$		
σ (MPa)	ϵ_p (%)	ϵ_t (%)
275	0,00016	0,16289
300	0,00114	0,17865
320	0,00476	0,19411
330	0,00943	0,20469
340	0,01829	0,21947
350	0,03479	0,24189
360	0,06502	0,27803
370	0,11942	0,33836
380	0,21583	0,44069
390	0,38413	0,61490
395	0,50963	0,74336
400	0,67374	0,91043
405	0,88761	1,12726
410	1,16542	1,40803
415	1,52515	1,77071
417	1,69687	1,94362

$\theta = 550\text{ }^{\circ}\text{C}$		
σ (MPa)	ϵ_p (%)	ϵ_t (%)
270	0,00017	0,16581
280	0,00045	0,17223
290	0,00118	0,17909
300	0,00298	0,18702
310	0,00727	0,19746
320	0,01728	0,21360
330	0,03999	0,24245
335	0,06026	0,26578
340	0,09025	0,29884
345	0,13437	0,34603
350	0,19691	0,41364
355	0,29283	0,51062
360	0,42875	0,64961
365	0,62448	0,84841
370	0,90493	1,13192
375	1,30480	1,53486
380	1,87227	2,10540

$\theta = 600\text{ }^{\circ}\text{C}$		
σ (MPa)	ϵ_p (%)	ϵ_t (%)
230	0,00013	0,15244
240	0,00063	0,15957
250	0,00297	0,16853
255	0,00628	0,17515
260	0,01310	0,18529
265	0,02696	0,20245
270	0,05472	0,23353
275	0,10965	0,29177
280	0,21699	0,40242
282	0,28413	0,47089
284	0,37135	0,55943
286	0,48442	0,67383
288	0,63078	0,82148
290	0,81980	1,01185
292	1,06358	1,25696
294	1,37740	1,57210
296	1,78070	1,97672

Table A3.1BS.6.1.1.2 (cont. 2)
MEAN STRESS σ INDUCING PLASTIC STRAIN ϵ_p AND TOTAL STRAIN ϵ_t AT TEMPERATURE θ

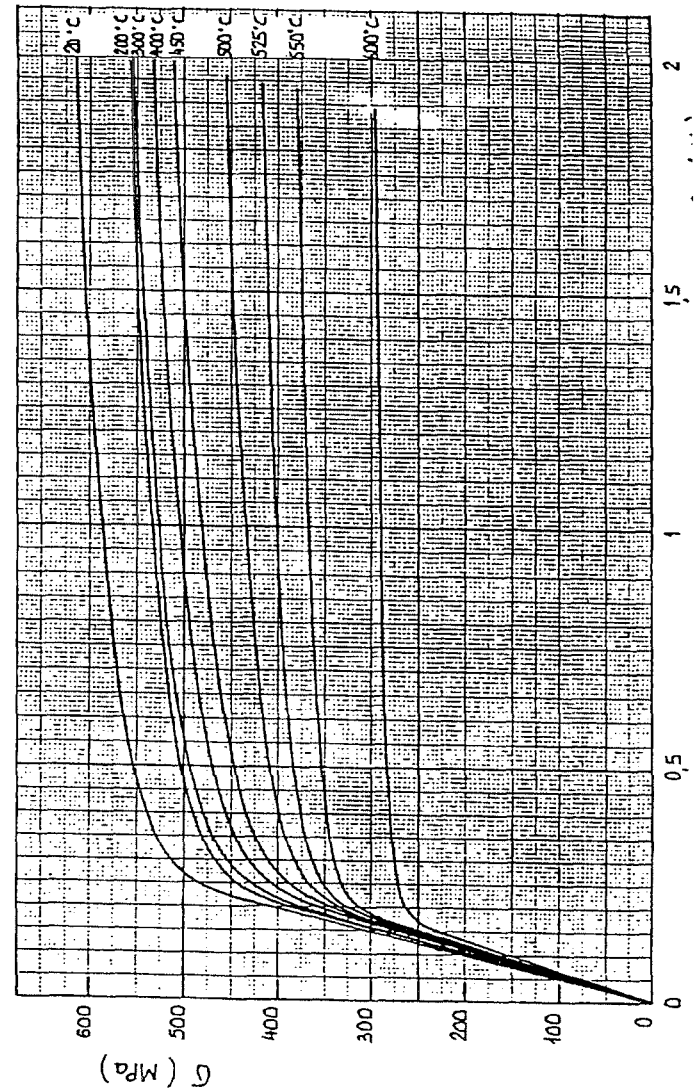


Figure A3.1BS.6.1.1.3
MEAN TENSILE CURVES

A3.18S.6.2 Bilinear curves

To be issued.

A3.18S.6.3 Creep-strain law

The mean value of the minimum creep rate is given by:

. formula 6.3.1

$$\log \epsilon_m = 27,3 + 0,025 265 \sigma + 3,2172 \log \sigma - 35,594/T$$

where

ϵ_m = minimum creep rate in % h⁻¹

σ = stress in MPa

T = temperature in degrees Kelvin T = 273 + θ

This formula is applicable for $480 \leq \theta \text{ } ^\circ\text{C} \leq 700$

$$10^{-5} \leq \epsilon_m (\%h^{-1}) \leq 10^{-1}$$

A3.18S.6.4 Fatigue curve

To be issued.

A3.18S.6.5 Maximum allowable strain : D_{max}

D_{max} = 1%.

A3.17S.6 ANALYSIS DATA (Cont.)

A3.17S.6.1 TENSILE HARDENING RULE

(Not supplied)

A3.17S.6.2 BILINEAR CURVES

(Not supplied)

A3.17S.6.3 CREEP STRAIN LAW

(Not supplied)

A3.17S.6.4 FATIGUE CURVES

The allowable strain range is given as a function of temperature and the number of cycles by the following:

- Table 6.4.1 (to be issued)
- Figure 6.4.2

Where applicable, the fatigue curves may be extrapolated for numbers of cycles greater than 10^6 by a straight line passing through the last two points of each curve in the $N\Delta\epsilon$ log-log diagram.

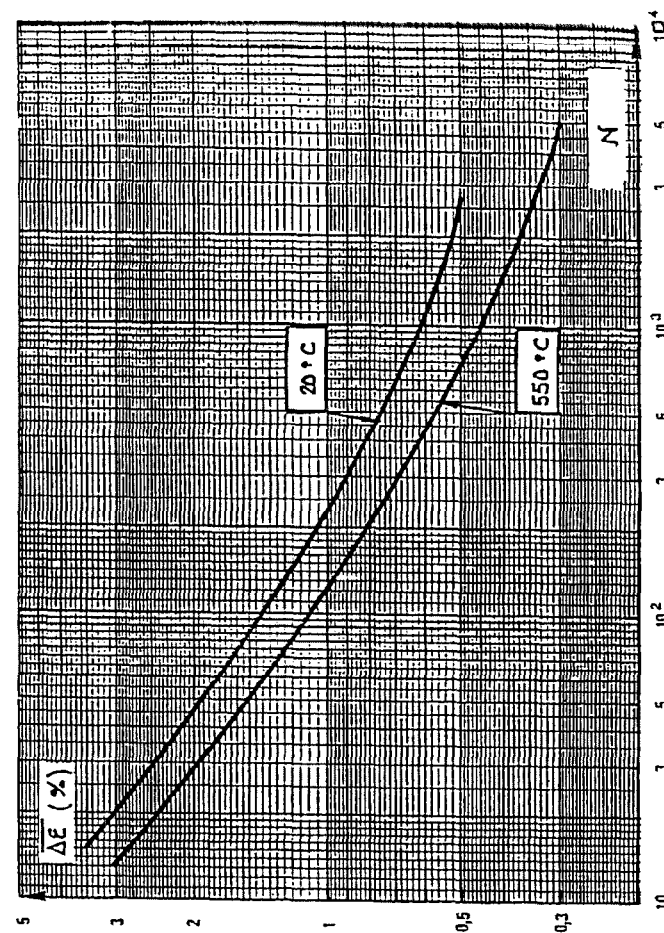


Figure A3.17S.6.4

FATIGUE CURVES

$\Delta\epsilon$ IN %, FUNCTION OF NUMBER OF CYCLES N

Appendix B Li_4SiO_4 pebble bed

Li_4SiO_4 has been chosen as reference material for the HCPB DEMO Blanket. They have to be placed in a gap of about 10 mm width between two cooling plates, and, to have high filling in the pebble bed, it is necessary to have pebbles with diameter smaller than 1 mm. On the other hand the pebbles should not be too small to avoid large pressure drops in the tritium purging gas flow. Therefore small pebbles with diameter in the range 250-630 μm are used. The pebbles are produced by melting a mixture of Li_4SiO_4 and SiO_2 and then spraying with a air jet the molten material. The pebbles contain an excess of SiO_2 over the stoichiometric composition ($\text{Li}_4\text{SiO}_4 + 2.2$ wt % SiO_2) [1]. The density of the Li_4SiO_4 pebbles is 98 % of the theoretical value [2].

Pebble characterization and mechanical properties

Pebbles produced by spraying liquid material have a dendritic structure with grains of up to 5 μm and 15 μm length. The dendritic structure spreads out over the whole cross section of the pebbles. The pebbles may also contain cracks because of the rapid quenching from melting temperature during the production process. Most of cracks observed by ceramographic analysis are microcracks that develop along grain boundaries during quenching.

In order to characterise the mechanical stability of the pebbles several different tests have been performed. First a simple test is applied to 0.5 mm diameter pebbles. A continuously increasing weight load is imposed by a piston to a single pebble until it breaks. The crush tests are performed at room temperature, and the measured fracture load is an important parameter in the optimisation of the fabrication route [3].

It is important to show that during blanket operation not too many pebbles break and powder is formed which could reduce or impede the flow of the gas purging the tritium produced in the Li_4SiO_4 . Particularly dangerous for the pebble integrity are rapid temperature changes. A series of thermal cycles tests have been thus performed for beds of Li_4SiO_4 . In these tests no attempt is made to obtain the maximum packing factor of the bed to be tested. This is done to avoid stresses caused by the relative dimensional variations between pebble bed and container during the temperature transients. The results of these experiments is that the pebbles can sustain very high thermal shocks (up to 60 $^\circ\text{C/s}$ [3]).

The thermomechanical behaviour of Li_4SiO_4 pebble beds is also investigated in tests where the pebble beds were axially loaded in cylindrical containers and the axial deformation was measured (Oedometer tests). These experiments were carried on at different temperatures and the Young modulus of the bed was obtained. First thermal creep data were also obtained [4].

The behaviour of Li_4SiO_4 pebbles in blanket relevant conditions was investigated in long term annealing tests (96 days at 970 $^\circ\text{C}$ and in He+0.1 vol % H_2 atmosphere) [5]. Before starting the experiment the pebbles were annealed at 1000 $^\circ\text{C}$ in air for two weeks in order to eliminate the high temperature metastable phase $\text{Li}_6\text{Si}_2\text{O}_7$, which is formed due to the rapid quenching in the production process, and decomposes completely into Li_4SiO_4 and Li_2SiO_3 at high temperatures. Afterwards,

during the long term annealing, the only significant change in orthosilicate pebbles was the diffusion of the present Li_2SiO_3 through the material.

Bed thermal conductivity

For a relevant bed configuration the bed thermal conductivity has been measured [6] and the heat transfer coefficient at the wall of the bed container has been calculated with the Schlünder correlation [7]. The measured thermal conductivity data have been correlated by a linear equation. The void fraction of the pebbles was 36 %. During the measurements helium was flowing through the bed with very low velocity, so that the heat transfer parameters were not affected by helium convection. For helium pressure higher than 1 bar the thermal conductivity is not function of the pressure of the gas, i.e. there is no Smoluchowski effect.

Lithium transport

The total lithium species vapour pressure in equilibrium with the $\text{Li}_4\text{SiO}_4 + 2.2 \text{ wt } \% \text{ SiO}_2$ pebbles in presence of the reference purge gas atmosphere ($\text{He} + 0.1 \text{ vol. } \% \text{ H}_2$) is 10^{-1} Pa at $1020 \text{ }^\circ\text{C}$ [8]. This partial pressure and thus the temperature correspond to a lithium transport over the 20000 hours of the DEMO blanket operation time of 0.1 %.

Compatibility with structural material

Out-of-pile tests of Li_4SiO_4 with austenitic steel 316L and with martensitic steel 1.4914 in presence of NiO (oxygen source) and of water vapour up to 100 Pa partial pressure indicate an upper temperature limit of $700 \text{ }^\circ\text{C}$ [9]. The results of the closed capsule irradiation COMPLIMENT [10] are in good agreement with the out of pile experiments.

Tritium Residence Time

Tritium residence time is the key parameter to calculate the tritium inventory in the ceramic materials. In the recent years several expressions have been formulated based on fitting or extrapolation of existing data. For the three ceramic materials, the following correlation of the tritium residence time τ [s] as function of the temperature T [K] has been used in the design calculations for HCPB blanket concepts [11]:

$$\tau = 4.608 \cdot 10^{-2} \cdot \exp(9720/T) \quad \text{for } \text{Li}_4\text{SiO}_4$$

$$\tau = 7.182 \cdot 10^{-3} \cdot \exp(10315/T) \quad \text{for } \text{Li}_2\text{TiO}_3$$

$$\tau = 1.135 \cdot 10^{-2} \cdot \exp(8581/T) \quad \text{for } \text{Li}_2\text{ZrO}_3$$

The tritium inventory I [g] in the breeder material can be calculated as follow

$$I = \int_{\Omega} \dot{m}(\vec{r}) \cdot \tau(T(\vec{r})) dV$$

with

$\dot{m}(\vec{r})$ local tritium production [$\text{g s}^{-1} \text{m}^{-3}$]

$\tau(T)$ tritium residence time [s] as function of the breeder temperature T [K].

The amount of tritium in the ceramic materials is almost negligible compared to the whole inventory of tritium in the blanket which is essentially determined by the tritium trapped in the beryllium. In particular the inventory in ceramics is less than that part of the tritium inventory in beryllium which is due to chemical trapping and can immediately be released during an accidental temperature excursion.

References

- [1] M. Dalle Donne et al., KfK 5429, Nov. 1994.
- [2] G. Schumacher et al., Improvement of the mechanical stability of lithium orthosilicate pebbles, Fusion Engineering and design 17 (1991) 31-36, p. 31.
- [3] M. Dalle Donne et al., Development work for lithium orthosilicate pebbles, Proceedings of the 19th SOFT, Lisbon, 16-20 Sept. 1996, p. 1483.
- [4] J. Reimann et al., 'Thermomechanical behaviour of ceramic breeder pebble beds', Proceedings of the CBBI-7, Petten (Holland), September 1998.
- [5] G. Piazza et al., 'Long term annealing of ceramic breeder pebbles for the HCPB DEMO blanket', Proceedings of the CBBI-7, Petten (Holland), September 1998.
- [6] G. Piazza, Nuclear Fusion Project annual report of the association Forschungszentrum Karlsruhe/EURATOM, January 1997.
- [7] M. Dalle Donne et al., Heat transfer and technological investigations on mixed beds of beryllium and Li_4SiO_4 pebbles, Journal of Nuclear Materials 212-215 (1994) 872-876.
- [8] R.-D. Penzhorn et al., Thermodynamic study of gas/solid reactors at the surface of Li_4SiO_4 in view of blanket sweep gas chemistry, 17th SOFT, Rome, 14-18 Sept. 1992, p. 1389.
- [9] P. Hofmann et al., chemical compatibility of oxide breeder materials with cladding steels, 17th SOFT, Rome, 14-18 Sept. 1992, p. 1374.
- [10] W. Dienst et al., Strength change and chemical reactivity of ceramic breeder materials near operation conditions, Journal of Nuclear Material, 212-215 (1994), p. 891
- [11] E.U. Contribution to the ITER MPH: Ceramic Breeder Materials. Compiled by N. Roux. Report of the Commissariat À L'Énergie Atomique, Saclay (France), April 1998.

Appendix C Beryllium pebble bed

Beryllium is a very effective neutron multiplier. Solid breeder blankets with lithiated ceramics as breeder and steel as structural material require beryllium to obtain a tritium breeding ratio sufficiently great to compensate for uncertainties in the calculations and for the tritium losses. In the present design the beryllium is used in form of small pebbles. This offers various advantages. Under neutron irradiation beryllium becomes brittle and swells. Within small pebbles the temperature differences in the pebble are small, thus the stresses caused by thermal gradients and by different swelling rates (swelling is temperature dependent) are considerably smaller. Because it is important to achieve a high beryllium density in the blanket, a binary bed of larger and smaller beryllium pebbles is used. The main structure of the pebble bed is given by the larger pebbles with a packing factor of 63.3%. In the space between them are placed the smaller beryllium pebbles with a packing factor of 17.5% [1]. The larger pebbles (diameter \approx 2 mm), which are fabricated by melting, are a relatively inexpensive intermediate product of the beryllium fabrication route, called Magnesium Reduction Method (MRM). On the other hand the smaller pebbles can be produced either by Melting and Spraying (MS) or by the Rotating Electrode Method (REM).

Pebble characterization and mechanical behavior [2]

The larger 2 mm MRM pebbles have a relatively large number of surface indentations. Optical microscopy revealed large pores of various size and a microporosity usually oriented along the crystal axis perpendicular to the basal plane. The average open porosity of the pebbles is 0.57% and the closed porosity is 0.84%. The smaller MS pebbles (0.1 - 0.2 mm) have an average open porosity of 0.86% and an average closed porosity of about 2.4%. Insoluble impurities have been usually observed on the grain boundaries, while iron and chrome are almost exclusively present in solid solution in the beryllium-matrix. The external surface of the large beryllium pebbles is usually covered by a 2 μ m thick SiO₂ layer and/or a fluorine layer (probably BeF₂) the thickness of which is generally lower than 2 μ m. Two extraneous phases are present in almost all the analyzed pebbles. Mostly a round bright phase looking like an eutectic stored in the beryllium matrix and occasionally a dark square phase which appears as a primary precipitated phase has been observed. The dominant precipitated phases are Be₁₃Mg, Be₁₃(Mg,Zr,U), Mg₂Si and Al₂O₃.

Almost all REM pebbles have a big pore at their center, produced by the volume reduction due to solidification (pebble density = 0.97% TD). The sphericity and the grain size were measured from the cross section of beryllium pebble by optical microscopy. The specific surface is measured by the BET method with nitrogen gas.

The mechanical behavior of the unirradiated MRM pebbles has been investigated by submitting them to compressive loads at room temperature. The plastic deformations of the pebbles have been measured and correlated with the applied loads. Relatively large variations have been observed in the mechanical response of the pebbles. However, probably due to the very small amount of BeO impurities, all the pebbles show a high ductility at room temperature. Pebbles loaded up to 400 N show

diameter reductions up to 13% but, in spite of evident large plastic deformations, no fracturing or crack formation has been observed. Pebbles loaded with 800 N (deformation up to 25%) or more, reveal cracks on their meridian planes.

The MRM pebbles irradiated in the HFR reactor at 420-530 °C and with a neutron fluence of 1.2×10^{21} n/cm² (E>1 MeV) have mechanical properties quite similar to the unirradiated ones.

The compression tests carried out at room temperature for the unirradiated REM pebbles and for REM pebbles irradiated in JMTR at 330 °C and with a neutron fluence of 1.3×10^{21} n/cm² (E>1 MeV) indicate that the fracture loads (about 150 N) of REM pebbles of 0.9 mm are unaffected by irradiation, while the fracture displacement decreased from 0.17 to 0.11 mm showing a certain degree of embrittlement.

Pebble bed heat transfer parameters

The heat transfer parameters (i.e. thermal conductivity and heat transfer coefficient) of the binary beryllium pebble bed have been obtained by experimental investigations at the Forschungszentrum Karlsruhe (FZK) and correlated as a function of temperature and of the interference between bed and constraining walls, due to the differential thermal expansion. In this test the beryllium pebble bed was contained in the annulus between an outer steel tube and an heater rod. The correlations allow an easy application for the calculations in the blanket.

However, these correlations have been obtained for a very stiff containment, so that they can be directly applied only in cases where very small deformations of the containing walls due to the pressure exerted by the bed are expected. This is the case, for instance, where containing plates have similar pebble beds on both sides.

Two kind of experiments were performed:

- a series of experiments with a thermal insulation on the outside surface of the outer tube. The heater rod was heated to temperatures ensuring that the differential thermal expansion between outer tube and beryllium pebble is zero, so that no constraint is exerted on the pebble bed;
- a series of experiments with a water cooling on the outside surface of the outer tube to ensure that various levels of constraint are exerted on the pebble bed.

The differential thermal expansion between bed and bed containment walls ("interference") produces a compression of the bed which increases the contact surface area of the pebbles.

Figure 1 shows the thermal conductivity of the binary pebble bed without constraint ($\Delta\ell/\ell = 0$) versus the average pebble bed temperature [3]. The bed thermal conductivity varies very little with bed temperature. This is because the beryllium thermal conductivity decreases with temperature, whereas the thermal conductivity of helium increases with temperature and the two effects somewhat compensate each other.

Figure 2 shows the results of the experiments with water cooling, i.e. with pebble bed constraint ($\Delta\ell/\ell > 0$), in the plots of Be pebble bed thermal conductivity $K/K(\Delta\ell/\ell = 0)$ versus the percentage ratio of the interference $\Delta\ell$ to the width of the pebble bed ℓ . As expected, the effect of $\Delta\ell/\ell$ [%] is linear, as the increase of the ratio of the contact surface to the cross section of the pebbles is also linear. Because this increase is

quite small in comparison to the pebble diameter, and neglecting a second order contribution, it is proportional to $\Delta\ell/\ell$ [%].

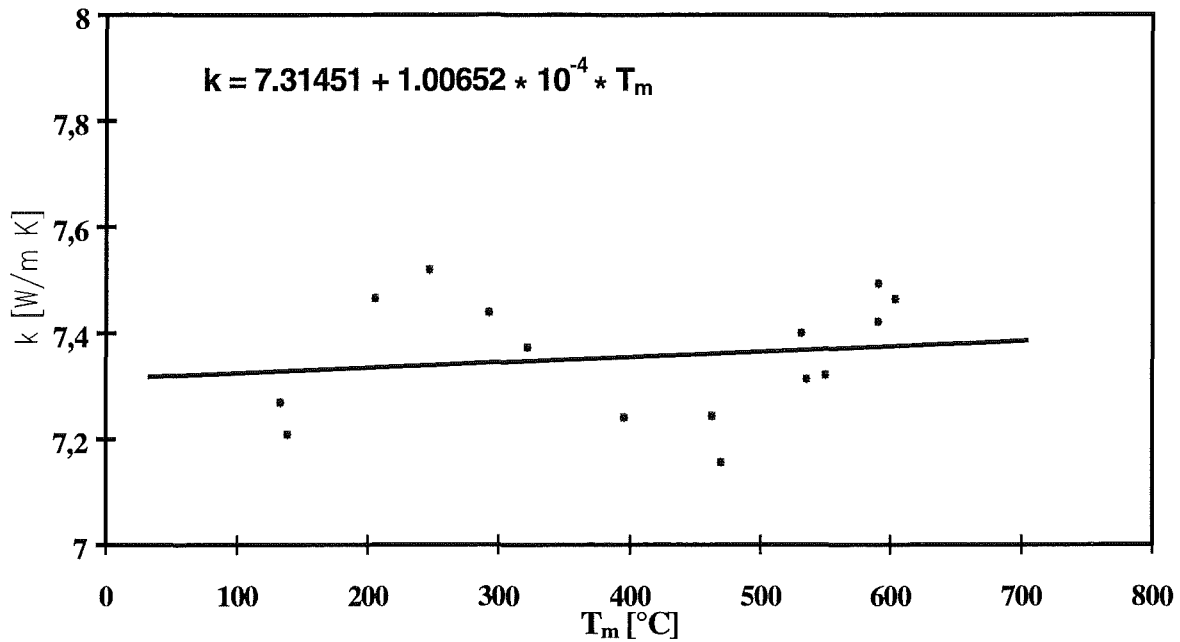


Figure 1: Thermal conductivity as a function of the mean bed temperature (case without constraint: $\Delta\ell/\ell = 0$).

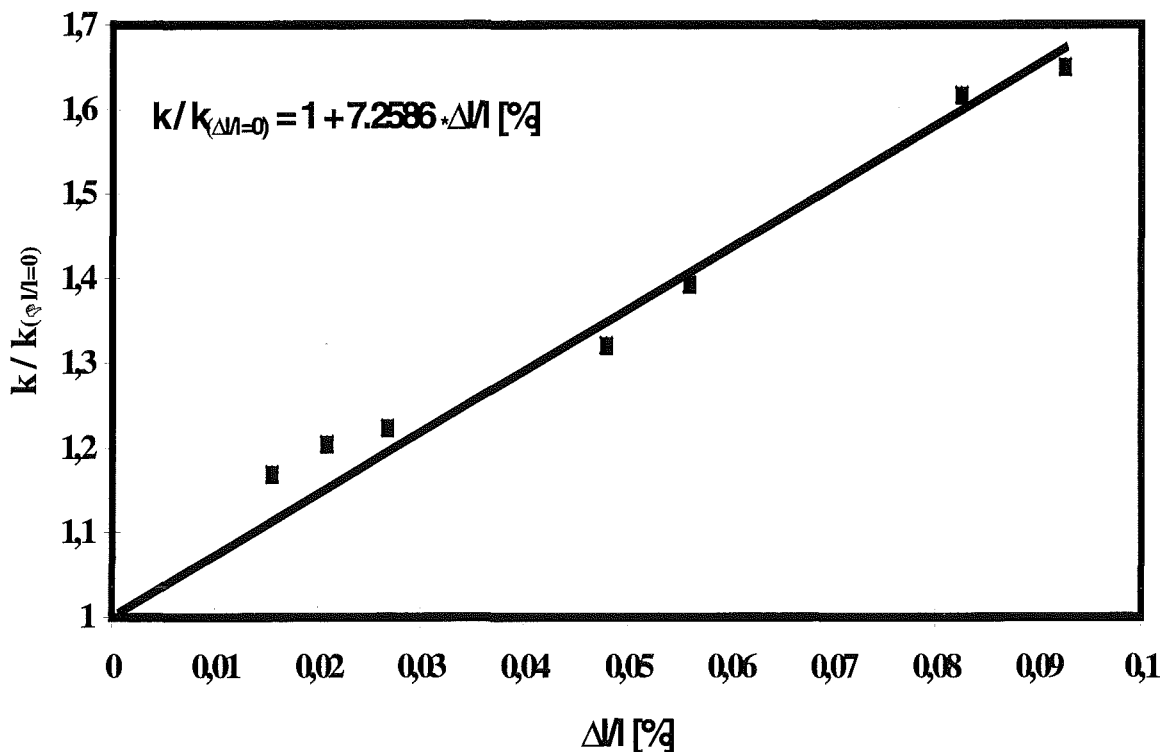


Figure 2: Thermal conductivity as a function of $\Delta\ell/\ell$ (case with constraint: $\Delta\ell/\ell \neq 0$).

The equation correlating the experimental results for the thermal conductivity and suggested for ITER design purposes is:

$$k [W / mK] = \left(7.3145 + 1.00652 \cdot 10^{-4} \cdot T_m \right) \cdot \left(1 + 7.259 \cdot \frac{\Delta \ell}{\ell} [\%] \right)$$

In case of $\Delta \ell / \ell = 0$ the experimental results for the temperature dependence of k are valid for T_m in the temperature range 130°C - 600°C. The values for the case of $\Delta \ell / \ell > 0$ are measured in the temperature range between 10° C and 160° C and are valid for $\Delta \ell / \ell$ [%] in the range 0-0.1 %.

Figure 3 shows the heat transfer coefficient at the inner tube wall of the pebble bed without constraint ($\Delta \ell / \ell = 0$) versus the temperature of the inner tube wall [3].

Figure 4 shows the results of the experiments with water cooling, i.e. with pebble bed constraint ($\Delta \ell / \ell > 0$), in the plot of Be pebble bed/wall contact heat coefficient $\alpha / \alpha (\Delta \ell / \ell = 0)$ versus the percentage ratio of the interference $\Delta \ell$ to the width of the pebble bed ℓ . As expected, also for the heat transfer coefficient the effect of $\Delta \ell / \ell$ [%] is linear, however only for $\Delta \ell / \ell$ [%] > 0.015 (see Figure 4), the increase for $\Delta \ell / \ell$ [%] < 0.015 being much stronger. More R&D work is necessary to determine the reasons for such a behavior at low values of $\Delta \ell / \ell$.

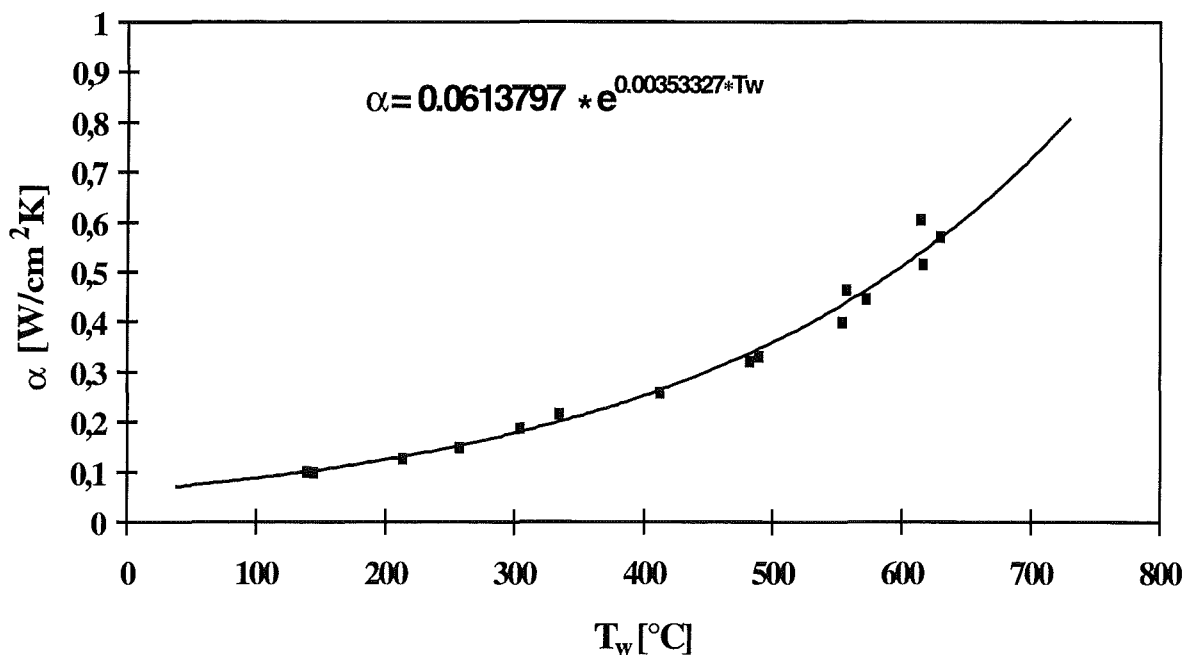


Figure 3 Heat transfer coefficient at the wall as a function of the wall temperature (case without constraint: $\Delta \ell / \ell = 0$).

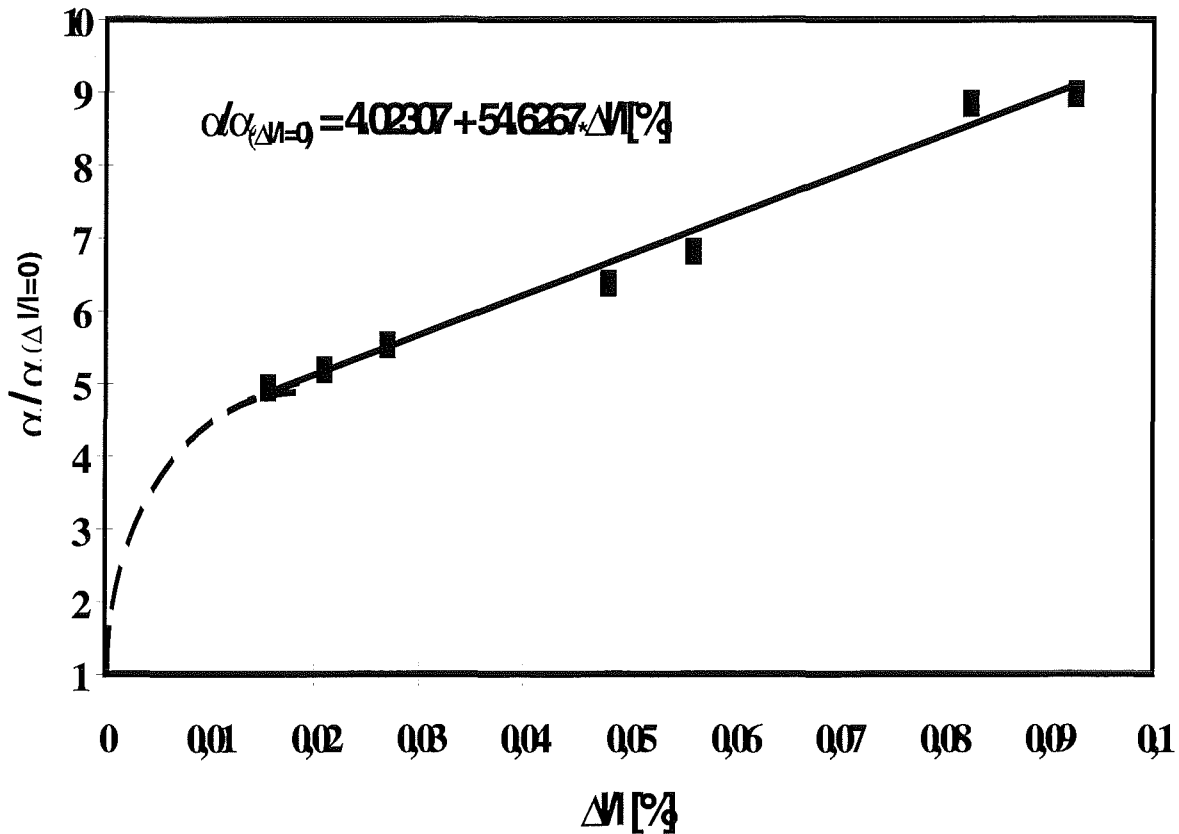


Figure 4: Heat transfer coefficient at the wall as a function of $\Delta l/l$ (case with constraint: $\Delta l/l \neq 0$).

The equation correlating the experimental results for the heat transfer coefficient and suggested for ITER design purposes is:

$$\alpha [W / cm^2 K] = 6.138 \cdot 10^{-2} \cdot f \cdot \exp(0.0035332 \cdot T_w)$$

with:

$$f = 4.023 + 54.63 \cdot \frac{\Delta l}{l} [\%] \quad \text{for } \frac{\Delta l}{l} \geq 0.015$$

and

$$f = 1 \quad \text{for } \frac{\Delta l}{l} [\%] < 0.015$$

In case of $\Delta l/l = 0$ the experimental results for the temperature dependence of α are valid for T_w in the temperature range 130°C-600 °C. The values for the case of $\Delta l/l > 0$ are measured in the temperature range between 10° C and 160° C and are valid for $\Delta l/l$ [%] in the range 0-0.1 %.

In case considerable deformations of the containing walls are expected, also the pressure effects have to be investigated experimentally. The results of these

investigations, together with the correlations from Ref. 3 (possibly extended to higher values of constraint) would allow to solve the problem also in the more general case.

Experiments with the measurement of the pressure on the containing walls are presently on going at FZK.

Swelling

The helium produced mainly by the reaction $9\text{Be}(n,2n)2x4\text{He}$ is the dominant cause of beryllium swelling. The blanket-end-of-life beryllium swelling has been calculated for the ITER Breeding Blanket with the use of older pebble bed heat transfer correlations obtained with the extrapolation of experimental data obtained for mixed beds of beryllium and Li_4SiO_4 pebbles [4]. The maximum calculated swelling (for the present reference design conditions of the HCPB TBM) was about 1%, i.e. considerably smaller than the pebble bed void fraction (20%). These calculations should be repeated with the new correlations obtained recently [3] or, even better, with the correlations of the experimental data which should be obtained in 1999.

Compatibility with structural materials

Under the conditions of high temperature and long heating time typical of a fusion reactor, the chemical interaction between beryllium and structural material could represent a concern. Several experimental tests carried out in Europe (FZK and CEA) showed that the out-of-pile compatibility limit of beryllium for 316 stainless steel and for ferritic martensitic steel are 600°C and 650°C respectively. Recent experimental data obtained in Japan (JAERI) showed that this limit is 600°C for stainless steel and between 600 and 800°C for the martensitic-ferritic steel F82H [2]. For reason of strength the martensitic steels have to be at temperatures less than 600°C.

References

- [1] M. Dalle Donne et al., Kernforschungszentrum Karlsruhe Report, KfK 5429, Nov. 1994
- [2] M. Dalle Donne, G. R. Longhurst, H. Kawamura and F. Scaffidi-Argentina, Beryllium R&D for Blanket Application, Proc. ICFRM-8, Sendai, Japan, 27-31 Oct. 1997
- [3] M. Dalle Donne, et al. "Measurement of the Thermal Conductivity and Heat Transfer Coefficient of a Binary Bed of Beryllium Pebbles". Proceedings of the 3rd IEA International Workshop on Beryllium Technology for Fusion, Mito, October 22-24, 1997.
- [4] M. Dalle Donne, A. Goraieb and G. Sordon, Measurement of the heat transfer parameters of mixed beds of beryllium and lithium orthosilicate pebbles, 1st IEA Int. Workshop on Beryllium for Fusion Application, Karlsruhe, 4-5- Oct. 1993. KfK Report 5271, Dec. 1993.